

**Université de Montréal**

**Strategies for revascularizing the ischemic retina**

**par Nicholas Sitaras**

**Département de pharmacologie, Faculté de Médecine**

Thèse présentée à la Faculté de Médecine en vue de  
l'obtention du grade de doctorat en pharmacologie  
option pharmacologie moléculaire

juillet 2014

© Nicholas Sitaras, 2014

## Résumé

Les rétinopathies ischémiques (RI) sont la cause majeure de cécité chez les personnes âgées de moins de 65 ans. Il existe deux types de RIs soit la rétinopathie du prématuré (ROP) ainsi que la rétinopathie diabétique (RD). Les RIs sont décrites en deux phases soit la phase de vasooblitération, marquée par une perte importante de vaisseaux sanguins, et une phase de néovascularisation secondaire à l'ischémie menant à une croissance pathologique de vaisseaux. Cette seconde phase peut générer des complications cliniques telles qu'un œdème dans l'humeur vitré ainsi que le détachement de la rétine chez les patients déjà atteints d'une RI. Les traitements approuvés pour les RIs visent à réduire la formation des vaisseaux pathologiques ou l'œdème; mais ceux-ci malheureusement ne règlent pas les problèmes sous-jacents tels que la perte vasculaire et l'ischémie.

La rétine est un tissu hautement vascularisé qui contribue à l'irrigation et à l'homéostasie des neurones. L'interaction neurovasculaire, comprenant de neurones, vaisseaux et cellules gliales, contribue au maintien de cette homéostasie. Durant le développement, les neurones et les cellules gliales jouent un rôle important dans la vascularisation de la rétine en sécrétant des facteurs qui stimulent l'angiogenèse. Cependant, nos connaissances sur l'interaction neurovasculaire dans les RIs sont limitées. En identifiant les interactions importantes entre les cellules composant cette unité neurovasculaire dans la rétine, nous pourrions viser des cibles qui engendreront une revascularisation saine afin de diminuer les signes pathologiques chez les patients atteints d'une RI.

Les travaux présentés dans cette thèse visent à mieux expliquer cette interaction neurovasculaire en soulignant des concepts importants propres aux RIs. En utilisant un modèle de rétinopathie induite par l'oxygène chez la souris, qui reproduit les caractéristiques importantes de la ROP (et en certaines instances, la RD), nous identifions quelques molécules clés jouant un rôle significatif dans les RIs soit la sémaphorine 3A (sema3A), l'IL-1 $\beta$ , ainsi que le récepteur PAR2.

Nos résultats démontrent que Sema3A, sécrétée par les cellules ganglionnaires rétiniennes (CGRs) durant une ischémie, empêche la revascularisation normale et que cette expression est induite par l'IL-1 $\beta$  provenant des microglies activées. En bloquant Sema3A directement ou via l'inhibition de l'IL-1 $\beta$ , nous remarquons une revascularisation saine ainsi qu'une diminution importante des vaisseaux pathologiques. Cela nous indique que Sema3A est impliquée dans la guidance vasculaire et qu'elle contribue à la pathogenèse des RIs. L'activation de façon exogène de PAR2, identifié aussi comme régulateur du récepteur de l'IL-1 $\beta$  (IL-1RI) sur les CGRs, se traduit par une diminution séquentielle de l'IL-1RI et de Sema3A ce qui mène également à une revascularisation saine.

En conclusion, ces travaux soulignent l'importance de l'interaction neurovasculaire ainsi que la guidance vasculaire dans les RIs. Ils renforcent l'importance de la communication entre neurone, vaisseau et microglie dans la pathogenèse des RIs. Finalement, nous identifions quelques molécules clés qui pourront servir comme cibles afin de lutter contre l'ischémie qui cause des problèmes vasculaires chez les patients atteints d'une RI.

## **Mots clés**

sémaphorine 3A, interleukine-1 $\beta$ , récepteur activé par protéase 2, vaisseaux, cellules ganglionnaires rétiniennes, microglies, vasooblitération, néovascularisation, revascularisation, rétinopathies ischémiques

## Abstract

Ischemic retinopathies (IRs), namely, retinopathy of prematurity (ROP) and diabetic retinopathy (DR), are the major cause of blindness in persons under the age of 65. IRs are biphasic disorders described by an initial vasoobliterative phase marked by a persistent microvascular degeneration, which leads to ischemia. Retinal ischemia, secondary to vessel loss, incites a second neovascularization phase represented by an aberrant, misdirected neovessel formation into the vitreous, which can cause adverse clinical complications including vitreous hemorrhaging and tractional retinal detachment. While current treatments aim at reducing vitreous/retinal hemorrhaging and/or pathological pre-retinal neovascularization, these regimens fail to address the underlying problem; that is, microvascular decay and retinal ischemia.

The retina is a highly metabolic tissue that requires a significant amount of nutrients and oxygen. This is supplied by an intricate and highly regulated vascular network required to maintain homeostasis and proper function. The intricate cellular interactions in the neurovascular unit – the consortium of vessel, neurons and support glia – are required for regulating and maintaining homeostasis under normal conditions. However, the understanding of how this unit functions under ischemic stress, that which is seen in patients suffering from IRs, is not well defined. The present work underlines several important concepts of neurovascular coupling in IRs in efforts to identify potential therapeutic agents that may help curb retinal ischemia by stimulating normal revascularization.

Using a mouse model of oxygen-induced retinopathy (OIR), which reproduces the salient features of ROP (and in some instances DR), we identified key players involved in generating the pathophysiological signatures associated with IRs; namely, semaphorin3A (Sema3A), interleukin-1 $\beta$  (IL-1 $\beta$ ) and protease-activated receptor 2 (PAR2). Our results show that neuronal-derived Sema3A, secreted by ischemic retinal ganglion cells (RGCs), acts as a potent vaso-repulsive molecules that impedes normal revascularization. Activated microglia contribute to this process by secreting

IL-1 $\beta$ , which induces paracrine release of Sema3A expression contributing to microvascular decay as well as pathological pre-retinal neovascularization. Inhibition of Sema3A or IL-1 $\beta$  translates to rapid revascularization and, as a result, a significant reduction in pathological neovessel formation. These results demonstrate that Sema3A is directly involved in vascular guidance and precipitates the pathophysiological features associated with IRs. PAR2, found on RGCs, was also identified as a key regulatory mechanism involved in dampening IL-1 $\beta$  induced Sema3A-mediated vascular decay by reducing IL-1 receptor (IL-1RI). Exogenous activation of neuronal PAR2 translates to a sequential reduction of both IL-1RI and Sema3A resulting in accelerated revascularization and consequentially pre-retinal neovascularization.

In conclusion, these studies highlight the importance of neurovascular coupling associated with IRs. Herein, we demonstrate the consorted interaction between neuron, vessel and glia and its impact on shaping the retinal vasculature during disease. Moreover, we underscore the significant impact of neuronal guidance cues in manifesting the salient vascular features of IRs. Finally, we identify key players that may serve as potential therapeutic avenues in curbing retinal ischemia in efforts to reduce vascular complications associated with IRs.

### **Key Words:**

Semaphorin 3A, Interleukin-1 $\beta$ , Protease-activated receptor 2, vessels, retinal ganglion cells, microglia, vaso-obliteration, neovascularization, revascularization, ischemic retinopathies

## Lay Summary

Ischemic retinopathies (IRs), which include Retinopathy of prematurity (ROP) and diabetic retinopathy (DR), are major causes of blindness worldwide. The onset of these diseases is complex and involves several factors, many of which have only begun to be unraveled. Extensive work has been conducted on retinal neovascularization, which is the pathological formation of new blood vessels. Notwithstanding, studies indicate that ischemia (or lack of nutrients and oxygen) precedes the pathological vessel formation has a significant impact on vision health.

There is growing evidence from our laboratory demonstrating the importance of neurons in the retina and their ability to influence their environment. This proposal aims at discerning the role of inflammation in vessel repair, growth and death, and the role of neurons in this process. Relevantly, we have shown that a population of retinal neurons called the ganglion cells can greatly influence the formation of new blood vessels both in physiological and pathological settings, as in IRs. A class of molecules that repel growing blood vessels called semaphorins, specifically Sema3A, have a significant impact on the severity of pathological neovascularization and thus IRs. Moreover, we identify that inflammation plays a significant role in generating Sema3A.

Our laboratory has unveiled preliminary data indicating the role of non-specific inflammatory responses (observed in most IR cases) as the underlying trigger of these repulsive cues. The PhD project presented here is designed to investigate the role of inflammation, which inadvertently constrains these vaso-sensitive neurons beyond a specific threshold thereby changing their initial pro-angiogenic phenotype for that of an anti-angiogenic profile. These findings will contribute to our greater understanding of factors that aggravate ROP and thus pre-disposes premature-born babies as well as diabetic patients to blinding retinal detachment.

## Table of Contents

List of Tables (by Chapter or Appendix) .....	4
List of Figures (by Chapter or Appendix).....	5
Abbreviations.....	9
Dedications .....	12
Acknowledgements.....	13
General Introduction .....	14
1. Brief Overview .....	14
2. Epidemiology of Ischemic Retinopathies .....	15
2.1. Retinopathy of prematurity (ROP).....	15
2.2. Diabetic retinopathy (DR).....	17
3. Etiology of Ischemic Retinopathies.....	18
3.1. Pathogenesis of Retinopathy of Prematurity.....	19
3.1.1. Risk factors for ROP .....	20
3.2. Pathogenesis of Diabetic Retinopathy .....	23
3.2.1. Risk factors for DR .....	25
4. Vascular biology in Ischemic Retinopathies .....	29
4.1. Angiogenesis, Vasculogenesis and Arteriogenesis .....	29
4.1.1. Vasculogenesis.....	29
4.1.2. Angiogenesis .....	31
4.1.3. Arteriogenesis .....	34
4.2. Formation of the retinal vascular network .....	35
4.3. Neurovascular coupling in angiogenesis.....	36
4.3.1. Nerve growth factor and neurotrophins.....	38
4.3.2. Netrins and their receptors.....	39
4.3.3. Semaphorins, Neuropilin and Plexins .....	40
4.3.4. Slits and Roundabouts .....	42
4.3.5. Ephrins and Eph receptors .....	43
4.4 Inflammation and angiogenesis .....	46
4.4.1. Cytokines and chemokines .....	46
4.4.2. Other relevant molecules .....	47
4.4.3. Inflammatory cells .....	48
5. Current treatments for Ischemic Retinopathies .....	50
5.1. Retinopathy of Prematurity (ROP).....	50
5.2. Diabetic retinopathy .....	51
6. Problem and general hypothesis.....	55
7. Description of the model: Oxygen-induced retinopathy .....	56
7.1 Mouse OIR model.....	56

7.2 Rat OIR model .....	57
<b>Chapter 1 .....</b>	<b>60</b>
<b>Ischemic neurons prevent vascular regeneration of neural tissue by secreting Semaphorin 3A .....</b>	<b>60</b>
Abstract .....	60
Introduction .....	61
Methods .....	63
Results .....	70
Discussion .....	76
Acknowledgements .....	78
Authorship .....	79
References .....	79
Specific contributions from the candidate .....	83
<b>Figures for Chapter 1 .....</b>	<b>84</b>
<b>Chapter 2 .....</b>	<b>106</b>
<b>Microglia and IL-1<math>\beta</math> in Ischemic Retinopathy elicit microvascular degeneration through neuronal Semaphorin3A .....</b>	<b>106</b>
Abstract .....	106
Introduction .....	107
Materials and Methods .....	109
Results .....	120
Discussion .....	126
Sources of Funding .....	129
Disclosures .....	129
References .....	129
Significance .....	134
Specific contributions from the candidate .....	134
<b>Figures for Chapter 2 .....</b>	<b>136</b>
<b>Chapter 3 .....</b>	<b>161</b>
<b>Retinal neurons curb inflammation and enhance revascularization in ischemic retinopathies via Protease-activated receptor 2 (PAR2) .....</b>	<b>161</b>
Abstract .....	162
Introduction .....	163
Materials and Methods .....	165
Results .....	170
Discussion .....	176
Acknowledgments .....	179
Authorship contributions .....	180
References .....	180
Specific contributions from the candidate .....	184
<b>Figures for Chapter 3 .....</b>	<b>186</b>
<b>Final Discussion .....</b>	<b>208</b>

<b>The importance of balancing vascular guidance cues in IRs: lessons from Sema3A and Netrin1 .....</b>	<b>209</b>
<b>Neurovascular interactions in IRs: RGCs, microglia and vessels .....</b>	<b>211</b>
<b>IL-1<math>\beta</math> and inflammation in IRs .....</b>	<b>213</b>
<b>Same protein, different roles: Lessons from PAR2 and Netrin1 .....</b>	<b>215</b>
<b>Conclusions .....</b>	<b>218</b>
<b>References: Introduction and Discussion .....</b>	<b>220</b>
<b>Appendix 1 .....</b>	<b>239</b>
<b>Supplementary Figures Joyal JS, Sitaras N, et al. Blood 2011 .....</b>	<b>239</b>
<b>Appendix 2 .....</b>	<b>251</b>
<b>Supplementary Figures for Rivera JC, Sitaras N et al. Arterioscler Thromb Vasc Biol 2013 .....</b>	<b>251</b>
<b>Appendix 3 .....</b>	<b>275</b>
<b>Supplementary Figures Sitaras N, et al. Am J Pathol 2014. ....</b>	<b>275</b>
<b>Appendix 4 .....</b>	<b>292</b>
<b>Neuronal ER Stress Impedes Myeloid-Cell-Induced Vascular Regeneration through IRE1a Degradation of Netrin-1 .....</b>	<b>292</b>
<b>Summary.....</b>	<b>292</b>
<b>Introduction .....</b>	<b>293</b>
<b>Experimental Procedures .....</b>	<b>296</b>
<b>Results .....</b>	<b>301</b>
<b>Discussion.....</b>	<b>312</b>
<b>Acknowledgments .....</b>	<b>317</b>
<b>References .....</b>	<b>318</b>
<b>Figures for Appendix 4 .....</b>	<b>326</b>

## List of Tables (by Chapter or Appendix)

Appendix 3 – Supplemental figures for Sitaras N et al. Am J Pathol 2014

**Supplementary Table 1.** Primers used for detecting mRNA expression both *in vivo* and *in vitro*.

## List of Figures (by Chapter or Appendix)

### Chapter 1 – Sema3A as an inducer of vascular repulsion

**Figure 1.** Sema3A expression is consistent with a role in retinopathy

**Figure 2.** IL-1 $\beta$  in the ischemic avascular retina induces Sema3A expression

**Figure 3.** RGC-derived Sema3A partakes in vasoobliteration, hinders vascular regeneration and contributes to pre-retinal neovascularization in OIR

**Figure 4.** Inhibition of RGC-derived Sema3A during proliferative retinopathy preserves neuro-retinal function

**Figure 5.** Sema3A produced by hypoxic RGCs prevents retinal endothelial cell growth

**Figure 6.** Sema3A produced by hypoxic RGCs repels nascent vessels

**Figure 7.** Intravitreal delivery of rSema3A suppresses pre-retinal neovascularization in OIR

### Chapter 2 – Microglia and IL-1 $\beta$ and their effects on vasculopathy

**Figure 1.** Hyperoxia triggers the production of inflammatory mediators and other factors in the retina

**Figure 2.** Inhibition of IL-1 $\beta$  activity decreases retinal vaso-obliteration and promotes revascularization.

**Figure 3.** Hyperoxia-induced generation of IL-1 $\beta$  is largely produced by activated microglia in the retina

**Figure 4.** IL-1 $\beta$  is released from microglial cells exposed to hyperoxia *in vitro*

**Figure 5.** Sema3A contributes to vaso-obliteration in rat pups exposed to hyperoxia

**Figure 6.** Activation of microglia is cytotoxic to endothelial cells through IL-1 $\beta$ -dependent generation of Semaphorin 3A by retinal ganglion cells

**Figure 7.** Endothelial apoptotic effects of RGC-conditioned media containing Sema3A obtained by stimulation of RGC-5 with IL-1 $\beta$  is abolished by the immunoneutralization of Sema3A or by blocking the activation of the IL-1 receptor

**Figure 8.** Microglia activation contribute to vascular regression in ROP through IL-1 $\beta$ -dependent stimulation of Semaphorin 3A in retinal ganglion cells: Inhibition of IL-1 $\beta$  activity decreases retinal vaso-obliteration and promotes revascularization

### Chapter 3 – PAR2 promotes revascularization

**Figure 1.** Neuronal PAR2 increases in mice retina during Oxygen-induced retinopathy (OIR)

**Figure 2.** Modulation of PAR2 activity during OIR affects vaso-obliteration and neovascularization

**Figure 3.** Increased expression of IL-1 $\beta$  in the retina during OIR stimulates PAR2 expression

**Figure 4.** PAR2 activation results in downregulation of IL-1RI in vivo

**Figure 5.** JNK activates downstream ERK1/2, which is required for PAR2-dependent inhibition IL-1RI in retinal neurons

**Figure 6.** Activation of PAR2 abolishes IL-1 $\beta$ -mediated Sema3A release, reducing endothelial cell death and promoting vascular sprouting

**Figure 7.** PAR2 on retinal ganglion cells enhances revascularization by suppressing IL-1RI

### Appendix 1 – Supplemental figures for Joyal JS, Sitaras N et al. Blood 2011

**Supplementary Figure 1.** Timeline of revascularization in OIR and depiction of laser-capture microdissection

**Supplementary Figure 2.** VEGF is upregulated in the central avascular region of the OIR retina

**Supplementary Figure 3.** Expression of IL-1RI in RGC-5 and astrocytes

**Supplementary Figure 4.** Intravitreal injection of Lentivirus efficiently infects RGCs

**Supplementary Figure 5.** Lv.shSema3A protects against vaso-obliteration and neovascularization

**Supplementary Figure 6.** *In vitro* assessment of RGC–derived Sema3A

Appendix 2 – Supplemental figures for Rivera JC, Sitaras N et al. *Arterioscler Thromb Vasc Biol* 2013

**Supplemental Figure 1.** NALP3 inflammasome expression in the retina and protein detection of different mediators induced by hyperoxia

**Supplemental Figure 2.** Administration of IL-1 antagonists does not affect normal retinal vascularization

**Supplemental Figure 3.** IL-1R inhibitors prevent pre-retinal neovascularization, and intravitreal IL-1 $\beta$  increases Sema3A expression and causes retinal microvascular injury

**Supplemental Figure 4.** The peptide 101.10 (*rytvela*) is mostly distributed in the retina in microglia and endothelial cells during hyperoxia

**Supplemental Figure 5.** Cellular internalization of 101.10 is dependent on the presence of the IL-1R

**Supplemental Figure 6.** IL-1 $\beta$  is minimally produced by astrocytes, neurons and endothelium during hyperoxia

**Supplemental Figure 7.** Localization of IL-1R in the retina

**Supplemental Figure 8.** NLRP3 inflammasome, IL-1 $\beta$  and Iba-1 expression in microglia cultures are increased during hyperoxia

**Supplemental Figure 9.** Autostimulation of IL-1 $\beta$  in HEK blue cells and macrophages

**Supplemental Figure 10.** Semaphorin 3A (Sema3A) is largely produced by retinal ganglion cells (RGC) in the retina under hyperoxia

**Supplemental Figure 11.** Conditioned media from retinal ganglion cells (RGC-5) stimulated with hyperoxic-microglia conditioned media (Hyp-MG-RGC-CM) induces activation of caspase-3 on endothelial cells (RBMVEC)

**Supplemental Figure 12.** IL-1 $\beta$  released from neuro-microvascular endothelial cells (RMBVEC) exposed to hyperoxia does not induced Sema3A release on RGC-5 cells

Appendix 3 – Supplemental figures for Sitaras N et al. Am J Pathol 2014

**Supplementary Figure 1.** PAR2 expression in neural retina

**Supplementary Figure 2.** Laser capture microdissection on sagittal P8 mouse retina

**Supplementary Figure 3.** PAR2 intact and transgenic mice share similar vascular phenotypes in OIR; shRNA-bearing Lentiviral constructs target PAR2 in retinal ganglion cells

**Supplementary Figure 4.** PAR2 transgenic mice do not respond to SLIGRL or Lv. shPAR2 treatment

**Supplementary Figure 5.** Kineret treatment in vivo successfully dampens IL-1 $\beta$  in whole retina and PAR2 expression in various cell lines

**Supplementary Figure 6.** SLIGRL treatment in normoxia raised mice pups; PAR2 transgenic mice respond to IL-1Ra but not to SLIGRL treatment

**Supplementary Figure 7.** PAR2-mediated regulation of IL-1RI in RBMVEC; PAR2-induced reduction of IRAK1 phosphorylation in RGC-5

**Supplementary Figure 8.** PAR2 stimulates production of VEGF in retinal ganglion cells and promotes VEGF-dependent vascular sprouting

Appendix 4 – Figures for Binet N et al. Cell Metab 2013

**Figure 1.** Neuronal ER Stress Is Induced in Hypoxic Retinas and Associated with Failure of Revascularization

**Figure 2.** Netrin-1 Is Downregulated by Hypoxia-Triggered ER Stress

**Figure 3.** Netrin-1 Is Cleaved by the RNase Activity of IRE1a

**Figure 4.** Administration of Netrin-1 to Ischemic Retinas Enhances Vascular Regeneration and Suppresses Pathologic Neovascularization

**Figure 5.** Netrin-1 Activates AA2BR on Macrophages and Provokes the Release of VEGF in an ERK1/ERK2-Dependent Manner

**Figure 6.** Netrin-1 Triggers a VEGF-Dependent Proangiogenic Response in Macrophages

**Figure 7.** Netrin-1-Dependent Vascular Regeneration Is Macrophage/Microglial Cell and VEGF Dependent

## Abbreviations

AA2BR = Adenosine 2B receptor  
ACE = angiotensin converting enzyme  
AGE = advanced-glycosylation end-products  
Akt = protein kinase B  
AMD = Age-related Macular Degeneration  
Ang = Angiopoietin  
ATF4 = Activating transcription factor 4  
BDNF = Brain-derived neurotrophin factor  
BM = basement membrane  
BRB = blood retina barrier  
CNS = central nervous system  
CNV = choroidal neovascularization  
COUP-TFII = Chicken ovalbumin upstream promoter transcription factor II  
COX = cyclooxygenase  
CXCR4 = C-X-C motif chemokine receptor 4  
DAG = diacylglycerol  
DCC = deleted in colorectal cancer  
DHA = docosahexaenoic acid  
DII4 = delta-like ligand 4  
DR = Diabetic Retinopathy  
EC = endothelial cell  
ECM = extracellular matrix  
EMA = Emergency Medical Association  
EPC = endothelial cell progenitors  
Epo = Erythropoietin  
ER stress = endoplasmic reticulum stress  
FDA = Food and Drug Administration  
FGF = fibroblast growth factor  
Flt1 = VEGFR2  
FOXC = Forkhead box C  
FSS = flow shear stress  
FVII = Coagulation factor VII  
GAP = GTPase activating protein  
GEF = guanine-nucleotide exchange factors  
GM-CSF = Granulocyte macrophage colony stimulating factor  
GPCR = G-protein coupled receptor  
GTPase = guanosine triphosphatase  
HIF-1 $\alpha$  = Hypoxia-inducible factor 1  $\alpha$   
Hh = Hedgehog  
ICAM-1 = intercellular adhesion molecule 1  
IGF = Insulin-like growth factor

IGFBP3 = Insulin-like growth factor binding protein 3  
ihh = Indian Hedgehog  
IL = Interleukin  
IL-1RI = Interleukin 1 receptor I  
IL-1Ra = Interleukin 1 receptor antagonist  
IOP = increased ocular pressure  
IR = Ischemic Retinopathy  
IRE1- $\alpha$  = inositol-requiring kinase 1 alpha  
ISV = intersegmental vessels  
Jag = Jagged  
LOX = lipoxygenases  
LPA = lysophosphatidic acid  
Lrp5 = low-density lipoprotein receptor protein 5  
MAPK = mitogen activated protein kinase  
MCP-1 or CCL2 = monocyte chemotactic protein-1  
MMP = matrix metalloprotease  
NICE = National Institute for Health and Clinical Excellence  
NF $\kappa$ B = nuclear factor kappa-light-chain-enhancer of activated B cells  
NGF = nerve growth factor  
NO = nitric oxide  
NOS = nitric oxide synthase  
NV = neovascularization  
Nrp = Neuropilin  
NT = neurotrophin  
OIR = oxygen-induced Retinopathy  
ONOO $^-$  = peroxynitrite  
PAF = platelet activating factor  
PAR = protease-activated receptor  
PDGF-B = Platelet-derived growth factor B  
PDGFR $\beta$  = Platelet-derived growth factor receptor  $\beta$   
PDR = Proliferative Diabetic Retinopathy  
PERK = protein kinase RNA-like endoplasmic reticulum kinase  
PI3K = phospo-inositol-3 kinase  
PKC = protein kinase C  
PLA $_2$  = phospholipases  
Plex = Plexin  
PPAR = peroxisome proliferator-activated receptor  
ProNGF = precursor form of NGF  
P75NTR = neurotrophin receptor P75  
RAGE = receptors for advanced-glycosylation end-products  
RASIP-1 = Ras-interacting protein 1  
RGC = retinal ganglion cell  
Robo = Roundabout  
ROCK = Rho kinase

ROP = Retinopathy of prematurity  
ROS = reactive oxygen species  
RPE = retinal-pigmented epithelium  
RTK = receptor tyrosine kinase  
RVO = retinal vein occlusion  
SDF-1 or CXCL12 = stromal-cell derived factor-1  
Sema = semaphorin  
shh = Sonic Hedgehog  
SHP-1 = Src homology-2-domain-containing-phosphatase-1  
SMC = smooth muscle cells  
SWEDROP = Swedish national register for retinopathy of prematurity  
TAA = trans-arachidonic acid  
TF = Tissue factor  
TGF- $\beta$  = transforming growth factor  $\beta$   
TNF- $\alpha$  = tumor necrosis factor  $\alpha$   
Trk = tropomyosin related kinase  
TSP-1 = thrombospondin-1  
UPR = Unfolded protein response  
VEGF = vascular endothelial growth factor  
VEGFR = vascular endothelial growth factor receptor  
VO = vaso-obliteration  
WINROP = weight, insulin-like growth factor I, neonatal, retinopathy of prematurity  
WHO = World Health Organization  
Wnt = Wingless  
 $\omega$ -3 PUFA = omega-3 poly-unsaturated fatty acids  
XPB1 = X-box binding protein 1

## Dedications

I dedicate this work to my father who passed away this year (2014) due to a brain ischemia. May you rest in peace forever.

I would also like to dedicate this work to my loving wife, Constanza, whom has supported me unabatedly throughout my PhD.

Love you always.

## **Acknowledgements**

I would like to thank my mother, Nella, my siblings, Jonathan, Cynthia and Christopher who unconditionally supported my efforts throughout the years.

My friends have also been key to my drive to success. They were there through and through supporting me without question.

I would like also like to thank Jose Carlos, Sylvain and Mike whom have made these years fruitful and memorable. They are the reason for my devout dedication to science and my constant strive to be better.

# General Introduction

## 1. Brief Overview

Ischemic retinopathies (IRs), namely, diabetic retinopathy (DR) and retinopathy of prematurity (ROP), are the leading cause of visual impairment and blindness affecting primarily working-age and pediatric populations, respectively. With the overwhelming incidence of diabetes increasing globally<sup>1</sup> as well as increased survival rate of prematurely born infants<sup>2</sup>, IRs are becoming a significant encumbrance on the health care system both directly and indirectly. The underlying causes of these diseases are predominantly vascular-based whereby a sudden microvascular dropout (phase I) translates to an overcompensated, uncontrolled vascular growth that protrudes into the vitreous (phase II). The latter accounts for multiple clinical complications including macular edema, vitreous hemorrhaging, fibrosis and tractional retinal detachment<sup>2,3</sup>. While current treatments involve tackling the problematic during the latter stages of the disease (excess vessel growth and extravasation into the retina and vitreous), there are few options that address the underlying problem leading to excess vessel growth; namely vessel loss and ischemia.

Recently, there is evidence demonstrating the importance of the neurovascular unit—the consortium of neurons, vessels and glia that make up the retina—in retinal diseases<sup>4</sup>. These cells bidirectionally communicate to maintain homeostasis and ensure proper functioning of the neuro-retina. When perturbations occur, as seen in ROP and DR, it affects the entire unit. We now know that IRs are not only vascular-based but also neuronal-based diseases. Notwithstanding, there is still a significant amount of knowledge regarding neurovascular coupling that remains to be unveiled. Formal understanding of the neurovascular coupling will help propagate the discovery of novel therapeutic avenues that will aid in curbing retinal ischemia and vessel loss that precedes excess vessel growth.

This investigation herein covers a series of topics related to neurovascular coupling between vessels, glia and neurons in efforts to discern the important interactions involved in propagating the disease. Using a mouse model of oxygen-induced retinopathy (OIR), which mimics the cardinal features of ROP (and to a certain extent DR), we highlight key players and concepts that contribute to the observed vessel loss and subsequent pathological vessel growth associated with IRs. Herein, we specifically target these molecules to essentially curb vessel loss, accelerate normal revascularization and prevent excess vessel growth; in other words, reestablishing a normal vascular network in the retina to reinstate homeostasis in the neurovascular unit.

## **2. Epidemiology of Ischemic Retinopathies**

The incidence of Ischemic Retinopathies (IRs), namely, retinopathy of prematurity (ROP) and diabetic retinopathy (DR), has increased drastically since the 1950's<sup>5</sup>. In 2000, the World Health Organization (WHO) published a report on the incidence of blindness globally, whereby 50,000 children and 1.7 million working-age persons were blinded as a direct cause of ROP and DR, respectively<sup>5</sup>. With increasing survival rates in preterm born children<sup>2</sup> and an alarming increase in diabetes globally<sup>1</sup>, these numbers are expected to surge drastically in the next 10 to 15 years; the WHO has now classified these eye ailments as “priority eye diseases”. Essentially, IRs will be the major contributing cause of irreversible blindness globally in persons below the age of 60, which will impart a significant burden to the health care systems.

### *2.1. Retinopathy of prematurity (ROP)*

Worldwide approximately 10% of all newborns are born before term (<37 gestational weeks)<sup>6</sup>. Although prematurity is still one of the leading causes of death in neonates<sup>7</sup>, there has been a drastic improvement in survival rates since the use of

supplemental oxygen incubators in the 1940's. This, however, has also led to a significant increase in ROP among neonates and is now one of the leading cause of blindness in children<sup>2,5</sup>.

ROP afflicts primarily extremely low birth-weight (typically  $\leq 1500$  g) and low gestational-age ( $\leq 30$  weeks) neonates accounting for the large majority of reported blindness<sup>8,9</sup>. However, the incidence of ROP also occurs in moderate birth weight ( $>1500$ g) and gestational age ( $> 31$  weeks) due to use of supplement oxygen, which remains one of the major risk factors for development of ROP (see below *Etiology of retinopathy of prematurity*)<sup>10,11</sup>. Statistically, while low incidence of ROP has been reported in some countries (in Australia and New Zealand  $<10\%$  neonates have severe ROP), other epidemiological studies report very high incidence of ROP among prematurely born babies (Sweden reports  $\sim 33\%$  of neonates have severe ROP)<sup>2</sup>. Although racial, genetic or environmental factors may influence epidemiological variations, infant mortality rates and ROP are highly correlated and vary widely between countries<sup>9</sup>. Notably, study design, survival rates and treatment use may also skew reported population statistics<sup>2,11</sup>. Complementary screening algorithms (e.g. WINROP) and centralized registries (e.g. SWEDROP) are now being employed in various countries in efforts to yield accurate numbers and reduce sampling errors between study groups<sup>2,12,13</sup>.

While the incidence of ROP may be high in some population groups<sup>9</sup>, less than 15% of neonates diagnosed with the disease develop sight-threatening vision loss requiring clinical intervention<sup>2,14</sup>. In most patients, characteristics of ROP spontaneously regress. Notwithstanding, neonates afflicted with moderate forms of ROP – not having suffered complete vision loss – often suffer from other ocular impairments including: significant reduction in visual acuity, refractory errors (e.g. myopia), amblyopia or strabismus, defects in ocular growth and retinal dysfunction<sup>15</sup>. Recent studies have associated abnormal or delayed child growth and perturbations in neurovascular homeostasis as underlying bases for these deficiencies<sup>15,16</sup>. Consequently, understanding the underlying mechanisms of ROP disease

progression will be beneficial in not only preventing blindness but also improving visual acuity and eye function in children.

## *2.2. Diabetic retinopathy (DR)*

In 2000, the World Health Organization reported an approximate 171 million people worldwide have been diagnosed with Diabetes Mellitus and was estimated that by 2030, approximately 366 million people will have diabetes globally<sup>5</sup>. The International Diabetes Federation, however, published a report in 2011 approximating that an 366 million have already been afflicted with this disease<sup>1</sup>. Thus, in nearly a third of the estimated time (11 years instead of 30 years) the incidence of Diabetes Mellitus has more than doubled globally. Pertinently, it is estimated that approximately 75% of all diabetes patients (type 1 and 2) will develop some form of DR after 20 years<sup>17</sup>. With a reported 93 million diabetic patients suffering from DR in 2010 (28 million having vision threatening DR)<sup>18</sup>, there has been a recent push to improve screening methods, increase metabolic control and patient follow-up, and research and develop novel treatment regimes in efforts to combat this sight-threatening ailment<sup>3,4</sup>.

Epidemiological studies show that uncontrolled glycemia, elevated blood pressure and lipid levels – commonly found in diabetes patients – are associated with increased incidence and progression of proliferative DR (PDR)<sup>4</sup>. While strict metabolic control reduces the incidence and development of DR<sup>19</sup>, up to 20% of patients diagnosed with diabetes still developed PDR after 30 years, which accounted for an estimated 17 million people globally in 2010<sup>18</sup>. Serum levels of adiponectin<sup>20</sup>, prolactin<sup>21</sup> and homocysteine<sup>22</sup> as well as non-alcoholic liver diseases<sup>23</sup>, genetic factors, insulin resistance and low levels of physical activity<sup>4</sup> have been proposed as potential risk factors in PDR; however, relative influences of these factors in the development of proliferative DR have thus far not been well established. Clinical macular edema also contributes to significant vision loss accounting for an estimated 6.8% of diabetic patients or 21 million people worldwide<sup>18</sup>. While similar risk factors

are associated with incidence and progression of diabetic macular edema and PDR<sup>4</sup>, distinct classification, management and treatment regimes for clinical macular edema are now being observed<sup>3</sup>. The underlying causes for onset and development of macular edema or PDR, however, still remain elusive.

While diabetic care has improved in the last few decades in most developed countries, insufficient eye care in emerging countries remains a significant problematic, particularly in areas where the incidence of diabetes is staggeringly high (~80% of diabetic persons live in low- or middle income countries)<sup>1,18</sup>. Moreover, there are a significant number of persons living with diabetes that have not yet been diagnosed<sup>1</sup>, thus creating a significant encumbrance to health care systems predominantly in countries where substantial eye care for diabetic patients are sub-optimal or unavailable. Thus, improved classification guidelines and effective screening methods will be necessary to help clinicians better diagnose DR in the coming years.

### **3. Etiology of Ischemic Retinopathies**

IRs are biphasic disorders caused by an imbalance in vascular homeostasis in the neural retina. The first phase is marked by a persistent degeneration of the retinal microvasculature leading to a state of ischemia. In ROP, the major underlying contributor leading to the abrupt vessel loss is excess oxygenation<sup>2</sup>, while in DR sustained hyperglycemia and inflammation are proposed as contributing factors to substantial vessel loss<sup>3</sup>. Improper oxygen supply due to sustained vessel loss (ischemia) results in significant biochemical changes in retinal cells (neurons and glia) that mount an overcompensated, uncontrolled vessel growth in attempt to reinstate vascular homeostasis – the second phase. This excessive and misguided neo-vascularization protrudes towards the vitreous and, if left untreated, can cause significant perturbations in visual acuity and irreversible vision loss. While similarities

exist between ROP and DR, the underlying pathophysiological mechanisms of disease onset, nonetheless, remain distinct.

### *3.1. Pathogenesis of Retinopathy of Prematurity*

Preterm birth causes an abrupt cessation in retinal vascular growth, which under normal circumstances matures only at term (e.g. week 40 gestational age)<sup>24</sup> [see *section 4.2*]. Since retinas of premature infants are only partly vascularized, the incidence and progression of ROP is directly proportional to the gestational age upon birth. As a result, the immature and highly susceptible retinal vasculature is vulnerable to a number of stressors including high levels of oxygen delivery, suppression of key vascular survival factors, including vascular endothelial growth factor (VEGF) and erythropoietin (Epo), and inadequate supply of maternally-derived cytoprotective factors, such as insulin-like growth factor (IGF-1). Clinically, this translates to a vaso-obliteration of retinal vessels known as the first phase of ROP (Stage 1 and 2 of ROP; see *Table 1* for details).

As the eye continues to grow and become functional, the metabolically active retinal cells prompt a rapid response in efforts to counter the relative hypoxia in the retina. In some ROP cases spontaneous revascularization does occur; however, hypoxia triggers massive increase in vaso-proliferative cues, such as VEGF<sup>25</sup> and Epo<sup>26</sup>, while simultaneous increase in non oxygen-regulated molecules, such as IGF-1<sup>27</sup> leads to an overcompensated vessel growth that protrudes into the vitreous cavity (Stage 3). Left unchecked, the immature and highly leaky vessels can lead to scarring fibrotic lesions, which result in, upon regression, tangential retinal shearing leading to partial (Stage 4) or complete detachment of the retina (Stage 5) and thus blindness.

Notwithstanding, clinical investigations<sup>8</sup> and use of animal models<sup>28,29</sup> has greatly enhanced our understanding of the pathophysiological changes that occur in the retina of preterm infants. We now understand that ROP is not only a vascular-based disorder but is also causes functional visual defects. Recent studies have underscored the important neurological changes that occur during ROP are mainly

due to hyperoxia and ischemia<sup>15,16</sup>. Although hyperoxia affects particularly the photoreceptors, likely via perturbations in choroidal development<sup>30</sup>, there is also mounting evidence showing the effect of oxidant stress on the inner retina structure<sup>15,31</sup> indicating that neurons in these layers also suffer from ensuing ischemia. The information regarding this occurrence, however, remains elusive.

While oxygenation remains a significant player in ROP, several other factors have also been attributed to the pathogenesis of the disease.

### 3.1.1. Risk factors for ROP

#### Hyperoxia

Excess oxygenation has been described as the most dominant factor in the development and severity of ROP in both human<sup>2,8</sup> and animal studies<sup>28,29</sup>. Hyperoxia, as a result of supplemental oxygen ventilation (typically between 85 – 100% O<sub>2</sub>), translates to an arrest in retinal vascular growth and regression of the pre-existing vasculature (vaso-obliteration). In humans, even room air—considered hyperoxic compared to *in utero* levels—can cause obliteration of retinal vessels. Relevantly, attempts to lower oxygen saturation levels (pO<sub>2</sub>) have been implemented in neonatal care units in efforts to lower ROP severity; however, this remains controversial, particularly since use of lower pO<sub>2</sub> correlates to increased neonatal mortalities<sup>2</sup>. Use of supplemental oxygen in the second vaso-proliferative phase, however, does not appear to affect the severity of ROP<sup>32,33</sup>.

At the molecular level, the hostile hyperoxic environment in the neonate retina promotes formation of various reactive oxygen species (ROS) and their peroxidation products, which contribute to microvascular injury during this first phase of ROP<sup>10,34</sup>. Increased enzymatic activities of cyclooxygenase (COX), phospholipases (PLA<sub>2</sub>) and nitric oxide synthase (NOS) in retinal endothelium contribute to observed vasoobliteration through release of thromboxane (TXA<sub>2</sub>), platelet activating factor (PAF), lysophosphatidic acid (LPA) and trans-arachidonic acid (TAA)<sup>10</sup>. Correspondingly, use of antioxidants or genetic ablation and pharmacological

inhibition of these enzymes translates to decreased microvascular decay in animal models of ROP<sup>10,35</sup>.

High oxygen levels also tips the balance between pro-angiogenic and anti-angiogenic cues whereby increased oxygen tension in the retina favors the latter. Hyperoxia downregulates important oxygen-regulated angiogenic factors, VEGF<sup>36,37</sup> and Epo<sup>26,38</sup>, which are indispensable vessel growth and survival factors required during this crucial phase of retinal vessel development. Conversely, release of anti-angiogenic factors, thrombospondin-1 (TSP-1)<sup>39</sup> and tumor necrosis factor  $\alpha$  (TNF- $\alpha$ )<sup>40</sup>, as a result of high oxygen tension contribute to observed vascular decay as seen in ROP patients by inducing endothelial cell apoptosis.

#### Gestational age, birth weight and postnatal weight gain

Aside from oxygen, gestational age ( $\leq 30$  weeks) and birth weight ( $\leq 1500$  g) are major risk factors in the outcome of ROP. Both factors impart a direct link to retinal development; low birth weight and low gestational age are proportionally related to underdeveloped neural and vascular networks, which are highly susceptible to injury. This is mainly associated with loss of key factors provided by the intrauterine environment and slow production of these factors in preterm neonates<sup>2</sup>, which can impact ROP progression. Moreover, birth weight is an important contributing factor in the outcome of ROP; low birth weight directly affects incidence and severity of ROP in preterm infants born before 31 weeks<sup>41-45</sup>. It has been proposed that intrauterine growth restrictions are attributed to this phenomenon<sup>2</sup>.

Weight gain post-conceptionally also contributes to the progression and severity of ROP in humans<sup>46</sup> and animals<sup>47</sup>. Essentially, animals and humans with inferior weight gain postnatally demonstrate increased exacerbation in ROP characteristics while excessive weight gain shows the inverse<sup>46,47</sup>. IGF-1 serum levels strongly correlate with preterm infant weight gain<sup>46</sup> and thus contributes both directly and indirectly in the outcome of ROP (see below). Notably, factors such as metabolic

rate, hyperglycemia, nutrition, infections and illnesses also affect premature infant weight gain and should be carefully monitored during postnatal weeks following birth<sup>2</sup>.

#### Maternally derived factors

One of the crucial disparities between babies born preterm and those born at term is loss of vital maternally-derived factors, the most important being IGF-1<sup>48,49</sup> and omega-3 polyunsaturated fatty acids ( $\omega$ -3 PUFAs)<sup>50</sup>. Preterm birth severs the maternal-fetal interaction thus preventing influx of these essential factors, which are particularly necessary during the third trimester of gestation<sup>48</sup>. Importantly, these essential nutrients and factors have a profound effect on infant development as well as incidence and progression of ROP and other disorders caused by prematurity (cerebral palsy, chronic lung disease)<sup>46,51,52</sup>.

IGF-1, a polypeptide protein hormone, is an essential factor for fetal development during all stages of pregnancy<sup>53</sup>. Premature birth severs the essential supply of IGF-1 from the placenta and utero thus slowing growth and development of the preterm infant<sup>49</sup>. Moreover, premature infants born before 33 weeks produce very low levels of IGF-1 compared to full term born infants<sup>48</sup>. Relevantly, serum levels of IGF-1 are inversely correlated the severity of ROP in preterm infants<sup>46</sup>; lack of IGF-1 and its binding protein (IGFBP3) results in significant loss of retinal vessels during the vaso-obliterative phase<sup>27,54</sup>. Experimental animal models of ROP have demonstrated that exogenous administration of recombinant human (rh) IGF-1 resulted in significant weight gain, rapid maturation and considerably less severity of OIR<sup>55</sup>. In this regard, use of fresh frozen placenta (a significant source of IGF-1) or rhIGF-1 and rhIGFBP3 is now commonly used in pediatric clinics to help augment serum IGF-1 in preterm infants to normal *in utero* levels in efforts to reduce ROP incidence and severity<sup>56,57</sup>.

$\omega$ -3 PUFA are essential nutrients obtained from our diet that exert powerful biological activities. An important influx of  $\omega$ -3 PUFA is normally transferred from mother to fetus during the third stage of pregnancy, which is lost as a result of premature birth. Since the eye contains the highest concentration of docosahexaenoic

acid (DHA, the major metabolite of  $\omega$ -3 PUFA) in the body, it is no surprise that exogenous supplementation of DHA in preterm infants correlated with increased visual acuity<sup>50</sup>. More recently, animal studies of ROP demonstrate that lactating mothers fed with  $\omega$ -3 PUFA enriched diets resulted in a significant decrease in vaso-obliteration and pathological neovascularization in mice pups<sup>58,59</sup>. Exploration into the molecular mechanisms shows that  $\omega$ -3 PUFA diet translated to significant increase in cytoprotective and anti-inflammatory resolvins and neuroprotectins, which impart their beneficial effects via suppression of TNF- $\alpha$ <sup>59</sup>, likely via peroxisome proliferator-activated receptor (PPAR $\gamma$ )<sup>58</sup>. The same group also demonstrated that 4-hydroxy-DHA (formed from  $\omega$ -3 PUFA via 5-lipoxygenase) potentiates anti-angiogenic properties by selectively activating PPAR $\gamma$  on endothelial cells (ECs). Although supplementation of  $\omega$ -3 PUFA in premature infants is not exercised clinically, anti-angiogenic effects of supplemented  $\omega$ -3 PUFA have been reported in patients suffering from related neovascular eye diseases, such as age-related macular degeneration (AMD)<sup>60,61</sup>.

### *3.2. Pathogenesis of Diabetic Retinopathy*

Although there is no established animal model for DR, the development of the OIR models in rodents<sup>28,29</sup> has shed much light on the mechanisms involved in vaso-proliferative phase of DR; however, the pathophysiological mechanisms underlying the onset of DR remain largely unknown. Nonetheless, a large body of data suggests that the dysfunctional changes that occur in the retina in DR patients are of neurovascular origin rather than a pure microvascular phenomenon. The interaction between inner retinal neurons (RGC, amacrine, bipolar cells), glia (microglia, astrocytes, Müller cells) and retinal microvasculature – cells that make up the neurovascular unit – is so finely tuned that perturbations can lead to neuronal dysfunction as seen in the brain<sup>62</sup>. In DR, these perturbations are quite often

asymptomatic but can lead to diabetic macular edema<sup>3</sup>, vitreous hemorrhaging and later tractional retinal detachment diminishing visual acuity and causing loss of vision.

The initial phase of vessel loss in diabetic patients begins with breakdown of the blood-retina-barrier (BRB), which often leads to noticeable microaneurysms in the retina<sup>3</sup>. The BRB is normally composed of endothelial cell (EC) tight-junction and adherence proteins as well as pericytes that wrap around blood vessels to limit extracellular fluid exchange between blood and retina<sup>62</sup> (see below *section 4*). Increased cytokine expression in the retina of DR patients, such as interleukin-1 $\beta$  (IL-1 $\beta$ ) and TNF- $\alpha$ <sup>63</sup>, which can induce intercellular adhesion molecule 1 (ICAM-1) expression<sup>64</sup> contribute to BRB breakdown by increasing leukocyte adhesion and activation in retinal vessels<sup>65</sup>. VEGF, first described as a vascular permeability factor<sup>66</sup>, increases significantly in the vitreous of patients with DR<sup>67</sup> and contributes directly to disruption of BRB integrity by disrupting EC tight-junction proteins and pericyte adhesion<sup>68</sup>. Other factors, such as increased activity of protein kinase C isoforms<sup>69</sup> (particularly PKC $\beta$ ), advanced-glycosylation end-products (AGE)<sup>70</sup> as well as increased activity of kallikrein-bradykinin<sup>71</sup> pathways also appear to contribute to compromised vessel integrity in the early stages of DR. This can lead to severe non-proliferative DR marked by venous bleeding, multiple blot hemorrhages and intraretinal microvascular abnormalities<sup>3</sup> which creates pockets of non-perfused tissue.

The resulting ischemia that occurs secondary to vessel loss induces an over-compensated albeit pathological neovascularization response similar to that observed in ROP patients. HIF-1 $\alpha$ , triggered by hypoxia, increases a plethora of vascular response cues, principally VEGF and Epo<sup>38,72</sup>, which play a central role in neovessel formation in proliferative DR<sup>73,74</sup>. However, this attempt to reinstate vascular homeostasis, instead of revascularizing non-perfused areas of the retina, grows aberrantly towards the posterior segments of the vitreous cavity<sup>3</sup>. The highly immature neovessels are often leaky resulting in bleeding into the vitreous and inner retina, which cause perturbations in visual acuity and obstruction of vision. Left

untreated, these immature and leaky neovessels can form fibrotic scars that, upon retraction, can cause blinding retinal detachment.

Poor blood sugar regulation in diabetic patients has been shown to increase the incidence and progression of DR<sup>4</sup>; however, despite proper metabolic control there is still a percentage of diabetic patients that develop DR<sup>19</sup> indicating that the appearance of retino-complications associated with DR may be multi-factorial. These include various facets of hyperglycemia, chronic inflammation and pathological angiogenesis discussed below.

### 3.2.1. Risk factors for DR

#### Hyperglycemia

In the CNS, glucose is the major metabolite used by cells in the neurovascular unit for supplying energy. In diabetic patients, hyperglycemia translates to a significant influx of glucose in the retina and brain and has is associated with observed microvascular complications in retinas of diabetic patients<sup>4</sup>. One complication linked directly to high glucose levels in the retina is formation of advanced-glycosylation end-products (AGE). AGEs form non-enzymatically from glucose or other glycation compounds, reacting with proteins lipids, or DNA<sup>70</sup>. Formation of AGEs can result in altered function of intracellular proteins, interrupt extracellular matrix proteins interactions as well as entitle their own functionality by binding to receptors for AGE (RAGE)<sup>75</sup>. Activation of RAGE results in increased ROS generation (discussed below) as well as activation of transcriptional factor NFκB, which lead to pathological gene expression changes<sup>76</sup>. Pertinently, accumulation of AGE in retinal pericytes can be detrimental precipitating cell death<sup>77</sup>; in retinal ECs, however, AGE-RAGE signaling can potentiate angiogenesis via upregulation of Ang2<sup>78</sup> and VEGF<sup>79</sup> indicating that AGEs can have a distinct roles in both phases of DR.

Hyperglycemia can also activate various protein kinase C (PKC) isoforms, which plays a pivotal role in disease progression of DR<sup>69</sup>. PKC activity is normally upregulated by intracellular  $\text{Ca}^{2+}$  and diacylglycerol (DAG); these molecules are significantly increased in retinal vessels by hyperglycemia, which lead to activation of various PKC isoforms in diabetic patients<sup>75</sup>. For instance, PKC $\beta$  increases as a result of hyperglycemia and is well known for disrupting tight-junction proteins on ECs causing subsequent breakdown of BRB<sup>69</sup>. Another study demonstrated that hyperglycemia-activated PKC $\delta$  phosphorylates and activates of mitogen activated protein kinase (MAPK) signaling via p38 $\alpha$ ; activation of p38 $\alpha$  translates to phosphorylation of SHP-1 (Src homology-2-domain-containing-phosphatase-1) and subsequent inactivation of PDGF receptor  $\beta$  (PDGFR $\beta$ ), which results in pericyte death and thus increased retinal extravasation in mice<sup>80</sup>. Moreover, PKC activity can lead to the formation of ROS, which imparts its own degenerative role in DR. PKC $\beta$  and  $\delta$  are also expressed in other retinal cell types albeit their relative contributions to the pathogenesis of DR has not been well established.

Hyperglycemia increases oxidative stress in the neurovascular unit through ROS formation via increased mitochondrial respiration, AGE-RAGE signaling and PKC activity. ROS formation can lead to increased lipid peroxidation in endothelial cells (and other retinal cells)<sup>75</sup>, which further exacerbate vessel loss similar to what is seen in ROP patients<sup>34</sup>. Excess ROS in the retina also augments endothelial cell death via indirect signaling pathways; for instance, oxidative stress can lead to the formation of peroxynitrite (ONOO<sup>-</sup>), which cause micro-vascular complications via inhibition of matrix metalloprotease-7 (MMP-7) activity<sup>81</sup>. MMP-7 is required for proteolytic processing of the precursor form of nerve growth factor (ProNGF) to its mature form and inhibition of MMP-7 leads to increased pro-apoptotic activity of ProNGF through neurotrophin receptor P75 (P75NTR)<sup>81</sup> on endothelial cells, which has shown to increase fluid extravasation in murine retinae<sup>82</sup> (as seen in DR patients).

Studies highlighting the mechanistic effect of hyperglycemia on retinal neurons and glia cells, however, remain limited.

## Chronic inflammation

Current research attributes inflammation as having a causal role in DR. There are studies pointing to a significant contribution of inflammatory molecules and cells having a direct contribution to the pathogenesis of DR. Inflammatory cytokines and chemokines have been detected in the vitreous of patients with DR (non-proliferative or proliferative), the most prominent being TNF- $\alpha$ , IL-1 $\beta$ , IL-6, IL-8 and monocyte chemoattractant protein-1 (MCP-1 or CCL2)<sup>4,83</sup>. These inflammatory molecules can have direct toxic effects on retinal endothelium (such as TNF- $\alpha$ <sup>40</sup>) but typically exacerbate vessel degradation via increased adhesion of circulating leukocytes (via elevated ICAM-1 expression)<sup>64,65</sup> and activation of resident microglia<sup>84</sup>. Moreover, during the vasoproliferative phase, inflammatory cytokines/chemokines can contribute to pathological angiogenesis via stromal-cell derived factor-1 (SDF-1/CXCL12), which stimulate migration and proliferation of endothelial cell progenitors (ECPs) into the retina<sup>85</sup>, or via upregulation of important vascular growth factors such as VEGF<sup>86</sup>.

In diabetes, there is an increase in circulating lipids resulting in a modification of the lipid profile in the retina<sup>87</sup>, which can cause elevated eicosanoid production in diabetic retinae. Arachidonic acid (AA), produced from lipid membranes by PLA<sub>2</sub>, is quickly metabolized into prostaglandins and leukotrienes via cyclooxygenases (COX) and lipoxygenases (LOX), respectively, which contribute to the pathogenesis of DR. For instance, increased COX-2 levels have been found in epiretinal membranes (fibrotic lesions between vitreous and retina)<sup>88</sup> of DR patients and has shown to be implicated in pericyte death and capillary dropout in diabetic animals<sup>89</sup>. Correspondingly, inhibition of COX-2 (but not COX-1) impedes diabetes-induced microvascular degeneration in these animals<sup>90</sup>. Other studies report increased leukotrienes (and leukotriene derivatives) in the vitreous of DR patients<sup>91</sup> and selective deletion of 5-LOX resulted in reduced microvascular degeneration in diabetic mice retina<sup>89</sup> highlighting the relative importance of leukotrienes in the DR.

Eicosanoids can also exacerbate vascular permeability via increase in inflammatory molecules, such as VEGF and NF- $\kappa$ B<sup>89</sup>.

### Pathological angiogenesis

The formation of pathological neovessels in the retina is major contributing cause of vision loss in DR. Pathological angiogenesis typically occurs around the optic disk and at the edge of non-perfused retinal tissue<sup>3</sup>. The exponential increase in VEGF, resulting from tissue hypoxia, has been revealed as the principal cause for the increase in pathological vessel formation in the retina and subsequent hemorrhaging into the vitreous<sup>92</sup>. Notwithstanding, other growth factors have shown to be involved in stimulating angiogenesis (e.g. Epo<sup>74</sup>), which may account for the reported non-responsiveness of some patients to diagnosed anti-VEGF treatment<sup>3</sup>. Potential targets are now being revealed as having a significant impact on aberrant vessel formation and inhibition thereof results in decreased pathological angiogenesis in various models of vaso-proliferative retinopathies<sup>93</sup>.

The apparent vascular response to tissue hypoxia originates principally from proximal neurons<sup>16</sup> and glia<sup>94</sup>. Studies are now beginning to underline the importance of these cells in releasing growth factors, or other factors, that potentiate pathological angiogenesis in the retina<sup>4</sup>. However, the observed pathological angiogenesis that protrudes into the vitreous in DR (and ROP) patients remains a puzzling phenomenon; that is, production of growth factors from the neuro-retina should maintain neovessels on the surface of the superficial plexus. Thus, it appears other forces are involved in misguiding these neovessels toward the vitreous. To understand this phenomenon, we must understand the functional aspects of vascular biology.

## 4. Vascular biology in Ischemic Retinopathies

Understanding the underlying mechanisms of vessel formation is important in developing novel treatments to combat sight-threatening IRs. This section covers the important processes involved in vessel formation highlighting key players that govern this phenomenon. Moreover, this section sheds light on the steps involved in vascularization of the retina, which becomes vital for in understanding ROP in preterm born infants. Finally, the last sections cover the importance in neuron and vessel cross talk—more aptly known as neurovascular coupling—involved in angiogenesis as well the vaso-modulatory effects of inflammatory molecules and cells in the retina (and the CNS).

### 4.1. Angiogenesis, Vasculogenesis and Arteriogenesis

The necessity for oxygen and nutrients from metabolically active tissue stimulates production of new blood vessels. Formation of neovessels occurs via two major pathways; namely, vasculogenesis and angiogenesis. Arteriogenesis is an also important process in higher animals that own complex circulatory systems. Understanding of the processes of vessel formation is crucial in determining potential targets involved in vessel degradation and pathological neovascularization in ischemic retinal diseases such as ROP and DR.

#### 4.1.1. Vasculogenesis

Vasculogenesis is the formation of vessels *de novo* via mesoderm-derived progenitor cells that migrate to non-perfuse tissues. Mesoderm-derived progenitor cells are pluripotent stem cells that can produce both hematopoietic stem cells, which give rise to all blood cell lineages, and angioblasts, that can differentiate into endothelial cells (EC)<sup>95</sup>. ECs are specialized and dynamic cells that line the inner wall of blood vessel; they maintain the integrity of vessels and respond to environmental changes. Aggregation of differentiated angioblasts, or ECs, leads to the formation of

tube-like structures (vessel cords)<sup>95</sup> that eventually disperse into an array of arteries, veins and capillaries.

Once formed, primary vessel cords have the capacity to form both arteries and veins. The exact fate of arterio-venous formation depends on the genetic signature of the ECs lining the vessel cord<sup>95,96</sup>. Notch signaling, which depends almost exclusively on cell-to-cell contact<sup>97</sup>, is one of the major contributors to arterial fate and its cell surface receptors, Notch1, and Notch4, and ligands, Jagged (Jag)1, Jag2 and delta-like ligand 4 (Dll4), are highly expressed in arteries via arterial-specific transcription factors, FOXC1 and FOXC2. In veins, however, Notch proteins are systematically suppressed via the vein nuclear receptor, COUP-TFII<sup>95</sup>. Mutations or deletion of *notch* genes give rise to arterial defects in mice that often die during embryonic stages. Notch signaling also regulates ephrin-Eph family of cell surface proteins that are important for arterio-venous formation<sup>95</sup>. Expression of ligand ephrinB2 is found exclusively in arteries while the EphB4 receptor is found singularly in veins and alteration of gene function of ephrinB2-EphB4 causes irregularities in arterial-vein remodeling.

The environment surrounding newly formed vessels cords can also promote arterio-venous formation. Typically, molecules are secreted from surrounding cells that help influence the differentiation process<sup>95</sup>. One class of secreted morphogens, namely, Hedgehog (Hh) proteins—sonic hedgehog (shh) and Indian hedgehog (ihh)—, have been shown to be involved in arterio-venous formation through patched (ptc) 1 receptor via downstream regulation of Notch ligands and receptors<sup>95</sup>. This phenomenon appears to be piloted indirectly via induction of VEGF-A, which stimulate Notch proteins via VEGFR and Neuropilin (Nrp) signaling<sup>98</sup>. Deletion of shh, ihh or downstream transcriptional factor, Smoothed, cause arterio-venous abnormalities and death in both zebrafish and mice embryos<sup>95</sup>. Embryonic deletions of VEGF-A or its cognate receptors, however, cause a more profound effect resulting in gross abnormalities in vasculogenesis, hematopoiesis and overall vascularization and causes embryonic lethality. On the other hand, increased expression of shh or VEGF-

A results in exacerbated arterial development<sup>95</sup> indicating that an appropriate balance of these genetic factors is required for proper arterio-venous formation and later development of a function circulatory system.

Blood flow and pressure also contributes to arterio-venous differentiation<sup>99</sup> although the underlying molecular processes involved in the fate of arterial or venous from primary vessel cords remains largely unknown. Once an established arrangement of arteries and veins form, expansion of subsequent vascular network proceeds mostly by angiogenesis.

#### 4.1.2. Angiogenesis

Angiogenesis is described as the formation of new vessels from pre-existing ones. There are two types of angiogenesis that exist: sprouting angiogenesis, spearheaded by specialized endothelial tip cells, and intussusception angiogenesis, which is defined as the splitting of vessels via insertion of tissue columns<sup>100</sup>. The exact mechanisms guiding intussusception, however, remain ill defined; as such this section will focus exclusively on sprouting angiogenesis.

Before sprouting can occur, vessels must liberate the mural cell encasing and degrade the basement membrane (BM) that lies between the mural cells and ECs. Growth factors (e.g. VEGF), mechanical stress and other cytokines can initiate this process by inducing expression of matrix metalloproteinases (MMPs) proximally<sup>101</sup>, which degrade the BM<sup>102</sup>. MMPs also breakdown the extracellular matrix (ECM) surrounding the vessels, which release additional growth factors that stimulate angiogenesis<sup>101</sup>. Endothelial-derived Angiopoietin2 (Ang2) release allows for rapid detachment of mural cells from ECs. This allows ECs to respond directly to growth factors and allow selection of specialized ECs, called tip cells, which lead the angiogenic growth front.

Notch signaling in ECs precipitates selection of tip cells versus stalk cells. Notch1 receptor is highly expressed in stalk cells compared to tip cells; tips cells express high levels of notch ligand Dll4, which upon binding to Notch1 inhibit tip cell

phenotype on adjacent stalk cells<sup>103</sup>. In contrast, stalk cells upregulate Jag1 that antagonizes Notch signaling (through Fringe glycosyltransferases) potentiating tip cell phenotype on the adjacent tip cells<sup>104</sup>. Loss-of-function studies demonstrate that inhibition of Dll4 leads to excessive tip cell formation while suppression of Jag1 results in blunted vascular front with few tip cells selection<sup>103</sup>. VEGF-A commences the process of tip cell formation by binding to Nrp1, VEGFR2 and VEGFR3 and rapidly upregulating Dll4 in ECs. Dll4-to-Notch1 signaling on adjacent cells increases VEGFR1 (stalk-specific) and downregulates Nrp1, VEGFR2 and VEGFR3 (tip cell specific) potentiating stalk cell phenotype in those adjacent cells<sup>68</sup>. A fine-tuned transcriptional control mechanism involving TEL/CtBP repressor complex at the *Dll4* promoter allows ECs to regulate tip cell/stalk cell ratios at the growing front. Essentially, tip cells help probe the environment migrating in response to external guidance cues.

Proximal cells (neurons, glia, etc.) secrete guidance molecules in efforts to chaperon the growing vascular front in a concerted manner towards non-perfuse areas. VEGF is a major chemoattractant cytokine that binds to VEGFR2 on tip cells activating Cdc42<sup>105</sup>, which coordinates filopodia formation. These cellular extensions, or arms, sense the environment ahead of the growing front. CXCR4 is also found on tip cells allowing it to respond chemotactically to secreted SDF-1/CXCL12. Conversely, repulsive cues also steer tip cells to avoid vascularization of unwanted areas. Netrins (1,2 & 4) family of secreted proteins can induce tip cell repulsion via its receptor, Unc5B<sup>106</sup>. Netrins can also bind to other receptors (DCC, neogenin) resulting in attraction<sup>107</sup>; however, this appears to depend on the differential expression of netrin receptors on tip cells. Roundabouts (Robos) receptors are known for their axon repulsive abilities via binding of Slit ligands and EC-specific Robo4 apparently induces vaso-repulsion; however, there is controversy on whether Slit ligands mediate this effect<sup>106</sup>. Semaphorins are a large family of secreted or membrane-bound ligands that bind to receptor complexes Nrp/plexin or plexin alone<sup>106</sup>. Class 3 secreted semaphorins, Sema3E and Sema3F, which bind to

PlexinD1<sup>108</sup> and Nrp2/PlexinA1<sup>109</sup> complexes, respectively, have been shown to be involved in vessel repulsion<sup>108,110</sup>. The relative contribution of membrane-bound semaphorins in vessel guidance, however, remains to be defined. Ephrin-Eph ligand-receptor signaling differs in their repulsive abilities as they are exclusively membrane-bound proteins<sup>111</sup>; however, ephrinB2-EphB4 signaling is also important for controlling tip cell behaviour as ECs lacking ephrinB2 have impaired sprouting<sup>112-115</sup>. Typically vaso-repulsive signals appear to mediate their effect via filopodia/lamellipodia retraction (Netrin1) and cytoskeleton collapse (Sema3F)<sup>109</sup> but can also affect tip cell guidance by modulating VEGFR2 activity (Sema3E, ephrinB2, ROBO4)<sup>108,114-117</sup>. Guidance cues become particularly important in vascular-based diseases where an imbalance in vaso-attractive and -repulsive cues can lead to uncoordinated vessel growth (see *section 4.3*).

Stalk cells that grow behind tip cells have an equally important role during angiogenesis by stabilizing vessels and forming lumen<sup>68</sup>. VEGF-A binding to VEGFR1 on stalk cells induces elongation and proliferation thus allowing the vascular front to advance<sup>118</sup>. Notch signaling helps stabilize stalk cells by laying down a BM and increasing EC adhesion<sup>103</sup>. Endothelial stalk cells subsequently adjust their shape via Rho kinase (ROCK) and Ras-interacting protein 1 (RASIP1) and establish a defined apical-basal polarity; this process allows adjacent ECs to form tube-like shapes using negatively charged glycoproteins on the apical cell surface to repel the surface juxtaposed to adjacent EC<sup>119</sup>.

Once properly formed, vessels recruit mural cells to protect and support it. In capillaries, differentiated pericytes line the endothelium while smooth muscle cells (SMCs) cover larger arteries and veins. Mural cell recruitment is initiated by release of transforming growth factor  $\beta$  (TGF- $\beta$ ) and PDGF-B, which induces migration, differentiation and proliferation of mural cells<sup>120,121</sup>. Defective PDGF-B or TGF- $\beta$  signaling can result in improper mural cell coverage of vessels and can lead to vascular deficiencies and hemorrhaging<sup>120</sup>. Recruited mural cells deploy an ECM to reinforce stability of neovessels while production of sphingosine-1-phosphate receptor

(S1PR), Notch3 and Ang1 help improve EC/mural cell interaction<sup>68</sup>. Finally, when vessels mature, ECs become quiescent and maintain their survival by autocrine release of fibroblast growth factor (FGF) and Ang1 that reinforce tight-junction proteins (claudins) and cell-adherence proteins (VE- and N-cadherin) as well as intracrine production of VEGF, which stimulates PI3K/Akt pro-survival molecules<sup>68</sup>.

#### 4.1.3. Arteriogenesis

Smaller vessels have the capacity to form larger vessels via a process known as arteriogenesis. Arteriogenesis, however, is not limited to simply to 'artery' formation as the name suggests; rather, smaller vessel also have the aptitude to form veins and venules as well. Vessels adjust their size and diameter to accommodate increased blood flow<sup>122</sup>. For this reason the largest arteries and veins are found where blood flow is maximal.

The major factor precipitating arteriogenesis is blood flow<sup>122,123</sup>. Increased flow in a vessel causes flow shear stress (FSS), which can activate ECs. The exact receptor or molecular response that occur on ECs as a result of FSS remains to be defined. What is known is that ECs increase cell-surface ICAM-1 and secrete GM-CSF to attract monocytes and leukocytes to the designated areas<sup>122</sup>. Monocytes differentiate into macrophages and along with leukocytes stimulate EC growth via proximal release of VEGF and TNF- $\alpha$ <sup>122</sup>.

Expansion and growth of vessels also requires multiplication of SMCs surrounding the engorging vessel. Macrophage-derived MMPs aid this process by breaking down the ECM, which liberate SMCs and allow them to proliferate and expand<sup>123</sup>. Release of basic FGF and PDGF-B from activated macrophages and ECs, respectively, provides the necessary proliferative potential for SMCs<sup>122,123</sup>. Proliferating SMCs cover the expanding vessel and reform the ECM.

Increased vessel diameter proportionally decreases FSS stunting further vessel expansion. EC return to their quiescent form and SMC redifferentiate into a

contractile phenotype<sup>122</sup>. Under normal circumstances, arteriogenesis rarely occurs in adulthood.

#### 4.2. Formation of the retinal vascular network

Vascularization of the human retina begins at 16<sup>th</sup> week of gestation and occurs by a combination of vasculogenesis and angiogenesis<sup>94</sup>. Vessels form *de novo* by aggregation of haemopoietic progenitor cells (angioblasts) near the optic disc that differentiate into endothelial cells (ECs) forming the primitive structures of the vessel network by vasculo-genesis<sup>124</sup>. Vessel sprouting occurs subsequently via sprouting angiogenesis, whereby new ECs are formed from pre-existing cells<sup>94,124-127</sup>.

Vascularization of the primary retinal surface augments in response to low tissue oxygen levels driving hypoxia inducible factor-1 $\alpha$  (HIF-1 $\alpha$ )-mediated increases in VEGF and Epo<sup>25,26,38,72</sup>. These guidance molecules are secreted from proximal neuroglia<sup>118</sup> as well as closely intertwined astrocytic bed<sup>128</sup> and retinal ganglion cells (RGC)<sup>129</sup> creating an effective gradient<sup>130</sup>, which help guide sprouting vessels towards non-perfused areas until it reaches the peripheral retina. Astrocytes and RGC lay appropriate scaffolding support for the growing vessel front via upregulation of R-cadherin<sup>131</sup> and integrin  $\alpha$ V $\beta$ 8<sup>132</sup>, respectively. Non-hypoxia mediated angiogenic cues, IGF-1 and angiopoietins also increase during retinal vasculature development<sup>27,133</sup>. Sprouting angiogenesis is piloted by tip cells enriched with receptors for VEGF (VEGFR2 and VEGFR3)<sup>118</sup>, Netrins (Unc5B)<sup>107</sup>, EphrinB (EphB2)<sup>114</sup> and semaphorins (Nrp1)<sup>134</sup>. This allows tip cells to sense their environment giving directionality to the advancing vessel front either by attraction or repulsion.

Stalk cells proliferate and form lumen in the wake of tip cells; they receive specific cues from the surrounding environment (VEGF) and the growing vascular front (Dll4)<sup>104,118</sup>.  $\beta$ -catenin and VE-cadherins are tight junction proteins up-regulated in stalk cells increasing cell-cell adherence and stability of proliferating ECs<sup>135</sup>. As the

growing vascular front reaches the periphery the pre-existing vascular bed undergoes leukocyte-mediated pruning and remodeling, thus avoiding over-oxygenation of the tissue<sup>136</sup>.

Once the primary plexus becomes vascularized, formation of the inner retinal vasculature ensues. Tip cells sprouting from the primary plexus dive towards the photo-receptors (outer vascular plexus) guided by resident myeloid cells via non-canonical Wnt5a-Flt1 (VEGFR1) signaling<sup>137</sup>. Vessels migrate using scaffolds provided by cell surface R-cadherin<sup>131</sup> and integrin  $\alpha V\beta 8$  expressed on Müller cells<sup>132</sup> while simultaneous secretion of Wnt proteins from these cells (Norrin, Wnt3a, 7a and 10a) activate canonical Wnt signaling on retinal endothelium via low-density lipoprotein receptor protein 5 (Lrp5) and Frizzled4 allowing migration of ECs into the deeper layers of the retina<sup>138-140</sup>. Upon reaching the photoreceptor layer, vessels turn and begin proliferating towards the peripheral retina, presumably through the vessel repulsive cue, Semaphorin 3F expressed by underlying retinal-pigmented epithelium (RPE)<sup>141</sup>, and via suppressive Wnt5a-Flt1 signaling on retinal myeloid cells<sup>137</sup>. Despite these recent advances, however, the mechanisms guiding vascularization of the intermediate vascular plexus (between superficial and outer vascular plexus) remain largely unknown.

Maturation of vessels is required for stability and maintenance of the final retinal vascular network. This is fulfilled by mural cell (pericytes or SMCs) recruitment via PDGF-B and TGF- $\beta$ <sup>120,121</sup>. Once ECs mature, they remain quiescent maintaining their own stability and homeostasis via autocrine or intracrine release of EC-specific FGF, VEGF and Ang1<sup>68</sup>. Complete vascularization of the retina concludes at term (i.e. 40 weeks)<sup>24</sup>.

### *4.3. Neurovascular coupling in angiogenesis*

The process of innervation and vascularization has been proposed as being anatomically coupled by Vesalius in the 16<sup>th</sup> century<sup>142</sup>. Later in the 19<sup>th</sup> century, use

of the light microscope permitted Ramon y Cajal to illustrate this phenomenon for the first time showing the coupling between neurons, glia and vessels<sup>143</sup>. Only recently, however, are we beginning to unravel the molecular mechanisms involved in the processes of innervation and vascularization, which is profoundly overlapping<sup>106</sup>.

Vessels and neurons share high similarities in their growth projection patterning, particularly in the skin and the CNS where neurons and vessels are in close proximity<sup>106</sup>. Although neurons differ slightly from vessels in that a single neuronal axon can travel large distances before reaching its target, the axonal terminal growth cone and the vascular sprouting tip cell share analogous anatomical structures demonstrating the overlapping similarities between nerves and vessels<sup>106,144</sup>. Nerve cell axons grow in an atypical manner protruding axonal growth cones towards potential innervated targets; these growth cones extend filopodia allowing them to sense their environment guided by varying gradients of growth factors and repulsive cues. In a similar way, tip cells protruding from pre-existing vessels extend their filopodia outward guiding the vascular front towards non-perfuse areas<sup>105,144</sup>. In this fashion, nerves and vessels extend their networks often in parallel.

Nerves and vessels cross communicate to satisfy their physiological needs; whereas neurons require oxygen and nutrients provided by the vascular network, vessels themselves require innervation to control vaso-dilation or constriction. Quite often, vessels and nerves grow in tandem utilizing similar growth paths. Evidence of this effect can be shown at the molecular level whereby neurons can release vascular proliferative factors (such as VEGF-A) in attempts to attract vessels<sup>106</sup>. Conversely, endothelial cells can secrete neuronal growth factors (such as NGF and Neurotrophin 3 [NT-3]) that draw axonal growth cones alongside growing vessels<sup>145</sup>. Many other secreted neuronal molecules have recently been shown to affect vascular patterning and are typically secreted proximally to help guide axonal growth cones and vascular tip cells<sup>106,144</sup>; these molecules are discussed in detail below. Similarly, vascular survival factors have been shown to induce survival pathways in neurons<sup>146</sup> further highlighting the importance of neurovascular coupling in maintaining homeostasis.

#### 4.3.1. Nerve growth factor and neurotrophins

Nerve growth factor (NGF) was one of the first neuronal secreted molecules identified as having post-natal angiogenic properties<sup>147</sup>. Initially, NGF (expressed also by ECs) was found to have pro-survival role in human umbilical cord ECs (HUVECs) and pig aortic ECs *in vitro*, but was later shown to have chemotactic properties on ECs expressing the trophic receptor for NGF, tropomyosin-receptor kinase (trk), which induce endothelial cell migration and proliferation *in vivo* and *in vitro*<sup>145</sup>. Moreover, over-expression of NGF during vascular injury enhances reparative angiogenesis<sup>148</sup> further highlighting the importance of NGF in vascular diseases. Later, other neurotrophins, BDNF, NT-4/5 as well as NT-3, were identified as having pro-angiogenic properties via their cognate trkB and trkC receptors, respectively<sup>145</sup>.

Downstream signaling of NTs (NGF, BDNF, NT-3) on trk receptors signal typically via Akt/PI3K, which in turn activate upregulate VEGF-A expression in ECs mediating their angiogenic actions. VEGF-A can, in turn, activate eNOS propagating EC migration, proliferation and survival<sup>145</sup>. NTs can also stimulate production of MMP-2<sup>145</sup>, which facilitates these processes *in vivo*. Conversely, NT can also signal apoptosis in ECs upon binding to its low-affinity neurotrophin receptors, P75<sup>NTR</sup> and sortilin<sup>149</sup>; this effect is typically observed whereupon pre-cursor neurotrophin isoforms (e.g. pro-NGF, pro-BDNF) accumulate during diseases (such as DR<sup>81,82</sup>), which have a markedly increased affinity for P75<sup>NTR</sup><sup>145,149</sup>. However, there are conflicting studies regarding the atypical expression of endothelial P75<sup>NTR</sup>; that is, its expression depends largely on organ type and disease under investigation<sup>150-152</sup>.

The importance cross-talk between NT and vessels can be demonstrated by gain-of-function or loss-of-function studies. In development, global knock out of BDNF reduces EC cell-cell contacts and increases intraventricular hemorrhaging<sup>153</sup>. Similarly, mice embryonically knocked out for trkB suffer from low blood vessel density and increased number of apoptotic ECs in the subepicardial regions of the heart<sup>154</sup> indicating that BDNF-trkB signaling is responsible for cell survival and stimulating angiogenesis. Moreover, defects in BDNF or trkB result in significantly

reduced CD133<sup>+</sup> endothelial stem cell (ESC) migration, which comprises a portion of the vascular response mediated by BDNF<sup>155</sup>. Embryonic deletion of NT-3 in mice generates abnormalities in larger vessels formation and causes defects in myofibril formation of the truncus arteriosus<sup>156</sup>. Although embryonic deletion of NGF causes severe neuronal defects, genetic modification studies demonstrating the effect of NGF in vascular development remain lacking. In adult pathological angiogenic studies, neutralizing antibody to NGF in a hindlimb ischemia model reduces the overall angiogenic response and subsequent blood flow recovery<sup>148</sup>. Exogenous administration of NGF or BDNF causes the inverse. BDNF has similar effects as NGF whereby both NTs induce VEGF-A-mediated vessel formation and increase blood flow recovery in a hindlimb ischemia model<sup>145</sup>. In the retina, mice exposed to OIR model show increased NGF expression during peak neovascularization<sup>157</sup>. In DR, both NGF and BDNF were found to be significantly increased in the retina of diabetic patients and can stimulate CD133<sup>+</sup> EPCs migration and proliferation both *in vivo*<sup>158</sup> and *in vitro*<sup>159</sup>. The latter study demonstrated that NGF had no direct effect on human retinal EC proliferation and migration<sup>159</sup> indicating that NT-activated EPCs may play a more pivotal role in vasculopathies in the retina.

#### 4.3.2. Netrins and their receptors

Netrins were first identified in the brain midline having chemoattractant abilities whence they bind to their receptor deleted in colorectal cancer (DCC)<sup>160</sup>. This would allow axons from commissural neurons to cross over the midline to reach their appropriate innervation target. Defects in DCC receptor or their ligands cause defects in midline crossing of commissural neurons<sup>161,162</sup>. Netrins can also bind to the Unc5 receptor family (a-d)<sup>144</sup>, which induces repulsion in other neuronal axons<sup>163,164</sup>.

In vessels, Netrin1 has shown to have an effect on vessel guidance inducing vessel repulsion by specifically binding to Unc5b receptor, which is enriched on endothelial tip cells. Treatment of netrin1 induces filopodia retraction on cultured endothelial cells and effectively guides intersegmental vessels (ISV) in zebrafish via

its receptor Unc5b<sup>165</sup>. Loss-of-function experiments in zebrafish show increased filopodia extension and misguidance of sprouting ISV upon inhibition of Unc5b. In mice, homozygous deletion of *unc5b* causes capillary defects increasing filopodia numbers and increasing vessel branching in embryos<sup>165</sup>. Similarly, in the retina injecting Netrin1 causes activation of Unc5b and retraction of endothelial cell filopodia<sup>165</sup>. Thus, Netrins play an important role in regulating normal vessel sprouting by controlling EC sprouting, migration and invasion. Also, Netrin1 and 4 expressions can be induced in EC following exhaustive VEGF stimulation, which can antagonize VEGF-induced cell migration and proliferation (as a negative feedback regulator)<sup>166</sup>. This effectively shows that EC have the capacity to regulate growth and invasion under normal circumstances via Netrin secretion. Interestingly, endothelial Netrin expression can potentially affect proximal neuronal axon projections that grow in parallel in the development; however, this phenomenon has yet to be explored.

In pathological settings, netrin appears to have dual roles. Several studies report inhibition of tumor invasion<sup>167</sup> or reduced neovascularization in animal models of pathological angiogenesis, such as laser-induced choroidal neovascularization (CNV)<sup>166</sup> and matrigel neovessel sprouting<sup>167</sup>, whereby Netrin1 and/or 4 effectively stalls proliferation and migration of ECs. Contrary to this, treatment of plasmids containing Netrin1 and 4 accelerated neovascularization in a hindlimb ischemia model in mice and can reverse neuropathy and vasculopathy in a diabetic mouse model<sup>107</sup>. The exact signaling mechanism, however, by which Netrins induce their differential roles in these pathological models, remains unclear. Reportedly, Netrin receptors have been found on cell types other than neurons and endothelial cells, such as macrophages/monocytes, which may have an indirect effect on angiogenesis<sup>144</sup> and account for the differential effect of Netrins *in vivo*.

#### 4.3.3. Semaphorins, Neuropilin and Plexins

Semaphorins are a large class of membrane-bound or secreted proteins that were initially described as having repulsive effects on neuronal axons in

grasshoppers<sup>168</sup>. The secreted family or Class 3 semaphorins have been extensively studied in both neuronal and vascular patterning; semaphorin3A (Sema3A), initially called Collapsin due its neuronal growth cone collapsing properties, was the first mammalian identified semaphorin<sup>169</sup>. Later on other semaphorins were identified and finally consolidated into a single family based on their homologous structures<sup>170</sup>. There are eight (8) classes of semaphorin, two of which are exclusive to invertebrates (Class 1 and 2), one belonging to virus (Class V) and five (5) mammalian semaphorins (Class 3 to 7)<sup>170</sup>. This section will focus only on mammalian semaphorins (3 through 7).

Semaphorin Classes 4 through 7 signal via direct binding to their Plexin receptors (A-D) while Class 3 semaphorins bind to their Neuropilin (Nrp1 and 2) co-receptor, which then recruit Plexins to signal downstream<sup>171</sup>. Nrps have shortened intracellular regions that cannot signal intracellularly, which is why Plexins and Nrps are typically co-expressed on receptive cells to potentiate secreted Sema3 signaling<sup>171</sup>. Commonly, plexins contain cytosolic GTPases, GTPase activating protein (GAP) activity, GTPase regulators or guanine-nucleotide exchange factors (GEFs) to transduce intracellular signals<sup>172</sup>. These signals frequently activate R-Ras or Rho (small G-proteins) that lead to downstream cytoskeleton rearrangements and repulsive axon guidance<sup>173,174</sup>. For instance, Sema4D binds to PlexB1 and stimulates RhoGEFs, which augments RhoA activity leading to actin-dependent reorganization of the cytoskeleton<sup>175</sup>. Similarly, Sema4D-PlexB1 complex signaling inhibits cell migration and axon outgrowth; this occurs via ErbB2, Rho kinase and 12-15 lipoxygenase, which are involved in cellular morphogenesis and collapse<sup>173</sup>. Conversely, Sema4D in complex with PlexB2 promotes cell migration and axon growth via Met and Ron receptors, Pyk2, Src, Akt and PI3K pathway<sup>176</sup>. Anomalies in semaphorin signaling have been associated with many neurological diseases including Parkinson's, retinal degradation and motor neuron degeneration<sup>177,178</sup>, which make semaphorins substantially important for neural development and have been recent targets for therapeutic venues.

Class 3 semaphorins are the most documented class having a substantial role in modulating angiogenesis. Sema3A competes directly with VEGF-A isoforms for binding to Nrp1 receptor to potentiate endothelial cell repulsion and inhibit angiogenesis<sup>179-181</sup>. When Sema3A binds to Nrp1, this complex can associate with PlexA1<sup>182</sup> to inhibit cell adhesion via downregulation of Integrin- $\alpha$ 5 $\beta$ 1. At higher concentrations, Sema3A can induce caspase-3-mediated EC apoptosis<sup>134,183</sup>. Despite these findings, the exact mechanism by which Sema3A directs tip cell guidance has not been yet been elucidated. Insights into this mechanism can be found in studies on Sema3F, which inactivates RhoA to induce cytoskeleton collapse in human glioma cells upon binding to Nrp2 and PlexA1<sup>109</sup>. Similarly, Sema3B has shown to have anti-angiogenic properties<sup>184</sup>. Sema3E-PlexD1 signaling also controls angiogenesis in a more intricate mechanism by negatively regulating VEGFR2 signaling in tip cells in the developing mouse retina<sup>108</sup>.

Semaphorins have also been linked to cancer, particularly with cell metastasis, angiogenesis, viability and tumorigenesis (review in <sup>185</sup>). Interestingly, studies show that some semaphorins exacerbate tumors while others diminish them. For example, Sema3F binds Nrp2, which inhibits E-cadherin-mediated cell adhesion and repulses breast and lung cancer cells, lowering their tumorigenicity<sup>186,187</sup>. Conversely, Sema3C maintains ovarian carcinoma survival by resisting *cis*-diammine-dichloroplatinum (CDDP)-mediated inhibition of metabolic enzymes (i.e. de-hydrogenases, synthases)<sup>188</sup>.

#### 4.3.4. Slits and Roundabouts

Slits are large secreted proteins that bind to single passage transmembrane receptors, roundabouts (Robo)<sup>189,190</sup>, typically found on axons growth cones to mediate repulsive actions but can stimulate branching and elongation depending on the neurons that they are expressed<sup>106</sup>. In mammals, there are three (3) Slit secreted proteins and four (4) Robo receptors, one of which being EC specific (Robo4)<sup>191</sup>.

While better known for their axon repulsion on commissural neurons crossing the midline<sup>192</sup>, Slits have also been implicated in kidney induction<sup>193</sup>, leukocyte migration<sup>194</sup> and angiogenesis<sup>195</sup>.

Robo4 plays an integral role in vessel formation by maintaining blood vessel integrity and number. In normal vessel development, Robo4 expression appears to be expressed in stalk cells, which inhibits VEGFR2 (directly or indirectly) to prevent sprouting angiogenesis behind the growing vascular front<sup>117</sup>. These results further contribute to the already complex mechanisms involved in regulating VEGF receptors in stalk cells involving Notch signaling pathways<sup>103,104</sup>. Intriguingly, Robo4 knockdown in zebrafish causes a lack of EC sprouting angiogenesis of ISV due to lack of proper tip cell guidance<sup>196</sup>, which differs significantly from the studies performed in mice whereby knockout of Slits2 and 3 or Robo4 causes significant increase in blood vessel density and complexity in breasts<sup>116</sup>. This indicates that although mice and fish share similar ectopic expression of Robo4 in ECs, the evolutionary function differs significantly.

Mammalian Slit-Robo4 signaling also contributes to decreased angiogenesis in various models of pathological vessel formation in the eye. In the retina and choroid, Slit2 can activate Robo4, which inhibit VEGFR2-induced Src and downstream Rac1 activation resulting in decreased pathological angiogenesis and hyper-permeability<sup>117</sup>. Interestingly, Robo1 has been reportedly found in the endothelium; however, there is much conflict in the literature regarding its localization and function in ECs<sup>116,144</sup>. More studies are required to identify the role of Robo1 in blood vessel formation.

#### 4.3.5. Ephrins and Eph receptors

Eph receptors and their Ephrin ligands make up another class of short range signaling molecules with capacities for attraction and repulsion. Ephrins were first identified as repellent axon guidance molecules in the establishment of RGC axonal projections towards the brain<sup>197,198</sup>, but were later found to have roles in axon guidance at the midline, dendritic spine formation, guidance of neuronal cells, and

synaptic plasticity. In mammals, Eph receptors are categorized into two classes, A (EphA1-8) and B (EphB1-4 and EphB6), although they share structural similarity belonging to a larger family of Receptor Tyrosine Kinases (RTKs), which are single passage transmembrane receptors<sup>199</sup>. Ephrin ligand classed into A and B nomenclature as well but are distinct from each other based structural properties; EphrinA are anchored to the membrane via a glycosyl-phosphatidyl-inositol modification while EphrinB ligands contain transmembrane passages and cytoplasmic regions<sup>199</sup>. Eph A or B receptors typically bind Ephrins ligands of similar class (e.g. EphrinB to EphB), although there has been reports of cross-reactivity<sup>106</sup>. The most intriguing characteristic of Eph and Ephrin family of proteins is their ability to initiate both 'forward signaling' and 'reverse signaling'; that is, upon binding Eph receptors initiate 'forward signaling' process on the receiving cell whereas the initiating cell signals simultaneously to propagate Ephrin-mediated 'reverse signaling'<sup>199</sup>.

Eph receptors and Ephrins have been extensively studied in the vascular system<sup>111</sup>. Much attention has been focused on Class B Ephs and Ephrins, which impart critical roles in various facets of vascular development; namely, vasculogenesis, sprouting angiogenesis and mural cell recruitment<sup>111</sup>. During early vascular development, for instance, EphB4 and ephrinB2—controlled by VEGF and Notch signaling—have important implications in arterial and venous specifications, respectively, and are critical for their maintenance<sup>95</sup>.

The studies demonstrating the role of class B Eph-Ephrins in angiogenesis remain, thus far controversial. For instance, in mice, ephrinB2 help navigate protruding EphB3/EphB4-expressing ISVs through tissue boundaries preventing them from entering the somites supporting the repulsive role of Eph-Ephrins in angiogenesis<sup>114,115</sup>. Knockdown of ephrinB2 or its receptors EphB2 or B3 causes significant impairment in angiogenesis and remodeling of the vascular system<sup>114,115</sup>. Other studies, however, demonstrate that ephrinB2-EphB4 through forward and reverse signaling can stimulate sprouting angiogenesis and EphB4 activation leads to increase EC migration and proliferation through PI3K, Akt and integrin activity<sup>200,201</sup>.

Moreover, ephrinB2 limits angiogenesis via regulation of VEGFR2 expressed on ECs<sup>112,113</sup>. While the role ephrinB-EphB signaling appears to demonstrate causal roles in angiogenesis, further studies are required to clarify their exact role of Eph-Ephrins in this process.

EphrinB2 also precipitates proper formation of mural cell-EC contact<sup>111</sup>; this occurs presumably through EphB binding on EC, although evidence alluding to this effect is lacking in the literature. Mural cell specific deletion of ephrinB2 results in poor mural cell adhesion and they fail to envelop endothelial monolayers<sup>202</sup>. Global deletion of ephrinB2 in mice results in perinatal lethality, edema and skin hemorrhaging<sup>202</sup>. EphrinA1-EphA4 also play a fundamental role in vSMC as well by controlling contractility, vascular tone and blood pressure via RhoA and Rac1<sup>203,204</sup>. Aside from its role in mural cell recruitment, EphrinA1 in cancer has been recently highlighted whereby ephrinA1 expressed on tumor cells help guide EphA2-expressing vessels towards the tumor and stimulate angiogenesis<sup>205</sup>.

The evidence supporting neurovascular coupling is substantial. Of course, several neuronal guidance cues appear to have controversial roles (Robo4, ephrinB2-EphB4); notwithstanding, their functional role in vessel formation remains substantiated. In this section we have covered the implicit role neuronal-derived proteins in modulating various facets of vascular biology, the coupling between neurons and vessels is unquestionably bidirectional<sup>106</sup>. In this regard, modulating factors through exogenous supplementation or inhibition of certain neurovascular cues can and most likely will affect both systems. This may be of particular importance in the advent of developing treatments for treating vascular- or neuronal-based diseases, such as in IRs.

#### 4.4 Inflammation and angiogenesis

The concept of inflammatory molecules and cells modulating angiogenesis is well established in the literature. Under normal conditions, acute inflammation can incite reparative angiogenesis; on the other hand, chronic inflammation results in significant perturbations in vascular homeostasis<sup>206</sup>. The contribution of inflammation in IRs, is highly pertinent; in DR, chronic inflammation is presumed to have a significant impact in the onset and progression of disease<sup>89</sup>, whereas in ROP, both hyperoxic and ischemic insults propagate inflammation as an innate response to the insult<sup>207</sup>. As such, targeting or suppressing key factors in inflammation in efforts to abate vasculopathies are now being employed in the treatment of IRs (see *section 5* below). Since immune response is associated with various pathological conditions, this section focuses specifically on the relative contributions of key inflammatory molecules and cells having potent vaso-modulatory effects in IRs.

##### 4.4.1. Cytokines and chemokines

Cytokines and chemokines are large classes of small molecules that impart a variety of different cellular functions. Pertinently, cytokines/chemokines have the ability to modulate angiogenesis via direct interaction with ECs or indirectly via inflammatory cell activation (see below). The most important of these being VEGF; first identified as a vascular permeability factor<sup>66</sup>, it was discovered to exert powerful vaso-proliferative effects upon binding to its receptor on retinal ECs<sup>25,73</sup>. Conversely, VEGF can also exacerbate inflammation by increases ICAM-1 and leukostasis in diabetic patients<sup>208</sup>. Another implicated cytokine is TNF- $\alpha$  that is commonly found in the vitreous of patients with IRs and corresponding animal models<sup>63,209</sup>. Animals lacking TNF- $\alpha$  are protected from OIR and inhibition of TNF- $\alpha$  using recombinant antibodies inhibits leukocyte adhesion, pericyte loss and capillary dropout in murine models of diabetic retinopathy<sup>89</sup>. However, mice devoid of the main TNF- $\alpha$  receptor, TNFR1, display defective neovascular regression and resolution following exposure to OIR<sup>210</sup>, indicating that TNF- $\alpha$  may have a dual role in IRs.

Interleukins (ILs) exert powerful immunological functions and have been shown to have vaso-modulatory effects. The most common of these is the IL-1 family (IL-1 $\beta$  and IL-18). IL-1 $\beta$  binds to its receptor IL-1RI to exert its biological action<sup>211</sup> and inhibition of IL-1RI protects from diabetes-induced capillary dropout in rats<sup>212</sup>, while use of IL-1 receptor antagonist (IL-1Ra) reduces neovascularization in a mouse model laser-induced choroidal neovascularization (CNV)<sup>213</sup>. IL-18 activation, on the other hand, protects mice from OIR-induced retinal NV<sup>214</sup> and laser-induced CNV<sup>215</sup>. IL-6 has also shown to be implicated in angiogenesis<sup>216</sup> and is reportedly elevated in patients with PDR and diabetic macular edema compared to non-diabetic control patients<sup>217</sup>; however, few studies have underlined their exact role in IRs.

Chemokines also contribute to ocular neovascularization. MCP-1 is a powerful chemotactic protein for monocytes (macrophages and microglia) and has been detected at high levels in the vitreous of patients with PDR<sup>83</sup>. Studies suggest that MCP-1 may be involved in angiogenesis by directly by stimulating VEGF in ECs<sup>218</sup> or indirectly by recruiting monocytes into the retina, although the latter has not been confirmed. CXCL8 (or IL-8) is also reportedly elevated in patients with PDR<sup>83</sup> and has shown to be directly involved in angiogenesis<sup>219</sup>. Another important chemokine is Stromal-cell derived factor-1 (SDF-1/CXCL12), which stimulates migration and proliferation of endothelial cell progenitors (ECPs) into the retina<sup>85</sup>, or angiogenesis by directly upregulating VEGF in ECs<sup>86</sup>.

#### 4.4.2. Other relevant molecules

NF $\kappa$ B is a major transcriptional factor commonly associated with inflammation. Its activity is upregulated in various cells in the retina (neurons, glia, ECs) of patients and animals suffering from IRs, and its activity further exacerbates the immune response by stimulating cytokines and other proteins (such as ICAM-1)<sup>83,206</sup>. As mentioned before, increased ICAM-1 expression in DR patients<sup>83</sup> and animal models of IRs<sup>136,220</sup> contribute to endothelial cell loss and BRB breakdown by increasing leukocyte adhesion and activation in diseased retinal vessels<sup>65,136</sup>.

Another class of signaling molecules that bridge the gap between inflammation and angiogenesis are protease-activated receptors, a unique class of G-protein coupled receptor (GPCR) that undergo proteolytic cleavage at their N-terminal to release their tethered ligand, thus activating it<sup>221</sup>. Classically associated with immunological response<sup>222</sup>, PARs (specifically PAR2) were found to generate reparative angiogenesis<sup>223</sup>. In the retina, activated PAR2 via proteolytic cleavage by Tissue Factor (TF) induces developmental and pathological angiogenesis in mice<sup>224,225</sup> and is associated with pathological vessel formation in DR patients<sup>225</sup>. Similarly, injection of the agonist peptide corresponding to the tethered ligand of PAR2 also stimulated angiogenesis in mice retina via TNF- $\alpha$  and sequentially Tie2<sup>133</sup>.

Lipid mediators of inflammation also contribute significantly to angiogenesis and pathogenesis of IRs. This has been thoroughly covered in *Section 3* and reviewed in detail in <sup>34</sup>.

#### 4.4.3. Inflammatory cells

Activated resident microglia and inflammatory cells recruited to the retina (leukocytes and monocytes/macrophages) have the ability to modulate vessel integrity both in development and in IRs. Generally, infiltration of leukocytes and to a lesser extent monocytes (which differentiate into macrophages) and activation of microglia are associated with pathogenesis of ROP and DR. Their respective roles are covered herein.

Resident microglia are typically the immuno-sensory cells of the retina engaging in the innate immune response to stressors, such as EC injury<sup>226</sup>. Initially, microglial precursors migrate into the retina during late embryonic development and early postnatal period<sup>227</sup>. Herein, they differentiate into their mature form performing largely phagocytotic actions and eliminating cellular debris from apoptotic neurons<sup>228</sup>. In retinal diseases, microglia—being the first line of defense in the retina—are majorly likely responsible for the increased inflammation in the retina observed in DR patients<sup>89</sup> and in various models murine of DR and OIR<sup>226</sup>. More specifically, in

diabetic patients, there is an important induction of cytokines produced locally in the retina<sup>229</sup>, which is accompanied by activation of resident microglia<sup>89</sup>, which associate with vascular lesions, pathological vessel formation and areas of hemorrhaging<sup>84</sup>. Non-selective inhibition of microglia by minocycline reduced retinal inflammation in diabetic rodents<sup>209</sup>, indicating that microglia contribute to vasculopathy in IRs. In ROP the exact role of microglia are not well defined although their numbers are known to increase in the retina of mice undergoing OIR<sup>226</sup>.

Leukocyte and monocyte infiltration are also hallmarks of inflammation and has shown to be upregulated in IRs. Increased expression of ICAM-1 in ECs in IRs<sup>83</sup>, coupled with increased expression of MCP-1<sup>83</sup> (likely from microglia<sup>226</sup>), causes increased leukostasis and adhesion of monocytes in the retinal vasculature<sup>89</sup>. Inhibiting ICAM-1 or CD18, another inflammatory cell adhesion protein, results in decreased retinal inflammation and EC degeneration<sup>136,220</sup>. Leukostasis contribute to microvascular damage by increasing cytokines, superoxide or by physically occluding capillaries<sup>89</sup>. Monocytes/macrophages appear to contribute to the latter stages of the disease whereby they associate with neovascular tufts<sup>230</sup>. Inhibiting macrophages using clodronate liposomes decreased neovascularization formation in mice exposed to OIR<sup>231</sup>.

Essentially, these studies highlight the important cross-talk between vessels and immune cells, which engage in bidirectional communication in both development and pathology in the retina, whereby Inflammatory molecules bridge the communication between vasculature and immune cells. In the retina, neurons also cross communicate with immune cells, which has been shown in the CNS<sup>232</sup>. However, to date there have been no studies highlighting a tripartite communication between neurons, vessels and immune cells in IRs. Since the neurovascular unit is quite dynamic and important in both development and pathology, it may be plausible that this cellular interaction contributes to vessel injury.

## 5. Current treatments for Ischemic Retinopathies

Treatment of IRs typically involves ablating pathological neovessel formation in the retina and diminishing vitreous and retinal bleeding. Physical methods still remain a standard for treating IRs (laser photocoagulation); however, with the advent of anti-VEGF treatment in 2006 biochemical products are now being employed in the clinic either alone or in combination with laser treatment. Unfortunately, accessing the neuro-retina has proven difficult due to the blood-retina-barrier; thus, these products are typically injected intravitreally, which often generates other complications (infection or raised intra-ocular pressure, IOP).

### 5.1. Retinopathy of Prematurity (ROP)

Laser photocoagulation is currently the only well-established therapy for treating ROP patients with threshold ROP (between stage 3 and 4)<sup>11</sup>. Typically an argon or diode laser is used for cauterizing pathological blood vessels and simultaneously burns peripheral tissue to reduce successive neovessel formation by damaging neuronal tissue that instigates the ensuing vascular response<sup>233</sup>. Although laser treatment improves visual outcomes and results in fewer side effects, there is significant loss of peripheral retinal function<sup>233</sup>. Furthermore, this treatment modality does not provide reconciliation for decreased central vision function that has been associated with ROP.

Anti-VEGF treatment has been introduced in the clinic for neovascular eye diseases such as age-related macular degeneration and DR (see below) but its use in ROP remains controversial. One study used bevacizumab (antibody targeting VEGF) as monotherapy and reported a reduction in neo-vascularization following intravitreal administration of bevacizumab; however, patients with zone 2 ROP (see *Table 1*) did not appear to benefit from anti-VEGF treatment and visual outcomes were not reported<sup>234</sup>. Another study demonstrated beneficial effects of bevacizumab injections on posterior neovascularization but the sample size was exceedingly low to draw conclusive results<sup>235</sup>. Pertinently, a retrospective review noted severe retinal

complications, including complete retinal detachment (stage 5), in ROP patients receiving bevacizumab monotherapy<sup>236</sup>. It should be highlighted that VEGF is a potent vascular growth factor<sup>118</sup> and crucial during development<sup>237</sup> and anti-VEGF treatment raises concerns on potential systemic complications (presence of anti-VEGF in circulation following intravitreal injection<sup>238</sup>). Moreover, VEGF has recently been shown to be a vital trophic and survival factor for retinal neurons<sup>146</sup> and RPE<sup>239</sup>, thus anti-VEGF therapy may not be an ideal regiment option for treating ROP.

A number of reviews are now highlighting the importance of preventative measures in efforts to improve ROP incidence and progression<sup>2,10,11</sup>. Lowering oxygen saturation levels has been exercised in the clinic with the goal to reduce the severity of ROP; however, conflicting studies report varying outcomes on ROP progression and is often scrutinized for augmenting mortalities<sup>2</sup>. Serum levels of IGF-1, a crucial maternal factor for fetal development, have been shown to inversely correlate with ROP severity<sup>46</sup> and animals studies demonstrate beneficial effects on ROP development by exogenously administrating IGF-1<sup>55</sup>. A recent study showed that use of recombinant human (rh)IGF-1 and rhIGFBP3 augments serum levels of these proteins in preterm infants<sup>56</sup> and clinical trials are now underway using exogenous administration of IGF-1 and IGFBP3 (NCT01096784) in efforts to reduce preterm complications including ROP.

## *5.2. Diabetic retinopathy*

Panretinal and grid laser treatment remains the main prescribed option for treating patients with diagnosed proliferative DR or diabetic macular edema, respectively<sup>3</sup>. Since its implementation in 1978<sup>240</sup>, there has been significant improvement in laser therapy. Use of diode lasers has now effectively replaced conventional green argon lasers<sup>241</sup>, which diminishes perturbations at the photoreceptor-RPE layer previously observed with green lasers<sup>3</sup>. Laser photocoagulation, however, does have its limitations; that is, it is not recommended for persons with predominant macular ischemia, bleeding in or near the fovea and

was found to be ineffective when repeatedly performed on patients with history of laser therapy<sup>3</sup>. In this regard, laser treatment has been superseded by anti-VEGF treatment for diabetic macular edema in some countries; however, panretinal laser treatment remains the only standard treatment for proliferative DR<sup>3,4</sup>.

The introduction of anti-VEGF therapy has facilitated the transition from physical methods to biochemical treatments for DR. While the main objective for anti-VEGF treatment is to reduce vascular leakage—typically recommended for diabetic macular edema<sup>3,4</sup>, there is also a potential benefit for reducing pathological neovascularization precipitated by VEGF<sup>92</sup>. Bevacizumab (Avastin®), a humanized mouse monoclonal antibody to VEGF-A, is an off-label treatment used for patients with diabetic macular edema having high efficiency and low cost<sup>242-244</sup>; however, it has yet to be approved for clinical use. Ranibizumab (Lucentis®), having a higher affinity for VEGF-A and is much smaller in size than bevacizumab, is typically prescribed in the clinic due to its high efficacy in reducing macular edema<sup>3</sup>. Aflibercept (Eyelea®), a fusion protein consisting of the VEGF binding domain of VEGFR 1 and 2 and the immunoglobulin domain (IgG), has a higher affinity for all VEGF-A isoforms and placental growth factor (PlGF) and competes well against the other anti-VEGF molecules due to fewer required injections<sup>245</sup>; this being the major setback for anti-VEGF molecules in that they have to be injected intravitreally, which imparts other complications including eye infection (endophthalmitis) that can significantly worsen vision<sup>3,4</sup>. There is also rising concern about anti-VEGF treatments entering the circulation and causing systemic complications; however, there are no studies that report any adverse systemic complications thus far. Despite its high cost, ranibizumab is the only anti-VEGF treatment approved by the Food and Drug Administration (FDA) and European Medical Association (EMA).

Inflammation plays a significant role in DR. Thus, the use of steroids has been recently employed in efforts to reduce inflammatory-mediated vascular permeability and hence diabetic macular edema. The fluocinolone implant (Iluvien®), which releases fluocinolone acetonide over a period of 36 months, is injected into the

vitreous cavity of patients suffering from diabetic macular edema. Despite the reportedly high occurrence of cataracts, the fluocinolone implants showed high effectiveness in reducing macular edema in DR patients<sup>246</sup>. Previously, Triamcinolone was prescribed for diabetic macular edema but prevalence of cataracts and glaucoma has restricted its use for diabetic macular edema<sup>247</sup>. Dexamethasone is one anti-inflammatory steroid that has been highly effective in treating macular edema in patients suffering from retinal vein occlusion (RVO) whereby a biodegradable drug-delivery implant is injected into the posterior segment of the vitreous cavity<sup>3,248</sup>. The EMA and National Institute for Health and Clinical Excellence (NICE) have approved this long-acting drug delivery system for RVO and clinical trials are underway for use in diabetic macular edema. Pertinently, steroids affect principally inflammatory cytokines, including VEGF, thus highlighting its potential for proliferative DR<sup>3</sup>; however, the use of steroids has consequently not been approved for patients with vaso-proliferative DR. Advantageously, long-acting steroid delivery system reduces the necessity of repeated injections often required with anti-VEGF treatment regimes. Nevertheless, there is the recurrent problem of cataracts and increased ocular pressure (IOP) in patients treated with intravitreal steroids, which often requires surgery.

Management of diabetes is now common practice in the clinic in efforts to delay or prevent the progression and onset of DR. Typically the most proliferative treatment prescribed is insulin injections in attempts to avoid chronically elevated blood sugar levels—which appear to precipitate the early phases of DR—and reduce the onset of DR (clinical trials NCT00360815; DCCT; UKPDS)<sup>249-251</sup>. This is usually coupled with strict glycemic control as well (food intake, for instance)<sup>3</sup>. Other treatments involve targeting the renin-angiotensin system, such as Lisinopril® (clinical trials EUCLID)<sup>252</sup>, an angiotensin converting enzyme (ACE) inhibitor, as well as beta blockers (clinical trials UKPDS)<sup>251,253</sup>, which are used to control blood pressure in patients with type 2 diabetes and have been shown to reduce the risk of incidence of DR. Enalapril®, an ACE inhibitor, in combination with Losartan® (clinical trials RASS;

NCT00143949)<sup>254</sup> and Candesartan® (clinical trials NCT00252720; DIRECT-1)<sup>255</sup>, angiotensin II receptor inhibitors, are used for type 1 diabetic patients to control blood pressure displaying positive effects on risk of progression and incidence of DR, respectively. It should be noted that these treatment regimes are directed for patients with no clinical signs of retinopathy. On the other hand, Fenofibrate®, an activator of peroxisome proliferator activating receptor alpha (PPARα) is prescribed typically to type 2 diabetic patients with mild-to-moderate DR to reduce lipid levels with effective reduction in progression to PDR and macular edema (clinical trials ISRCTN647833481; NCT00542178; FIELD; ACCORD-eye)<sup>256</sup>. Advantageously, these metabolic-targeting treatment regimes help hinder DR progression and onset, which, in some cases, reduces the necessity of intravitreal injections of anti-VEGF and laser therapy<sup>253,257</sup>. While proper diabetes management may prevent the progression and onset of DR there are still some patients that progress into mild or severe forms of DR indicating that are other unknown factors involved in disease onset.

While many treatments aim to curb vascular leakage or neo-vessel formation in IRs, there are no existing regimes that focus on curbing vascular decay or the ensuing hypoxia secondary to vessel loss. Preventative measures attempt to minimize, retard or even prevent vascular degeneration but there are a subset of patients that accede to the onset of retinopathy. Moreover, as summarized above, IRs are multifactorial indicating that monotherapy may not be sufficient to curb vascular anomalies associated with these diseases. Thus, other therapeutic avenues must be introduced—in combination with the current therapies—to combat these sight-threatening illnesses.

## 6. Problem and general hypothesis

Evidence highlighted above demonstrates that the neurovascular unit engages in bidirectional cross-talk between neurons, neuroglia and vessels. While we may have sufficient understanding of these processes in the developing tissue, few studies have demonstrated this phenomenon in pathological settings. Ischemic Retinopathies (IRs) are classified as such due to the systematic vessel loss that precipitates retinal cell ischemia, which can cause significant biochemical changes (inflammation, for instance) or even cell death. During this ischemic phase, lack of nutrients and oxygen prompts a massive vascular response in efforts to reinstate retinal homeostasis; however, instead of vascularizing the appropriate areas, vessels are misguided towards the vitreous. This appears rather counterintuitive in that surrounding hypoxic neurons and glia secrete angiogenic factors (particularly VEGF) that should retain vessel on the retinal surface. Thus, other forces are likely at play. It may be plausible that, in the retina, cells undergoing massive ischemia may secrete signals in efforts to divert metabolic stores away from perishing tissue.

Based on these premises, we hypothesize that, 1) stimulating angiogenic factors while removing endothelial pro-apoptotic molecules from underlying neuronal or glia cells can help curb vessel loss and reduce retinal ischemia and, 2) specifically targeting neuronal-derived secreted molecules involved in vascular repulsion (semaphorins, for instance) can reduce misguidance of nascent vessels toward the vitreous. Essentially, the purpose of these studies is to identify therapeutic avenues that can promptly *revascularize* neuronal tissue to reduce ischemic stress and, consequentially, pathological vessel formation.

## 7. Description of the model: Oxygen-induced retinopathy

The use of animal models has greatly augmented our understanding of pathology. In ischemic retinopathies (IR), the development of the oxygen-induced retinopathy (OIR) mouse model<sup>28</sup> and rat models<sup>29</sup> has led to an exponential increase in the understanding of the pathology. Relevantly, over the last 20 years, the use of the OIR model has translated to over 10,000 peer-reviewed publications (National Centre for Biotechnology Information [NCBI] search using keywords “murine and oxygen induced retinopathy” October 31<sup>st</sup>, 2014) as well as the development of various treatment modalities for both ROP and DR<sup>2,3,93</sup>.

The main premise for using murine OIR models in this context is to reproduce the salient features of ROP (as seen in preterm born babies) in efforts to better understand the neurovascular interactions involved in IRs. Notwithstanding, there are notable differences between human and murine retinopathologies; they are discussed herein. Importantly, the OIR model also reproduces several key features of DR—particularly the second vaso-proliferation phase—, although the cause of vessel loss is vastly different in patients with DR.

### 7.1 Mouse OIR model

The mouse model was originally developed by LE Smith, et al.<sup>28</sup> to reproduce human ROP in a laboratory setting in efforts to better understand the mechanisms involved in disease progression. Pre-term birth stunts retinal vasculature progression and the ensuing hyperoxic environment *ex utero* causes retinal vascular degeneration. Since the development of the vascular superficial plexus in mice begins post-natally (as of day 0)—corresponding to gestational week 16 in infants<sup>94</sup>— mice pups are exposed from post-natal day 7 (P7) to P12 to a high oxygen environment (75% O<sub>2</sub>) resulting in a halt in vascular growth followed by a substantial decay of retinal

vessels<sup>125</sup>. This first phase of obliteration occurs centrally in mice retina while in humans loss of vessels occurs exclusively in the peripheral retina. Once the mice are returned to normal air, revascularization occurs and, as a result of the substantial vessel loss, retinal ischemia sets in (as seen in pre-term infants). Thus, the retina mounts an over-compensated uncontrolled vessel growth that, instead of perfusing the ischemic core, is misguided towards the vitreous. In humans, neovascularization typically occurs at the threshold between the central vascularized and peripheral avascular areas forming a ridge; in mice, neovascular ‘tufting’ occurs in an around the central area. This disparity likely accounts for why retinal detachment is almost never observed in mice. Notwithstanding, the pathomechanisms involved in the vessel loss and neovascularization are similar in mice and humans, despite geographical discrepancies.

There are several advantages in using the mouse model of OIR; firstly, the ability to genetically manipulate mice DNA in order to insert or remove genes has provided enormous insight into the functional roles of certain genes in the pathogenesis of IRs. For this reason, in chapter 3, we utilized the mice model to genetically remove PAR2 gene in efforts to determine its contribution in OIR. Second, the size of the litters (between 5 – 10 pups) provides sufficient animal numbers to attain appropriate statistical differences. Moreover, the gestational period in mice is only three weeks allowing for rapid sample collection. Finally, the reproducibility of the model allows for easily manipulation of experimental conditions (injections, modifications, etc) in efforts to determine their effects on vessel loss and neovessel formation.

## *7.2 Rat OIR model*

The rat model of OIR consists of two types of distinct models described by JS Penn *et al.*<sup>29</sup>. As in mice, the development of the retinal vasculature occurs post-natally. Thus, high oxygen model is used for replicating the first phase of ROP in rats by exposing them from post-natal day 5 (P5) to P10 to 80% oxygen, which causes a

central obliteration of retinal vessels. However, rats exposed to constant high oxygen develop much less pathological neovessel formation<sup>29</sup>; the exact reason why this occurs in rats and not mice is not fully understood. For this reason the cycling oxygen model is used (to measure neovascularization), whereby rat pups are exposed to 10 and 50% oxygen from P1 to P14 in 24 h cycles. Importantly, obliteration of the retinal vessels and subsequent neovascularization occurs almost exclusively in the peripheral retina, which better represents the human pathology as it developed in pre-term infants exposed to high oxygen levels. Thus, this second model of rat OIR offers more suitable insight into the patho-mechanisms involved in neovessel formation while the first constant oxygen rat OIR model is used for determining the effects of high oxygen on retinal vessel loss.

The use of both high oxygen and cycling rat models allows one to easily monitor disease progression of IRs separately; that is, to see how experimental conditions distinctly affect vaso-obliteration and neovascularization. Another advantage of the rat cycling model of OIR is the geographical similarities in the areas of vaso-obliteration and neovascular formation, as seen in human ROP patients, which occur in the peripheral retina. Moreover, in comparison to mice, rat eyes are much larger allowing for easy user handling (enucleating and dissecting retinas, injections, etc). Also, the litter numbers are typically larger than mice (between 10 – 12 pups) allowing for rapid attainment of statistical significance. Finally, as in mice, the reproducibility of the rat high oxygen and cycling models permits easy manipulation of experimental conditions in efforts to determine their effects on vessel loss and neovessel formation.

Although, while some features of the models vary from the actual human pathology, our aim was to reproduce the major findings in both models to better understand the actual patho-mechanisms occurring in patients suffering from IRs; these include: 1) the importance of neurovascular coupling—between neurons, vessels and glia—in vascular-based retinal diseases; 2) the contribution of inflammatory cytokines (more specifically IL-1 $\beta$ ) in exacerbating these retinal pathologies; and 3)

the importance of vascular guidance cues (Sema3A) in perpetuating vascular pathophenotypes as seen in patients with IRs. It should be noted that several of the unprecedented findings unraveled herein using murine OIR models can be (or have been) directly measured in ROP and DR patients (e.g. increased vitreous levels of IL-1 $\beta$ <sup>63</sup> or Sema3A<sup>258,259</sup>, elevated microglial counts<sup>226</sup>, etc.).

## Chapter 1

### Ischemic neurons prevent vascular regeneration of neural tissue by secreting Semaphorin 3A

**Authors:** Jean-Sébastien Joyal<sup>1,2</sup>, **Nicholas Sitaras**<sup>2,3</sup>, François Binet<sup>3</sup>, Jose Carlos Rivera<sup>2</sup>, Andreas Stahl<sup>5</sup>, Karine Zaniolo<sup>2</sup>, Zhuo Shao<sup>1</sup>, Anna Polosa<sup>6</sup>, Tang Zhu<sup>2</sup>, David Hamel<sup>3</sup>, Mikheil Djavari<sup>6</sup>, Dario Kunik<sup>3</sup>, Jean-Claude Honoré<sup>2</sup>, Emilie Picard<sup>2</sup>, Alexandra Zabeida<sup>2</sup>, Daya R Varma<sup>1</sup>, Gilles Hickson<sup>2</sup>, Joseph Mancini<sup>2,3</sup>, Michael Klagsbrun<sup>7</sup>, Santiago Costantino<sup>3</sup>, Christian Beauséjour<sup>2</sup>, Pierre Lachapelle<sup>6</sup>, Lois E.H. Smith<sup>4</sup>, Sylvain Chemtob<sup>1,2,3</sup> and Przemyslaw Sapieha<sup>3,8</sup>

**Institutions:** <sup>1</sup>Department of Pharmacology and Therapeutics, McGill University, Montreal, Québec, Canada; <sup>2</sup>Departments of Pediatrics, Ophthalmology and Pharmacology, CHU Sainte-Justine Research Center, Montreal, Quebec, Canada; <sup>3</sup>Department of Ophthalmology, Maisonneuve-Rosemont Hospital Research Centre, University of Montreal, Montreal, Quebec, Canada; <sup>4</sup>Department of Ophthalmology, Children's Hospital Boston, Harvard Medical School, Boston, Massachusetts, USA; <sup>5</sup>Department of Ophthalmology, University of Freiburg, Germany; <sup>6</sup>Department of Ophthalmology and Neurology-Neurosurgery, McGill University-Montreal Children's Hospital Research Institute, Montreal, Quebec, Canada; <sup>7</sup>Vascular Biology Program, Children's Hospital Boston, Harvard Medical School, Boston, Massachusetts, USA and the <sup>8</sup>Department of Neurology-Neurosurgery, McGill University, Montreal, Quebec, Canada.

#### *Abstract*

The failure of blood vessels to revascularize ischemic neural tissue represents a significant challenge for vascular biology. Examples include proliferative retinopathies (PRs) such as retinopathy of prematurity and proliferative diabetic retinopathy, which are the leading causes of blindness in children and working age adults. PRs are characterized by initial microvascular degeneration, followed by a compensatory albeit pathological hyper-vascularization mounted by the hypoxic retina attempting to reinstate metabolic equilibrium. Paradoxically, this secondary revascularization fails to grow into the most ischemic regions of the retina. Instead, the new vessels are misdirected towards the vitreous, suggesting that vaso-repulsive forces operate in the

avascular hypoxic retina. Here we demonstrate that the neuronal guidance cue Semaphorin3A (Sema3A) is secreted by hypoxic neurons in the avascular retina in response to the pro-inflammatory cytokine Interleukin-1 $\beta$ . Sema3A contributes to vascular decay and later forms a chemical barrier that repels neo-vessels towards the vitreous. Conversely, silencing Sema3A expression enhances normal vascular regeneration within the ischemic retina, thereby diminishing aberrant neovascularization and preserving neuro-retinal function. Overcoming the chemical barrier (Sema3A) released by ischemic neurons accelerates the vascular regeneration of neural tissues, which restores metabolic supply and improves retinal function; findings may be applicable to other neurovascular ischemic conditions such as stroke.

Submitted October 4, 2010.

J.S.J. and N.S. contributed equally to this study.

The online version of the article contains a data supplement.

### *Introduction*

Proliferative retinopathies (PRs) are traditionally perceived as disorders limited to the microvasculature, given the characteristic profuse and deregulated growth of retinal vessels<sup>1</sup>. The mechanisms by which neo-vessels grow towards the vitreous and fail to revascularize ischemic zones are thought to result from high concentrations of pro-angiogenic factors, such as vascular endothelial growth factor (VEGF), in the vitreous of patients. However, if such an explanation was sufficient, retinal glial cells (astrocytes and Muller cells)<sup>2</sup> and neurons<sup>3</sup> that produce vast amounts of growth factors under hypoxic conditions should retain vessels on the retinal surface and ensure revascularisation of the retina proper. It is therefore compelling to hypothesize the presence of a vaso-repulsive force originating from the significantly hypoxic avascular retina, which repel neo-vessels away from the vasoobliterated retina and

grow towards the vitreous.

Neurovascular crosstalk shapes vascular development but has received limited attention in a pathologic setting. In PRs, evidence points to an early decline in the function of ischemic regions of the neural retina as noted by multifocal electroretinogram (mfERG)<sup>4,5</sup>. Throughout the vaso-obliterative phase of retinopathy, the local retinal environment is hostile to both vasculature and neurons<sup>6</sup>. Following blood vessel degeneration, neurons are metabolically starved and undergo a number of adaptive cellular changes to counter the ischemic state of the tissue<sup>3,6</sup>. If adequate vascular supply is not reinstated in time to salvage deprived neurons, it is conceivable that these severely hypoxic cells mount a repulsive front in an attempt to shunt metabolic resources away from the perishing ischemic tissue toward less affected regions of the retina. In the process, excessive production of VEGF<sup>7</sup> induces exaggerated neovascularization at the periphery of the ischemic and repulsive zones, into the pre-retinal region (normally devoid of vasculature), since re-establishing a vascular network to neurons that are unsalvageable would be wasteful.

Attractive candidates that may mediate misguided growth of neovessels away from the ischemic retina include classic neuronal guidance cues given their established role in influencing endothelial cell (EC) behaviour<sup>8</sup>. During embryonic development, nerves and blood vessels establish architecturally optimized networks to ensure adequate transmission of sensory information and tissue perfusion. Of particular interest are the class III Semaphorins such as Sema3A. Sema3A binds to Neuropilin-1 (Nrp-1) to elicit (neuronal) cytoskeletal collapse<sup>9,10</sup>. In addition, VEGF165 also binds to Nrp-1 to promote its angiogenic effects<sup>10-12</sup>. These opposing actions of Sema3A and VEGF, whereby Sema3A directly provokes EC apoptosis and inhibits VEGF-dependent chemotaxis, may be important contributors to the vascular phenotypes observed in PRs.

Using an oxygen-induced model of PRs (OIR)<sup>13,14</sup>, we demonstrate that the inflammatory environment present in the ischemic neural retina, notably involving Interleukin-1 $\beta$  (IL-1 $\beta$ ), induces robust production of Sema3A specifically in retinal

ganglion neurons. Sema3A was found to contribute to vascular decay and curtail revascularization of the ischemic zones, resulting in misguided intravitreal vascular growth in ischemic retinopathies. Our findings reach beyond previously reported anti-angiogenic properties of Sema3A as we provide evidence for a counterintuitive uncoupling of neuronal metabolism and vascular supply. We show that in response to hypoxia, neurons secrete a chemical barrier (Sema3A) to repulse new vessels and in turn prevent revascularization of hypoxic retinal tissue; conversely, we demonstrate that rapid enhancement of retinal revascularization during early ischemic stages effectively prevents aberrant pre-retinal neovascularization.

### *Methods*

**Animals.** All studies adhered to the Association for Research in Vision and Ophthalmology (ARVO) Statement for the Use of Animals in Ophthalmic and Vision Research and were approved by the Animal Care Committee of the University of Montreal in accordance with the guidelines established by the Canadian Council on Animal Care. C57 Bl/6 wild-type, GFP-mice (C57BL/6-Tg(UBC GFP) 30Scha/J stock number 004353) and RGC-YFP-mice (B6.Cg-Tg (Thy1-YFPH) 2Jrs/J stock number 003782) were purchased from Jackson Laboratories.

**O<sub>2</sub>-induced retinopathy.** This model serves as a proxy to human ocular neovascular diseases such as ROP and diabetic retinopathy characterized by a late phase of destructive pathological angiogenesis<sup>1,15</sup>. Mice were exposed to 75% oxygen from P7 to P12. Upon return to room air, hypoxia-driven neovascularization (NV) develops from P14 onwards<sup>16,13</sup>. Intravitreal injections were performed as described below. Twice daily intraperitoneal injections of IL-1R antagonist (Kineret; 20 mg/Kg) were administered from P10 for 4 days. The eyes were collected at documented time points. Retinal vasoobliteration was evaluated at P12, P14 and P17, while NV was evaluated at the disease peak (P17) as described previously<sup>52</sup>. Briefly, mice were given a lethal dose of Avertin (Sigma-Aldrich) and eyes were enucleated and fixed in

4% paraformaldehyde for 1h at room temperature. Retinas were dissected and stained overnight at room temperature with fluoresceinated Isolectin B4 (Alexa Fluor 594 – I21413, Molecular Probes) in 1 mM CaCl<sub>2</sub> in PBS. Lectin-stained retinas were whole-mounted onto Superfrost/Plus microscope slides (Fisher Scientific) with the photoreceptor side down and imbedded in SlowFade Antifade reagent (Invitrogen). For quantification of retinal neovascularization (NV) 20 images of each whole mounted retinas were obtained at  $\times 5$  magnification on by fluorescence microscopy (Nikon Eclipse E800). Vaso-obiterated areas were assessed as the retinal area devoid of vasculature over total retinal retina. Neovascularization was analysed using the SWIFT\_NV method<sup>17</sup>. All mice of less than 5.5g at p17 were excluded from the study eliminating all runty animals<sup>18</sup>.

**Reverse transcription and quantitative real-time PCR analysis.** Eyes were rapidly enucleated and whole retinas (or laser-captured retinal layers or vessels) processed for RNA using TRizol (Invitrogen), followed by treatment with DNase I (QIAGEN) to remove any contaminating genomic DNA. The DNase-treated RNA was then converted into cDNA using M-MLV reverse transcriptase (Invitrogen). PCR primers targeting mouse and rat VEGFA, Sema3A, Sema3E, Sema3F, Neuropilin-1, IL-1 $\beta$ , IL-6, TNF $\alpha$  and the control genes cyclophilin A and 18S were designed using Primer Bank and NCBI Primer Blast software. Quantitative analysis of gene expression was generated using an ABI Prism 7700 Sequence Detection System and the SYBR Green Master mix kit (BioRad) and gene expression was calculated relative to cyclophilin A or 18S universal primer pair (Ambion) expression using the  $\Delta\Delta C_T$  method.

**Western Blot.** Retinal samples were obtained as described above. Samples were centrifugated and 50  $\mu$ g of pooled retinal lysate from a minimum of three different animals was loaded on an SDS-PAGE gel and electroblotted onto a PVDF membrane. After blocking, the membranes were incubated overnight with 1:200 rabbit antibody to mouse VEGFA (sc-152 ; SantaCruz Biotechnology), 1:1000 rabbit antibody to mouse

Sema3A (ab23393; Abcam), 1:1500 rabbit antibody to mouse IL-1RI (sc-689; Santa Cruz Biotechnology), 1:200 goat antibody to rat IL-1 $\beta$  (MAB501; R&D) and 1:1000 mouse antibody to mouse  $\beta$ -actin (sc-47778; Santa Cruz Biotechnology). After washing, membranes were incubated with 1:5,000 horseradish peroxidase-conjugated anti-rabbit, anti-goat or anti-mouse secondary antibodies (Amersham) for one hour at room temperature. Bands were assessed using densitometry plugins in Image Pro 4.5 (Media Cybernetics).

**Laser capture microdissection.** Eyes with oxygen-induced retinopathy (OIR) or normoxic controls were enucleated at P14 or P17 and embedded in OCT compound. The eyes were sectioned at 12  $\mu$ m in a cryostat, mounted on RNase-free polyethylene naphthalate glass slides (11505189, Leica), and immediately stored at -80°C. Slides containing frozen sections were fixed in 50% ethanol for 15 seconds, followed by 30 seconds in 75% ethanol, before being washed with DEPC-treated water for 15 seconds. Sections were stained with Haematoxylin/Eosin or fluoresceinated Isolectin B4 (Alexa Fluor 594 –I21413, Molecular Probes, 1:50 dilution in 1mM CaCl<sub>2</sub> in PBS) and treated with RNase inhibitor (03 335 399 001, Roche) at 25°C for three minutes. Layers or neovessels were laser-microdissected with the Leica LMD 6000 system (Leica Microsystems) and collected directly into lysis buffer from RNeasy Micro kit (Qiagen, Chatsworth, CA).

**Immunohistochemistry.** For immunohistochemistry, eyes were enucleated from mice and fixed in 4%paraformaldehyde at room temperature for 4h incubated in 30% sucrose overnight and then frozen in OCT compound. Sagittal cross-sections were permeabilized overnight at 4 °C and incubated with rabbit IL-1RI (sc-689; Santacruz Biotechnology) or rabbit Sema3A (ab23393; Abcam) and mouse Thy1.1 (Millipore), followed by fluoresceinated secondary antibodies (goat anti-mouse IgG Alexa Fluor 594 and goat anti-rabbit IgG Alexa Fluor 488 and 594; Invitrogen) for localization studies according to manufacturers' recommendations. Flatmount retinas were

stained with 0.1% Triton X-100 (T-8787, Sigma) in PBS, and stained with fluoresceinated Isolectin B4 (Alexa Fluor 594 – I21413, Molecular Probes) in 1 mM CaCl<sub>2</sub> in PBS for retinal vasculature. Antibodies to rabbit Nrp-1 (sc-5541; Santa Cruz Biotechnology) were applied overnight and secondary Abs as above. Samples were visualized using 40x objectives by fluorescence microscopy (Nikon Eclipse E800).

**Lentivirus production.** Lentiviral vectors (HIV-1-derived) were prepared by transfecting HEK293T cells with a vector plasmid containing the small hairpin RNA against Sema3A or Green Fluorescent Protein together with the third generation packaging plasmids; pV-SVG, pMDL and pREV (Open Biosystems). Approximately 10<sup>7</sup> cells were seeded and transfected with the above plasmids in DMEM complete media (Invitrogen) and incubated for 30h. Subsequently, supernatant was replaced with fresh complete DMEM media and incubated for an additional 30h. Secreted virus was collected and ultracentrifuged at 50,000g, resuspended in PBS, aliquoted and stored at -80°C.

**Intravitreal injections.** Postnatal day 2 or day 14 C57BL/6 pups were anesthetized with 3.0% isoflurane and injected intravitreally with 0.5µl of lentivirus (see below) or recombinant Sema3A (rSema3A, 100ng/µl) respectively, using a 10 µl Hamilton syringe fitted with a 50 gauge glass capillary tip. Approximately 254 ± 11.0 ng/µl of lentivirus shGFP and 323.3 ± 15.3 ng/µl containing shSema3A was injected (virus titers were assessed by p24 ELISA kit; ZeptoMetrix).

**ERG Recordings and analysis.** Adult (50 days old) mice subjected to OIR and receiving Lv.shSema3A in the left eye and Lv.shGFP in the contra-lateral right eye were used in this study and compared to room air raised controls. Mice were housed in the animal care facilities under a cyclic light environment (12h light at 80 lux / 12h dark). ERG recordings were obtained as previously described<sup>19</sup>. Briefly, prior to the recordings, the animals were dark adapted for a period of 12 hours and

anaesthetized. Drops of 1% cyclopentolate hydrochloride (Alcon, Texas, USA) were used to dilate the pupils. The animals were then placed in a chamber with a photostimulator (model PS22, Grass Instruments, Quincy, MA) and a rod desensitizing background of 30 cd.sec/m<sup>2</sup>. The active DTL fibre electrode (27/7 X-Static Silver coated conductive nylon yarn, Sauquoit Industries, Scranton, PA, USA) was placed on the cornea, a reference electrode was positioned in the mouth (Grass E5 disc electrode, Grass Instruments, Quincy, MA, USA) and a ground electrode (Grass E2 subdermal electrode) was inserted in the tail. Simultaneous recordings of full-field ERGs (bandwidth: 1-1000 Hz; 10 000 X; 6 db attenuation; Grass P-511 amplifiers) was performed with the Biopac data acquisition system (Biopac MP 100 WS, Biopac System Inc., Goleta, CA, USA). Scotopic ERGs were obtained in response to progressively brighter flashes of white light ranging in intensity from -6.3 log cd.s/m<sup>2</sup> to 0.9 log cd.s/m<sup>2</sup> in 0.3 log-unit increments (Grass photostimulator, interstimulus interval: 10 sec, flash duration 20 $\mu$ s, average of 2-5 flashes). ERG amplitudes were measured according to a method commonly used<sup>20</sup>. In brief, the amplitude of the a-wave was measured from baseline to trough and the b-wave from the trough of the a-wave to the highest peak of the b-wave.

**Preparation of Conditioned Media (CM) from hypoxic RGC-5.** The RGC-5 cell line was kindly provided by Neeraj Agarwal of the University of North Texas Health Science Center. All cells were terminally differentiated and prepared as previously described<sup>6</sup>. Approximately 10<sup>6</sup> cells were seeded prior to exposure to 2.0% O<sub>2</sub> levels. Supernatant was collected at appropriate time points and centrifuged remove debris, filtered with 0.2 $\mu$ m filters (Millipore) and distributed for proliferation assays (see below).

**IL-1 $\beta$  stimulation of cultured RGC-5.** Terminally differentiated RGC-5 cells (10<sup>5</sup>/well) were seeded in 6-well plates and incubated for 0-8 hours with recombinant murine IL-1 $\beta$  (500 pg/mL; PeproTech Inc. Cat# 211-11B). Cells were collected at

each time point using TRIzol reagent for mRNA extraction as described in “RT-PCR and Real-Time qPCR”.

**Cell proliferation assay.** Rat brain microvascular endothelial cells (RBMVEC) were obtained from Cedarlane Laboratories (Applications) and used from passage 2–7. Cell number and division rates were determined using thymidine incorporation whereby [methyl-<sup>3</sup>H]-Thymidine (1μCi/well; Amersham) was introduced to RGC-5 conditioned media upon seeding in 24-well plates. Cell proliferation was assessed after 24 hrs.

**Aortic explant microvascular growth assay.** Aortae were explanted from adult C57BL/6 mice, sectioned into 1mm rings and placed into growth-factor reduced Matrigel (BD Biosciences) in 24-well plates. Rings were cultured in supplemented Endothelial Basal Medium (Lonza) prior to a 40h exposure to RGC-5 conditioned media. Treated rings were photographed using an inverted phase contrast microscope (Eclipse TE300, Nikon) and microvascular growth assessed using Image Pro 4.5 (Media Cybernetics, Silver Spring, USA) as described<sup>6</sup>.

**Real-time migration assay.** RBMVEC migration rates were assessed following exposure to the CM described above using an Xcelligence Real Time Cell Analyzer with Dual Plate (RTCA DP) apparatus from Roche Applied Science. This migration assay provides a real-time measurement of endothelial cell migration by extrapolating changes in electrical impedance with the number of cells passing through a porous membrane. Briefly, 160 μl of complete RBMEC medium with or without 0.5 or 1.0 μg/ml Sema3A was loaded on the lower chamber of the Cellular Invasion and Migration (CIM)-plate 16 (Roche). The upper chamber was then fitted on the lower chamber and loaded with 50μl RBEC basal medium. After one hour of equilibration,  $2.8 \times 10^4$  of RBMVEC were loaded on each well of the upper chamber. The CIM-plate was subsequently placed on a RTCA analyzer in a 37°C incubator. The cellular

migration was recorded every 15min (100 Sweeps at 15min Interval) using the cellular index provided by the RTCA DP instrument (Roche). RBMVEC basal medium was used as negative control. Four independent reactions were assayed for each condition.

**Micro-deposition of Sema3A.** Aortic explants from adult GFP-mice (see above) were plated on polycarbonate slides adjacent to micro-deposited Sema3A (100ng/ $\mu$ l) and vehicle controls using micropipettes. Samples were covered with growth factor reduce Matrigel as described above. Nascent vessels were visualized using 63X objectives by fluorescence microscopy (Nikon Eclipse E800).

**Morphometric analysis and live cell imaging.** Rat brain microvascular endothelial cells (RBMVECs) incubated with Sema3A and RGC supernatants were photographed using a 40X air objective on a Leica DMI6000 microscope coupled to a Ultraview Vox spinning disc confocal unit (Perkin Elmer). The camera was a Hamamatsu Orca-R2. Cells were maintained at 37 degrees using an environment chamber system from Pathology Devices. Images were acquired each 2 min for 45 min and surface areas were calculated using the Image J software.

**Actin network visualization and RhoA pull down.** RBMVECs were incubated for 1 hour with RGC CM or Sema3A and cells were fixed with 4% PFA and permeabilized with 0,2% Triton X-100. Subsequently, cells were stained using rhodamine-phalloidin (0,15 $\mu$ M) for 30min and DAPI (0,1 $\mu$ g/mL) for an additional 5min. Actin network collapse was assessed by confocal microscopy (Zeiss LMS5). RhoA activity was determined using a RhoA pull down kit from Pierce Biotechnology following manufacturer instructions. Briefly, active RhoA (GTP-bound) fraction was isolated from 200 $\mu$ g of protein lysates from RBMVEC incubated with RGC CMs. Five  $\mu$ g of total RhoA was presented here as loading controls.

**Statistical analysis.** Data are presented as means  $\pm$  s.e.m. Two-tailed independent Student's *t*-tests was used to analyse data. Comparisons between groups were made using one-way analysis of variance followed by post-hoc Tukey's multiple comparisons test among means.  $P < 0.05$  was considered statistically significant.

## *Results*

*The expression pattern of Sema3A is temporally and geographically consistent with a role in both vaso-obliterative and vaso-proliferative phases of PRs.*

In humans, the initial retinal vascular degeneration observed in PRs yields pockets of non-perfused neuronal tissue resulting in local hypoxia. Similarly in mice, the OIR model (75% oxygen from P7-P12 and room air until P17) provokes a central avascular retinal region (Fig 1A; left and central panels). As the retina revascularizes, aberrant neo-vascularization peaks at P17<sup>3,21</sup> (Supplementary Fig 1) where vascular-tufts protruding into the vitreous are found bordering the avascular zone (Fig 1A; centre and right panels). In accordance with a role in retinopathy, Sema3A levels in whole retina (determined by RT-PCR) surge 3-fold ( $p=0.0015$ ) during the height of vascular obliteration immediately following exposure to high O<sub>2</sub> concentrations at P8 and persists during pre-retinal NV formation at P14 ( $p=0.0157$ ) (Fig 1B). At P14, when pre-retinal NV commences (Supplementary Fig 1), this increase in Sema3A is precisely located to central avascular (A) zones in micro-dissected retinas (Fig 1C). Although, VEGF levels significantly increase in this avascular zone (Supplementary Fig 2), nascent vessels fail to enter. Moreover, Sema3A mRNA expression (by RT-PCR) is markedly increased in OIR in the ganglion cell layer (GCL) (Fig 1D) ( $p=0.0075$ ) isolated by laser capture micro-dissection (Fig 1F), while lesser expression was noted in the inner nuclear layer (INL) (Fig 1D). These findings are confirmed by immunohistochemical localization of Sema3A in the GCL of the central avascular retina in OIR (P14), specifically in retinal ganglion cells expressing Thy1.1 (Fig 1E). Importantly, at P19 when physiological revascularization progresses after

the earlier peak of NV (Supplementary Fig 1)<sup>13,15</sup>, Sema3A levels decrease in the central avascular zones to values detected at the periphery (Fig 1C), consistent a revascularization of the retina (see below). Bordering the Sema3A rich avascular retina, Nrp-1 expression is increased in pathological pre-retinal vascular tufts. In contrast to Sema3A, which is mainly found within the avascular zone, Nrp-1 is increased in pre-retinal vascular tufts (P17) (Supplementary Fig 1B) that are present in the periphery of this central avascular zone (Fig 1G,H). Together, these data suggest that Sema3A generated by RGCs is induced during the vasoobliterative phase of PRs, and positioned to block subsequent desirable revascularization during the proliferative phase (Fig 7C).

#### *IL-1 $\beta$ in the ischemic core of the retina induces Sema3A expression*

During vascular injury, the neural retina mounts an inflammatory response to the insult. Accordingly, levels of various cytokines such as, IL-1 $\beta$ <sup>22,23</sup>, IL-6<sup>23-25</sup> and TNF- $\alpha$ <sup>7,26</sup> are increased in the vitreous fluid of patients with proliferative diabetic retinopathy, in the retina of diabetic rats and during the proliferative phase of ROP. We determined whether the induction of Sema3A in the ischemic core of the retina was dependent on inflammation. Retinal levels of key inflammatory mediators IL-6, TNF- $\alpha$  and IL-1 $\beta$ , were increased at P14 in OIR (Fig 2A) ( $p < 0.05$ ). Although cytokine signaling is inter-related, we focused on IL-1 $\beta$ , which was markedly elevated and largely confined to the avascular retina (Fig 2B) in regions of elevated Sema3A expression (Fig 1C). Stimulation of IL-1RI-expressing RGCs (Supplementary Fig 3A) with IL-1 $\beta$  induced a robust rise in Sema3A expression (Fig 2C). Importantly, the induction of Sema3A was only noted after prolonged exposure to IL-1 $\beta$  (starting at 8 h), and therefore suggests that a sustained inflammatory stress is required to trigger the production of this cue. Concordant with RGCs being the main source of Sema3A, we localized IL-1RI in this neuronal population in retinal cross-sections (Fig 2D) and in retinal astrocytes (Supplementary Fig 3B). To ascertain the role of the inflammatory stimulus, specifically IL-1 $\beta$ , in the generation of Sema3A in OIR, we determined the

effects of IL-1 receptor antagonist (IL-1ra; Kineret) on Sema3A expression. IL-1ra administered twice daily starting at P10 fully inhibited the production of Sema3A in OIR at P14 (Fig 2E), further confirming a role for inflammatory stress in governing expression of this repulsive cue.

*RGC-derived Sema3A partakes in vasoobliteration, hinders vascular regeneration and contributes to pre-retinal neovascularization in OIR.*

Physiological and pathological retinal vascularization is orchestrated by the coordinated interplay of ECs, astrocytes, microglia<sup>2,27,28</sup>, and neurons such as RGCs<sup>3</sup>. Given the pivotal role of the latter in retinal vascular homeostasis<sup>3</sup> and the relative abundant expression of Sema3A in RGCs (Fig 1D,E), we proceeded to knockdown Sema3A mRNA in these neurons using small hairpin interfering RNA (shRNA) encoded in lentivectors (Lv); this approach was favoured over the use of Sema3A transgenic mice which exhibit high mortality rates and confounding neuronal deficits<sup>29</sup>; surviving Sema3A transgenic pups are also small for gestational age<sup>30</sup>, which would independently alter their OIR phenotype<sup>18</sup>. Intraocular injection of Lv at P2 effectively infects ~70% of RGCs as determined 72 h post infection<sup>3</sup> (GFP colocalization with RGC marker Thy1.1; Supplementary Fig 4A) and leads to a ~50% reduction ( $p < 0.05$ ) in retinal Sema3A, while the Sema3A levels in contralateral control eyes infected with Lv.shGFP are unaffected (Supplementary Fig 4B,C). Importantly, expression of related Semaphorins and VEGF remains unaltered, confirming specificity of the Lv.shSema3A (Supplementary Fig 4C,D).

Mice injected with Lv.shSema3A exhibit 32% less O<sub>2</sub>-induced vaso-obliteration at P12, consistent with Sema3A's pro-apoptotic properties in ECs<sup>31</sup> ( $p < 0.01$ ) (Fig 3A; Supplementary Fig 5A). Moreover, prior and during the vaso-proliferative phase (P12-P17) revascularization of the central avascular zone is accelerated by 3.7 folds in animals treated with Lv.shSema3A ( $p = 0.02$  linear reg) (Fig 3A). Of note, more rapid restoration of retinal vasculature is associated with less pre-retinal neovascularisation (Fig 3B; Supplementary Fig 5B), as expected<sup>21,32,33</sup>. These findings introduce a new neurovascular paradigm where stressed neurons express Sema3A and contribute to

promoting the degeneration of surrounding vasculature, which deviates nascent vessels away from the most severely ischemic areas, in an attempt to redistribute metabolic resources to areas deemed “more salvageable”<sup>34</sup>.

*Inhibition of RGC-derived Sema3A during proliferative retinopathy preserves neuro-retinal function.*

Maintaining neural function in ischemic tissue requires preservation of local vascular supply. Accelerated post-ischemic revascularization is associated with improved neural recovery<sup>35,36</sup>. OIR is associated with sustained depression in retinal function<sup>37</sup>, primarily in the inner retina (reflected by b-wave amplitude of the ERG)<sup>5</sup>. To assess the functional benefits of inhibition of RGC-derived Sema3A, we performed short-flash electroretinogram (ERG) analysis in 50 day-old OIR mice. We find that suppression of Sema3A (using Lv.shSema3A) in animals subjected to OIR preserves inner neuro-retinal function as demonstrated by enhanced scotopic (mixed cone-rod) b-wave amplitudes when compared to Lv.shGFP injected controls ( $p=0.0049$ ) (Fig 4A,B). This Lv.shSema3A-induced improvement in amplitude was accompanied by renormalization of the delayed b-wave peak times ( $p=0.001$ ) (Fig 4C). Outer retinal function as determined by a-wave amplitudes, is not significantly affected (Fig 4B).

*Sustained hypoxia in RGCs induces Sema3A and blocks endothelial cell growth.*

Given the inferred neurovascular cross-talk observed, we sought to decipher the cellular dynamics governing Sema3A expression and actions. We first explored Sema3A production using an *in vitro* model of RGCs<sup>38</sup> exposed to hypoxia (2% O<sub>2</sub>)<sup>3</sup>. In response to hypoxia, VEGF mRNA rises promptly (within 6 h) as expected (Fig 5A) and is consistent with the initial attempt of VEGF to protect ischemic neurons and promote vascular re-growth. This is confirmed by increased proliferation of primary rat neuromicrovascular endothelial cells (RBMVEC) and vascular sprouting of aortic explants exposed to 12 h hypoxia RGC media; addition of rSema3A (800 ng/ml) to this VEGF-rich media abolished its proliferative effect (Fig 5B,C). By 24 h of hypoxia,

VEGF levels subside and are followed at 36 h and 48 h by sharp rises in Sema3A mRNA ( $p < 0.0001$ ) (Fig 5A), in line with hypoxia and/or oxidant stress-induced regulation of other semaphorins 39. Accordingly, conditioned media from hypoxic RGCs taken at 40 h reduces basal RBMVEC division by 70% (suggestive of cell death) ( $p < 0.01$ ) as well as vessel sprouting from aortic explants (Fig 5B,C); these effects are abolished by Sema3A knockdown in the hypoxic RGCs using Lv.shSema3A [ $\sim 95\%$  infection efficiency & 50% knockdown (Supplementary Fig 6A)] compared to Lv.shGFP controls. Taken together, our findings reveal that Sema3A is produced by hypoxic stress-injured neurons and support our hypothesis that these injured RGCs participate in hindering revascularization of ischemic retinal tissue.

Revascularization of ischemic tissues begins with the selection at the vascular front of highly motile ECs known as tip cells that express a number of chemosensitive receptors such as Sema3A-responsive Nrp1, and are believed to follow guidance and growth cues with their elaborate filopodial extensions<sup>10</sup>. Accordingly, in control (as well as in Lv.shGFP-treated) mice subjected to OIR, tip cells at the retinal vascular front bordering the avascular zone rich in Sema3A exhibited mostly short and dystrophic filopodia (Fig 5D). Conversely, in mice with RGC knockdown of Sema3A, vascular filopodia are 3-fold more abundant (Fig 5D). These data underscore the role of neuron-derived Sema3A in stalling vascular regeneration of ischemic tissues.

*RGC-derived Sema3A repels nascent vessels.*

Aberrant vessel guidance as an etiology of disease has thus far not been considered; although Sema3A has been reported to affect EC motility<sup>9</sup>, its role in guiding vessels remains elusive. We corroborated this influence on cell motility in a real-time migration assay demonstrating that hypoxic RGCs produce sufficient Sema3A to significantly impede EC movement and thus reduce rates of migration ( $P < 0.05$ ) (Fig 6A). The effect of Sema3A in specifically deviating vessels is also observed as nascent vessels (from aortic explants of germ-line-GFP mice) steer away from micro-

deposited Sema3A (Fig 6B,C).

Steering endothelial tip cells towards desired trajectories requires dynamic cytoskeletal rearrangement involving actin polymerization, the formation of stress fibres and focal adhesion points, which together modulate cytoplasmic morphology and are required to instigate movement. In line, RGC-derived Sema3A influences EC shape. Conditioned media from hypoxic RGCs (40 h) caused rapid endothelial cell deformation (assessed using live spinning-disk imaging) (Fig 6D) to a similar extent as that observed with rSema3A (Fig 6E, Supplementary Fig 6B). The effects on cell shape and motility translate into a loss of stress fibres (determined by F-actin staining with rhodamine-phalloidin) by hypoxia-inducing Sema3A (Fig 6F); these changes are abrogated by Sema3A knockdown in RGCs (Fig 6D,F).

Actin alignment, cell shape and stress fibre formation is under the control of small GTPases, such as RhoA, which activate Rho Kinase leading to myosin light chain phosphorylation and in turn contributes to actomyosin contraction and cell motility. In line with the promotion of tip cell formation and subsequent growth of vessels, conditioned media from RGCs silenced of Sema3A, promotes RhoA activation in endothelial cells (as determined by RhoA-GTP pull-down; Supplementary Fig 6C). Altogether, these findings are consistent with changes in endothelial cell migration affected by Sema3A (Fig 6A-C), and by the tip cell phenotype observed at the vascular front of OIR mice (Fig 5D).

The source of Sema3A release dictates the direction of the repulsive and anti-angiogenic force acting upon tip cells. In OIR (as presented in Fig 1), Sema3A is produced by ischemic RGCs of the avascular zone under the superficial retinal vascular layer (Fig 7A) causing neovessels to steer away from the central zone towards the vitreous to form pathologic vascular tufts. Intravitreal injections of rSema3A (into the pre-retinal vitreous) following OIR (P14) prevent entry of neovessels in the vitreous body and hence decrease vascular tuft formation at P17 (Fig 7B). Although a trend was noted, vaso-obliteration in rSema3A-treated retinas also tended to decrease, albeit not significantly (Fig 7B). Collectively, our data

suggest that regional production of Sema3A by markedly hypoxic RGCs participates in deviating neovessels away from the avascular ischemic retina thus hindering functional revascularization of avascular retinal zones, as depicted in the schematic diagram in Fig 7C.

### *Discussion*

Neuronal metabolism is tightly coupled to vascular supply by regulating vasomotricity and in a more sustained manner through the release of a number of growth factors<sup>3</sup>. However the reasons why vessels fail to invade distinct zones of ischemic yet salvageable neural tissue are to date poorly understood. This study provides the first proof of concept for a neuronal factor implicated in microvascular degeneration, and identifies neuronal-derived Sema3A as a vascular repulsive cue that also actively participates in mediating the key features of PRs. Paradoxically, our findings uncover that hypoxic ischemia causes neurons to reverse their signaling machinery from VEGF production to expression of the vascular chemo-repellent and cytotoxic cue Sema3A at the expense of VEGF (Fig 5A). This sacrifice of injured neurons could be a mechanism to preserve the integrity of the remaining neurovascular network by shunting revascularization away from irreversibly damaged tissue (sustained loss of inner retinal function). In doing so, neurons mount a chemical barrier that deviates neovessels, isolating the damaged retina away from healthy regions. This novel mechanism involving Sema3A also provides an alternative explanation for the pathognomonic phenotype of ridge and tufts formation observed in ischemic PRs.

However, the factors that regulate expression of Sema3A remain elusive. Although general hypoxia and/or oxidant stress have been shown to affect other semaphorins<sup>39,40</sup>, our study is the first to draw a direct link between the inflammatory stress present in ischemic neural tissue and the induction of semaphorins. Consistent with the theory of segregating damaged areas of tissue, the induction of Sema3A requires prolonged exposure to inflammatory cytokines (here notably IL-1 $\beta$ ) - a

scenario akin to prolonged exposure to damaging ischemia. Our findings thus expose a new patho-physiological role for neuronal-derived Sema3A that extends beyond its previously reported anti-angiogenic properties.

The paradigm presented herein may also apply to other areas of the eye and the central nervous system. Increased levels of repulsive guidance cues (including Sema3A) are released from choroidal neovascular retinal pigmented epithelium<sup>41</sup>. Guidance cues may therefore also contribute to diseases of the outer retina, such as age-related macular degeneration. Shortly after an ischemic stroke<sup>42</sup>, Sema3A is produced by injured cells<sup>43,44</sup> and localizes to regions immediately adjacent to the infarct<sup>44</sup>. A similar pattern is observed after spinal cord injury, where neurons near the site of lesion increase production of Sema3A<sup>45</sup>. The timing of this increase corresponds to the early phases of the response to injury when vascular remodeling occurs and axonal sprouting is induced. However, besides direct effects of repulsive cues such as Semaphorins on cellular proliferation in models of tumorigenesis<sup>46,47</sup>, the involvement of guidance cues in pathological settings has not previously been explored. In light of the ubiquitous release of Sema3A by injured neurons elsewhere in the central nervous system, the present study suggests that modulation of this guidance cue could be harnessed as a therapeutic strategy to promote prompt revascularization of ischemic neural tissue.

In line with our current mechanistic understanding of PRs, VEGF has been the most promising therapeutic target for ocular vasoproliferative diseases, albeit with concerns. Notwithstanding the contribution of excessive levels of VEGF in PRs, this growth factor also plays a pivotal protective role in the normal physiologic development and health of the retina<sup>48,49</sup>. Inhibiting VEGF may curb neovascularization but may also cause unwanted damage to neuronal networks; accordingly, the appropriate dose of anti-VEGF treatment remains a challenge<sup>50</sup>. Alternatively, inhibiting the repulsive forces that are only present during a pathological insult may prove to be a more selective therapeutic approach.

Although mechanisms governing vascular degeneration and ensued pre-retinal

neovascularization in PRs have been studied<sup>13,51-55</sup>, there are currently no strategies to accelerate revascularization of the vasoobliterated area and consequently limit aberrant pre-retinal neovascularization. We propose that inhibition of neuronal-derived Sema3A aids the physiological vascular regeneration of the retina by overriding the vaso-inhibitory status of the injured tissue and thus alleviates the hypoxic stress that is central to disease progression. Accordingly, inhibition of RGC-derived Sema3A or upstream inflammatory mediators (notably IL-1 $\beta$ ), while harnessing the growth potential of VEGF (Supplementary Fig 2 & 4) may force vessels to promptly revascularize injured neurons and improve retinal function. rSema3A may also curb pathological neovascularization; however as is the case with anti-VEGF therapy, this approach would curtail beneficial rapid retinal revascularization. Thus modulation of RGC-derived Sema3A may be a preferable therapeutic modality to remedy PRs without directly sequestering growth factors such as VEGF that are essential for endothelial and neuronal homeostasis. Since Sema3A is also released by injured neurons elsewhere in the central nervous system<sup>9,44,45</sup>, the concept proposed herein may not only apply to ischemic retinopathies, but also to other pathologies such as cerebral infarct where vascular growth is a key determinant of outcome<sup>35,36</sup>.

### *Acknowledgements*

J.-S.J. is a recipient of the Canadian Child Health Clinician Scientist Program, a Canadian Institute of Health Research (CIHR) training initiative. NS is supported by and Frederick-Banting scholarship from the CIHR. FB holds a *Fonds de la Recherche en Santé du Québec* (FRSQ) fellowship. JCR is supported by the Heart and Stroke Foundation of Canada (HSCF) and the Canadian Stroke Network (CSN). LS is supported by NIH EY017017, EY017017-04S1 P01 HD18655, RPB Senior Investigator Award, Lowy Medical Institute (MacTel), Rosche Foundation for Anemia Research and V. Kann Rasmussen Foundation (LEHS). SC holds a Canada Research Chair (Translational Research in Vision) and the Leopoldine Wolfe Chair in

translational research in age-related macular degeneration and is supported by grants from the CIHR. PS holds a Canada Research Chair in Retinal Cell Biology and is supported by grants from the CIHR and the Canadian National Institute for the Blind. J.-S.J and N.S. are PhD candidates at McGill University and Université de Montréal respectively and this work is submitted in partial fulfillment of the requirement for the PhD.

### *Authorship*

Contribution: J.-S.J., N.S., S. Chemtob, P.S. conceived and designed the experiments. J.-S.J., N.S., F.B., K.Z., A.S., J.C.R., Z.S., A.P., T.Z., D.H., M.D., D.K., J.C.H., E.P., A.Z., G.H., S. Costantino., C.B., P.S. performed experiments. D.R.V., G.H., J.M., M.K., S. Costantino, C.B., P.L., L.E.H.S. provided expert advices. M.K. and C.B. provided gene expression vectors. All of the authors analyzed the data. J.-S.J., N.S., S. Chemtob and P.S. wrote the paper.

Conflict-of-interest disclosure: The authors declare no competing financial interests

Correspondence: Przemyslaw (Mike) Sapieha, Ph.D. and Sylvain Chemtob, M.D., Ph.D.

Maisonneuve-Rosemont Hospital Research Centre, and CHU Ste-Justine, Research Centre 5415 Assomption Boulevard, Montreal, Qc, H1T 2M4, Canada

### *References*

1. Sapieha P, Joyal J-S, Rivera JC, et al. Retinopathy of prematurity: understanding ischemic retinal vasculopathies at an extreme of life. *J Clin Invest.* 2010;120:3022-3032.
2. Stone J, Itin A, Alon T, et al. Development of retinal vasculature is mediated by hypoxia-induced vascular endothelial growth factor (VEGF) expression by neuroglia. *J Neurosci.* 1995;15:4738-4747.
3. Sapieha P, Sirinyan M, Hamel D, et al. The succinate receptor GPR91 in neurons has a major role in retinal angiogenesis. *Nat Med.* 2008;14:1067-1076.
4. Dorfman A, Dembinska O, Chemtob S, Lachapelle P. Early manifestations of

- postnatal hyperoxia on the retinal structure and function of the neonatal rat. *Invest Ophthalmol Vis Sci.* 2008;49:458-466.
5. Dorfman AL, Polosa A, Joly S, Chemtob S, Lachapelle P. Functional and structural changes resulting from strain differences in the rat model of oxygen-induced retinopathy. *Invest Ophthalmol Vis Sci.* 2009;50:2436-2450.
  6. Sapieha P, Hamel D, Shao Z, et al. Proliferative retinopathies: Angiogenesis that blinds. *Int J Biochem Cell Biol.* 2009.
  7. Stahl A, Sapieha P, Connor KM, et al. Short communication: PPAR gamma mediates a direct antiangiogenic effect of omega 3-PUFAs in proliferative retinopathy. *Circ Res.* 2010;107:495-500.
  8. Carmeliet P, Tessier-Lavigne M. Common mechanisms of nerve and blood vessel wiring. *Nature.* 2005;436:193-200.
  9. Miao HQ, Soker S, Feiner L, Alonso JL, Raper JA, Klagsbrun M. Neuropilin-1 mediates collapsin-1/semaphorin III inhibition of endothelial cell motility: functional competition of collapsin-1 and vascular endothelial growth factor-165. *J Cell Biol.* Vol. 146; 1999:233-242.
  10. Klagsbrun M, Eichmann A. A role for axon guidance receptors and ligands in blood vessel development and tumor angiogenesis. *Cytokine Growth Factor Rev.* 2005;16:535-548.
  11. Klagsbrun M, Takashima S, Mamluk R. The role of neuropilin in vascular and tumor biology. *Adv Exp Med Biol.* 2002;515:33-48.
  12. Mamluk R, Gechtman Z, Kutcher ME, Gasiunas N, Gallagher J, Klagsbrun M. Neuropilin-1 binds vascular endothelial growth factor 165, placenta growth factor-2, and heparin via its b1b2 domain. *J Biol Chem.* 2002;277:24818-24825.
  13. Smith LE, Wesolowski E, McLellan A, et al. Oxygen-induced retinopathy in the mouse. *Invest Ophthalmol Vis Sci.* Vol. 35; 1994:101-111.
  14. Aiello LP, Pierce EA, Foley ED, et al. Suppression of retinal neovascularization in vivo by inhibition of vascular endothelial growth factor (VEGF) using soluble VEGF-receptor chimeric proteins. *Proc Natl Acad Sci USA.* 1995;92:10457-10461.
  15. Stahl A, Connor KM, Sapieha P, et al. The mouse retina as an angiogenesis model. *Invest Ophthalmol Vis Sci.* 2010;51:2813-2826.
  16. Connor KM, Krah NM, Dennison RJ, et al. Quantification of oxygen-induced retinopathy in the mouse: a model of vessel loss, vessel regrowth and pathological angiogenesis. *Nat Protoc.* 2009;4:1565-1573.
  17. Stahl A, Connor KM, Sapieha P, et al. Computer-aided quantification of retinal neovascularization. *Angiogenesis.* 2009;12:297-301.
  18. Stahl A, Chen J, Sapieha P, et al. Postnatal weight gain modifies severity and functional outcome of oxygen-induced proliferative retinopathy. *Am J Pathol.* 2010;177:2715-2723.
  19. Cayouette M, Behn D, Sendtner M, Lachapelle P, Gravel C. Intraocular gene transfer of ciliary neurotrophic factor prevents death and increases responsiveness of rod photoreceptors in the retinal degeneration slow mouse. *J Neurosci.* 1998;18:9282-9293.
  20. Marmor MF, Fulton AB, Holder GE, Miyake Y, Brigell M, Bach M. ISCEV Standard

- for fullfield clinical electroretinography (2008 update). *Doc Ophthalmol.* 2009;118:69-77.
21. Connor KM, SanGiovanni JP, Lofqvist C, et al. Increased dietary intake of omega-3-polyunsaturated fatty acids reduces pathological retinal angiogenesis. *Nat Med.* 2007;13:868-873.
  22. Abu el Asrar AM, Maimone D, Morse PH, Gregory S, Reder AT. Cytokines in the vitreous of patients with proliferative diabetic retinopathy. *Am J Ophthalmol.* 1992;114:731-736.
  23. Carmo A, Cunha-Vaz JG, Carvalho AP, Lopes MC. L-arginine transport in retinas from streptozotocin diabetic rats: correlation with the level of IL-1 beta and NO synthase activity. *Vision Res.* 1999;39:3817-3823.
  24. Funatsu H, Yamashita H, Shimizu E, Kojima R, Hori S. Relationship between vascular endothelial growth factor and interleukin-6 in diabetic retinopathy. *Retina.* 2001;21:469-477.
  25. Canataroglu H, Varinli I, Ozcan AA, Canataroglu A, Doran F, Varinli S. Interleukin (IL)-6, interleukin (IL)-8 levels and cellular composition of the vitreous humor in proliferative diabetic retinopathy, proliferative vitreoretinopathy, and traumatic proliferative vitreoretinopathy. *Ocul Immunol Inflamm.* 2005;13:375-381.
  26. Limb GA, Chignell AH, Green W, LeRoy F, Dumonde DC. Distribution of TNF alpha and its reactive vascular adhesion molecules in fibrovascular membranes of proliferative diabetic retinopathy. *Br J Ophthalmol.* 1996;80:168-173.
  27. Checchin D, Sennlaub F, Levavasseur E, Leduc M, Chemtob S. Potential role of microglia in retinal blood vessel formation. *Invest Ophthalmol Vis Sci.* 2006;47:3595-3602.
  28. Fruttiger M, Calver AR, Kruger WH, et al. PDGF mediates a neuron-astrocyte interaction in the developing retina. *Neuron.* 1996;17:1117-1131.
  29. Behar O, Golden JA, Mashimo H, Schoen FJ, Fishman MC. Semaphorin III is needed for normal patterning and growth of nerves, bones and heart. *Nature.* 1996;383:525-528.
  30. Gu C, Rodriguez ER, Reimert DV, et al. Neuropilin-1 conveys semaphorin and VEGF signaling during neural and cardiovascular development. *Dev Cell.* 2003;5:45-57.
  31. Guttman-Raviv N, Shraga-Heled N, Varshavsky A, Guimaraes-Sternberg C, Kessler O, Neufeld G. Semaphorin-3A and semaphorin-3F work together to repel endothelial cells and to inhibit their survival by induction of apoptosis. *J Biol Chem.* 2007;282:26294-26305.
  32. Chen J, Smith L. Retinopathy of prematurity. *Angiogenesis.* 2007;10:133-140.
  33. Dorrell M, Friedlander M. Mechanisms of endothelial cell guidance and vascular patterning in the developing mouse retina. *Progress in Retinal and Eye Research.* 2006;25:277-295.
  34. Hou X, Roberts LJ, 2nd, Gobeil F, Jr., et al. Isomer-specific contractile effects of a series of synthetic f2-isoprostanes on retinal and cerebral microvasculature. *Free Radic Biol Med.* 2004;36:163-172.

35. Chopp M, Zhang ZG, Jiang Q. Neurogenesis, angiogenesis, and MRI indices of functional recovery from stroke. *Stroke*. 2007;38:827-831.
36. Li L, Jiang Q, Zhang L, et al. Angiogenesis and improved cerebral blood flow in the ischemic boundary area detected by MRI after administration of sildenafil to rats with embolic stroke. *Brain Res*. 2007;1132:185-192.
37. Fulton AB, Hansen RM, Moskowitz A, Akula JD. The neurovascular retina in retinopathy of prematurity. *Prog Retin Eye Res*. 2009;28:452-482.
38. Frassetto LJ, Schlieve CR, Lieven CJ, et al. Kinase-dependent differentiation of a retinal ganglion cell precursor. *Invest Ophthalmol Vis Sci*. 2006;47:427-438.
39. Sun Q, Zhou H, Binmadi NO, Basile JR. Hypoxia-inducible factor-1-mediated regulation of semaphorin 4D affects tumor growth and vascularity. *J Biol Chem*. 2009;284:32066-32074.
40. Barisani D, Meneveri R, Ginelli E, Cassani C, Conte D. Iron overload and gene expression in HepG2 cells: analysis by differential display. *FEBS Lett*. 2000;469:208-212.
41. Martin G, Schlunck G, Hansen LL, Agostini HT. Differential expression of angioregulatory factors in normal and CNV-derived human retinal pigment epithelium. *Graefes Arch Clin Exp Ophthalmol*. 2004;242:321-326.
42. Fujita H, Zhang B, Sato K, Tanaka J, Sakanaka M. Expressions of neuropilin-1, neuropilin-2 and semaphorin 3A mRNA in the rat brain after middle cerebral artery occlusion. *Brain Res*. 2001;914:1-14.
43. Carmichael ST. Cellular and molecular mechanisms of neural repair after stroke: making waves. *Ann Neurol*. 2006;59:735-742.
44. Carmichael ST, Archibeque I, Luke L, Nolan T, Momiy J, Li S. Growth-associated gene expression after stroke: evidence for a growth-promoting region in peri-infarct cortex. *Exp Neurol*. 2005;193:291-311.
45. De Winter F, Oudega M, Lankhorst AJ, et al. Injury-induced class 3 semaphorin expression in the rat spinal cord. *Exp Neurol*. 2002;175:61-75.
46. Geretti E, Klagsbrun M. Neuropilins: novel targets for anti-angiogenesis therapies. *Cell Adh Migr*. 2007;1:56-61.
47. Casazza A, Finisguerra V, Capparuccia L, et al. Sema3E-Plexin D1 signaling drives human cancer cell invasiveness and metastatic spreading in mice. *J Clin Invest*;120:2684-2698.
48. Robinson GS, Ju M, Shih SC, et al. Nonvascular role for VEGF: VEGFR-1, 2 activity is critical for neural retinal development. *FASEB J*. 2001;15:1215-1217.
49. Alon T, Hemo I, Itin A, Pe'er J, Stone J, Keshet E. Vascular endothelial growth factor acts as a survival factor for newly formed retinal vessels and has implications for retinopathy of prematurity. *Nat Med*. 1995;1:1024-1028.
50. Schlingemann RO, Witmer AN. Treatment of retinal diseases with VEGF antagonists. *Prog Brain Res*. 2009;175:253-267.
51. Michaelson I. The mode of development of the vascular system of the retina with some observations on its significance for certain retinal disorders. *Trans Ophthalmol Soc UK*. 1948;68:137-180.
52. Campbell K. Intensive oxygen therapy as a possible cause of retrolental

fibroplasia; a clinical approach. *Med J Aust.* 1951;2:48-50.

53. Lundbaek K, Christensen NJ, Jensen VA, et al. Diabetes, diabetic angiopathy, and growth hormone. *Lancet.* 1970;2:131-133.

54. D'Amore PA, Sweet E. Effects of hyperoxia on microvascular cells in vitro. *In Vitro Cell Dev Biol.* 1987;23:123-128.

55. Smith LE. Pathogenesis of retinopathy of prematurity. *Growth Horm IGF Res.* 2004;14 Suppl A:S140-144.

### *Specific contributions from the candidate*

Dr. P Sapieha initially developed the central idea explaining why ischemic neurons repulse growing vessels away from perishing tissue. I, along with Dr. JS Joyal, under the guidance of Dr. P Sapieha and Dr. S Chemtob, began underlying the exact role of semaphorin3A (Sema3A) in Ischemic Retinopathies, which gave rise to the current study published in *Blood* in 2011. My contribution was determining the characteristic mechanism by which Sema3A repulses vessels using a variety of techniques.

Precisely, I contributed enormously to the development of the project, which include planning, designing, optimizing and performing the majority of the experiments. Several specialized techniques were performed by other contributing authors (ERG – A Polosa, M Djavari; Laser capture microdissection – A Stahl, JS Joyal; Live cell imaging – F Binet, JS Joyal; Microprinting – D Kunik, S Constantino). I partook in gathering and analyzing data, and preparing figures for the manuscript. Finally I contributed to the writing, proofing and finalizing of the manuscript.

Dr. D Varma, Dr. J Mancini, Dr. M Klagsbrun, and Dr. LE Smith provided expert opinion in the study.

## Figures for Chapter 1

**Figure 1**

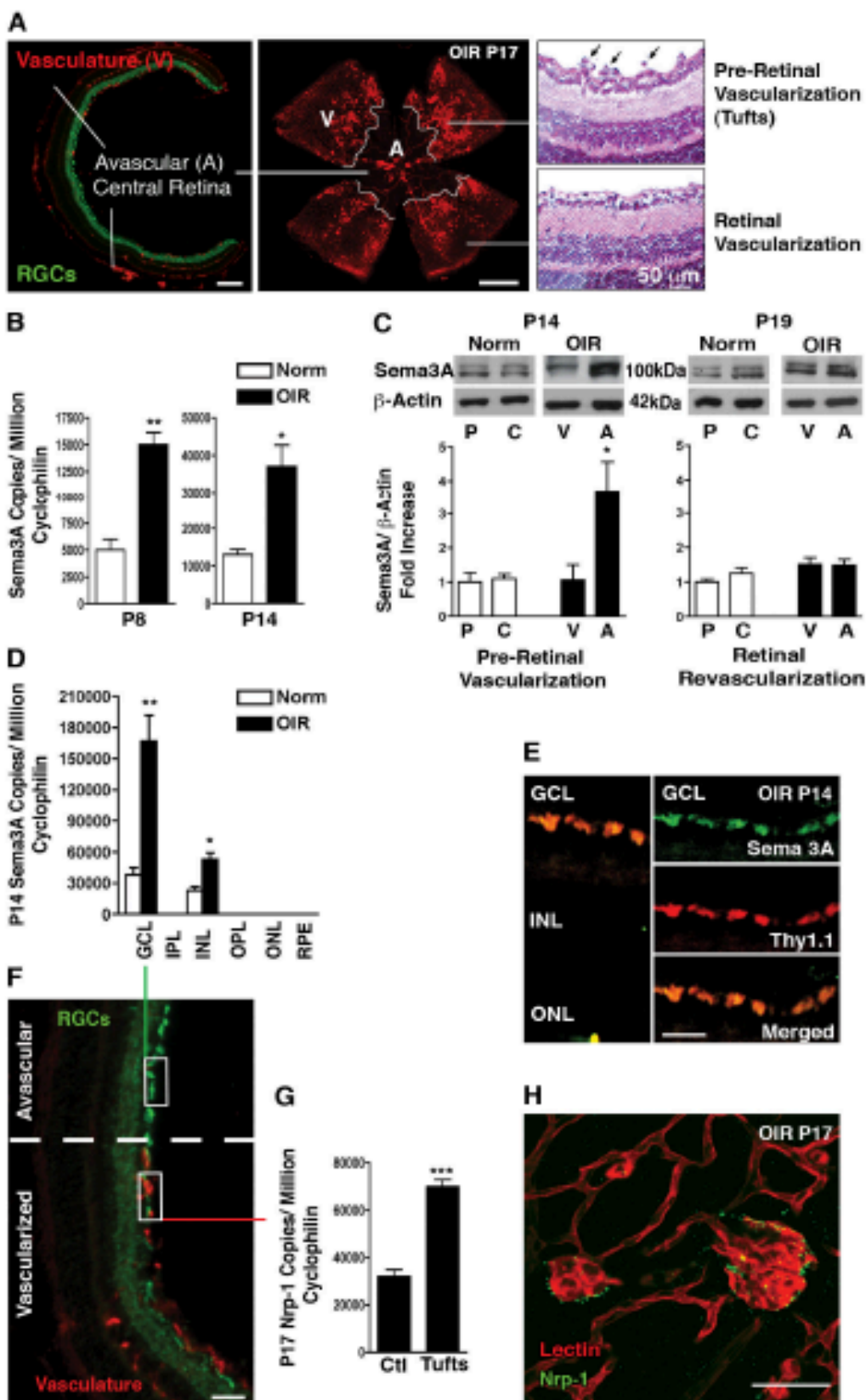


**Fig 1. Sema3A expression is consistent with a role in retinopathy.** (A) Frozen cross section (left panel) and flat mount retinas (central panel) taken at P17 of OIR demonstrating the principal characteristics of PRs including avascular (A) and vascular (V) zones. Paraffin sections (right panel) demonstrating preretinal neovascular tufts (black arrows). (B) Real-time PCR on whole retinas taken at P8 and P14 demonstrates a ~3-fold increase in Sema3A during the vaso-obliterative and neovascular phases of PRs respectively (n=3). Values are gene copy number normalized to *CyclophilinA* standards  $\pm$  s.e.m. \*\*p=0.0015 and \*p=0.0157 compared to Normoxia (Norm). (C) Micro-dissection of avascular regions of the OIR retina at P14 reveals a 3.5-fold induction in Sema3A protein levels in the avascular area (n=3). Values are shown relative to vascularized areas  $\pm$  s.e.m. \*p=0.0447 compared to vascularised zone (V). At P19 when physiological retinal re-vascularization is reinstated, Sema3A in the avascular retina returns to control levels. Levels of Sema3A in the peripheral (P) and central (C) retina of normoxic controls are comparable. (D) Laser Capture Microdissection on retinal layers (F, and Suppl Fig 1B) demonstrates that Sema3A is primarily produced in the Ganglion Cell Layer (GCL) with lower expression in the inner nuclear layer (INL). Levels of Sema3A surge 4.4-fold in the GCL at P14 following OIR (n=3). \*\*p=0.0075 and \*p=0.0143 relative to normoxia (Norm). (E) Confocal imaging of IHC on central avascular retinal cross-sections (OIR P14) reveals a predominant expression of Sema3A by RGCs as confirmed by merging with RGC marker Thy1.1. (G) At P17, LCM and RT-PCR of normal vessels versus neovascular tufts revealed a 2.2-fold induction in Neuropilin-1 (Nrp-1) in tufts (n=3). Values are gene copy number normalized to *CyclophilinA* standards  $\pm$ s.e.m.\*\*\*p=0.0007 compared to controls (Ctl). (H) Immunohistochemistry on flat-mount retinas confirms pronounced staining of Nrp-1 on lectin-stained neovascular tufts (P17). Images are representative of 5 experiments. Scale bars: (A) 300  $\mu$ m (right panel), 500  $\mu$ m (central panel) and 50  $\mu$ m (right panel). (E) 25  $\mu$ m, (F) 100  $\mu$ m and (H) 25  $\mu$ m.

**Relative contributions: Figure 1**

- A) Immunohistochemistry, imaging and analysis performed by JS Joyal and K Zaniolo
- B) qPCR analysis performed by A Stahl and P Sapieha
- C) Western blot performed by **N Sitaras**
- D) and G) Laser-capture microdissection and qPCR analysis performed by A Stahl and P Sapieha
- E) Immunocytochemistry and imaging performed by **N Sitaras** and JS Joyal
- F) And H) Immunocytochemistry and imaging performed by JS Joyal and K Zaniolo

Animal handling and sample collection: **N Sitaras**, JS Joyal, Z Shao and K Zaniolo

Figure preparation: JS Joyal, **N Sitaras**, P Sapieha and S Chemtob

Approximate Figure contribution: 25%

**Figure 2**

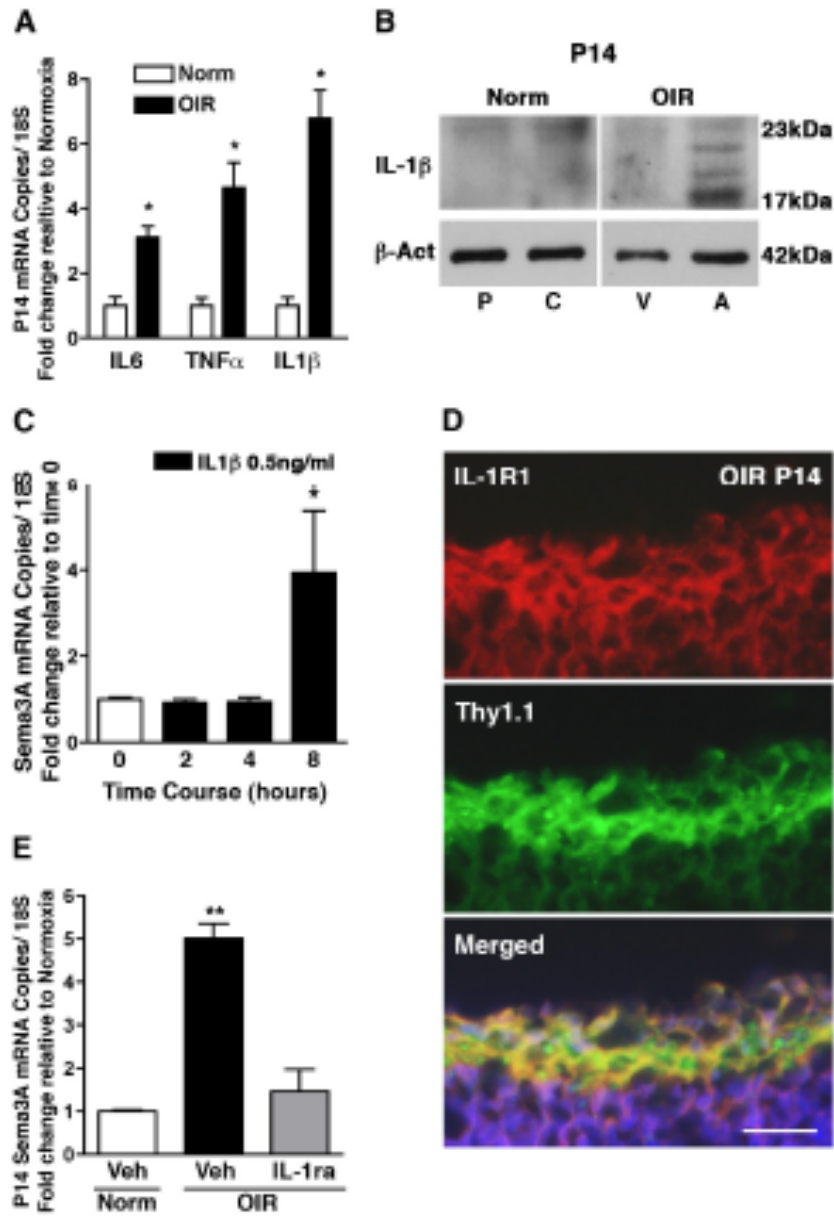


**Fig 2. IL-1 $\beta$  in the ischemic avascular retina induces Sema3A expression. (A)** Inflammatory cytokines IL-6, TNF- $\alpha$  and IL-1 $\beta$  are induced in OIR retinas, in particular IL-1 $\beta$  which was upregulated 6.8 fold compared to normoxia. n=3; p<0.01 compared to normoxia (Norm). **(B)** Micro-dissection of avascular (A) regions of the OIR retina reveals a marked induction in IL-1 $\beta$  (17 KDa) protein levels compared to the vascular regions (V) and the central (C) and peripheral (P) normoxic retina; higher molecular weight bands correspond to pro-IL-1 $\beta$ . n=3; p<0.01 compared to time 0. **(C)** RGC-5 stimulated with IL-1 $\beta$  (0.5 ng/ml) elicit a delayed (8 h) but significant 4-fold increase in Sema3A (n=3-4). **(D)** Confocal imaging of IHC on retinal cross-sections (OIR P14) reveals a predominant expression of IL-1RI by RGCs as confirmed by merging with RGC marker Thy1.1. **(E)** Interleukin receptor (IL-1RI) antagonist IL-1ra (Kineret) abrogated the OIR-dependent induction of Sema3A compared to vehicle-treated normoxia and OIR controls. Values are fold-increase of control  $\pm$ s.e.m. n=3; \*\*p<0.01 compared to normoxic vehicle (Veh). **(D)** Scale bar: 25 $\mu$ m.

**Relative contributions: Figure 2**

- A) qPCR analysis performed by **N Sitaras**
- B) Western blot analysis performed by **N Sitaras**
- C) In vitro experiment and qPCR analysis carried out by **N Sitaras**
- D) Immunocytochemistry and imaging performed by JS Joyal and T Zhu
- E) Kineret administration and qPCR analysis performed by **N Sitaras** and JC Rivera

Animal handling and sample collection: **N Sitaras**, JS Joyal and JC Rivera

Figure preparation: JS Joyal, **N Sitaras**, P Sapieha and S Chemtob

Approximate Figure contribution: 60%

**Figure 3**

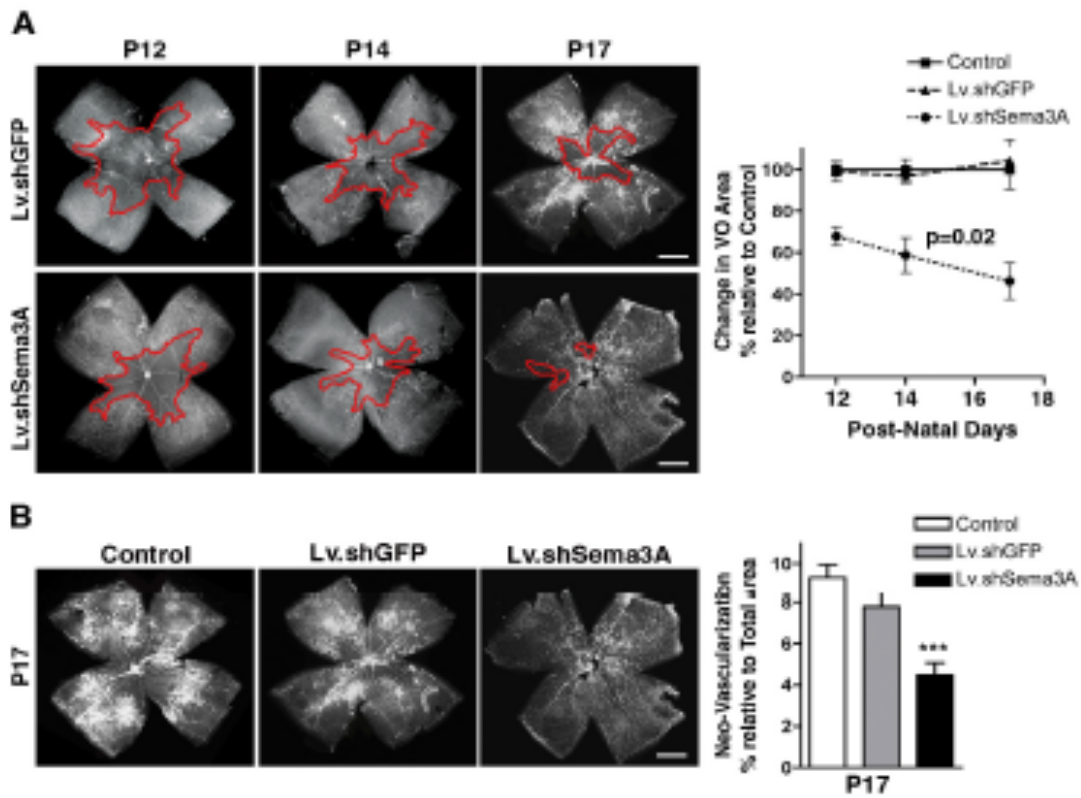


**Fig 3. RGC-derived Sema3A partakes in vasoobliteration, hinders vascular regeneration and contributes to pre-retinal neovascularization in OIR. (A)** Representative photo-micrographs of *Griffonia simplicifolia* lectin stained flatmount retinas at P12 reveal that mice receiving an intravitreal injection of Lv.shSema3A show a 32% reduction in the area of vaso-obliteration compared to contralateral eyes receiving Lv.shGFP injections and non-injected eyes (basal) revealing the vaso-toxic properties of Sema3A in the first phase of OIR (n=13-15; additional quantification is presented in **Supplementary Fig 4A**). The inhibition of RGC-derived Sema3A significantly enhanced the rate of vascular regeneration secondary to OIR as determined at P12 (n=13-15), P14 (n=12-13) and P17 (n=15-18). Values are presented as rate change in vaso-obliterated area relative to Lv.shGFP treated controls  $\pm$  s.e.m.  $p=0.02$  by anova factoring for time and group. **(B)** At peak neovascularization (P17) lectin-stained flatmount retinas reveal that inhibition of Sema3A (n=9-12) significantly reduced areas of pathological neovascularization from 9.3% to 4.5% as determined using the Swift NV quantification protocol (**Supplementary Fig 4B**). Values are presented as area of neovascularization relative to total retinal area  $\pm$  s.e.m.  $***p=0.0002$  compared to control. Scale bars: **(A)** and **(B)** 500 $\mu$ m.

**Relative contributions: Figure 3**

A) and B) Lentiviral preparations performed by **N Sitaras**, JS Joyal, D Hamel and  
C Beauséjour

Intravitreal injections performed by **N Sitaras**, K Zaniolo and Z Shao

Sample preparation performed by **N Sitaras**, K Zaniolo and Z Shao

Imaging and calculation performed by **N Sitaras**, K Zaniolo, Z Shao and A  
Zabeida

Animal handling and sample collection: **N Sitaras**, JS Joyal, Z Shao and K Zaniolo

Figure preparation: JS Joyal, **N Sitaras**, P Sapieha and S Chemtob

Approximate Figure contribution: 60%

**Figure 4**

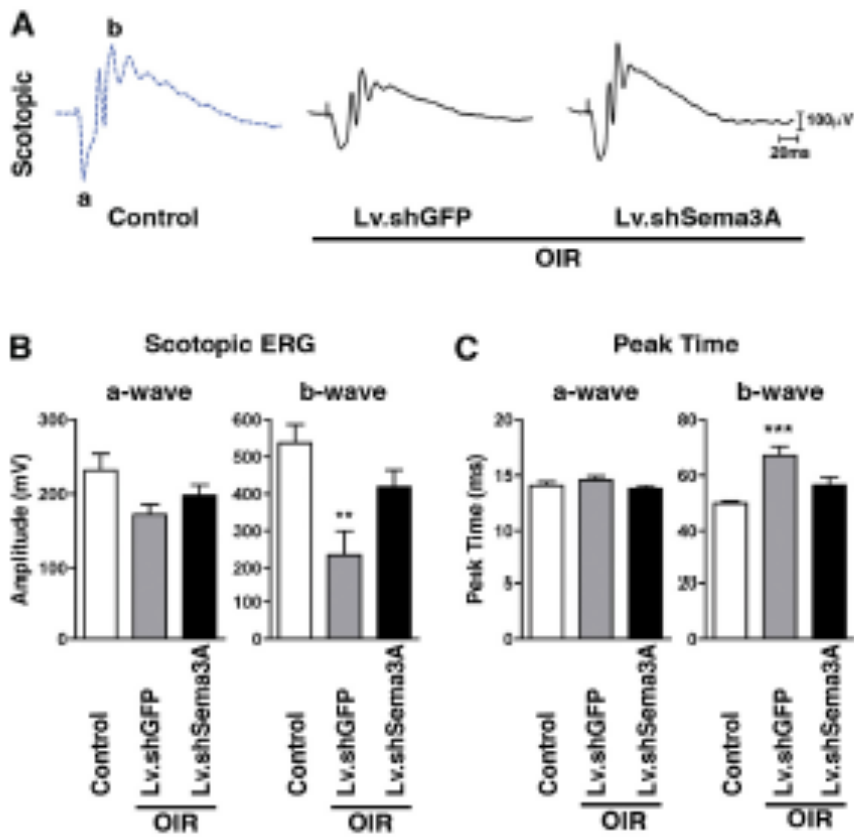


**Fig 4. Inhibition of RGC-derived Sema3A during proliferative retinopathy preserves neuro-retinal function.** (A) Representative recordings of full field scotopic ERGs in response to progressively brighter flashes of white light ranging in intensity from -6.3 log cd.s/m<sup>2</sup> to 0.9 log cd.s/m<sup>2</sup> in 0.3 log-unit increments (Grass photostimulator, interstimulus interval: 10 sec, flash duration 20 $\mu$ s, average of 2-5 flashes). (B) Lv.shSema3A-treated mice show a significant gain in inner-retinal scotopic (mixed conerod) b-wave response (418.2  $\mu$ V; n=6) when compared to control contra-lateral Lv.shGFP  $\mu$ V (234.3; n=8) injected eyes. \*\*p<0.01 and p<0.001 compared to corresponding control. Similarly, knockdown of Sema3A enhances the response time to light stimulus as illustrated by a decreased peak times (56.4 ms) with respect to controls (67.1 ms). Inner retinal function determined by a-wave amplitudes and peak times was not significantly affected.

**Relative contributions: Figure 4**

A) and B) Lentiviral preparations performed by **N Sitaras**, JS Joyal, D Hamel and C Beauséjour

Intravitreal injections performed by N Sitaras, K Zaniolo and Z Shao

Electroretinogram performed by A Polosa and M Djavari

Analysis of data performed by JS Joyal, **N Sitaras**, P Lachapelle and P Sapieha

Figure preparation: JS Joyal, **N Sitaras**, P Sapieha and S Chemtob

Approximate Figure contribution: 10%

**Figure 5**

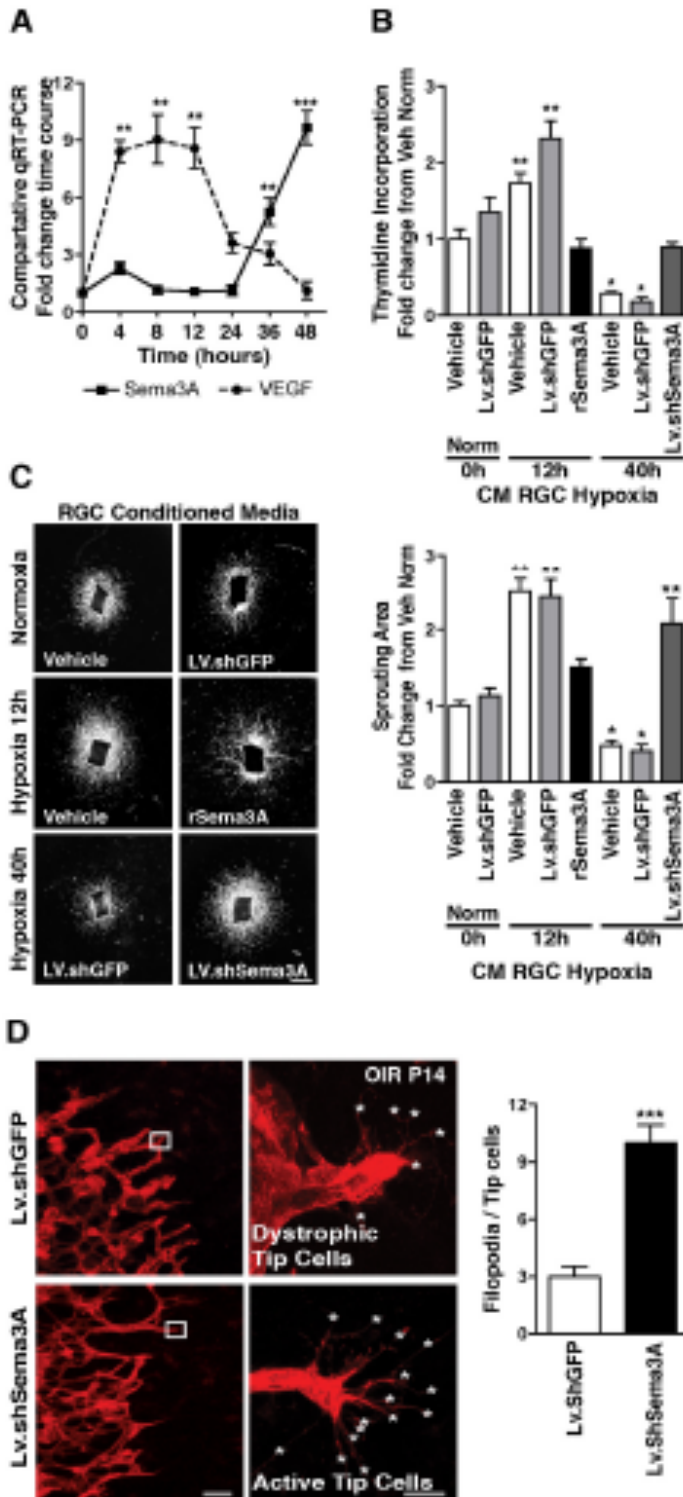


**Fig 5. Sema3A produced by hypoxic RGCs prevents retinal endothelial cell growth.** **(A)** VEGF and Sema3A release by cultured RGC-5 cells exposed to hypoxia (2%). In the initial 12 h after hypoxia, VEGF levels rapidly rise ~9-fold while Sema3A remains unaffected. Later as hypoxic exposure is prolonged, Sema3A levels rise (6-fold at 36 h and 10-fold at 48 h). Values represent fold increase relative to time 0. \*\* $p < 0.01$  and \*\*\* $p < 0.0001$  compared to corresponding time 0. **(B)** Neuro-microvascular endothelial cells (EC) proliferation measured by thymidine incorporation. Incubation of EC with conditioned media (CM) from RGCs exposed to hypoxia for 12 h (high VEGF, low Sema3A) caused a 1.7- (vehicle) and 2.3- (non-specific shRNA; LV.shGFP) fold increase in cell number within 24 h; this effect is abrogated by rSema3A (800 ng/ml). Conversely, ECs treated with CM from RGCs exposed to hypoxia for 40 h (low VEGF, high Sema3A), show a Sema3A-dependent reduction in EC division (5-fold diminution). Knockdown of Sema3A in hypoxia-exposed RGCs using Lv.shSema3A prevents the noted drop in EC division compared to vehicle and Lv.shGFP treated RGCs.  $n=4-6$ ; \* $p < 0.05$ , \*\* $p < 0.01$  compared to vehicle during normoxia (Norm) at time 0. **(C)** Aortic sprouting more than doubled in explants grown in CM from vehicle- and LV.shGFP-treated RGCs exposed to 12 h hypoxia; this vascular growth was curbed by rSema3A (800 ng/ml). CM from RGCs exposed to 40 h hypoxia reduce their sprouting by ~60% compared to normoxic media controls. When Sema3A is knocked-down in RGCs, vascular sprouting is doubled compared to Lv.shGFP underscoring the inhibitory properties of Sema3A towards nascent vessels. Values are represented as fold change relative to controls.  $n=3-6$ ; \* $p < 0.05$ , \*\* $p < 0.01$  compared to vehicle during normoxia (Norm) at time 0. **(D)** Representative confocal images of the re-vascularization front (images on left) and high magnification of tip cells (images on right) at OIR P14. The number of filopodia (asterix) per tip cell is increased 3-fold in Lv.shSema3A animals, whereas contralateral eyes treated with Lv.shGFP showed less filopodia and dystrophic tip cells.  $n=10$ ; \*\*\* $p < 0.0001$  compared to value for Lv.shGFP. Scale bars: **(C)** 1mm, **(D)** 50  $\mu\text{m}$  (left) and 10  $\mu\text{m}$  (right).

**Relative contributions: Figure 5**

- A) In vitro preparation and qPCR analysis performed by **N Sitaras**, JS Joyal and A Zabeida
- B) In vitro preparation and data analysis performed by **N Sitaras**, JS Joyal and K Zaniolo
- C) Aortic ring explant preparation performed by **N Sitaras** and JC Honoré  
Sample preparation, imaging and analysis performed by **N Sitaras**, JS Joyal and P Sapieha
- D) Lentiviral preparations performed by **N Sitaras**, JS Joyal, D Hamel and C Beauséjour  
Intravitreal injections performed by JS Joyal, Z Shao and K Zaniolo  
Immunocytochemistry and data analysis performed by JS Joyal, E Picard and P Sapieha

Figure preparation: JS Joyal, **N Sitaras**, P Sapieha and S Chemtob

Approximate Figure contribution: 30%

**Figure 6**

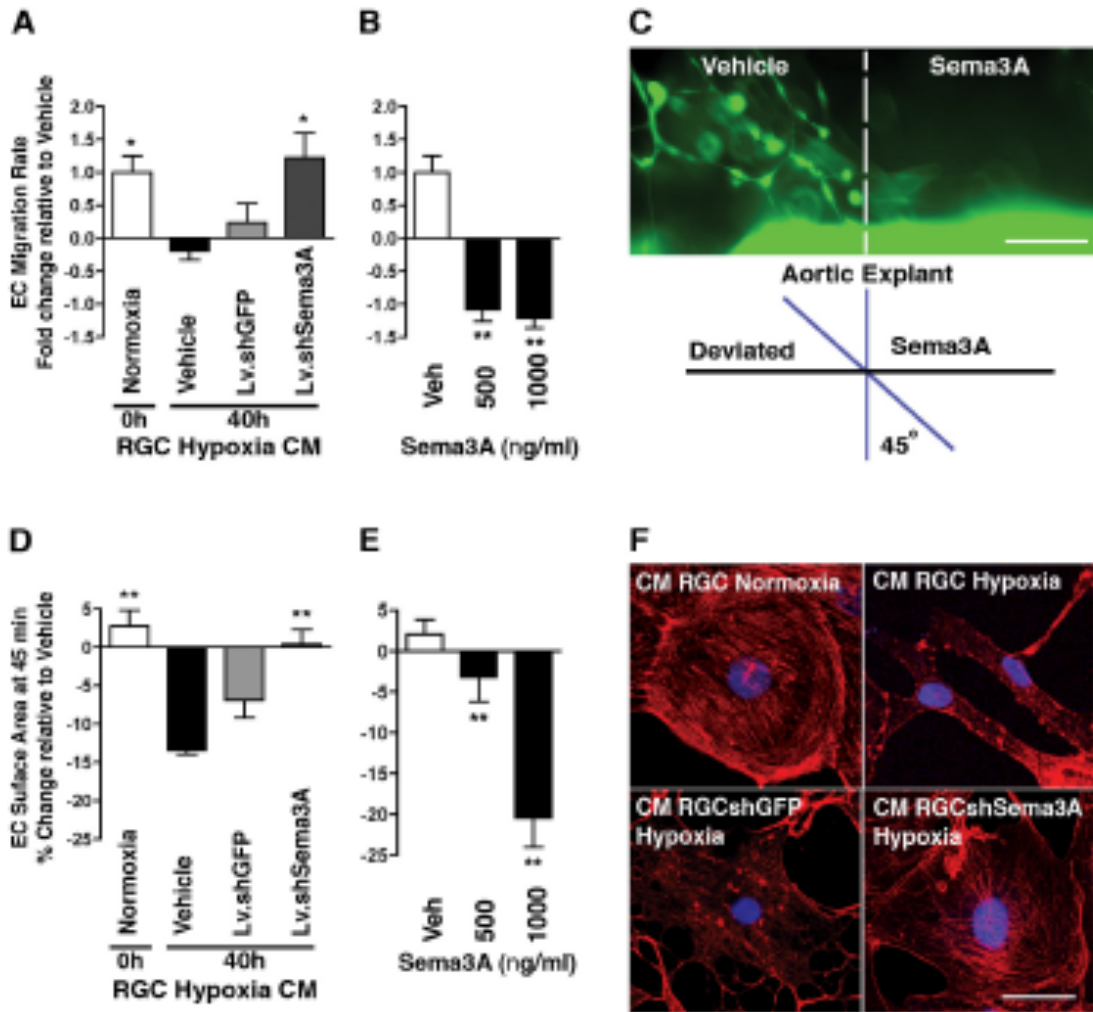


**Fig 6. Sema3A produced by hypoxic RGCs repels nascent vessels.** (A) Rates of RBMEC migration using a real-time cell analyzer. EC motility was significantly blocked by hypoxia-induced Sema3A (4.2 fold) and rescued by CM from hypoxic RGC where Sema3A was silenced (40 h). n=4; \*p<0.05 compared to vehicle at 40 h of hypoxia. (B) Effect of rSema3A on EC migration rate (over 45 min). n=3; \*\*p<0.01 compared to vehicle (Veh). (C) Propensity of Sema3A to deviate (repel) nascent vessels was established using micro-deposited Sema3A adjacent to aortic explants from GFP-mice. Vascular sprouts invaded vehicle-coated regions but avoided Sema3A-coated zones. (D) RGC-derived Sema3A modulates EC cytoskeletal arrangements and morphology, as demonstrated by time-lapse morphometric analysis of RBMEC subjected to CM (**Supplementary Fig 6B**). ECs exposed for 45 min to CM from hypoxic RGCs (40 h) contracted, while knock-down of Sema3A in the RGCs largely abrogated this effect. n=3; \*\*p<0.01 compared to vehicle at 40 h of hypoxia. (E) rSema3A provokes a dose-dependent cellular contraction (22.5%), similar in magnitude to 40 h hypoxic CM presented in panel. n=3; \*\*p<0.01 compared to vehicle (Veh). (F) Actin stress fibers in ECs. Treatment of ECs with hypoxic CM from hypoxic retinas resulted in loss of actin stress fibres and collapse of the actin network (as determined by rhodamine-phalloidin staining [red]); knockdown of Sema3A in RGCs abrogated this effect. Hence, changes in actin are consistent with those on cell shape and movement (panels A-E). Images are representative of 4 experiments. Nuclei are stained with DAPI in blue. Scale bars: (C) 20  $\mu\text{m}$ , (F) 50  $\mu\text{m}$ .

**Relative contributions: Figure 6**

- A) In vitro preparation performed by **N Sitaras**, F Binet and T Zhu  
EC Migration and analysis performed by F Binet, T Zhu, JS Joyal and T Zhu
- B) Same as A
- C) Aortic ring explant preparation performed by D Kunik, S Constantino and P Sapieha  
Sample preparation, imaging and analysis performed by JS Joyal, A Stahl and P Sapieha
- D) Lentiviral preparations performed by **N Sitaras**, JS Joyal, D Hamel and C Beauséjour  
Sample preparation, imaging and analysis performed by F Binet, JS Joyal, G Hickson and P Sapieha

Figure preparation: JS Joyal, **N Sitaras**, P Sapieha and S Chemtob

Approximate Figure contribution: 20%

Figure 7

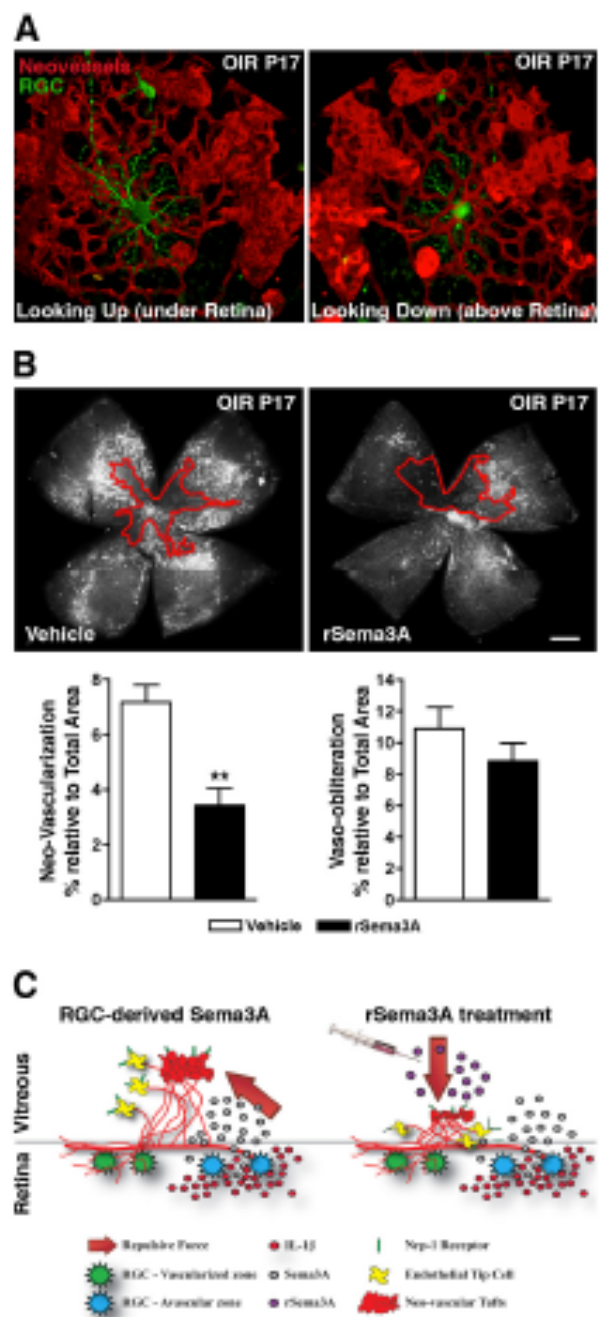


**Fig 7. Intravitreal delivery of rSema3A suppresses pre-retinal neovascularization in OIR.** (A) 3D reconstructions of pathological neovessels and RGC-YFP at P17 following OIR. The spatial distribution of retinal neurons and vessels results in the repulsion of neo-vascular tufts towards the vitreous. (B) Intravitreal injection of rSema3A (100 ng; P14) halved the formation of pre-retinal vascular tufts at P17. n=7; \*\*p=0.0012 compared to corresponding vehicle. (C) Schematic summary illustrates ischemic neurons in the avascular zones producing Sema3A secondary to inflammatory stress (IL-1 $\beta$ ). Pathologic neo-vascular tufts are enriched in Neuropilin-1 (Nrp-1). RGC-derived Sema3A impedes revascularization and repels neo-vessels away from the avascular neural-retina towards the vitreous (left). Whereas intravitreal rSema3A (injected) prevents pre-retinal invasion of pathological neovessels (right).

**Relative contributions: Figure 6**

- A) Sample preparation, imaging and analysis performed by JS Joyal, A Stahl and P Sapieha
- B) Intravitreal injections performed by JC Rivera and **N Sitaras**  
Sample preparation, imaging and analysis performed by **N Sitaras**, JS Joyal, JC Rivera and P Sapieha
- C) Schematic provided by P Sapieha

Figure preparation: JS Joyal, **N Sitaras**, P Sapieha and S Chemtob

Approximate Figure contribution: 30%

## Chapter 2

### Microglia and IL-1 $\beta$ in Ischemic Retinopathy elicit microvascular degeneration through neuronal Semaphorin3A

**Short Title:** IL-1 $\beta$  induces retinal vaso-obliteration via Sema3A

José Carlos Rivera<sup>1,2</sup>, **Nicholas Sitaras**<sup>2</sup>, Baraa Noueihed<sup>1</sup>, David Hamel<sup>1</sup>, Ankush Madaan<sup>1</sup>, Tianwei Zhou<sup>2</sup>, Jean-Claude Honoré<sup>1</sup>, Christiane Quiniou<sup>1</sup>, Jean-Sébastien Joyal,<sup>1</sup> Pierre Hardy<sup>1</sup>, Florian Sennlaub<sup>3</sup>, William Lubell<sup>4</sup>, Sylvain Chemtob<sup>1,2</sup>

<sup>1</sup>Department of Pediatrics, Ophthalmology and Pharmacology, CHU Sainte-Justine Research Center, Université de Montréal, Montréal, Québec, Canada.

<sup>2</sup>Department of Ophthalmology, Maisonneuve-Rosemont Hospital Research Center, Université de Montréal, Montréal, Québec, Canada.

<sup>3</sup>INSERM, UMR S 872, Paris, France

<sup>4</sup>Department of Chemistry, Université de Montréal, Montréal, Québec, Canada.

**Corresponding author:** Sylvain Chemtob, M.D., Ph.D. CHU Sainte-Justine, Research Center, Departments of Pediatrics, Ophthalmology and Pharmacology. 3175 Chemin Côte Ste Catherine, Montréal, Québec, Canada, H3T 1C5.

**Key words:** Interleukin-1 $\beta$ , microglia, Semaphorin 3A, vaso-obliteration, retinopathies.

#### Non-standard abbreviations and Acronyms

101.10                      Allosteric modulator of IL-1R1  
RGC-CM                    Retinal ganglion cell conditioned medium

#### *Abstract*

**Objective:** Pro-inflammatory cytokines contribute to the development of retinal vasculopathies. However the role of these factors and the mechanisms by which they elicit their effects in retina are not known. We investigated whether activated microglia during early stages of ischemic retinopathy produces excessive interleukin-1 $\beta$  (IL-1 $\beta$ ), which elicits retinal microvascular degeneration, not directly but rather by triggering

the release of the pro-apoptotic/repulsive factor Semaphorin3A (Sema3A) from neurons.

**Approach and results:** Sprague Dawley rats subjected to retinopathy induced by hyperoxia (80% O<sub>2</sub>; O<sub>2</sub>-induced retinopathy [OIR]) exhibited retinal vaso-obliteration associated with microglial activation, NLRP3 upregulation, and IL-1 $\beta$  and Sema3A release; IL-1 $\beta$  was mostly generated by microglia. Intraperitoneal administration of IL-1 receptor antagonists (IL-1Ra [Kineret], or *rytvela* [101.10]) decreased these effects and enhanced retinal revascularization; knockdown of Sema3A resulted in microvessel preservation and conversely, administration of IL-1 $\beta$  caused vaso-obliteration. In vitro, IL-1 $\beta$  derived from activated primary microglial cells cultured under hyperoxia, stimulated the release of Sema3A in retinal ganglion cells (RGC-5), which in turn induced apoptosis of microvascular endothelium; antagonism of IL-1R decreased microglial activation and on RGC-5 abolished the release of Sema3A inhibiting ensuing endothelial cell apoptosis. IL-1 $\beta$  was not directly cytotoxic to endothelial cells.

**Conclusions:** Our findings suggest that in the early stages of OIR retinal microglia are activated to produce IL-1 $\beta$ , which sustains the activation of microglia and induces microvascular injury through the release of Sema3A from adjacent neurons. Interference with IL-1 receptor or Sema3A actions preserves the microvascular bed in ischemic retinopathies and consequently decreases ensued pathological pre-retinal neovascularization.

### *Introduction*

Ischemic vasoproliferative retinopathies characterized by a retinal microvascular degeneration followed by an abnormal intravitreal neovascularization have recently been associated with neuro-inflammatory responses<sup>1-3</sup>. Interleukin-1 $\beta$  (IL-1 $\beta$ ), a major mediator of inflammation<sup>4-6</sup>, has generally been implicated in the development of vasoproliferative retinopathies such as in diabetes<sup>7</sup> and choroidal

neovascularization<sup>8,9</sup>. Yet, IL-1 $\beta$  exerts neurotoxicity<sup>2,10,11</sup>, vascular repulsion<sup>1</sup>, capillary degeneration<sup>12</sup>, induction of neovascular tumor growth,<sup>13-15</sup> and seems to modulate angiogenesis by directly interacting with vascular endothelial cells or by enhancing the production of pro-angiogenic factors in a paracrine manner<sup>6,16-18</sup>. In the eye, under ischemic conditions IL-1 $\beta$  is markedly increased in neutrophils recruited into the retina, endothelial and retinal glial cells<sup>19</sup>. Microglia are phagocytic sentinels in the central nervous system including the retina, and are also needed for neuronal homeostasis and innate immune defense<sup>20,21</sup>. However, under severe insults including hypoxic/ischemic injury, microglia become over-activated and function as a prominent source of cytotoxic oxidant stress and pro-inflammatory factors<sup>22-24</sup>. In this regard, microglial overactivation can contribute to the production of IL-1 $\beta$ , TNF- $\alpha$ , and IL-6 found in high concentrations in tissues of patients and animals with vasoproliferative retinopathy<sup>25-27</sup>, and have been linked to the development of ischemic retinopathies in humans<sup>28</sup> and animal models<sup>27, 29, 30</sup>.

IL-1 $\beta$  exerts its biological effects by interacting with the IL-1 receptor type I (IL-1RI), which is composed of a ligand binding unit and a signaling unit named the accessory protein (IL-1RacP)<sup>4</sup>. This activity is modulated endogenously by the natural IL-1 receptor antagonist (IL-1Ra) - a 17.5-kDa protein that competes with IL-1 for its binding site on IL-1RI<sup>31,32</sup>. IL-1Ra is considered an important endogenous anti-inflammatory cytokine that blocks all known actions of IL-1 $\beta$ . Previous studies have shown that recombinant IL-1Ra (Kineret) protects against IL-1 $\beta$  and excitotoxin-induced neurotoxicity<sup>33</sup>. *In vitro*, the presence of IL-1Ra has been shown to transform amoeboid microglia into ramified cells<sup>34</sup>, and inhibit endothelial cell death induced by IL-1 $\beta$  by decreasing NF $\kappa$ B and caspase-3 activation<sup>7</sup>. IL-1Ra-deficient mice are susceptible to neuronal injury following cerebral ischemia<sup>35</sup>, and conversely recombinant IL-1Ra attenuates the neurotoxicity<sup>36</sup>. Intravitreal IL-1Ra also markedly reduces laser-induced choroidal neovascularization<sup>8</sup>.

Our laboratory recently highlighted the influence of neuron-derived signalling molecules on endothelial cell function in the retina<sup>1</sup>. These signals include classic neuronal guidance cues, particularly the class III Semaphorins, implicated among its functions in inducing apoptosis<sup>37,38</sup>. However, the specific interplay of microglia and neurons in the pathogenesis of ischemic retinopathies (such as of prematurity [and diabetes]), particularly as it applies to IL-1 $\beta$ , on the critical vascular degenerative component, which precedes the aberrant vasoproliferative phase, is not known.

In this work we found in the oxygen-induced model of retinopathy of prematurity (OIR) that hyperoxia activates microglia in the retina to produce IL-1 $\beta$ , which sustains the activation of microglia and induces microvascular injury not directly, but through the release of proapoptotic/repulsive factor Sema3A from adjacent neurons. Administration of two distinct inhibitors of IL-1R (IL-1Ra, and an all-d [protease resistant] oligopeptide *rytvela* labeled 101.10<sup>39</sup>) abrogated microglial activation, IL-1 $\beta$  release and Sema3A expression in the retina and resulted in a significant decrease in vaso-obliteration and acceleration of revascularization of the avascular retina in OIR, as seen after knockdown of Sema3A.

## *Materials and Methods*

### *Animal Care*

All experimental procedures were approved by the Animal Care Committee of the Hôpital Ste-Justine in accordance with guidelines established by the Canadian Council on Animal Care.

### *Retinal vaso-obliteration model*

Since we focused on retinal vaso-obliteration we utilized a well-established model of retinopathy of prematurity—the oxygen-induced retinopathy model (OIR)-, characterized by exposing the animals to 80% O<sub>2</sub> during the first days of birth, when vasculature is still immature, and susceptible to damage caused by hyperoxia leading to retinal vaso-obliteration, a hallmark of the initial phase of ischemic retinopathies in

humans<sup>1, 2</sup>; relevantly, this model mimicks the relative hyperoxia premature infants are exposed to relative to levels in utero. Hence, Sprague- Dawley albino rat pups were placed with their mothers in an 80% oxygen environment from P5 to P10, when normal retinal vasculature reaches the periphery. The ability of IL-1Ra or 101.10 to curb vaso-obliteration was tested in two different animal groups exposed to O<sub>2</sub> from P5-P8 (first group) and P5-P10 (second group). Briefly, in each group the pups were randomly selected to receive twice daily 20 µl saline (vehicle), IL-1Ra (10 mg/kg) or 101.10 (1.5 mg/kg) intraperitoneally from P5 to P8 in the first group and from P8 to P10 in the second group; pups were euthanized respectively on P8 and P10. Eyes were enucleated and retinas dissected. Vaso-obliteration was evaluated in retinal flat-mounts. Control animals were maintained in room air (21% O<sub>2</sub>). All other conditions (e.g., light exposure, temperature, feeding, etc.) were similar for both treatment groups.

#### *Retinal neovascularization model*

Within 4 hours after birth, litters of Sprague-Dawley albino rats (Charles River, St. Constant, Québec, Canada) were placed with their mothers in an oxygen regulated environment (OxyCycler A820CV; BioSpherix Ltd., Redfield, NY) adjusted to alternate between 50% and 10% of oxygen every 24 hours for 14 days. At postnatal day 14 (P14), pups were transferred to room air (21% O<sub>2</sub>) for 4 days<sup>40</sup>. Pups were randomly selected to receive twice daily 20 µl saline (vehicle), commercial interleukin-1 receptor antagonist Kineret® [(Amgen, Canada, Inc) by intraperitoneal injections (10 mg/kg) or twice daily the recently reported allosteric modulator of IL-1 receptor, labelled 101.10 [(peptide sequence: rytvela; synthesized by Elim Biopharmaceuticals, Hayward, CA) by intraperitoneal injections (1.5 mg/kg) from birth to sacrifice<sup>39</sup>; the efficacy of doses used has previously been demonstrated<sup>39,41</sup>. This treatment protocol aimed at preventing vaso-obliteration (induced by high O<sub>2</sub>) and consequently neovascularisation. On day P18, rats were anaesthetized with isoflurane (2%) and sacrificed by decapitation. Eyes were enucleated and retinas dissected.

Neovascularization was evaluated in retinal flat-mounts stained with lectins. Control animals were maintained in room air (21% O<sub>2</sub>) throughout the 18 days. All other conditions (e.g., light exposure, temperature, feeding, etc.) were similar for both treatment groups.

### *Retinal Flat-Mounts*

In all cases the eyes were enucleated and fixed in 4% paraformaldehyde for one hour at room temperature and then stored in PBS at 4°C until used. The cornea and lens were removed and the retina was gently separated from the underlying choroid and sclera under a dissecting microscope. Then, the retinas were subjected to 100% cold methanol (-20°C) for 10 minutes, and incubated overnight at 4°C in 1% Triton X-100-1 mM CaCl<sub>2</sub>/phosphate-buffered saline (PBS) with the TRITC-conjugated lectin endothelial cell marker *Bandeiraea simplicifolia* (1:100; Sigma-Aldrich, St. Louis, MO). Retinas were washed in PBS and mounted on microscope slides (Bio Nuclear Diagnostics Inc, Toronto, ON) under cover slips with Fluoro-Gel® (Electron Microscopy Sciences, Hatfield, PA) as the mounting media.

Retinas were photographed under an epifluorescence microscope (Nikon, Eclipse E800, Rockland, MA) using a digital camera (Nikon, DXM1200, Rockland, MA) and vascular density was calculated for the full retina surface by using the software AngioTool recently described<sup>42</sup>. AngioTool computes several morphological and spatial parameters including vascular density by assessing the variation in foreground and background pixel mass densities across an image<sup>42</sup>. Vascular density in study groups was normalized with that of untreated groups raised in 21% O<sub>2</sub>. Vaso-obiterated areas were assessed as the retinal area devoid of vasculature over the total retinal area. Neovascularization was analyzed using the SWIFT-NV method<sup>43</sup>, that consists of a set of macros that was developed to quantify all the pixels represented by neovascular tufts and clusters, but not normal vessels in lectin-stained retinal whole mounts.

### *Retinal uptake of 101.10 in vivo.*

Pups were randomly selected to receive 40 µl of the peptide 101.10 labelled with fluorescein isothiocyanate (101.10-FITC), or FITC (alone; Sigma-Aldrich) as control by intraperitoneal injections (3 mg/kg) or enteral administration (5 mg/kg) in rats exposed to normoxia (21% O<sub>2</sub>) or hyperoxia (80% O<sub>2</sub>). Animals were euthanized 3 hours after drug administration, and retinas were evaluated in retinal flat-mounts co-stained with lectins and 4,6-diamidino-2-phenylindole, dihydrochloride (DAPI; 0.1 µg/mL; Molecular Probes).

### *Intravitreal injections of IL-1β*

On day P5, pup rats were anaesthetized with isoflurane (2%) and intravitreally injected into the left eye with 5ng/1µl of IL-1β, and sterile PBS was injected into the contralateral eye as control. Twenty-four hours after the administration of IL-1β, the animals were euthanized, the eyes were removed, and retinal flat-mounts stained by the lectin technique and vascular density evaluated using image J.

### *Immunofluorescence in retinal cryosections*

Seventy two hours after exposure to hyperoxia, eyes of rats treated or not with IL-1Ra or 101.10 and their corresponding controls (n=3 in each group) were enucleated and fixed in 4% paraformaldehyde at room temperature for 4 hours, incubated in 30% sucrose overnight, and then frozen and cut. Sagittal cryosections were blocked in PBS containing 1% bovine serum albumin, 1% normal goat serum, 0.1% Triton X-100 and 0.05% Tween-20 for 1 h and double labeled overnight at 40C with a 1:300 dilution of anti-IL-1β polyclonal (R&D Systems), 1:300 dilution of anti-IL-1RI polyclonal (Santa Cruz Biotechnology, inc), 1:200 of anti-Sema3A polyclonal (Abcam, Inc) or a 1:100 dilution of the anti-IL-1β monoclonal antibodies and antibodies for cell-specific proteins: microglia [Iba-1, 1:500; Wako Chemicals USA, Inc], astrocytes [GFAP, 1:500; Dako, Carpinteria, CA], neurons [NeuN, 1:100, Chemicon] and endothelium [anti-CD31, 1:100 Immunologicals Direct). The primary antibodies were labeled for 2

h with Alexa-594-conjugated goat anti-rabbit or anti-mouse IgG, or Alexa-488 goat anti-rabbit or anti-mouse IgG obtained from Molecular Probes (Eugene, OR) and used at dilutions of 1:1000 (anti-rabbit) or 1:500 (anti-mouse), respectively. Incubation with isotype antibody was used as control. Labeled retinas were examined with a laser scanning confocal microscope (Zeiss LSM 510).

#### *Primary cultures of retinal microglia cells*

Microglial cells were isolated from retinas of rats (6 days old) according to the method described previously<sup>2,44</sup>. Briefly, the eyes were enucleated, and the retinas were collected in ice-cold 0.01 M PBS. They were soaked in Dulbecco's modified Eagle's medium/F12 (1:1) (DMEM; Invitrogen, CA, USA) supplemented with 100 U/ml penicillin and 100 µg/ml streptomycin, and then washed in Hank's balanced salt solution, cut into small pieces, and digested with 0.5% trypsin for 30 min at 37°C. Then DMEM/F12 (1:1) with 10% fetal bovine serum (FBS; Hyclone, Logan, UT, USA) was added to terminate trypsinization, the retinal pieces were manually dissociated by trituration and centrifuged. The supernatant was eliminated and the cell pellet was resuspended in DMEM/F12 (1:1) + 10% FBS supplemented with 10 ng/ml recombinant murine granulocyte-macrophage colony-stimulating factor (rmGM-CSF, PreproTech, Rocky Hill, NJ, USA) and allowed to grow at 37°C in 5% CO<sub>2</sub> in 75-cm<sup>2</sup> flasks at a density of 1X10<sup>6</sup> cells/mm<sup>2</sup>. All cultures were maintained in a humidified CO<sub>2</sub> incubator (Sanyo Biomedical) and fed every 2 days. After 2 weeks, microglia were harvested by shaking the flasks at 200 rpm for 4 h in an orbital shaker at 37°C. The cell suspension was centrifuged at 1000 rpm for 5 min, and the cell pellet was resuspended in DMEM/F12 (1:1) + 10% FBS. The purity of the microglia in the cultures was determined by immunostaining the cells with Ionized Calcium Binding Adaptor Molecule-1 (Iba-1), Glial Fibrillar Acidic Protein (GFAP), or Neuronal Nuclei (NeuN), as specific markers for microglia, astrocytes and neurons, respectively. The percentage of microglial cells was about 97%, which was established after 2 weeks.

### *Microglia activation in vitro and quantification in vivo*

To study whether IL-1 $\beta$  regulates the activation of microglia, isolated retinal microglial cells (150, 000 cells/well) were treated with IL-1 $\beta$  (0.5 ng/ml) in presence or absence of IL-1Ra or 101.10. After 24 hours, the mRNA expression of IL-1 $\beta$  and Iba-1 was analyzed by qPCR. For microglia quantification, retinal flat-mounts stained with an anti-Iba-1 polyclonal antibody were used. Four representative fields in the central (vasoobliterated) zone were randomly selected in each retina. Activated microglial cells were recognized by their short and thick processes and their increased immunoreactive staining of Iba-1 (as well as IL-1 $\beta$ )<sup>45,46</sup>. The average number of Iba-1 positive cells from the four fields for each retina was calculated by using Image J. The mean and standard error of these averages from at least 4 retinas in each group was calculated.

### *Preparation of microglia-conditioned media (MGCM)*

To study the effects of hyperoxia on expression of IL-1 $\beta$ , microglial cells (250, 000 cells) were cultured in plates of 25 cm<sup>2</sup> (Sarstedt, Inc, Newton, NC, USA) with DMEM/F12 (1:1) + 10% FBS. After 24 hours the cells were starved with DMEM/F12 (1:1) free of FBS for 24 hours. Then the cells were exposed to hyperoxia (80% oxygen and 20% nitrogen; Hyp-MGCM) in a modular incubator chamber (Billups-Rothenberg, Inc) and maintained in a humidified CO<sub>2</sub> incubator at 37<sup>o</sup> C for 4, 12, and 24 h. Microglial cells in matching controls (Nor-MGCM) were incubated at 37<sup>o</sup> C in an incubator with 95% air and 5% CO<sub>2</sub> and collected at the same time points.

### *Reverse transcription and quantitative real-time PCR analysis.*

Eyes were enucleated and retinas were rapidly dissected and processed for RNA using TRizol (Invitrogen). Total cellular RNA was isolated by acidic phenol/chloroform extraction followed by treatment with DNase I (Roche Diagnostics, Mannheim, Germany) to remove any contaminating genomic DNA; 500 ng of RNA was reverse transcribed into cDNA with Moloney murine leukemia virus reverse transcriptase

(Promega, Madison, WI) in 25 $\mu$ L of reaction mixture. PCR primers targeting for IL-1 $\beta$ ; (5'-CATCTTTGAAGAAGAGCCCG-3' and 5'- GGGATTTTGTGCGTTGCTTGT-3'), Sema3A; (5'-GAGTCCCTTATCCACGACCA-3' and 5'- AATGCTTTCTCCGCTCTGAA-3'), VEGF; (5'-CAATGATGAAGCCCTGGAGT-3'and 5'- AATGCTTTCTCCGCTCTGAA-3'), Iba-1; (5'- AGAGGTGTCCAGTGGCTCCGA-3' and 5'- GTCCTCGGTCCCACCGTGTT-3'), ICAM1; (5'-TGCAGCCGGAAAGCAGATGGT3' and 5'- CACGATCACGAAGCCCGCAAT-3'), IL1Ra; (5'-TCTGTTGGCTAACCCAATCC3' and 5'- ACTTGGGGGATTGTCAAGTG-3'), Caspase-1; (5'- AAGGCACGAGACCTGTGCGAT-3' and 5'- ACCACTCGGTCCAGGAAATGCG-3'), TNF- $\alpha$ ; (5'-CTATGTGCTCCTCACCCACA-3' and 5'- TGAAGACTCCTCCCAGGTA-3'), IL-1R1; (5'-TGAATGTGGCTGAAGAGCAC-3' and 5'- CGTGACGTTGCAGATCAGTT-3'), NLRP3; (5'-TGCATGCCGTATCTGGTTGT-3' and 5'- ACGGCGTTAGCAGAAATCCA-3') were designed using Primer Bank and NCBI Primer Blast software. Quantitative analysis of gene expression was generated using an ABI Prism 7700 Sequence Detection System and the SYBR Green Master mix kit (BioRad) and gene expression was calculated relative to 18S universal primer pair (Ambion) expression using the  $\Delta$ C<sub>T</sub> method.

### *Western Blot*

Retinal samples were obtained as described above. Three retinas from different animals per sample (n=3 samples per group) were collected in tubes (Precellys Lysing Kit, 0.5 ml, MEDICORP, Montreal, CA) containing 100  $\mu$ l lyses buffer and proteases inhibitors and then homogenized in a tissue homogenizer (Precellys®24 Cat. 03119.200.RD000) at 5000 rpm- 3x15seg. The samples were then centrifuged at 10,000 rpm during 10 minutes at 40C and the supernatant was collected. 50  $\mu$ g of protein was loaded on an SDS-PAGE gel and electroblotted onto a PVDF membrane. After blocking, the membranes were incubated overnight with 1:200 rabbit antibody to VEGF-A (sc-152; Santa Cruz Biotechnology), 1:1000 rabbit antibody to Sema3A

(ab23393; Abcam), 1:200 goat antibody to rat IL-1 $\beta$  (MAB501; R&D), 1:500 rabbit antibody to IL-1R (sc-689; Santa Cruz Biotechnology) and 1:1000 mouse antibody to  $\beta$ -actin (sc-47778; Santa Cruz Biotechnology). After washing, membranes were incubated with 1:5000 horseradish peroxidase conjugated anti-rabbit, anti-goat or anti-mouse secondary antibodies (Amersham) for one hour at room temperature.

#### *MTT assay*

MTT [3-(4,5-dimethylthiazol-2-yl)-2,5-diphenyltetrazolium bromide] assays were performed to assess endothelial or microglia cell viability. Briefly, rat brain microvascular endothelial cells (RBMVEC, Cell Applications, Inc,  $1.8 \times 10^5$  cells) were seeded in 48-well plates and treated for 24 h with recombinant rat IL-1 $\beta$  (500 pg/mL; 400-01B; PeproTech), recombinant Sema3A (R&D Systems), normoxic or hyperoxic microglia-conditioned media (Norm-MGCM or Hyp-MGCM), Norm-MG-RGC-CM or Hyp-MG-RGC-CM or with normoxic or hyperoxic endothelial-RGC-conditioned media (Nor-EC-RG-CM or Hyp-EC-CM) in presence or absence of IL-1Ra or 101.10. To analyze microglia cells viability, the cells were cultured in 6-well plates ( $2.4 \times 10^5$ ) and exposed to hyperoxia (80% O<sub>2</sub>) or normoxia (21% O<sub>2</sub>) in presence or absence of *N*-acetylcysteine (NAC; 8 mM). After treatment in both types of cultures, the medium was removed and MTT (5 mg/mL, 30  $\mu$ l/well) was added followed by incubation at 37°C for 4 h. Afterwards, supernatants were carefully removed, and DMSO (30  $\mu$ l/well, Sigma-Aldrich, St. Louis, MO) was added to the cells. After insoluble crystals were completely dissolved, absorbance at 590 nm was measured using microplate reader (Awareness Technology, Inc). Cell viability was expressed as a percentage of optical density relative to control.

#### *TUNEL assay*

Retinal ganglion cell line (RGC-5,  $2.5 \times 10^4$  cells) was kindly provided by Neeraj Agarwal (University of North Texas Health Science Center, Fort Worth, TX). RGC-5 supernatant (RGC- CM) was collected after 24 hours of stimulation with Hyp-MGCM,

Norm-MGCM or directly with pure recombinant rat IL-1 $\beta$  (0.5 ng/ml) in presence or absence of IL-1Ra or 101.10. Hyp-MG- RGC-CM, Norm-MG-RGC-CM or RGC-CM+IL-1 $\beta$  was centrifuged to remove debris and filtered with 0.2- $\mu$ m filters (Millipore). To eliminate the Sema3A present in the RGC-CM, the collected medium was filtered with a Centricon (10000 MWCO, Millipore). The concentrated medium was discarded and the filtered media was immu-neutralized with a polyclonal anti-Sema3A antibody (2 $\mu$ g/ml, Abcam) in the RBMVEC assay. RBMVEC (1.8  $\times$  10<sup>5</sup> cells) were seeded in 48-well plates and treated for 24 h with Hyp-MG-RGC-CM, Norm-MG-RGC-CM or IL-1 $\beta$ -RGC-CM. After the treatment, the medium was removed and TUNEL assay was performed with an *in situ* cell- death detection kit (ApopTag® Plus, Chemicon International.) according to the manufacturer's instructions. After TUNEL staining, the samples were counterstained with 4,6-diamidino-2- phenylindole, dihydrochloride (DAPI; 0.1  $\mu$ g/mL; Molecular Probes).

#### *Immunofluorescence in RBMVEC cells*

After the treatment with Norm-MG-RGC-CM or Hyp-MG-RGC-CM for 24 hours, the medium was removed and rat brain microvascular endothelial cells (RBMVEC, Cell Applications, Inc) were washed two times with PBS, fixed with 4% paraformaldehyde for 10 minutes and incubated with a 1:500 dilution of activated caspase-3 polyclonal antibodies (Cell Signaling Technology) or a 1:300 dilution of the anti- $\beta$ -actin monoclonal antibodies (Santa Cruz Biotechnology, Inc). The primary antibodies were labelled for 2 h with Alexa-488 goat anti-rabbit (1:1000) or Alexa-594-conjugated goat anti-mouse (1:500). RBMVEC cell were co-stained with DAPI (0.1  $\mu$ g/mL; Molecular Probes) and examined with a laser scanning confocal microscope (Zeiss LSM 510).

#### *ELISA*

Conditioned media from microglial cells exposed to hypoxic or hyperoxic conditions in presence or absence of N-acetyl cysteine (NAC; Sigma-Aldrich) was collected and concentrated in Ultrafree-4 centrifugal filter unit (10,000 NMWL, Millipore) at 3,500

rpm for 10 minutes at 40C. The concentrated media (5 times) was collected and analyzed by ELISA according to the manual instructions (Rat IL-1 $\beta$ /1L-1F2 immunoassay R&D Systems, Inc, Cat. RLB00) to determine the IL-1 $\beta$  concentration in each condition.

#### *Internalization of 101.10 in HEK cells*

HEK-Blue<sup>TM</sup> IL-33/IL-1 $\beta$  cells (InvivoGen) designed to detect bioactive IL-1 $\beta$  (generated by stable transfection of the IL1-RL1 gene) and HEK293 cells (ATCC<sup>®</sup>) that do not express the IL-1RI were used. Both cell types were cultured following the manufacturer's protocols. Briefly, HEK-Blue<sup>TM</sup>IL-1 $\beta$  and HEK-293 cells were cultured in 24 well plates at densities of approximately 50,000 cells/well in 500  $\mu$ l of complete growth medium consisting of DMEM supplemented with 4.5 g/l glucose, 10% FBS, 50 U/ml penicillin, 50 mg/ml streptomycin, 100 mg/ml Normocin<sup>TM</sup> and 2 mM L-glutamine for HEK-Blue<sup>TM</sup> IL-1 $\beta$  cells or ATCC-formulated Eagle's Minimum Essential Medium, supplemented with 10% fetal bovine serum [FBS], 100 U/ml penicillin, and 100  $\mu$ g/ml streptomycin for HEK 293 cells. All cultures were maintained in a humidified incubator at 5% CO<sub>2</sub> and 37 °C. After overnight incubation, the cells were starved with Eagle's Medium or DMEM free of FBS for 4 hours. Then the cells were stimulated with human recombinant IL-1 $\beta$  (50 ng/ml/well) and incubated with 101.10-FITC or FITC alone (control) for 3, 6 and 9 hours. After incubation the cells were washed three times with PBS, fixed with 4% paraformaldehyde, stained with DAPI. Microphotographs showing the uptakes 101.10- FITC were made by confocal microscopy.

#### *IL-1 $\beta$ stimulation in RAW-Blue mouse macrophage and HEK blue cells*

Transfection with siRNA macrophages was performed as follows. Twenty micrograms of siRNA complex was mixed with 8 ml of 1mg/ml polyethylenimine solution (Polyscience Inc.) for 30 minutes and added to RAW-Blue mouse macrophages (Invivogen). The following day cells were treated with mL-1 $\beta$  (50 ng/ml) at 37°C for 4

hours. HEK blue and 293 cells were treated with human recombinant IL-1 $\beta$  in presence or absence of 1x10<sup>6</sup> M of IL-1Ra or 101.10. After treatment, the cells were collected in TRIzol (Invitrogen) and total RNA was isolated. 500 ng of RNA was combined to qScript cDNA SuperMix (Quanta Bioscience) and cDNA synthesis was performed following the manufacturer's protocol. Quantitative real-time PCR was performed on MxPro3000 (Stratagene) using iTaq SYBR Green SuperMix with ROX (Bio-Rad). siRNA primers and qPCR primers were synthesized by Alpha DNA and sequences were: siRNA: simIL-1RF557AGUAACCGUAACUGUUATT; simIL-1R-R557U AACACAGUUACGGUUACUTT; simIL-1RF1794GAAAGACCACAGUCUGCAATT ; mL1RF:AACCTTTGACCTGGGCTGTC ; mL1bF: AGATGAAGGGCTGCTTCCAAA ; expression levels were normalized against 18S rRNA endogenous control levels in each sample and calculated relative to control vehicle-treated cells. simIL1RR1794UUGCAGACUGUGGUCUUUCTT; mL1RR :CAGAGGATGGGCTCTTCTTCAA ; mL-1bR:GGAAGGTCCACGGGAAAGAC ; mRNA expression levels were normalized against 18S rRNA endogenous control levels in each sample and calculated relative to control vehicle-treated cells.

#### *Lentivirus production*

Lentiviral vectors (HIV-1 derived) were prepared as we previously reported<sup>1</sup> by transfecting HEK293T cells with a vector plasmid containing the small hairpin RNA (shRNA) against Sema3A or green fluorescent protein together with the third generation packaging plasmids pV-SVG, pMDL, and pREV (Open Biosystems).

#### *Intravitreal injections of lentivirus*

P2 rat pups were anesthetized with 3.0% isoflurane and injected intravitreally with 1  $\mu$ L of lentivirus using a 10- $\mu$ L Hamilton syringe fitted with a 50-gauge glass capillary tip. Approximately 500 ng/ $\mu$ L of lentivirus shGFP or containing shSema3A was injected. From P5 to P8 the animals were exposed to hyperoxia (80% oxygen). At P8,

the animals were sacrificed and vaso-obliteration was assessed in retinal flat-mounts.

### *Statistical Analysis*

Results are expressed as mean  $\pm$  SEM. Two-tailed independent Student *t* tests was used to analyze data. Comparisons between groups were made using 1-way ANOVA followed by the post hoc Bonferroni's multiple comparison test. Statistical significance was set at  $p < 0.05$ .

### *Results*

*Oxygen-induced retinopathy (OIR) triggers early production of IL-1 $\beta$  and other inflammatory mediators in the retina; inhibition of IL-1 $\beta$  activity decreases inflammation and retinal vaso-obliteration*

Animals were subjected to OIR as described<sup>40</sup>. At postnatal day 6 (P6) following exposure to hyperoxia (80% O<sub>2</sub>) for 20 hours there was an increase in the retinal mRNA expression of the proinflammatory cytokine, IL-1 $\beta$  (4.1-fold;  $p < 0.001$ ), the microglial marker, Iba-1 (2.6-fold;  $p < 0.01$ ), and the cytotoxic factor, Sema3A (2.1-fold;  $p < 0.05$ ), as well as other inflammatory mediators such as TNF- $\alpha$  (2.1-fold;  $p < 0.01$ ) and ICAM-1 (1.5-fold;  $p < 0.05$ ), compared to the normoxic retinas (Fig. 1); interestingly, the major inflammasome protein NOD-like receptor family pyrin domain containing-3 (NLRP3) was also increased in retina of P6 and P8 hyperoxia-exposed pups (Supplemental Fig. IA). mRNA expression of endogenous IL-1Ra did not significantly increase, and that of Caspase-1 and VEGF also remained unchanged (Fig. 1). IL-1Ra and 101.10 (started at P5) significantly attenuated hyperoxia-induced changes in IL-1 $\beta$ , TNF- $\alpha$ , ICAM-1, Iba-1, and Sema3A.

At P8, 72 h after exposure to high oxygen IL-1 $\beta$  and Iba-1 mRNA expression was greater than values in normoxia, albeit lower than at P6 (Fig. 1); IL-1Ra decreased further to below normoxia values. In contrast, Caspase-1, ICAM-1 and VEGF mRNA increased relative to values at P5; while TNF- $\alpha$  and Sema3A remained

steady. Western blot analysis confirmed the hyperoxia-induced increase in IL-1 $\beta$  and Sema3A, while VEGF expression decreased (Supplemental Fig. IB). IL-R antagonists generally decreased values for all parameters except IL-1Ra and VEGF (Fig. 1 and Supplemental Fig. IB).

At P10, 120 h after exposure to hyperoxia the mRNA expression of all inflammatory and apoptotic factors subsided, while that of the anti-inflammatory IL-1Ra and of the cytoprotective VEGF increased relative to changes at P8 (during this vaso-obliterative phase).

Both antagonists of IL-1R prevented retinal vaso-obliteration and tended to renormalize vascular density of animals subjected to hyperoxia (Fig. 2). Moreover, pups treated with both IL-1R antagonist starting at P8 (3 days after exposure to hyperoxia which leads to vaso-obliteration) till P10 exhibited a significant increment in normal revascularization (compared with the vehicle-treated rats) (Fig. 2G), as noted by a gradual decrease in vaso-obliteration; this was further substantiated by a lack of increase in VEGF by P10 (Fig. 1). In control normoxic pups IL-1Ra and 101.10 did not affect developmental retinal vascular density (Supplemental Fig. II), consistent with absence of inflammation under normal conditions. Hence, the overall decreased vaso-obliteration by IL-1R inhibitors tended to abolish the hypoxia-driven surge in VEGF (Fig. 1H). Thus as anticipated, treatments with inhibitors of the IL-1 receptor consequently diminished ensued aberrant pre-retinal neovascularization (Supplemental Fig. IIIA). Additional evidence to substantiate cytotoxic effects of IL-1 $\beta$  on retinal microvasculature was demonstrated by intravitreal injection of IL-1 $\beta$  in normoxia-raised pups (P5), which resulted 24 h later in a loss of microvasculature (Supplemental Fig. IIIB).

To ascertain actions of the all-d peptide 101.10 in retina, its local distribution was studied. 101.10 was conjugated to FITC and fluorescence detected by microscopy in retinas of injected animals. 101.10 localized principally in microglial and endothelial cells in normoxia-raised rats (Supplemental Figure IV). Animals exposed to hyperoxic conditions exhibited a significant increase in vascular and perivascular

fluorescence; FITC alone (not conjugated to 101.10) was negligibly detected in retina. Hence, 101.10 distributes in retina – more so during hyperoxia when IL-1R (to which 101.10 binds<sup>39</sup>) expression increases (Supplemental Figure ID). To determine the need for IL-1R expression for uptake of 101.10, HEK-Blue cells (that express constitutively IL1-R) and HEK293 cells devoid of IL-1R were stimulated with 1L-1 $\beta$  (0-9 h) in presence of 101.10-FITC; 101.10-FITC internalization was only observed in IL-1R-expressing cells, indicative of the need for IL-1R for cell uptake (Supplemental Fig. V).

Together these results reveal that hyperoxia induces an early increase in the expression of inflammatory mediators in the retina, and show that exogenous IL-1Ra and 101.10 comparably reduce the expression of these inflammatory components, and in turn protect the retina from retinal vascular degeneration allowing for an accelerated normal vascular regrowth and preventing against ensued pre-retinal neovascularization.

*Hyperoxia leads to activation of microglia, which in turn is the main generator of IL-1 $\beta$  in retina*

Increased Iba-1 mRNA expression in hyperoxic rats (Fig. 1B) was suggestive of microglial activation. We elaborated on this observation by examining microglial Iba-1 immunoreactivity and morphology *in situ*. IL-1 $\beta$  was mostly found in the inner retina of hyperoxic rats (at P8), largely confined to microglia (Iba-1 immunopositive; a calcium-binding protein expressed by activated microglial cells) (Fig. 3); baseline immunoreactivity (under normoxic conditions) was very weak (Fig. 3). Both exogenous IL-1Ra and 101.10 reduced intensity of IL-1 $\beta$  immunoreactivity in hyperoxic rats (Fig. 3). A slight localization of IL-1 $\beta$  was found on endothelium (CD31 immunopositive; Supplemental Fig. VI), but hardly on retinal ganglion cells (NeuN immunopositive) and astrocytes (GFAP immunopositive; Supplemental Fig. VI). IL-1R1 expression was increased by hyperoxia (at P8), and found throughout all layers of the

retina, consistent with its ubiquitous distribution (Supplemental Fig. VII); no immunoreactivity to isotype control antibody was detected.

Upon closer examination one noted overall increased Iba-1 immunoreactive cells in retinas of hyperoxic rats compared to normoxic ones (Fig. 3). Retinal microglia from normoxic rats possessed thin processes that branched as they extended from the cell soma (Fig. 3), characteristic of resting microglia. Microglia in retinas of hyperoxic rats were hypertrophied often with amoeboid shape, had fewer processes, which were thicker and shorter, consistent with differentiation into an activated phagocyte (Fig. 3). Treatment with inhibitors of IL-1R, IL-1Ra or 101.10, renormalized the number of activated microglia as well as their morphology which was more branched out similar to that in normoxic animals (Fig. 3); these observations along with those showing decreased Iba-1 mRNA in IL-1R inhibitor-treated animals (Fig. 1) suggested that IL-1 $\beta$  participates in the activation of microglia.

#### *IL-1 $\beta$ is released from microglial cells exposed to hyperoxia in vitro*

Microglia is activated and IL-1 $\beta$  is released during the hyperoxia-induced vaso-obliteration in OIR (Figs. 1 and 3). To confirm microglia as a prominent source of IL-1 $\beta$  under hyperoxic conditions, primary retinal microglial cells from pup rats at P6 were isolated and cultured (Fig. 4). Nearly all (>98%) of the isolated DAPI-positive cells from retinas of rats were immunopositive for the microglial specific marker Iba-1 (Fig. 4A) as well as lectin *Bandeiraea simplicifolia* (Fig. 4B); cells were immunonegative for macroglial marker glial fibrillary acidic protein (GFAP; Fig. 4C) and for neural marker NeuN (Fig. 4D). Exposure of microglial cells to hyperoxia (80% O<sub>2</sub>) (compared to normoxia [21%]) for 4-24 hours revealed a time-dependent robust increase in IL-1 $\beta$  mRNA expression (in cells) and protein (in cell media) (Fig. 4E and F), which was not due to an increase in viable microglial cells (Supplemental Fig. VIIIA).

Since hyperoxia results in oxidant stress in retina of young developing subjects<sup>41</sup> we determined its role in inducing IL-1 $\beta$ . The antioxidant glutathione

precursor N-acetyl cysteine markedly prevented hyperoxia-induced microglial activation as attested by diminished Iba-1, NLRP3 and IL-1 $\beta$  expression (Supplemental Fig. VIII B-E).

We also verified in isolated microglia if IL-1 $\beta$  controls activation of microglia and stimulates further generation of IL-1 $\beta$ , as inferred *in vivo* using the inhibitors of IL-1R (Fig. 1). Indeed, stimulation of microglial cells with IL-1 $\beta$  induced Iba-1 and IL-1 $\beta$  (mRNA) expression, and this effect was abrogated by inhibitors of IL-1R (Fig. 4G). This auto-amplification of IL-1 $\beta$  expression by exogenous IL-1 $\beta$  was reproduced in IL-1RI-expressing HEK cells as well as in raw-blue mouse macrophages (Supplemental Fig. IX A,B). Essentially, stimulation with exogenous IL-1 $\beta$  induced an increase in IL-1 $\beta$  mRNA in IL-1RI-expressing HEK cells; this effect was abrogated by IL-1RI antagonists; no induction of IL-1 $\beta$  was observed in IL-1RI-devoid HEK293 cells (Supplemental Fig. IX A). A similar pattern of response was observed in raw-blue mouse macrophages (Supplemental Fig. IX B).

*Activation of microglia is cytotoxic to endothelial cells through IL-1 $\beta$ -dependent induction of Semaphorin 3A in retinal ganglion cells*

Since microglial activation and increased IL-1 $\beta$  are associated with vaso-obliteration during hyperoxia *in vivo* (Figs. 2-4), we next investigated *in vitro* if conditioned media from activated microglia in culture (which contains IL-1 $\beta$  [Fig. 4F]) or if IL-1 $\beta$  is directly cytotoxic to retinal microvascular endothelial cells. Neither conditioned media from hyperoxia-exposed microglia nor exogenous IL-1 $\beta$  were directly cytotoxic to retinal microvascular cells (Fig. 4H,I). Interestingly, IL-1 $\beta$  has been reported to induce the release of the endothelial pro-apoptotic and repulsive cue Sema3A from RGC<sup>1</sup>. We first confirmed the contribution of Sema3A in vaso-obliteration as seen upon exposure to hyperoxia (when IL-1 $\beta$  levels are high [Fig. 1]). We started by showing that exposure to hyperoxia induced an increase in Sema3A expression specifically in RGC and that this increase was abolished by IL-1R antagonists (Supplemental Fig. X). We then determined the role of Sema3A on vaso-

obliteration using shRNA encoded in lentiviral vectors (Lv) as we previously reported<sup>1</sup>. Rat pups were injected at P1 with Lv.shSema3A and the contralateral (control) eye with Lv.shGFP; the shSema3a- but not the shGFP-encoded lentivirus knocked down Sema3A expression (Fig. 5). As anticipated, Lv.shSema3A but not Lv.shGFP (control) attenuated the OIR-associated vaso-obliteration at P8 (Fig. 5).

We further explored the link between IL-1 $\beta$  and Sema3A. IL-1 $\beta$  induced a time-dependent increase in Sema3A mRNA expression in cultured RGC, which was significantly attenuated by inhibitors of IL-1R (Fig. 6A); similar changes were seen on the protein by Western blot (Supplemental Fig. IE). In addition, RGC stimulated with conditioned media from hyperoxia-exposed (24 h) microglia (containing IL-1 $\beta$  [Fig. 4F]) triggered endothelial cell apoptosis as attested by activated caspase-3 (Supplemental Fig. XI) and TUNEL positivity (Fig. 6); similar results were observed with recombinant IL-1 $\beta$  (Fig. 7). Inhibitors of IL-1RI as well as anti-Sema3A antibody protected the endothelial cells (Fig. 6B,C and Fig. 7), and conversely application of Sema3A to endothelial cells triggered death (Fig. 7; Supplemental Fig. XIIA); apoptotic effects of Sema3A were unrelated to VEGF expression (Supplemental Fig. XIIB) as reported<sup>38</sup>. In contrast, hyperoxia-exposed endothelial cells did not exhibit augmented IL-1 $\beta$  formation, and treatment of RGC with conditioned media from hyperoxia-exposed endothelium did not cause endothelial cytotoxicity (Supplemental Fig. XIIC,D). Together with *in vivo* evidence that IL-1R inhibitors prevent the early hyperoxia-induced surge in Sema3A (Fig. 1C, and Supplemental Fig. X), the present findings strongly support an IL-1 $\beta$ -induced Sema3A expression and in turn endothelial cell death, consistent with Sema3A-dependent impaired vascular sprouting. Our results provide evidence for a role for IL-1 $\beta$ , (largely) from sustained activated microglia (Figs. 3 and 4), in contributing significantly to hyperoxia-induced vaso-obliteration through a mechanism involving the pro-apoptotic factor, Sema3A.

## *Discussion*

A number of studies have proposed a role for inflammatory mediators in ischemic retinopathies. In this context, the major proinflammatory cytokine IL-1 $\beta$  has been suggested to contribute to the development of proliferative diabetic retinopathy in humans as well as in animal models<sup>7,12,25,42</sup> choroidal neovascularization and retinal degeneration<sup>8,9</sup>; its role in retinopathy of prematurity has never been specifically evaluated. On one hand, IL-1 $\beta$  is primarily associated with angiogenesis.<sup>8,9,18,43</sup> Whereas, on the other hand, IL-1 $\beta$  has also been linked to retinal vascular degeneration<sup>44</sup>; this latter aspect remains unexplained. Although microglia are thought to contribute significantly to the generation of cytokines in neural tissue,<sup>2,45</sup> their involvement in retinovascular degeneration is elusive; along these lines, microglia (nonactivated) are reported to participate in normal developmental angiogenesis.<sup>46</sup> In this study, we show that retinal microglia are overactivated during the vaso-oblivation phase of ischemic retinopathies, and serve as an important source of IL-1 $\beta$ , which induces vascular degeneration not directly but rather by stimulating the generation of proapoptotic/repulsive cue Sema3A from adjacent neurons. Inhibitors of the IL-R, notably exogenous recombinant IL-1Ra and the IL-1R modulator 101.10,<sup>39</sup> decreased microglial activation and IL-1 $\beta$  release, and in turn Sema3A expression, consequently diminishing vaso-oblivation, enhancing revascularization and, thus, attenuating resultant pathological preretinal neovascularization in the established model of OIR.

A major feature in this study applies to the pivotal role of microglia not only in generating IL-1 $\beta$ , but also through this cytokine in orchestrating neurovascular degeneration through the release of Sema3A. Although microglia are known to be in intimate contact with neovascular tufts<sup>29,30</sup> because they guide the proliferating vascular bed,<sup>46</sup> mechanisms for their role in vascular degeneration is vague. We found that in response to hyperoxic stress, microglia are activated and release IL-1 $\beta$  (in vivo and in vitro), which in turn induces its endothelial cytotoxic effects via RGC-derived Sema3A; our findings do not fully exclude a contribution of cytokines by other

retinal cells.<sup>19</sup> Consistent with these findings, hyperoxic stress is tightly intertwined with inflammation<sup>47</sup> through receptors activated by products of peroxidation, such as CD<sup>36,48</sup> TLR4, and stimulation of the inflammasome<sup>49</sup>; this oxidant stress<sup>41</sup> seems to explain the generation of IL-1 $\beta$  during hyperoxia as observed here and by others.<sup>50</sup> Conversely, we found that interfering with IL-1R actions preserved retinal vasculature, enhanced revascularization, and, as a result, prevented preretinal neovascularization.

In this context, we observed that it is not so much the number of microglia that changes with the stress stimulus (hyperoxia) but rather their activation. These observations are consistent with microglial activation in human diabetic retinopathy<sup>28</sup> as well as in experimental ischemic retinopathies.<sup>30</sup> Interestingly, we also found that IL-1 $\beta$  maintains activation of microglia, and inhibition (or downregulation) of IL-1R prevents increased Iba-1 in microglia and IL1 $\beta$  expression in different cell types. Along these lines, inhibition of microglial activation (using minocycline) has been found to diminish cytokine release and reduce progression of ischemic retinopathy<sup>27</sup>; whereas exogenous IL-1Ra reduces intercellular adhesion molecule-1 expression and reinstates microglial ramification (resting condition)<sup>34</sup>; microglial activation is also reduced in IL-1R1 null mice subjected to hypoxic/ischemic insults.<sup>51</sup> Together our observations, supported by other reports, suggest an autoactivation of microglia through IL-1 $\beta$ .

In the present work, we uncover a new mechanism for IL-1 $\beta$  in inducing retinal microvascular degeneration, specifically by stimulating RGCs to produce the proapoptotic/repulsive factor Sema3A. By 20 hours of hyperoxia, microglia were activated through an IL-1 $\beta$ -dependent process, resulting in release of IL-1 $\beta$  (along with other inflammatory markers) and (consequently) in Sema3A; this *in vivo* induction in IL-1 $\beta$  expression could be reproduced and better characterized *in vitro* on cultured microglia exposed to hyperoxia; in turn, IL-1 $\beta$  was also shown to induce Sema3A in isolated RGCs. Consequently, Sema3A was responsible for microvascular endothelial cell death (*in vitro* and *in vivo*); hence, inhibition of IL-1R or of Sema3A (anti-Sema3A, or through silencing shRNA-Sema3A) exerted a relative preservation of retinal

endothelium. By 120 hours of hyperoxia (at P10), retinal vascular degeneration was found to be pronounced, resulting in a relatively hypoxic inner retina, which triggers an increase in VEGF expression in an attempt to reestablish O<sub>2</sub> supply; this does not exclude a direct role for IL-1 $\beta$  in inducing VEGF expression<sup>52-54</sup>; however, there was a general suppression of inflammatory markers at P10 (compared with P8), which may be attributable to the relative increase in IL-1Ra. Interestingly, one also notes at P10 unaltered levels of Sema3A (compared with normoxia), consistent with a rate of vaso-obliteration, which decreases from P8-P10 compared with P5-P8. Inhibition of IL-1R prevents the early (P8) rise in Sema3A, which contributes to vaso-obliteration, and facilitates revascularization; re-establishment of the O<sub>2</sub> supply to the retina suppresses a hypoxia-driven surge in VEGF at P10. A schematic model depicting our overall observations is presented in Figure 8.

A new aspect conveyed in this study applies to the efficacy of the IL-1R modulator 101.10 in ischemic retinopathies. This small stable peptide was as effective as recombinant IL-1Ra. Recombinant IL-1Ra is approved for rheumatoid arthritis, but exhibits certain drawbacks, such as pain at the site of administration, need for injection (rather than oral administration), and increased risk for infections. The allosteric modulator of IL-1R 101.10 may offer certain advantages, including possibly through its pharmacological selectivity diminish certain adverse effects such as the risk for infections.<sup>39</sup> 101.10 may represent a prototype for a new class of small (molecule) inhibitors of IL-1R, which so far are all large molecules requiring parenteral administration.<sup>55</sup>

In summary, we hereby present a critical role for IL-1 $\beta$  in contributing to the early (and consequently as well to the late) phase of OIR, by activating microglia that are major contributors in IL-1 $\beta$  generation; on one hand, IL-1 $\beta$  sustains microglial activation, and on the other induces adjacent RGCs to produce Sema3A. The latter causes microvascular degeneration contributing to the early vaso-obliteration detected in ischemic retinopathies, which predisposes to subsequent preretinal neovascularization. Distinct inhibitors of IL-1R, notably recombinant IL-1Ra and the

modulator 101.10, prevent hyperoxia-induced microglial activation, the surge in IL-1 $\beta$  formation, retinal vaso-obliteration and, consequently, preretinal neovascularization.

### *Sources of Funding*

J.C.R and J-C.H. were supported by the Heart and Stroke Foundation of Canada (HSCF) and the Canadian Stroke Network (CSN). J-S.J. is a recipient of a fellowship from the Canadian Institutes of Health Research (CIHR). N.S., B.N. and T.Z. are recipients of studentships from the Fond de la Recherche du Québec en Santé. S.C. holds a Canada Research Chair (Translational Research in Vision) and the Leopoldine Wolfe Chair in translational research in age-related macular degeneration, and grants from the CIHR.

### *Disclosures*

None

### *References*

1. Joyal JS, Sitaras N, Binet F, Rivera JC, Stahl A, Zaniolo K, Shao Z, Polosa A, Zhu T, Hamel D, Djavari M, Kunik D, Honore JC, Picard E, Zabeida A, Varma DR, Hickson G, Mancini J, Klagsbrun M, Costantino S, Beausejour C, Lachapelle P, Smith LE, Chemtob S, Sapielha P. Ischemic neurons prevent vascular regeneration of neural tissue by secreting semaphorin 3a. *Blood*. 2011;117:6024-6035
2. Sivakumar V, Foulds WS, Luu CD, Ling EA, Kaur C. Retinal ganglion cell death is induced by microglia derived pro-inflammatory cytokines in the hypoxic neonatal retina. *J Pathol*. 2011;224:245-260
3. Ishida S, Yamashiro K, Usui T, Kaji Y, Ogura Y, Hida T, Honda Y, Oguchi Y, Adamis AP. Leukocytes mediate retinal vascular remodeling during development and vaso-obliteration in disease. *Nat Med*. 2003;9:781-788

4. Dinarello CA. Immunological and inflammatory functions of the interleukin-1 family. *Annu Rev Immunol.* 2009;27:519-550
5. Dinarello CA. The biological properties of interleukin-1. *Eur Cytokine Netw.* 1994;5:517-531
6. Dinarello CA. Biologic basis for interleukin-1 in disease. *Blood.* 1996;87:2095-2147
7. Kowluru RA, Odenbach S. Role of interleukin-1beta in the pathogenesis of diabetic retinopathy. *Br J Ophthalmol.* 2004;88:1343-1347
8. Olson JL, Courtney RJ, Rouhani B, Mandava N, Dinarello CA. Intravitreal anakinra inhibits choroidal neovascular membrane growth in a rat model. *Ocul Immunol Inflamm.* 2009;17:195-200
9. Lavalette S, Raoul W, Houssier M, Camelo S, Levy O, Calippe B, Jonet L, Behar-Cohen F, Chemtob S, Guillonneau X, Combadiere C, Sennlaub F. Interleukin-1beta inhibition prevents choroidal neovascularization and does not exacerbate photoreceptor degeneration. *Am J Pathol.* 2011;178:2416-2423
10. Allan SM, Tyrrell PJ, Rothwell NJ. Interleukin-1 and neuronal injury. *Nat Rev Immunol.* 2005;5:629-640
11. Basu A, Krady JK, Levison SW. Interleukin-1: A master regulator of neuroinflammation. *J Neurosci Res.* 2004;78:151-156
12. Kowluru RA, Odenbach S. Role of interleukin-1beta in the development of retinopathy in rats: Effect of antioxidants. *Invest Ophthalmol Vis Sci.* 2004;45:4161-4166
13. Voronov E, Shouval DS, Krelin Y, Cagnano E, Benharroch D, Iwakura Y, Dinarello CA, Apte RN. Il-1 is required for tumor invasiveness and angiogenesis. *Proc Natl Acad Sci U S A.* 2003;100:2645-2650
14. Song X, Voronov E, Dvorkin T, Fima E, Cagnano E, Benharroch D, Shendler Y, Bjorkdahl O, Segal S, Dinarello CA, Apte RN. Differential effects of il-1 alpha and il-1 beta on tumorigenicity patterns and invasiveness. *J Immunol.* 2003;171:6448-6456
15. Nakao S, Kuwano T, Tsutsumi-Miyahara C, Ueda S, Kimura YN, Hamano S, Sonoda KH, Saijo Y, Nukiwa T, Strieter RM, Ishibashi T, Kuwano M, Ono M. Infiltration of cox-2-expressing macrophages is a prerequisite for il-1 beta-induced neovascularization and tumor growth. *J Clin Invest.* 2005;115:2979-2991
16. Mantovani A, Bussolino F, Dejana E. Cytokine regulation of endothelial cell function. *Faseb J.* 1992;6:2591-2599
17. Torisu H, Ono M, Kiryu H, Furue M, Ohmoto Y, Nakayama J, Nishioka Y, Sone S, Kuwano M. Macrophage infiltration correlates with tumor stage and angiogenesis in human malignant melanoma: Possible involvement of tnfa and il-1alpha. *Int J Cancer.* 2000;85:182-188
18. Carmi Y, Voronov E, Dotan S, Lahat N, Rahat MA, Fogel M, Huszar M, White MR, Dinarello CA, Apte RN. The role of macrophage-derived il-1 in induction and maintenance of angiogenesis. *J Immunol.* 2009;183:4705-4714

19. Hangai M, Yoshimura N, Yoshida M, Yabuuchi K, Honda Y. Interleukin-1 gene expression in transient retinal ischemia in the rat. *Invest Ophthalmol Vis Sci.* 1995;36:571-578
20. Langmann T. Microglia activation in retinal degeneration. *J Leukoc Biol.* 2007;81:1345-1351
21. Kreutzberg GW. Microglia: A sensor for pathological events in the CNS. *Trends Neurosci.* 1996;19:312-318
22. Block ML, Zecca L, Hong JS. Microglia-mediated neurotoxicity: Uncovering the molecular mechanisms. *Nat Rev Neurosci.* 2007;8:57-69
23. Chao CC, Hu S, Molitor TW, Shaskan EG, Peterson PK. Activated microglia mediate neuronal cell injury via a nitric oxide mechanism. *J Immunol.* 1992;149:2736-2741
24. Burguillos MA, Deierborg T, Kavanagh E, Persson A, Hajji N, Garcia-Quintanilla A, Cano J, Brundin P, Englund E, Venero JL, Joseph B. Caspase signalling controls microglia activation and neurotoxicity. *Nature.* 2011;472:319-324
25. Demircan N, Safran BG, Soylu M, Ozcan AA, Sizmaz S. Determination of vitreous interleukin-1 (il-1) and tumour necrosis factor (tnf) levels in proliferative diabetic retinopathy. *Eye (Lond).* 2006;20:1366-1369
26. Mocan MC, Kadayifcilar S, Eldem B. Elevated intravitreal interleukin-6 levels in patients with proliferative diabetic retinopathy. *Can J Ophthalmol.* 2006;41:747-752
27. Krady JK, Basu A, Allen CM, Xu Y, LaNoue KF, Gardner TW, Levison SW. Minocycline reduces proinflammatory cytokine expression, microglial activation, and caspase-3 activation in a rodent model of diabetic retinopathy. *Diabetes.* 2005;54:1559-1565
28. Zeng HY, Green WR, Tso MO. Microglial activation in human diabetic retinopathy. *Arch Ophthalmol.* 2008;126:227-232
29. Davies MH, Eubanks JP, Powers MR. Microglia and macrophages are increased in response to ischemia-induced retinopathy in the mouse retina. *Mol Vis.* 2006;12:467-477
30. Fischer F, Martin G, Agostini HT. Activation of retinal microglia rather than microglial cell density correlates with retinal neovascularization in the mouse model of oxygen-induced retinopathy. *J Neuroinflammation.* 2011;8:120
31. Carter DB, Deibel MR, Jr., Dunn CJ, Tomich CS, Laborde AL, Slightom JL, Berger AE, Bienkowski MJ, Sun FF, McEwan RN, et al. Purification, cloning, expression and biological characterization of an interleukin-1 receptor antagonist protein. *Nature.* 1990;344:633-638
32. Gabay C, Smith MF, Eidlen D, Arend WP. Interleukin 1 receptor antagonist (il-1ra) is an acute-phase protein. *J Clin Invest.* 1997;99:2930-2940
33. Thornton P, Pinteaux E, Gibson RM, Allan SM, Rothwell NJ. Interleukin-1-induced neurotoxicity is mediated by glia and requires caspase activation and free radical release. *J Neurochem.* 2006;98:258-266

34. Wirjatijasa F, Dehghani F, Blaheta RA, Korf HW, Hailer NP. Interleukin-4, interleukin-10, and interleukin-1-receptor antagonist but not transforming growth factor-beta induce ramification and reduce adhesion molecule expression of rat microglial cells. *J Neurosci Res.* 2002;68:579-587
35. Pinteaux E, Rothwell NJ, Boutin H. Neuroprotective actions of endogenous interleukin-1 receptor antagonist (il-1ra) are mediated by glia. *Glia.* 2006;53:551-556
36. Relton JK, Rothwell NJ. Interleukin-1 receptor antagonist inhibits ischaemic and excitotoxic neuronal damage in the rat. *Brain Res Bull.* 1992;29:243-246
37. Gagliardini V, Fankhauser C. Semaphorin iii can induce death in sensory neurons. *Mol Cell Neurosci.* 1999;14:301-316
38. Guttmann-Raviv N, Shraga-Heled N, Varshavsky A, Guimaraes-Sternberg C, Kessler O, Neufeld G. Semaphorin-3a and semaphorin-3f work together to repel endothelial cells and to inhibit their survival by induction of apoptosis. *J Biol Chem.* 2007;282:26294-26305
39. Quiniou C, Sapieha P, Lahaie I, Hou X, Brault S, Beauchamp M, Leduc M, Rihakova L, Joyal JS, Nadeau S, Heveker N, Lubell W, Sennlaub F, Gobeil F, Jr., Miller G, Pshezhetsky AV, Chemtob S. Development of a novel noncompetitive antagonist of il-1 receptor. *J Immunol.* 2008;180:6977-6987
40. Zaniolo K, Sapieha P, Shao Z, Stahl A, Zhu T, Tremblay S, Picard E, Madaan A, Blais M, Lachapelle P, Mancini J, Hardy P, Smith LE, Ong H, Chemtob S. Ghrelin modulates physiologic and pathologic retinal angiogenesis through ghsr-1a. *Invest Ophthalmol Vis Sci.* 2011;52:5376-5386
41. Hardy P, Beauchamp M, Sennlaub F, Jr Gobeil F, Jr., Mwaikambo B, Lachapelle P, Chemtob S. Inflammatory lipid mediators in ischemic retinopathy. *Pharmacol Rep.* 2005;57 Suppl:169-190
42. Abu el Asrar AM, Maimone D, Morse PH, Gregory S, Reder AT. Cytokines in the vitreous of patients with proliferative diabetic retinopathy. *Am J Ophthalmol.* 1992;114:731-736
43. BenEzra D, Hemo I, Maftzir G. In vivo angiogenic activity of interleukins. *Arch Ophthalmol.* 1990;108:573-576
44. Vincent JA, Mohr S. Inhibition of caspase-1/interleukin-1beta signaling prevents degeneration of retinal capillaries in diabetes and galactosemia. *Diabetes.* 2007;56:224-230
45. Kaur C, Rathnasamy G, Ling EA. Roles of activated microglia in hypoxia induced neuroinflammation in the developing brain and the retina. *J Neuroimmune Pharmacol.* 2012
46. Checchin D, Sennlaub F, Levavasseur E, Leduc M, Chemtob S. Potential role of microglia in retinal blood vessel formation. *Invest Ophthalmol Vis Sci.* 2006;47:3595-3602
47. Rahman I, Biswas SK, Jimenez LA, Torres M, Forman HJ. Glutathione, stress responses, and redox signaling in lung inflammation. *Antioxid Redox Signal.* 2005;7:42-59

48. Li W, Febbraio M, Reddy SP, Yu DY, Yamamoto M, Silverstein RL. Cd36 participates in a signaling pathway that regulates ros formation in murine vsmcs. *J Clin Invest.* 2010;120:3996-4006
49. Shichita T, Hasegawa E, Kimura A, Morita R, Sakaguchi R, Takada I, Sekiya T, Ooboshi H, Kitazono T, Yanagawa T, Ishii T, Takahashi H, Mori S, Nishibori M, Kuroda K, Akira S, Miyake K, Yoshimura A. Peroxiredoxin family proteins are key initiators of post-ischemic inflammation in the brain. *Nat Med.* 2012;18:911-917
50. Beauchamp MH, Sennlaub F, Speranza G, Gobeil F, Jr., Checchin D, Kermorvant-Duchemin E, Abran D, Hardy P, Lachapelle P, Varma DR, Chemtob S. Redox-dependent effects of nitric oxide on microvascular integrity in oxygen-induced retinopathy. *Free Radic Biol Med.* 2004;37:1885-1894
51. Basu A, Lazovic J, Krady JK, Mauger DT, Rothstein RP, Smith MB, Levison SW. Interleukin-1 and the interleukin-1 type 1 receptor are essential for the progressive neurodegeneration that ensues subsequent to a mild hypoxic/ischemic injury. *J Cereb Blood Flow Metab.* 2005;25:17-29
52. Konishi N, Miki C, Yoshida T, Tanaka K, Toiyama Y, Kusunoki M. Interleukin-1 receptor antagonist inhibits the expression of vascular endothelial growth factor in colorectal carcinoma. *Oncology.* 2005;68:138-145
53. Moore JE, McMullen TC, Campbell IL, Rohan R, Kaji Y, Afshari NA, Usui T, Archer DB, Adamis AP. The inflammatory milieu associated with conjunctivalized cornea and its alteration with il-1 ra gene therapy. *Invest Ophthalmol Vis Sci.* 2002;43:2905-2915
54. Biswas PS, Banerjee K, Zheng M, Rouse BT. Counteracting corneal immunoinflammatory lesion with interleukin-1 receptor antagonist protein. *J Leukoc Biol.* 2004;76:868-875
55. Zhang H. Anti-il-1beta therapies. *Recent Pat DNA Gene Seq.* 2011;5:126-135

## *Significance*

IL-1 $\beta$  is a major pro-inflammatory cytokine that is vasoproliferative for endothelium from tumors and choroid. Although it is detected in high levels in retina in ischemic retinopathies such as that associated with diabetes (and prematurity), its role in the corresponding vasculopathy is unknown. We found in ischemic retinopathies, that the majority of IL-1 $\beta$  arises from activated microglia and participates in its auto-activation. IL-1 $\beta$  was cytotoxic to retinal vasculature. However, this effect was not direct but rather occurs through a complex process involving activation of neurons to produce Semaphorin 3A, which in turn induces apoptosis of retinal microvascular endothelium. Inhibition of IL-1 $\beta$  (using IL-1Ra [Kineret], or a novel allosteric modulator d-peptide *rytvela*) or of Semaphorin 3A preserves retinal microvasculature and prevents ensuing aberrant intra-vitreous neovascularization – a predisposition to blindness. IL-1 $\beta$  is thus an important target which so far has attracted little attention for ischemic retinopathies; approved inhibitors may yield clinical benefits.

## *Specific contributions from the candidate*

The contribution of IL-1 $\beta$  and microglia in Ischemic Retinopathies (IRs) is not so well defined; elevated levels of both cytokine and cell in the retina have been documented in the literature in patients with DR and ROP and they appear to have a causal role in exacerbating IRs. Dr. JC Rivera and Dr. S Chemtob initially set out to explore how microglia and IL-1 $\beta$  effectively contribute to the pathogenesis of IRs. In the previous study, published in *Blood*, we crudely outlined the contribution of inflammation and IL-1 $\beta$  in the induction of Sema3A expression; my contribution in this

study was determining the precise interaction between microglia cells and neurons in producing Sema3A (via IL-1 $\beta$ ), which, in turn, cause vascular decay.

Precisely, I contributed to the development of the project through planning, designing and performing the experiments. I partook in gathering and analyzing data, and preparing figures for the manuscript. Finally I contributed to scripting and editing the manuscript.

Dr. JS Joyal, Dr. P Hardy, Dr. F Sennlaub and Dr. W Lubell provided expert opinion in the study.

## Figures for Chapter 2

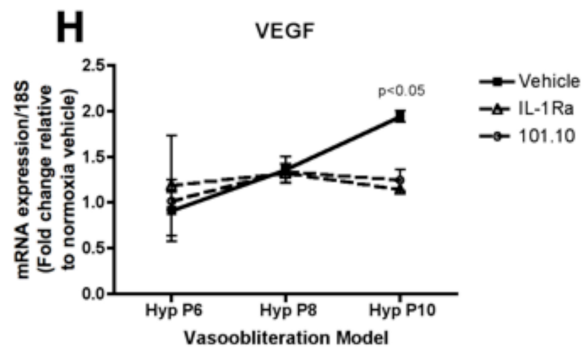
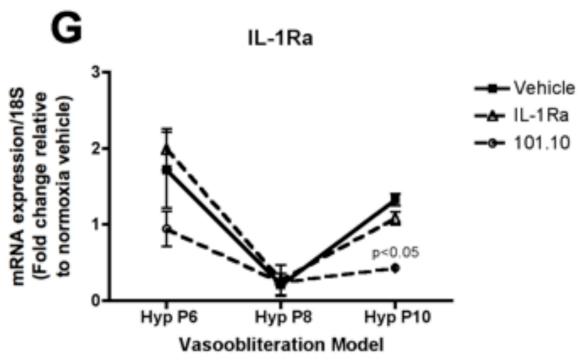
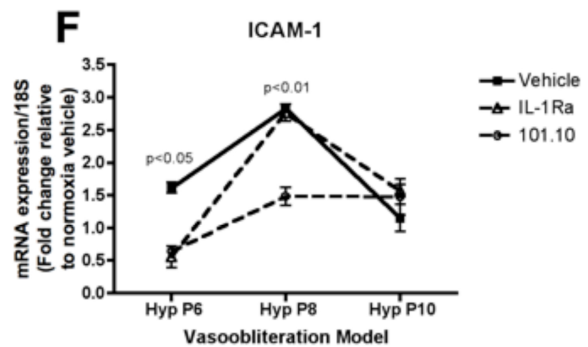
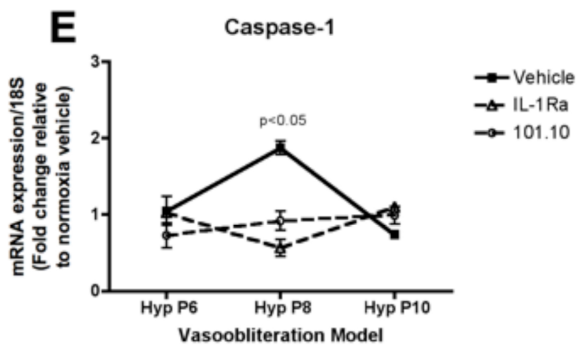
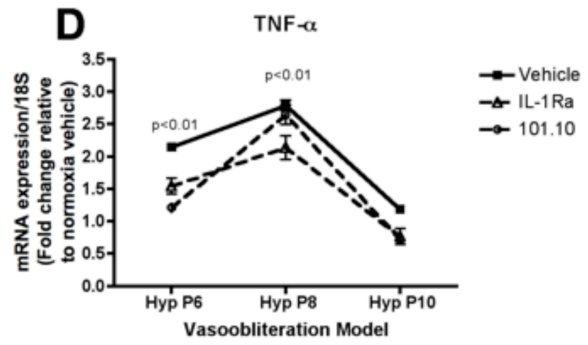
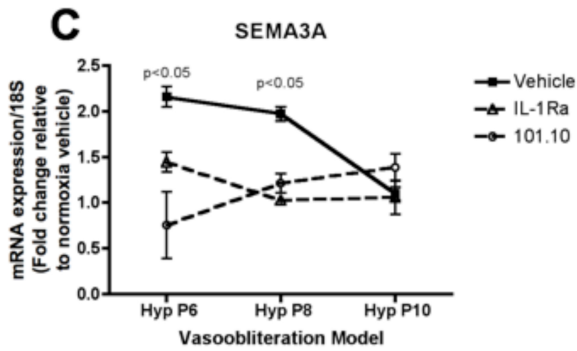
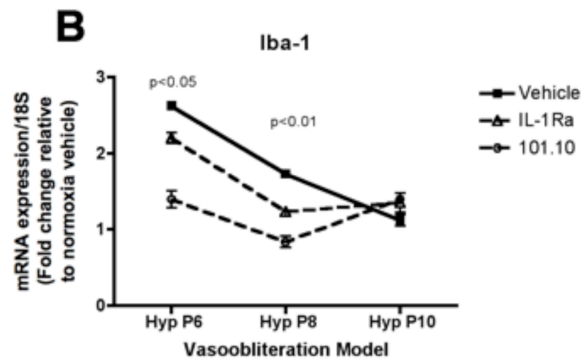
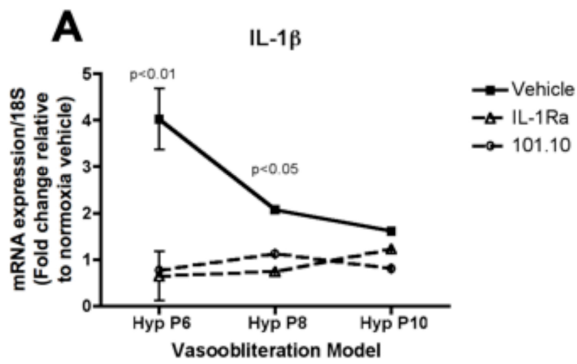


**Figure 1. Hyperoxia triggers the production of inflammatory mediators and other factors in the retina.** Quantitative RT-PCR analysis on whole retinas from animals exposed to hyperoxia (80% O<sub>2</sub>) for 20 hours (HypP6) and from P5 to P8 (HypP8) or P5 to P10 (HypP10) treated intraperitoneally with vehicle, IL-1Ra or 101.10; normoxic control values were set at 1. An increment in the retinal mRNA expression of IL-1 $\beta$ , Iba-1, Sema3A, TNF- $\alpha$  and ICAM-1, was seen 20 hours after exposure to hyperoxia (80%) (at P6) compared to the normoxic retinas. By P8 and P10 the mRNA expression of IL-1 $\beta$ , Iba-1 and Sema3A gradually decreased compared to values at P6. IL-1R inhibitors decreased IL-1 $\beta$ , Iba-1 and Sema3A values at P6 and P8. Values are mean  $\pm$  SEM of 3-4 experiments. The fold changes were normalized to 18S as internal control. Significant differences (p value) in the mRNA levels between vehicle and IL-1Ra or 101.10 treatments are shown in the graphs.

**Relative contributions: Figure 1**

A) through H) Drug administration, sample preparation performed by JC Rivera and JC Honoré

qPCR and analysis performed by **N Sitaras** and JC Rivera

Animal handling and sample collection: JC Rivera and **N Sitaras**

Figure preparation: JC Rivera, **N Sitaras** and S Chemtob

Approximate Figure contribution: 50%

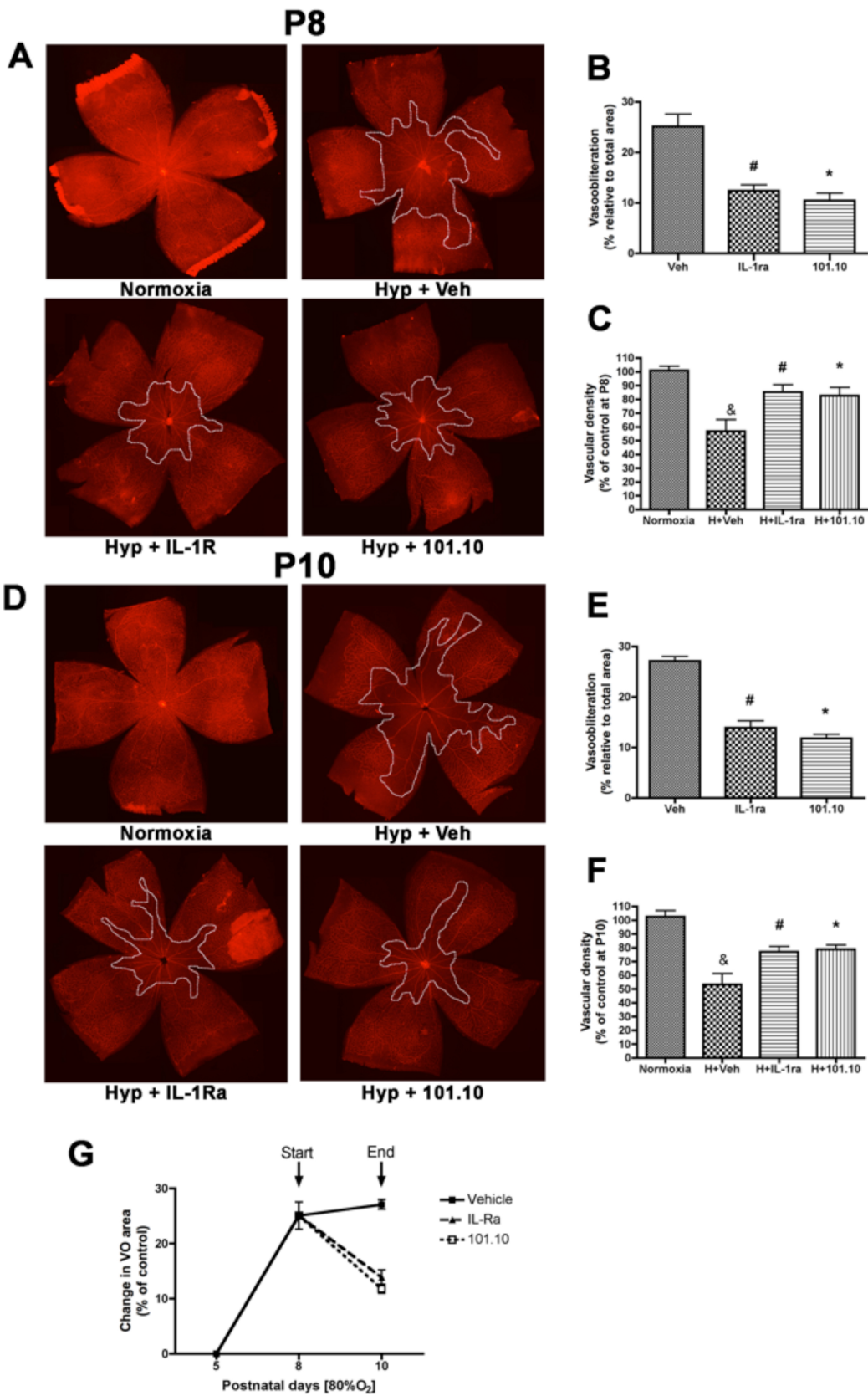


**Figure 2. Inhibition of IL-1 $\beta$  activity decreases retinal vaso-obliteration and promotes revascularization.** Representative images of flat-mounted retinas labeled with *Griffonia simplicifolia* lectin to examine vascularization at P8 (**A**) and at P10 (**D**); the central outline delimits the vasoobliterated (VO) region. In the top panels (**A-C**) rat pups (n=5-6 per group) were treated with vehicle or IL-1R antagonists, and maintained in hyperoxia (80% oxygen) from P5 to P8; one notes a 26% central capillary dropout area (white areas) and 44% decrease in vascular density in controls (compared to pups exposed to 21% oxygen). Whereas IL-1Ra and 101.10 treatments significantly reduced the capillary dropout areas to ~10% (**B**; #\*p<0.05 versus hyperoxia [vehicle-treated], and increased vascular density to ~85% [**C**; &p=0.001 vs normoxia, #\*p<0.05 versus hyperoxia [vehicle]). In lower panels (**D-G**) rat pups (n=5-6) were maintained in hyperoxia (80% oxygen) from P5 to P10 (**D**) and treated with vehicle or IL-1R antagonists from P8 (when vaso-obliteration was already present) until P10. In vehicle-treated animals there was a 29% central capillary dropout area and 48% reduction in vascular density compared to the control. Treatment with both antagonists of IL-1R (starting at P8 and ending at P10, see arrows in Fig. G) reduced significantly the central capillary dropout area to ~13% (**E**; #\*p<0.05 versus hyperoxia [vehicle]), and increased vascular density to ~78% (**F**), and promoted revascularization as noted by decrease in vaso-obliteration between P8 and P10 (**G**; &p<0.001 vs normoxia, #p<0.01 and \*p<0.001 versus hyperoxia [vehicle]).

**Relative contributions: Figure 2**

A) through G) Drug administration, sample preparation performed by JC Rivera, **N Sitaras** and JC Honoré

Imaging and analysis performed by JC Rivera and **N Sitaras**

Animal handling and sample collection: JC Rivera

Figure preparation: JC Rivera and S Chemtob

Approximate Figure contribution: <10%

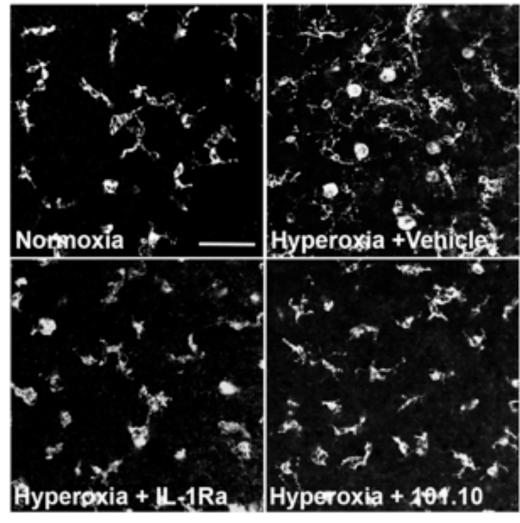
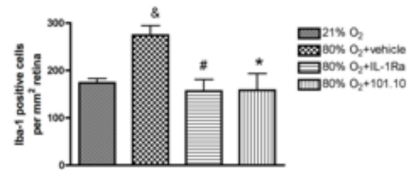
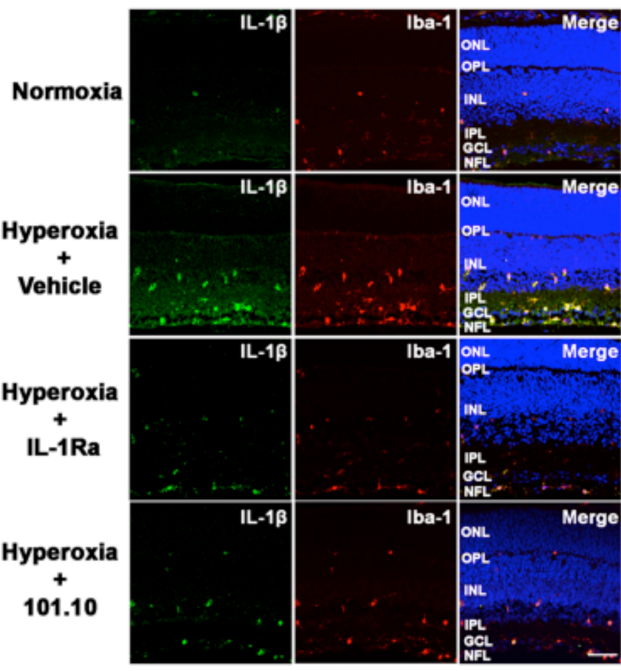


**Figure 3. Hyperoxia-induced generation of IL-1 $\beta$  is largely produced by activated microglia in the retina. (Left panels)** Representative confocal images showing immunoreactivity of IL-1 $\beta$  (green) and Iba-1 (red) merged with DAPI (blue and yellow) in retinal cryosections from 8-day-old rats (n=3 per group) after 3 days in normoxia (21% O<sub>2</sub>) or hyperoxia (80% O<sub>2</sub>). Co-staining of IL-1 $\beta$  with Iba-1 was detected mainly on activated microglial cells localized in the nerve fiber layer (NFL) or the ganglion cell layer (GCL) in retinas from hyperoxic pups treated with vehicle. Retinas from hyperoxic rat pups treated with IL-1Ra or 101.10 reveal a decrement in IL-1 $\beta$  staining and a resting microglia phenotype (Iba-1 labeling) similar to the normoxic animals in the outer nuclear layer (ONL) and GCL. Scale bar = 50  $\mu$ m. **(Right panels)** Quantitative analysis of the number of Iba-1 immunopositive cells in retinal flat-mounts (n=3-4 per group) from pups exposed to normoxia (21% O<sub>2</sub>) or hyperoxia (80% O<sub>2</sub>) from P5 until P8 and treated with vehicle, IL-1Ra or 101.10; &p<0.01 vs normoxia, # p<0.01 vs hyperoxia. Representative photomicrographs from retinal flat-mounts stained with Iba-1 (white) showed a predominant labeling of ramified, non-activated microglia in animals exposed to normoxic conditions, whereas a large number of amoeboid/activated cells were present in retinas under hyperoxic conditions. Hyperoxic animals receiving IL-1Ra or 101.10 administrations displayed a reverse phenotype of microglia with long protrusions typical of resting microglia. Scale bar = 50  $\mu$ m.

**Relative contributions: Figure 3**

Drug administration performed by JC Rivera, **N Sitaras** and JC Honoré

Imaging and analysis performed by JC Rivera and **N Sitaras**

Animal handling and sample collection: JC Rivera

Figure preparation: JC Rivera and S Chemtob

Approximate Figure contribution: <10%

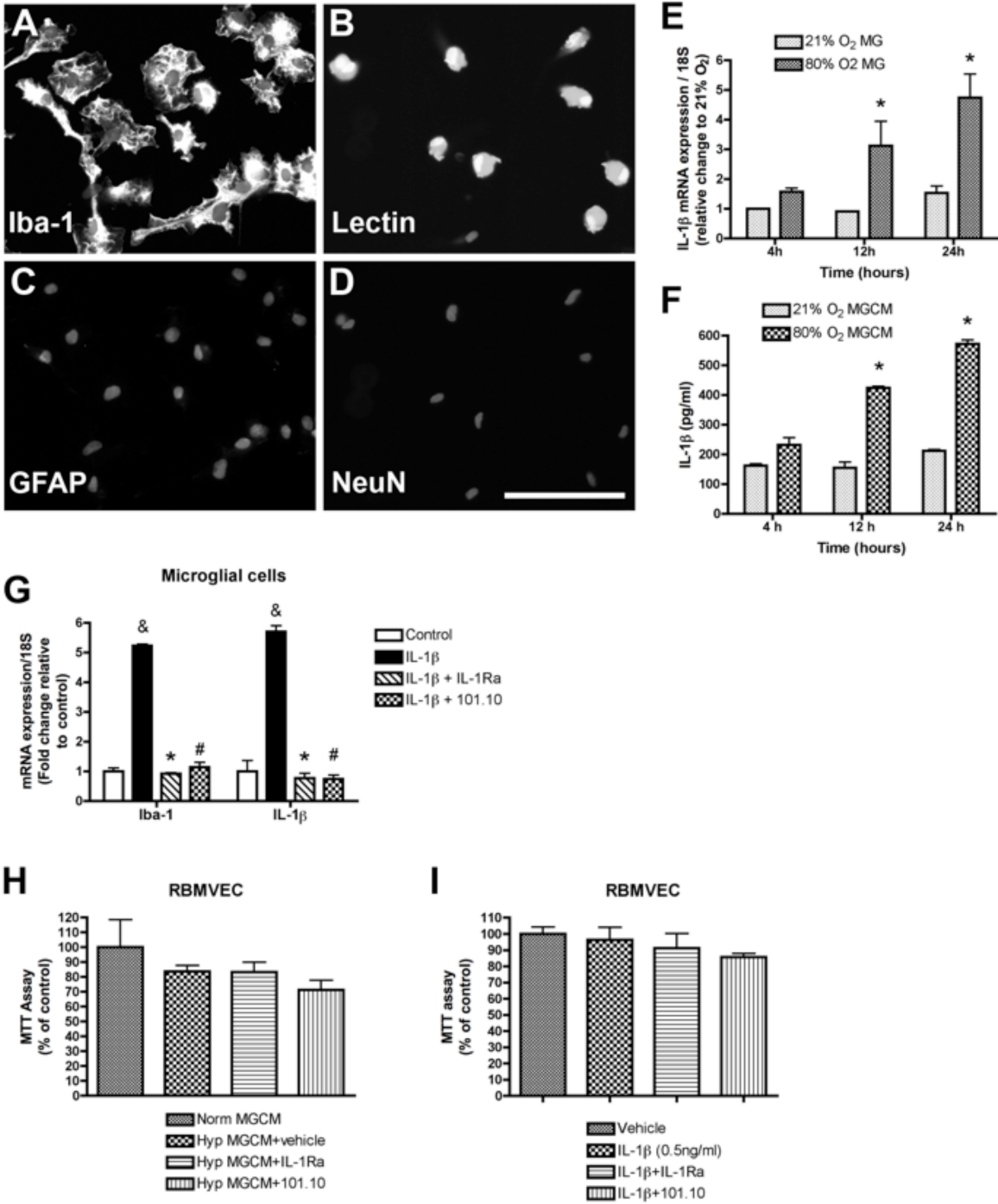


**Figure 4. IL-1 $\beta$  is released from microglial cells exposed to hyperoxia *in vitro*.**

Representative retinal microglial cultures isolated from 6 days old rats, and characterized by double immunostaining for the classic microglial markers Iba-1 (**A**), and lectin (**B**); cultures (n=4) were immune-negative for the specific astrocyte marker glial fibrillary acidic protein (GFAP, **C**) and the specific neural marker neuronal nuclei (NeuN, **D**). Scale bar = 50  $\mu$ m. mRNA and protein expression of IL-1 $\beta$  were evaluated respectively by qRT-PCR on cell culture lysates (**E**) or by ELISA in the conditioned media (**F**) from primary microglia cells (n=3-4 per condition) exposed to 21% and 80% of oxygen levels for 4, 12 and 24 hours. \*p<0.001 vs 21% O<sub>2</sub>. Microglial cell cultures (n=4) exposed to IL-1 $\beta$  (0.5 ng/ml) resulted in an increment in mRNA expression for Iba-1 and IL-1 $\beta$ , that was significantly suppressed with both IL-1R antagonists treatment (**G**). & p<0.001 vs control and \*# p<0.001 vs IL-1 $\beta$  treatment. No changes were observed in cell viability evaluated by MTT reduction assay on neuro-microvascular endothelial cells (RBMVEC; n=3) treated with hyperoxic (80% O<sub>2</sub>) microglial media (**H**) or IL-1 $\beta$  protein (**I**; 0.5 ng/ml), in absence (vehicle) or presence of IL-1Ra or 101.10 for 24 hours. Conditioned media from microglial cells exposed to normoxia (21%) or PBS (vehicle) were used as controls.

**Relative contributions: Figure 4**

A) through D) Microglial isolation, expansion and characterization performed by JC Rivera and C Quiniou

E) and F) In vitro assay and qPCR analysis performed by JC Rivera, **N Sitaras**, B Noueihed and A Madaan

H) and I) In vitro assay and analysis performed by JC Rivera, **N Sitaras**, B Noueihed and A Madaan

Animal handling and sample collection: JC Rivera

Figure preparation: JC Rivera, **N Sitaras**, B Noueihed and S Chemtob

Approximate Figure contribution: 30%

# OIR

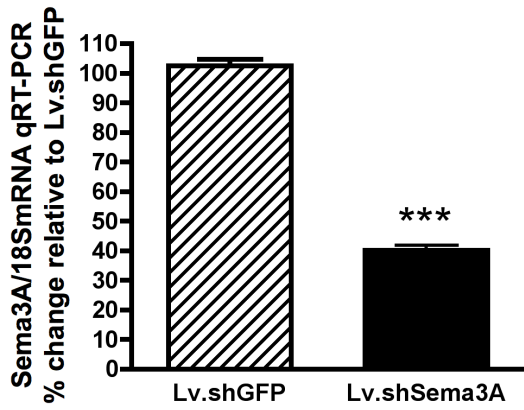
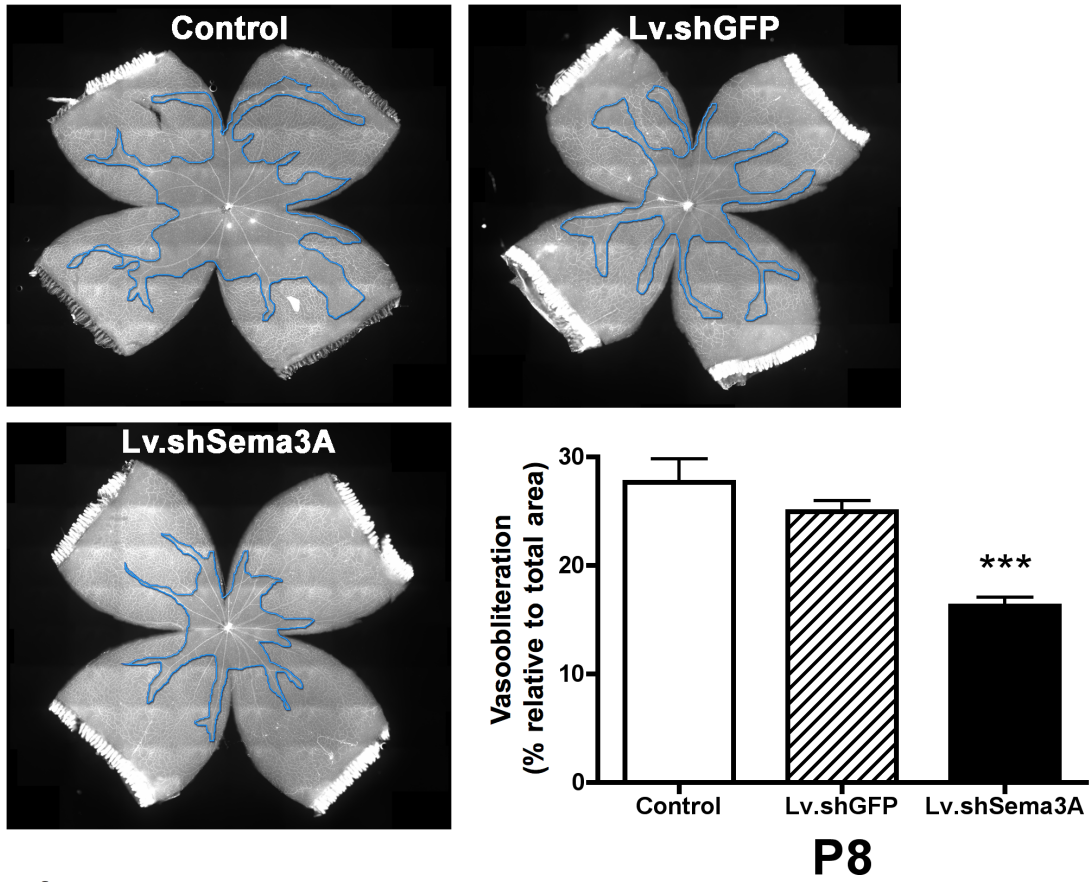


**Figure 5. Sema3A contributes to vaso-obliteration in rat pups exposed to hyperoxia.** Representative photomicrographs of *Griffonia simplicifolia* lectin-stained flat-mount retinas at P8 reveal that rat pups (n=4-5) receiving an intravitreal injection of Lv.shSema3A show a 36 % reduction in the area of vaso-obliteration (central outline) compared with contra-lateral eyes receiving Lv.shGFP injections and noninjected eyes (control). Specificity of shSema3A was confirmed by qRT-PCR, where Sema3A expression was diminished (vs Lv.shGFP). n=3; \*\*\*p<0.01 compared to corresponding Lv.shGFP. Values in the histogram are presented as the rate change in vaso-obliterated areas relative to Lv.shGFP-treated controls  $\pm$  SEM. \*\*\*p<0.01 vs Lv.shGFP.

**Relative contributions: Figure 5**

Lentiviral preparation performed by **N Sitaras** and D Hamel

Intravitreal injections performed by JC Rivera and **N Sitaras**

Immunohistochemistry, imaging and analysis performed by JC Rivera and **N Sitaras**

Animal handling and sample collection: JC Rivera and **N Sitaras**

Figure preparation: JC Rivera, **N Sitaras** and S Chemtob

Approximate Figure contribution: 40%

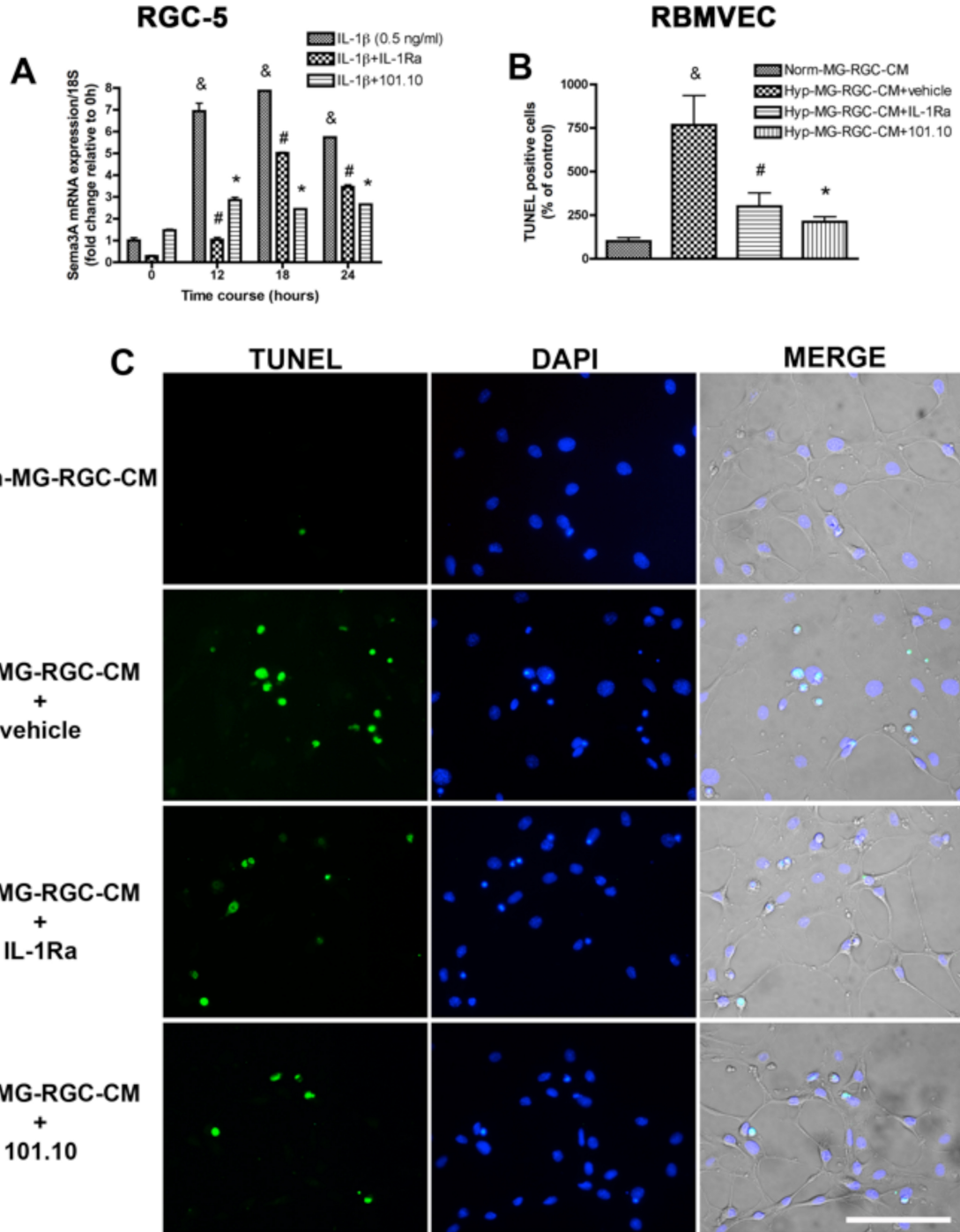


**Figure 6. Activation of microglia is cytotoxic to endothelial cells through IL-1 $\beta$ -dependent generation of Semaphorin 3A by retinal ganglion cells. (A)** RGC-5 stimulated with IL-1 $\beta$  (0.5 ng/ml; n=3) elicited an increase in Sema3A expression (at 12, 18 and 24 hours), that was suppressed by IL-1Ra or 101.10. <sup>&</sup>p<0.001 vs 0 hours, <sup>#</sup>p<0.001 vs IL-1 $\beta$  effect. Representative photomicrographs of apoptotic cells (**C**; green nuclei) detected by TUNEL on RBMVEC treated for 48 hours with conditioned medium from RGC-5 cells which were previously stimulated with normoxia- (21% O<sub>2</sub>; Norm-MG-RGC-CM) or hyperoxia-exposed (80% O<sub>2</sub>) media from microglia untreated (vehicle; Hyp-MG-RGC-CM) or treated with IL-1Ra or 101.10. Co-localization of RBMVECs nucleus stained with DAPI (blue) and TUNEL staining were merged with phase contrast. Scale bar = 50 $\mu$ m. (**B**) Histogram compiles percent TUNEL-positive cells determined in three different fields for each group (n=3) and normalized to the control (Normoxia). <sup>&</sup>p=0.01 vs Norm-MG-RGC-CM, <sup>#</sup>p<0.05 vs Hyp-MG-RGC-CM-vehicle.

**Relative contributions: Figure 6**

- A) In vitro assay and qPCR analysis performed by JC Rivera, **N Sitaras** and B Noueihed
- B) In vitro assay and TUNEL analysis performed by JC Rivera, **N Sitaras**
- C) Immunocytochemistry, imaging and analysis performed by JC Rivera

Figure preparation: JC Rivera, **N Sitaras** and S Chemtob

Approximate Figure contribution: 20%

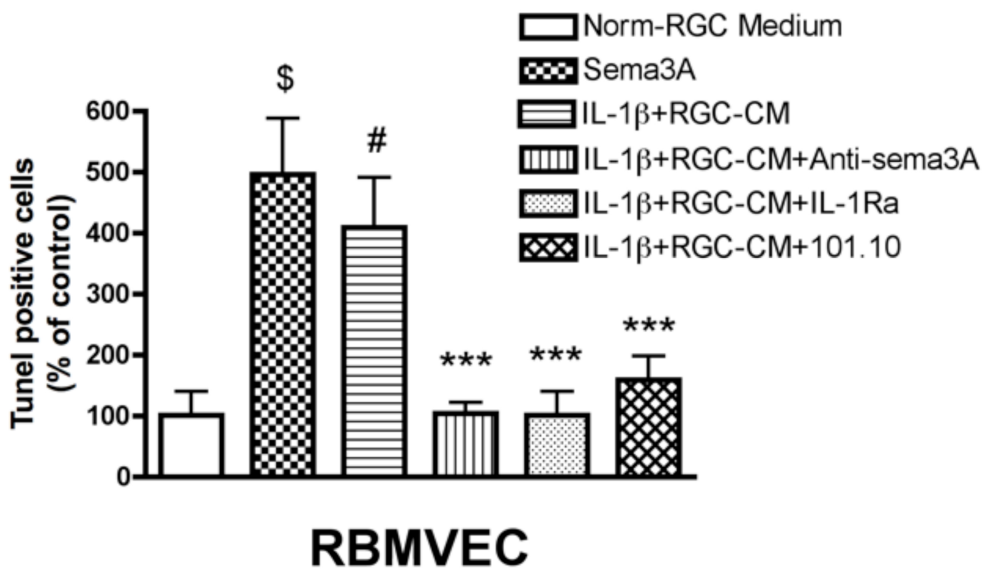
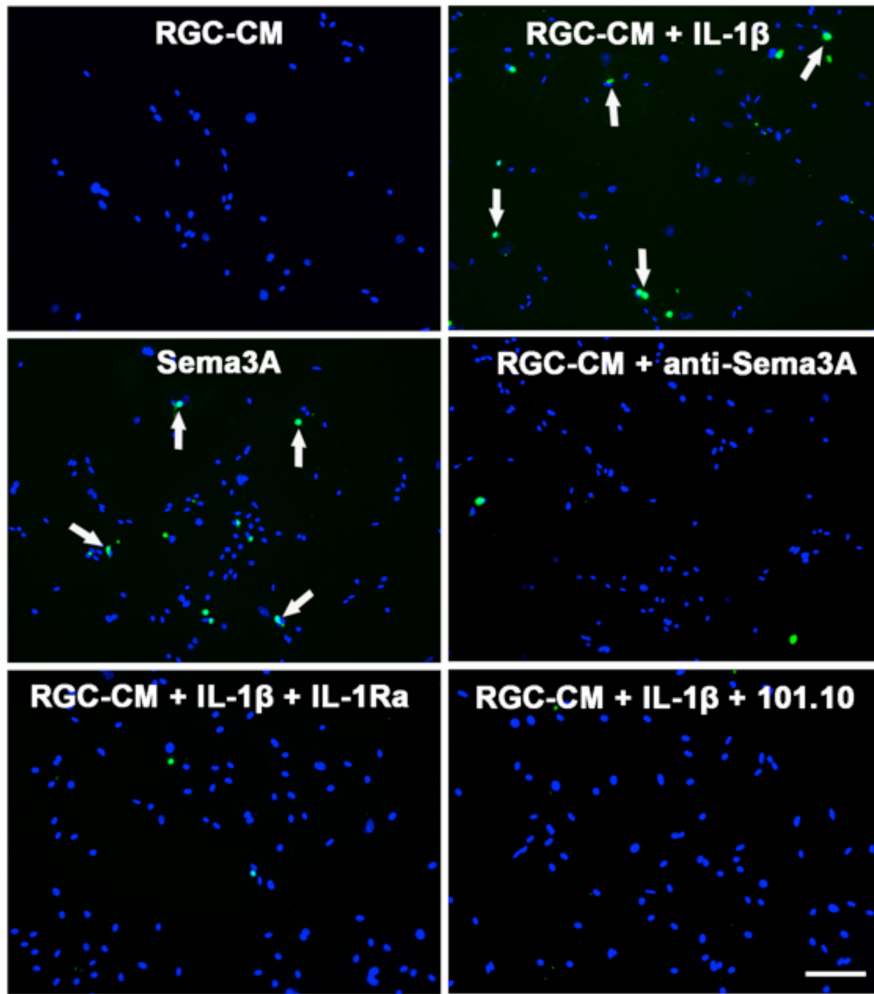


**Figure 7. Endothelial apoptotic effects of RGC-conditioned media containing Sema3A. obtained by stimulation of RGC-5 with IL-1 $\beta$  is abolished by the immunoneutralization of Sema3A or by blocking the activation of the IL-1 receptor.** Representative micrographs of apoptotic neuro-microvascular endothelial cells (RBMVEC) detected by TUNEL (green nuclei) 24 h after treatment of RGC-5 stimulated or not with IL-1 $\beta$  (RGC-CM), recombinant Sema3A (Sema3A) or conditioned media from RGC-5 cells previously stimulated with IL-1 $\beta$  (0.5 ng/ml) in absence (RGC-CM+IL-1 $\beta$ ) or presence of IL-1R antagonists (RGC-CM+IL-1 $\beta$ +IL-1Ra and RGC-CM+IL-1 $\beta$ +101.10), or RGC-CM+IL-1 $\beta$  immunoneutralized with a polyclonal anti-Sema3A antibody (2 $\mu$ g/ml, RGC-CM+anti-Sema3A). Cells were counter-stained with DAPI (blue) to detect nuclei. Scale bar = 100 $\mu$ m. Histogram compiles the percentage of TUNEL-positive cells determined in three different fields for each group (n=3) and normalized to the control (RGC-CM). <sup>\$#</sup>p=0.05 vs Norm-RGC Medium, <sup>\*\*\*</sup>p<0.05 vs RGC-CM+IL-1 $\beta$ .

**Relative contributions: Figure 7**

In vitro assay performed by JC Rivera and **N Sitaras**

Immunocytochemistry, imaging and TUNEL analysis performed by JC Rivera and **N Sitaras**

Figure preparation: JC Rivera and S Chemtob

Approximate Figure contribution: 10%

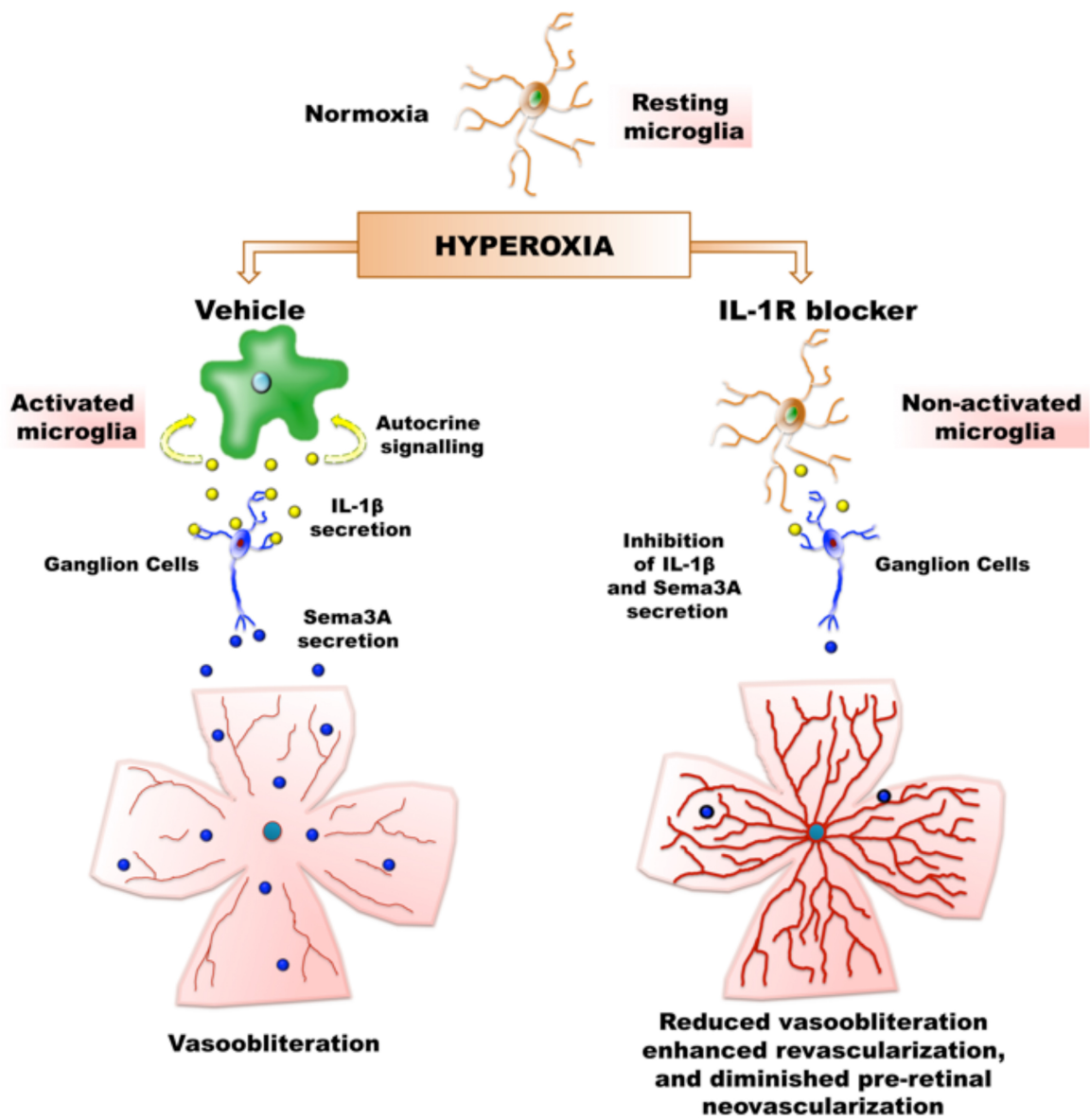


**Figure 8. Microglia activation contribute to vascular regression in ROP through IL-1 $\beta$ -dependent stimulation of Semaphorin 3A in retinal ganglion cells: Inhibition of IL-1 $\beta$  activity decreases retinal vaso-obliteration and promotes revascularization.** Microglial cells maintain the neuronal homeostasis and immunological integrity of the healthy retina. Hyperoxia as seen in OIR and retinopathy of prematurity activates microglia, which become a prominent source of pro-inflammatory auto-activating interleukin-1 $\beta$  (IL-1 $\beta$ ). IL-1 $\beta$  then stimulates in a paracrine manner the production of Sema3A from adjacent retinal ganglion cells, and in turn induces endothelial cell death. Pre-treatment with IL-1R blockers prevent this cascade, retinal vaso-obliteration, and subsequent pre-retinal neovascularization.

**Relative contributions: Figure 8**

Schematic provided by JC Rivera

Figure preparation: JC Rivera, **N Sitaras** and S Chemtob

Approximate Figure contribution: <10%

## Chapter 3

### **Retinal neurons curb inflammation and enhance revascularization in ischemic retinopathies via Protease-activated receptor 2 (PAR2)**

**Running title:** PAR2 augments revascularization via IL1R

**Authors:** Nicholas Sitaras<sup>1,2</sup>, José Carlos Rivera<sup>1,2</sup>, Baraa Noueihed<sup>3</sup>, Milsa Bien-Aimé<sup>2</sup>, Karine Zaniolo<sup>4</sup>, Samy Omri<sup>1,2</sup>, David Hamel<sup>1</sup>, Pierre Hardy<sup>5</sup>, Przemyslaw Sapiaha<sup>2</sup>, Jean-Sébastien Joyal<sup>5</sup> and Sylvain Chemtob<sup>1,2,3,5</sup>

**Institutions:** <sup>1</sup>Department of Pharmacology, CHU Sainte-Justine Hospital, University of Montréal, Montréal, Québec, Canada

<sup>2</sup>Department of Ophthalmology, Maisonneuve-Rosemont Hospital Research Center, University of Montréal, Montréal, Québec, Canada

<sup>3</sup>Department of Pharmacology and Therapeutics, CHU Sainte-Justine Hospital, McGill University, Montréal, Québec, Canada

<sup>4</sup>LOEX-CUO Research Center, Saint-Sacrement Hospital, Québec, Québec, Canada

<sup>5</sup>Department of Pediatrics, CHU Sainte-Justine Hospital, University of Montréal, Montréal, Québec, Canada

Correspondence to Sylvain Chemtob, MD, PhD, FRCPC, FCAHS, Jean-Sébastien Joyal MD, PhD, or José Carlos Rivera, PhD. CHU Sainte-Justine Research Center, 3175 Côte Sainte-Catherine, Montreal, Quebec, Canada H3T 1C5.

Conflict of interest: The authors declare no competing financial interest.

Sources of funding: Canadian Institute of Health Research (CIHR; MOP12532)

Number of pages: 31

Number of figures: 7

## *Abstract*

**Background:** Ischemic retinopathies (IRs) are characterized by sequential vasoobliteration followed by abnormal intra-vitreous neovascularization predisposing to retinal detachment and blindness. IRs are associated with robust inflammation leading to generation of IL-1 $\beta$ , which causes vascular degeneration and impairs retinal revascularization. Yet, revascularization of the retina occurs in subjects with IRs. Because inflammation leads to activation of proteases involved in formation of vasculature, we hypothesized that PAR2 may modulate deleterious effects of IL-1 $\beta$ .

**Methodology and Results:** PAR2 - detected mostly in retinal ganglion cells – was upregulated in Oxygen-induced retinopathy (OIR). Surprisingly, OIR-induced vasoobliteration and neovascularization were unaltered in PAR2-knockout mice, suggesting compensatory mechanisms. We therefore conditionally knocked down retinal PAR2 with shRNA-PAR2-encoded lentivirus. PAR2 knockdown interfered with normal revascularization, resulting in pronounced intra-vitreous neovascularization; conversely PAR2 agonist peptide (SLIGRL) accelerated normal revascularization. *In vitro* and *in vivo* exploration of mechanisms revealed that IL-1 $\beta$  induced PAR2 expression, which in turn, downregulated IL-1RI through ERK1/2-dependent process.

**Significance:** Collectively, our findings unveil an important mechanism, by which IL-1 $\beta$  regulates its own endothelial cytotoxic actions by augmenting PAR2 expression to repress sequentially IL-1RI and Sema3A expression. Timely activation of PAR2 may be a promising therapeutic avenue in IRs.

## **Key Words:**

Ischemic retinopathies, inflammation, revascularization, protease-activated receptor 2, interleukin-1 beta, Semaphorin 3A

## *Introduction*

Ischemic retinopathies, such as retinopathy of prematurity (ROP) and in some circumstances diabetic retinopathy (DR), are the main causes of severe visual impairment in children and working class population in industrialized countries<sup>1, 2</sup>. Ischemic retinopathies are biphasic diseases characterized by a degeneration of the retinal vascular bed, resulting in tissue hypoxia that leads to an anarchic, deregulated vessel proliferation into the vitreous, which in severe instances can result in retinal detachment and blindness<sup>3</sup>. Importantly, the vascular decay-induced retinal ischemia can also cause neuronal dysfunction and loss<sup>4</sup>. Therefore, therapeutic interventions that help alleviate ischemic stress of the neural retina would be desirable to prevent these adverse neuronal consequences in patients suffering from Ischemic retinopathies.

In Ischemic retinopathies, oxidative stress elicits sustained inflammation associated with a release of inflammatory cytokines<sup>5-8</sup>, notably interleukin-1b (IL-1b), which participates in recruiting and activating inflammatory cells in the retina<sup>8-10</sup>. We recently showed in a murine model of oxygen-induced retinopathy (OIR) that hyperoxia-activated microglia through an autocrine feedback loop to secrete IL-1b. IL-1b in turn induces in a paracrine manner the release of the pro-apoptotic repulsive cue Semaphorin3A (Sema3A) from neighbouring retinal ganglion cells (RGC), which contributes to vaso-oblivation<sup>8</sup> and hinders normal revascularization<sup>11</sup>. This self-sustained and potentially unrelenting destructive inflammatory cascade, if kept unchecked, could result in severe obliteration of the microvascular network of the retina; however, this is not the case as revascularization eventually does occur, albeit slowly (over several days)<sup>12</sup>. Simple homologous downregulation of IL-1RI by its own natural ligand, however, is usually not the case; in fact, the contrary often happens<sup>13</sup>.

<sup>14</sup>. It is thus reasonable to postulate the existence of alternate intrinsic regulatory mechanism that counteracts the self-sustained and potentially harmful IL-1b-induced inflammatory cascade.

Inflammation is associated with the release and activation of various proteases involved in ensued vascularization<sup>15</sup>. A number of these proteases activate a class of G protein-coupled receptors (GPCR) the Protease-activated receptors (PARs), through cleavage of their N-terminus thus revealing their tethered ligand, which can subsequently bind to the second extracellular loop of the PARs to elicit intracellular signaling<sup>16</sup>. Of the four members of the PAR family, PAR1 through 4<sup>16</sup>, PAR2 is recognized for its marked pro-angiogenic properties in the retina<sup>17, 18</sup>. Interestingly, PAR2 is robustly activated by IL-1b in different cell types, including neurons and endothelial cells<sup>19-22</sup>; and IL-1b-mediated inflammation can further induce the expression of various proteases, which can cleave and activate PAR2<sup>23</sup>. This may appear rather counterintuitive as amplified IL-1b increases endothelial cell death in OIR<sup>8, 11</sup>. We therefore hypothesize that in OIR PAR2 exerts its angiogenic properties by countering the cytotoxic actions of IL-1b.

Using a mouse model of OIR<sup>24</sup>, which mimics the cardinal features of ischemic retinopathies, we uncover a new mechanism of action for PAR2 in retinal revascularization. By conditionally knocking down PAR2 (utilizing a lentiviral-encoded shRNA), we hereby show that IL-1b regulates neuronal PAR2 expression, which in turn reduces oxygen-induced vaso-obliteration and enhances desirable revascularization of the retina. The effect of PAR2 is mediated (in large part) by downregulating IL-1RI specifically in RGCs, which in turn diminishes Sema3A release, to facilitate revascularization. Our findings unveil a novel property for PAR2 in modulating inflammation, which in the context of ischemic retinopathies limits the vaso-obliterative effects of amplified IL-1b, allowing desirable revascularization and consequently reducing pathological intra-vitreous neovascularization.

## *Materials and Methods*

### *Animals*

Adult C57BL6/J mice and PAR2 transgenic mice (B6.Cg-F2r11<sup>tm1Mslb</sup>) were purchased from Jackson laboratories (Bar Harbour, Maine, USA). PAR2 transgenic mice were genotyped as described by Jackson Laboratories. Adoptive CD-1 lactating females were purchased from Charles Rivers Laboratories (Sainte-Hyacinthe, Canada) to tend to hyperoxia-exposed mice pups. All experiments were conducted in accordance with ARVO statement regarding use of animals in ophthalmic and vision research and were approved by Maisonneuve-Rosemont and Sainte-Justine research center animal care committees.

### *Oxygen-induced retinopathy (OIR)*

Mice pups were exposed from postnatal day 7 (P7) to P12 to 75 % oxygen using BioSpherix oxycycler. Vasoobliteration (VO) and neovascularization (NV) were assessed in hyperoxia-exposed mice pups at P12 and P17, respectively, as described previously<sup>24, 25</sup>. Concisely, mice pups were fully anesthetized in 3 % isoflurane in oxygen and decapitated using a guillotine. Eyes were enucleated and fixed in 4 % paraformaldehyde solution for 1 h at room temperature. Retinas were dissected and stained overnight at 4°C with fluorescein-labeled GSL 1, isolectin B4 (Vector Labs; 1:100). Lectin-stained retinas were whole-mounted onto Superfrost/Plus microscope slides (Fisher Scientific) with the photoreceptor side down and imbedded in Fluoro-gel (Electron Microscopy Sciences) and imaged at 10x using a Zeiss AxioObserver.Z1. Images were merged into a single file using the MosiaX option in the AxioVision 4.6.5 software (Zeiss). Quantification of VO and NV was assessed using the SWIFT\_NV methods as previously described<sup>26</sup>. Commercial interleukin-1 receptor inhibitor Kineret® (Amgen Canada Inc.) was administered intraperitoneally from P7 to P8 at 20mg/kg/day.

### *Preparation of lentiviral particles*

Third generation Lentivirus (HIV-1) was prepared by as previously described<sup>27</sup>. p24 ELISA kit (Clontech) was used to quantify lentiviral titers for Lv. shGFP (8.5 ng/mL), Lv. shPAR2 (9.6 ng/mL) and Lv. GFP (15.0 ng/mL).

### *Intravitreal injections*

Animals were anesthetized in 3 % isoflurane in oxygen and injected intravitreally either at P3 with 1.0  $\mu$ L of lentiviral particles (described above) or at P7 with 10  $\mu$ mol of Kineret® or P7 and P9 or P12 and P14 with 100  $\mu$ mol of NH<sub>2</sub>-SLIGRL (Elim Biopharm) using a Hamilton syringe equipped with 50 gauge glass capillary.

### *Immunohistochemistry*

Eyes were enucleated from mice pups and fixed in 4 % paraformaldehyde at room temperature for 2 h and saturated overnight at 4°C in a 30 % sucrose solution prior to embedding in OCT compound (TissueTek®). Coronal sections of 10  $\mu$ m were sectioned using a Cryostat (Leica). Sections were subsequently washed with PBS, blocked and permeabilized for 1 h at room temperature and subsequently incubated with fluorescein-labeled GSL 1, isolectin B4 (Vector Labs; 1:100) for retinal vasculature. Antibodies to rabbit  $\beta$ -tubulin (ECM Biosciences; 1:1000), mouse  $\beta$ -tubulin (Sigma; 1:1500), mouse PAR2 (Invitrogen; 1:500), rat CD31 (BD Biosciences; 1:100), rabbit IL-1RI (Santa Cruz Biotechnology; 1:400), rabbit Sema3A (Abcam, 1:500) or rabbit VEGF (Santa Cruz Biotechnology; 1:200), while fluoresceinated secondary antibodies (goat anti-mouse IgG Alexa Fluor 488, 594 and/or 647 and goat anti-rabbit IgG Alexa Fluor 488, 594 and/or 647; Invitrogen) were used for localization studies according to manufacturers' recommendations. Samples were visualized using 30x or 60x objectives with an IX81 confocal microscope (Olympus), and images were obtained with Fluoview 3.1 software (Olympus).

### *Laser-capture microdissection*

Eyes were enucleated and immediately embedded in OCT compound and snap frozen in liquid nitrogen and subsequently cut into 16 mm coronal sections onto MembraneSlide 1.0 PEN nuclease free slides (Zeiss). To visualize vessels, sections were prepared as previously described<sup>11</sup>. Retinal sections were laser-microdissected (LCM) with the Zeiss (Observer.Z1) Palm Microbeam LCM microscope system. Isolated retinal RNA was transcribed into cDNA for quantitative real-time PCR analysis (see Reverse Transcription PCR).

#### *Western Blot*

Eyes were enucleated and retinas dissected and placed into commercial RIPA buffer (Cell Signalling) and homogenized using Precellys 24 homogenizer. Samples were centrifuged and 30 µg of pooled retinal lysate from two different animals was loaded on an SDS-PAGE gel and subsequently electro-blotted onto either PVDF or nitrocellulose membrane (BioRad). After blocking, the membranes were blotted with 1:400 mouse antibody to PAR2 (35-2300, Invitrogen), 1:1000 mouse antibody to  $\beta$ -actin (Santa Cruz Biotechnology), 1:200 rabbit antibody to VEGF (SantaCruz Biotechnology), 1:400 rabbit antibody to IL-1RI (sc-689; Santa Cruz Biotechnology), 1:400 goat antibody to IL-1b (R&D Systems), 1:1000 rabbit antibody to Sema3A (Abcam), 1:500 rabbit antibody to total (Cell Signaling) or phosphorylated IRAK1 (Sigma), 1:1000 rabbit or mouse antibody to total and phosphorylated ERK1/2 (Cell Signaling), 1:1000 rabbit antibody to total and phosphorylated p38 (Cell Signaling) or 1:1000 rabbit or mouse antibody to total and phosphorylated c-jun N-terminal kinase [JNK] (Cell Signaling). After washing, membranes were incubated with 1:5000 horseradish peroxidase-conjugated (HRP) anti-mouse or 1:2000 HRP anti-goat or -rabbit secondary antibodies (Millipore). Membranes were imaged with LAS-3000 imager and bands were assessed using densitometry plugins in Multi Gauge 4.0 software (FujiFilm).

#### *Reverse-transcription PCR and quantitative real-time PCR*

Freshly dissected whole retina or laser-capture microdissected samples were processed using RiboZol (AMRESCO) as described by manufacturer's instructions. Genomic DNA was removed using DNase I (Invitrogen). Approximately 1 mg of total RNA was reverse-transcribed into cDNA using iScript RT Supermix (BioRad) as described by manufacturer's instructions. cDNA was analysed by Quantitative real-time PCR using iQ<sup>TM</sup> SYBR® Green Supermix (BioRad) with primers targeting mouse PAR2 (Fwd 5'-TGACCACGGTCTTTCTTCCG-3' and Rev 5'-TCAGGGGGAACCAGATGACA), rat PAR2 (Fwd 5'-TGGGAGGTATCACCCCTTCTG-3' and Rev 5'-GGGGAACCAGATGACAGAGA-3'), mouse Sema3A (Fwd 5'-GCTCCTGCTCCGTAGCCTGC-3' and Rev 5'-TCGGCGTTGCTTTCGGTCCC-3'), mouse VEGF-A (Fwd 5'-GCCCTGAGTCAAGAGGACAG-3' and Rev 5'-CTCCTAGGCCCTCAGAAGT-3'), mouse and rat IL-1RI (Fwd 5'-TGAATGTGGCTGAAGAGCAC-3' and Rev 5'-CGTGACGTTGCAGACAGTT-3') and mouse IL-1b (Fwd 5'-CTGGTACATCAGCACCTCACA-3' and Rev 5'-GAGCTCCTTAACATGCCCTG-3') (designed using Primer3<sup>TM</sup> [NCBI]; see Supplemental Table 1). Quantitative gene expression analysis was assessed using ABI 7500 Real-Time PCR system (Applied Biosystems) and compared to control genes cyclophilin A (Fwd 5'-CAGACGCCACTGTGCTTT-3' and Rev 5'-TGTCTTTGGAACCTTGTCTGCAA-3') or 18S primers (Ambion) using the DDCT quantification.

#### *Preparation of stable cell lines*

Neeraj Agarwal of the University of North Texas Health Science Center at Fort Worth kindly provided the RGC-5 cell line and was prepared as previously described<sup>28</sup>. Undifferentiated RGC-5 were incubated overnight with lentiviral particles containing shRNA. Next day, media was changed and incubated for 48h prior to selection with 5 ug/mL puromycin (Sigma) for 7 days. Cells were differentiated thereafter with 1 mM staurosporine (Sigma).

#### *Stimulation of RGC-5 and RBMVEC*

Rat brain microvascular endothelial cells (RBMVEC) were obtained from Cederlane Laboratories (Cell Applications; cat #: R840-05a) and used between passages 2 – 7. RGC-5 were cultured in DMEM (Invitrogen) supplemented with 10 % FBS (Cell Applications) and 1 % penicillin/streptomycin (Cell Applications) at 37°C and 5 % CO<sub>2</sub> while RBMVEC were cultured as described by manufacturer's instructions. Cells were starved 4 h prior to treatment with 1.0 or 10.0 ng/mL of recombinant murine IL-1b (PeproTech) or 0, 40 or 100 mM SLIGRL-NH<sub>2</sub>. Commercial inhibitors for ERK1/2 (U0126), JNK (SP600125) and p38 (SB203580) were purchased from Sigma and used at 10 μM approximately 60 min prior to SLIGRL-NH<sub>2</sub> treatment.

#### *Preparation of RGC-5 conditioned media (CM)*

Terminally differentiated RGC-5 were seeded (10<sup>6</sup> cells) and starved 4 h prior to treatment with 0 or 100 mM NH<sub>2</sub>-SLIGRL and exposed to 5.0 ng/mL of recombinant murine IL-1b (PeproTech). Supernatants were collected 24 h later, centrifuged briefly and filtered through 0.22 μm filters (Millipore) and distributed for proliferation assays (see below).

#### *Cell survival assay*

Approximately 10<sup>4</sup> RBMVEC cells/well were seeded in 24-well plates and starved 4 h prior to exposure to RGC-5 CM. Neutralizing antibody to Sema3A was used at 2 mg/mL (Abcam). After 24 h, 50 μL of a 5 mg/mL solution of Thiazolyl Blue Tetrazolium bromide (Sigma) was added and cells incubated for 2-3 h. Supernatants were aspirated and cells were lysed and resuspended in acidified isopropanol. Duplicate absorbance readings were taken at 565 nm using Infinite® M1000 Pro plate reader (TECAN).

#### *Aortic explant microvascular growth assay*

Aortae were isolated from adult PAR2 null mice, sectioned into 1 mm rings and placed into growth-factor reduced Matrigel (BD Biosciences) in 24-well plates. Rings

were cultured in supplemented Endothelial Basal Medium (Lonza) 4-5 days prior to a 48 h exposure to RGC-5 CM. Treated rings were photomicrographed using AxioObserver (Zeiss) and microvascular growth assessed using Image Pro 4.5 (Media Cybernetics, USA). Neutralizing antibody to mouse VEGF<sub>164</sub> was used at concentrations of 20 mg/mL (R&D Systems)

### *Statistical analysis*

Results are presented as mean  $\pm$  s.e.m. for all studies. One-way or two-way analysis of variance with significance  $\alpha=0.05$  or higher were used for processing data. Bonferroni post-hoc analysis was used for calculating significance between groups. Two-tailed student t-tests were used to test for significance between two means.

### *Results*

#### *Neuronal PAR2 expression augments during oxygen-induced retinopathy (OIR)*

Retinas from C57BL/6 mice subjected to 75% oxygen for 5 days (P7 to P12)<sup>24</sup> were analyzed at different time points during OIR. During the early phases of vaso-obliteration (at P8) protein levels of PAR2 surged ~3-fold compared to normoxic controls (Figure 1A,B), and relative to values at P5 (normalized vs. P5). PAR2 expression in retina remained high during the hyperoxic phase at P12 (Figure 1A,B); by P17, PAR2 levels were comparable to normoxic controls.

Immunofluorescence analysis on sagittal sections from P8 and P12 normoxic retinas demonstrates preferential distribution of PAR2 in  $\beta$ III-tubulin positive RGCs (Figure 1C and Supplementary Figure 1A, upper panels) and robustly increases in these cells during OIR (Figure 1C and Supplementary Figure 1A, lower panels). PAR2 also slightly co-localized with retinal endothelial cells at P8 (CD31-positive) [Supplementary Figure 1B]. Laser-capture microdissection of retinal tissue followed by qPCR analysis revealed significantly higher PAR2 mRNA in the ganglion cell layer

(GCL) relative to microdissected vessels (Figure 1D and Supplementary Figure 2A and B), particularly in OIR-subjected animals (~3.5-fold increase,  $p < 0.001$ ). Low levels of PAR2 mRNA were also detected in the INL likely owing to the invading blood vessels that protrude into these layers in retinas from P8 mice pups (supplementary Figure 2A and B); in OIR, the vasoobliteration leads to disappearance of PAR2 expression in these layers. At P17, PAR2 expression remained localized to the retinal endothelium in both room air and hyperoxia-raised mice retina. Altogether, our data demonstrate that PAR2 increases sharply during the early phases of OIR and that this expression is localized preferentially to the RGCs.

*PAR2 protects the retina from oxygen-induced vaso-obliteration and induces retinal revascularization*

To explore the role of PAR2 in OIR, we exposed transgenic mice lacking PAR2 gene (PAR2<sup>-/-</sup>) to 75 % O<sub>2</sub> from P7 until P12. As previously reported<sup>17</sup>, mice lacking PAR2 gene surprisingly showed no changes in vaso-obliteration or pre-retinal neovascularization compared to age-matched wild-type mice (supplementary Figure 3A, B and C). Because, compensatory mechanisms are regularly reported with germ cell line gene modulation,<sup>29</sup> and signaling redundancies exist between different PARs<sup>16</sup> (as reported in PAR2 transgenic mice<sup>30</sup>), we attempted to circumvent this drawback, by conditional knockdown of PAR2 using lentiviral (Lv.) constructs bearing shRNAs targeting PAR2 (Lv. shPAR2) injected intravitreally in C57BL/6 mice pups at P3; lentiviral vectors show high tropism for RGCs (see co-localization of GFP [encoded in Lv] with βIII-tubulin, supplementary Figure 3D and references<sup>11, 28, 31, 32</sup>). In wildtype mice Lv. shPAR2 successfully down-regulates retinal PAR2 expression by P7 compared to contralateral eyes injected with control Lv. shGFP (supplementary Figure 3E). PAR2 knockdown caused a significant reduction in the rate of revascularization between P12 and P17 (by 20.9%,  $p < 0.001$ ) [Figure 2C] resulting in augmented retinal vaso-obliteration at these corresponding ages [Figure 2A and 2B, upper panels]. Consequently, Lv. shPAR2 treated animals exhibited increased

aberrant pre-retinal neovascularization at P17 compared to control Lv. shGFP injected pups (Figure 2B); Lv. shPAR2 was ineffective in PAR2<sup>-/-</sup> pups (supplementary Figure 4A and B), consistent with the specificity of the shPAR2.

We next proceeded to evaluate the effects of exogenous PAR2 stimulation with PAR2 activating peptide (PAR2-AP), SLIGRL (corresponding to tethered ligand),<sup>33</sup> injected intravitreally. Since expression of PAR-2 increased robustly at P8 and P12, we administered SLIGRL via intravitreal injection during early (P7) and late (P12) hyperoxic exposure. Administration of SLIGRL at P7 caused a significant reduction in vaso-obliteration at P12 compared to vehicle-injected animals [Figure 2A, lower panels]; a successive injection at P9 further diminished vaso-obliteration [Figure 2A, lower right panel]. Likewise, intravitreal injections of SLIGRL after the hyperoxic exposure (P7-P12) at P12 and P14 reduced dose-dependently the size of the avascular area measured at P17 [Figure 2B, lower panels], which reflected into an accelerated rate of revascularization between P12 and P17 [Figure 2C]. Consequently and as expected, SLIGRL treatment diminished pathological pre-retinal neovascularization at P17 (Figure 2B; lower histogram). PAR2<sup>-/-</sup> mice were unresponsive to SLIGRL (Supplementary Figure 4A and B). Collectively, these data indicate that PAR2 enhances the integrity of the inflammation-challenged<sup>8,11</sup> retinal vascular bed during hyperoxic stress by promoting normal revascularization, which in turn reduces undesirable aberrant pre-retinal neovascularization.

#### *IL-1 $\beta$ induces PAR2 expression in neuronal and endothelial cells*

Oxidative stress and inflammation are intimately intertwined<sup>34</sup>. Accordingly, augmented levels of inflammatory cytokines, such as IL-1 $\beta$ , IL-6 and TNF- $\alpha$  are found in the vitreous of patients with ischemic retinopathies and corresponding animal models<sup>5-8, 11</sup>. Of relevance, IL-1 $\beta$  has been shown to increase PAR2 expression in cultured endothelial cells<sup>20</sup>, chondrocytes<sup>21</sup>, synovial cells<sup>19</sup> and neuronal cells<sup>22</sup>. We explored the relationship between IL-1 $\beta$  and PAR2 *in vivo* in OIR. IL-1 $\beta$  levels were increased during hyperoxia, particularly at P8 (Figure 3A), corresponding to the peak

of PAR2 expression in OIR. (Figures 1A, 3B). Pre-treatment of hyperoxia-exposed mice with IL-1 receptor antagonist (IL-1Ra) Anakinra (Kineret®), reduced IL-1 $\beta$  mRNA expression (supplementary Figure 5) as reported<sup>8</sup>, and significantly lowered PAR2 mRNA levels at P8 (Figure 3B), suggesting that IL-1 $\beta$  may regulate PAR2 expression *in vivo*.

*In vivo* findings were ascertained *in vitro*. Cultured mouse retinal neuronal cells (RGC-5) and RBMVEC displayed dose-dependent increases in PAR2 mRNA expression upon treatment with recombinant murine IL-1b [rmIL-1b] (Figure 3C and D); these effects were abolished by IL-1Ra (Figure 3E and F). PAR2 mRNA increased within 2-4 h after stimulation with IL-1b, but was not sustained thereafter; whereas increased PAR2 protein translation was detected by 6-12 h in both cells, but remained sustained at 24 h only in RGC-5 (Figure 3G and H), consistent with changes in PAR2 expression in micro-dissected retinas of animals subjected or not to OIR (Figure 1D). Hence, IL-1b upregulates PAR2 expression in retinal ganglion neurons in a sustained manner but yields a limited and transient response in vascular endothelial cells.

#### *PAR2 is involved in negative feedback regulation of IL-1 response*

Chronic inflammation can be detrimental to the nascent vessels, either directly via cytokine or chemokine signaling<sup>35-39</sup> or indirectly through inflammatory cell activation<sup>9, 10, 40</sup>. Previous studies from our laboratory reveal that in OIR IL-1 $\beta$  - predominantly generated by microglia - interferes with normal revascularization of the retina by eliciting paracrine release of the pro-apoptotic endothelial repulsive cue Sema3A, from RGCs.<sup>8,11</sup> On the other hand, we hereby show that IL-1 $\beta$  upregulates PAR2 (Figure 3), which enhances normal revascularization of the retina (Figure 2C). We therefore set out to determine how PAR2 promotes retinal revascularization in OIR, by examining its modulation of IL-1 signaling. We determined IL-1 $\beta$  and IL-1RI expression in retinas from P9 C57BL/6 mouse pups exposed to OIR and injected intravitreally with SLIGRL or Lv.shPAR2. Both IL-1 $\beta$  and IL-1RI expression increased in vehicle-injected retinas of animals exposed to hyperoxia. SLIGRL attenuated the

OIR-provoked increase in IL-1RI expression predominantly localized on  $\beta$ III-tubulin positive RGCs (Figure 4A,B); normoxic animals treated with SLIGRL also exhibited moderate reductions in IL-1RI (Supplementary Figure 6A,B). Conversely Lv.shPAR2 further augmented IL-1RI expression in OIR (Figure 4A); whereas SLIGRL and Lv.shPAR2 had no effect on IL-1 $\beta$  (Figure 4A).

To determine whether inhibition of IL-1 and stimulation of PAR2 acted synergistically in enhancing revascularization, wildtype mice subjected to OIR were treated with either IL-1Ra, SLIGRL or both. The effects on vaso-obliteration were comparable (Figure 4C), suggesting that PAR2 stimulation did not induce any additional mechanism to that through IL-1RI suppression to enhance retinal revascularization in OIR; as anticipated, PAR2-null mice were only responsive to IL-1Ra (Supplementary Figure 6C).

*PAR2 stimulation reduces IL-1RI expression in retinal neurons via JNK and downstream ERK1/2 signalling*

To elucidate signaling pathways by which PAR2 regulates IL-1RI expression, we first corroborated our *in vivo* observations on cultured cells. In RGC-5 cells, SLIGRL reproduced its *in vivo* effects, as it time- and dose-dependently suppressed IL-1RI mRNA expression (Figure 5A; Supplementary Figure 7A); a similar profile was observed for IL-1RI protein (Figure 5B); this reduction was abrogated in cells previously infected with Lv.shPAR2 (Figure 5A,B and Supplementary Figure 7B). Interestingly, in RBMVEC IL-1RI mRNA increased 1 h after stimulation with SLIGRL and IL-1RI protein increased by 2 h following SLIGRL stimulation only (Supplementary Figure 7C), suggesting distinct pathways in different cell types. In addition in RGC-5 cells, IL-1 induced IRAK-1 phosphorylation as expected (Supplementary Figure 6D); this effect was attenuated by pre-treatment with SLIGRL, which suppresses IL-1RI (Figure 4); RGC-5 cells infected with Lv.shPAR2 were unresponsive to SLIGRL (Figure 5A,B).

PAR2 stimulation results in activation of several downstream effectors including  $\text{Ca}^{2+}$  transients and MAPK signaling<sup>16, 41,42</sup>. RGC-5 cells treated with SLIGRL exhibited a time-dependent increase in MAPK signaling including ERK1/2, c-jun N-terminal kinase (JNK) and p38 phosphorylation (Figure 5C). Inhibition of p38 using SB203580 did not affect SLIGRL-dependent suppression of IL-1RI mRNA; however, pre-treatment with MEK1/2 inhibitor, U0125, or JNK inhibitor, SP600125, prevented SLIGRL-induced IL-1RI mRNA suppression (Figure 5D). Western blot analysis demonstrate that the JNK inhibitor, SP600125, effectively abolished ERK1/2 phosphorylation while the MEK1/2 inhibitor, U0125 had no effect on JNK phosphorylation indicating that PAR2 stimulation suppresses IL-1RI in RGCs by signaling downstream first via JNK and subsequently via ERK1/2 pathway. RBMVEC cells stimulated with MET kinase inhibitor, PD98059, did not abolish SLIGRL-induced IL-1RI upregulation further supporting distinct signaling pathways in different cells types (Supplemental Figure 7E and F).

*PAR2 activation inhibits IL-1 $\beta$ -mediated Sema3A release and ensuing endothelial cell death and promotes angiogenesis by concomitant VEGF release*

OIR-induced increase in IL-1 $\beta$  leads to Sema3A release and ensuing endothelial cell death resulting in increased vaso-obliteration<sup>8,11</sup> and hindered normal revascularization<sup>11</sup>. Since PAR2 negatively regulates IL-1 signaling (Figures 4 and 5), we proceeded to investigate if this was associated with suppressed Sema3A expression. OIR-induced Sema3A expression was indeed suppressed by PAR2 stimulation with SLIGRL (Figure 6A,B); as expected, Lv.shPAR2 increased Sema3A levels compared to Lv.shGFP. Concomitantly, VEGF levels increased sharply in RGCs upon SLIGRL stimulation (Supplementary Figure 8A,B), facilitating angiogenesis (Supplementary Figure 8C,D).

To ascertain *in vivo* findings, we stimulated RGC-5 cells with IL-1 $\beta$  and measured Sema3A in presence or absence of SLIGRL. Sema3a mRNA was markedly induced by IL-1 $\beta$  (Figure 6C), and this effect was abrogated by SLIGRL, which was

ineffective in Lv.shPAR2-infected cells (Figure 6D); importantly, SLIGRL in absence of IL-1 $\beta$  did not affect Sema3a expression.

Next, we determined the functional role of PAR2 in angiogenesis by treating RBMVEC to assess cell survival, using conditioned media (CM) from RGC-5 cells stimulated with IL-1 $\beta$  in the presence or not of SLIGRL. Endothelial cell death triggered by IL-1 $\beta$  stimulation of RGC-5 cells was Sema3A-dependent, as this was abrogated using a neutralizing antibody to Sema3A (Figure 6E). IL-1 $\beta$ -induced endothelial cell death was also abolished by PAR2 stimulation (Figure 6F). Similarly, CM from PAR2 stimulated RGC-5 cells elicited aortic explant vascular sprouting (Figure 6G) due to concomitant VEGF release from these cells (Supplementary Figure 8C,D); whereas CM from IL-1 $\beta$  stimulated RGC-5 cells diminished aortic explant vascular sprouting, and this effect was abolished by co-treatment of RGC-5 with SLIGRL (Figure 6G). Altogether these data demonstrate that the actions of PAR2 in the retina negatively modulate IL-1 $\beta$  actions, and thus prevent IL-1 $\beta$ -induced Sema3A release while maintaining elevated levels of VEGF; these effects dampen endothelial cell death during oxygen-induced vaso-obliteration and augment desirable revascularization through retino-vascular proliferation.

## *Discussion*

Sustained inflammation is an established cause of vessel network injury<sup>5-10, 35, 43</sup>. Resident microglia cells, a dominant source of inflammatory IL-1 $\beta$ , are auto-activated by this cytokine, which contributes to exacerbating vaso-obliteration in ischemic retinopathies<sup>8</sup>. Despite this auto-amplified inflammation, vasoobliteration eventually ceases to progress and instead – as seen in some patients – normal retinal revascularization takes place,<sup>12, 44</sup> suggesting the presence of an intrinsic regulatory mechanism. In this study, we demonstrate that neuronal PAR2 acts as an important regulatory mediator for dampening IL-1 $\beta$ -induced vessel degeneration and prompts preferential revascularization of vaso-obliterated retinal tissue. In this context

rapid IL-1 $\beta$  release induces PAR2 expression, which in turn negatively regulates IL-1 $\beta$  signaling by downregulating its receptor IL-1RI; this system essentially counteracts the otherwise homologous upregulation of IL-1RI by its natural ligand<sup>13, 14</sup>. These events occur in IL-1RI- and PAR2-expressing RGCs where the pro-apoptotic Sema3A is produced<sup>8,11</sup>, to limit its formation, while concomitantly enhancing secretion of VEGF to allow nascent vessels to invade and perfuse the ischemic vaso-obiterated regions, as depicted in the schema in Figure 7.

There is growing evidence to show that neurons play a crucial role in the formation of retinal vessel network. For instance, mice pups lacking retinal ganglion cells (*brn3b*<sup>Z-dta/+</sup>; *six3-cre* mice) are devoid of an inner retinal capillary network<sup>28</sup>. In OIR, neurons appear to contribute beneficially early in disease by releasing pro-angiogenic signals such as GPR91, VEGF and Netrin1 in attempts to counteract ischemic stress<sup>11, 28, 31</sup>; however, if unchecked, sustained hypoxia and inflammation can result in suppression of VEGF and secretion of vaso-repulsive cue Sema3A, as well as activation of endoplasmic reticulum stress pathways that translates to an IRE1-a-dependent cleavage of Netrin1 mRNA<sup>8,11, 31</sup>; this results in diversion of metabolic stores away from perishing tissue<sup>11</sup>. On the other hand, we hereby show that amplified IL-1 $\beta$  rapidly signals an increase in PAR2 expression on RGCs in an attempt to regulate and overcome excessive vascular decay elicited by Sema3A, and reestablish normal revascularization by inducing expression of VEGF (independently of HIF-1a<sup>45</sup>). PAR2 exerts these beneficial effects by suppressing IL-1RI expression in RGCs, which in turn limits IL-1 $\beta$ -regulated Sema3A release, despite high IL-1 $\beta$  retinal levels during OIR. Altogether this study highlights a central role for neurons in governing retino-vascular network integrity in ischemic retinopathies, and more specifically uncovers an important regulatory mechanism in PAR2 that avoids excessive vascular decay and reestablishes normal retinal revascularization in these conditions.

PAR2 is ubiquitously expressed in various organs and can have distinct cellular functions depending on the cell type where it is expressed<sup>46, 47</sup>. Herein, we

show that PAR2 in the retina is most prominently localized on RGCs and to a lesser extent on endothelium, where it exhibits functionally distinct cellular processes. Tissue Factor, which is expressed on endothelium (but not on neurons), has been shown when constitutively activated to robustly stimulate angiogenesis of the vascular plexus during development via PAR2<sup>18</sup>; however in OIR, endothelial PAR2 activation by Tissue Factor fails to curb oxygen-induced vaso-obliteration and subsequent pathological neovascularization<sup>17</sup>. Correspondingly, we show that endothelial PAR2 activation increases IL-1RI (and IL-1 $\beta$ <sup>20</sup>) expression, which may potentiate vascular injury, and does so seemingly via distinct intracellular signaling pathways. Neuronal PAR2, on the other hand, dampens oxygen-induced endothelial cell death by inhibiting IL-1 $\beta$ -mediated Sema3A release while maintaining elevated levels of VEGF in the retina, thus allowing normal growth of intra-retinal neovessels (and consequently avoid extra-retinal neovessel formation). In the brain as well as other organs, a similar dichotomy is apparent. PAR2 activation can have opposing effects depending on the tissue or cell where it is expressed<sup>48, 49</sup>. For instance, experimental models of neurodegenerative disorders demonstrate that PAR2 in glial cells evoke distinct cellular mechanisms from neuronal PAR2 to initiate neuroprotection<sup>22, 50-53</sup>. Hence targeting PAR2 on specific cell populations may selectively modulate downstream effectors in an attempt to limit pathological processes.

Importantly, this study also highlights the drawback associated with embryonic gene deletion. As previously reported<sup>17</sup>, OIR-induced vaso-obliteration and neovascularization were unaltered in mice having embryonic deletion of PAR2. Herein, we show that PAR2 mice, whereupon they are exposed to OIR, not only demonstrate comparable vascular phenotypes but also show similar molecular signatures compared to PAR2-intact mice. This indicates that embryonic gene deletion may – in some circumstances – unobtrusively induce compensatory mechanisms that may guise the native function of genes under investigation.

Overall our findings uncover an important unprecedented physiologic mechanism induced by inflammation to limit vascular injury. In this process, the major

pro-inflammatory IL-1 $\beta$  induces PAR2 expression, which in turn suppresses IL-1RI to curb IL-1 $\beta$ -triggered Sema3A-dependent vasoobliteration and prompt desirable revascularization of the hypoxic retina, thus preventing aberrant pre-retinal neovascularization in ischemic retinopathies. We hereby identify PAR2 as an important physiologic mediator that regulates the inflammatory hypoxic-ischemic retinal environment in ischemic retinopathies, thus allowing for normal vascular regeneration of the retina. To date considerable attention has been focused on inhibiting pathological neovascularization<sup>54-57</sup>, whereby anti-VEGF administration is currently accepted as a possible treatment regime for patients suffering from ischemic retinopathies<sup>58</sup>. However, there are no clinical treatments that prompt desirable revascularization in an effort to reduce ischemic stress that is crucial to neuro-retinal dysfunction and pre-retinal neovascularization. The current study offers an approach for alleviating ischemic stress using PAR2 agonists.

### *Acknowledgments*

We acknowledge Hensy Fernandez and Isabelle Lahaie for valuable technical assistance. We would also like to thank Dr. Christian Beauséjour for providing us with lentiviral constructs. This study was supported in part by grants from the Canadian Institutes of Health Research (CIHR; S.C.). NS, SO and BN are supported by studentship from the Fond de Recherche en Santé du Québec; DH was supported by a studentship from Centre Hospitalier Sainte-Justine; JCR was supported by a fellowship from the Heart and Stroke Foundation of Canada and the Canadian Stroke Network; KZ was recipient of a fellowship award from Foundation Fighting Blindness. JSJ is supported by a Burrough Wellcome Fund Career Awards for Medical Scientists and holds a Career development Award from the Canadian Child Health Clinician Scientist Program (CCHCS), a training initiative of the CIHR. PS holds a Canada Research Chair (Cell and Molecular Vision) and is supported by grants from CIHR.

SC holds a Canada Research Chair (Translational Research in Vision) and the Leopoldine Wolfe Chair in translational research in age-related macular degeneration.

### *Authorship contributions*

N.S., J.C.R. and S.C. conceived and designed the experiments; N.S., J.C.R., B.N., M.B.-A., K.Z., S.O., D.H. performed the experiments; N.S., J.C.R. and S.C. analyzed the data; J.C.R., P.H., P.S. and J.-S.J. provided expert advice; N.S. and J.C.R. prepared the figures; N.S., J.C.R. and S.C. wrote the manuscript.

### *References*

1. Yau JWY, Rogers SL, Kawasaki R, Lamoureux EL, Kowalski JW, Bek T, Chen SJ, Dekker JM, Fletcher A, Grauslund J, Haffner S, Hamman RF, Ikram MK, Kayama T, Klein BEK, Klein R, Krishnaiah S, Mayurasakorn K, O'Hare JP, Orchard TJ, Porta M, Rema M, Roy MS, Sharma T, Shaw J, Taylor H, Tielsch JM, Varma R, Wang JJ, Wang N, West S, Xu L, Yasuda M, Zhang X, Mitchell P, Wong TY, The Meta-Analysis for Eye Disease (Meta-eye) Study Group: Global Prevalence and Major Risk Factors of Diabetic Retinopathy, *Diabetes Care* 2012, 35:556-564
2. Gilbert C, Rahi J, Eckstein M, O'Sullivan J, Foster A: Retinopathy of prematurity in middle-income countries, *Lancet* 1997, 350:12-14
3. Sapiha P, Hamel D, Shao Z, Rivera JC, Zaniolo K, Joyal JS, Chemtob S: Proliferative retinopathies: Angiogenesis that blinds, *Int J Biochem Cell Biol* 2010, 42:5-12
4. Fulton A, Hansen R, Moskowitz A, Akula J: The neurovascular retina in retinopathy of prematurity, *Prog Retin Eye Res* 2009, 28:452-482
5. Demircan N, Safran BG, Soylu M, Ozcan AA, Sizmaz S: Determination of vitreous interleukin-1 (il-1) and tumour necrosis factor (tnf) levels in proliferative diabetic retinopathy, *Eye (Lond)* 2006, 20:1366-1369
6. Mocan MC, Kadayifcilar S, Eldem B: Elevated intravitreal interleukin-6 levels in patients with proliferative diabetic retinopathy, *Can J Ophthalmol* 2011, 41:747-752
7. Krady JK, Basu A, Allen CM, Xu Y, LaNoue KF, Gardner TW, Levison SW: Minocycline reduces proinflammatory cytokine expression, microglial activation, and caspase-3 activation in a rodent model of diabetic retinopathy, *Diabetes* 2011, 54:1559-1565
8. Rivera JC, Sitaras N, Noueihed B, Hamel D, Madaan A, Zhou T, Honore J,

- Quiniou C, Joyal J, Hardy P, Sennlaub F, Lubell W, Chemtob S: Microglia and IL-1 $\beta$  in Ischemic Retinopathy elicit microvascular degeneration through neuronal Semaphorin3A, *Arterioscler Thromb Vasc Biol* 2013, 133:1881-1891
9. dell'Omo R, Semeraro F, Bamonte G, Cifariello F, Romano MR, Costagliola C: Vitreous Mediators in Retinal Hypoxic Diseases, *Mediators Inflamm* 2013, 1-16
  10. Ishida S, Yamashiro K, Usui T, Kaji Y, Ogura Y, Hia T, Honda Y, Oguchi Y, Adamis A: Leukocytes mediate retinal vascular remodeling during development and vaso-obliteration in disease, *Nat Med* 2003, 9:781-789
  11. Joyal JS, Sitaras N, Binet F, Rivera JC, Stahl A, Karine, Polosa A, Zhu T, Hamel D, Djavari M, Kunik D, Honoré JC, Picard E, Zabeida A, Varma DR, Hickson G, Mancini J, Klagsbrun M, Costantino S, Beauséjour C, Lachapelle P, Smith LEH, Chemtob S, Sapieha P: Ischemic neurons prevent vascular regeneration of neural tissue by secreting semaphorin 3A, *Blood* 2011, 117:6024-6035
  12. Dorfman A, Dembinska O, Chemtob S, Lachapelle P: Early Manifestations of Postnatal Hyperoxia on the Retinal Structure and Function of the Neonatal Rat, *Invest Ophthalmol Vis Sci* 2008, 49:458-466
  13. Teshima S, Nakanishi H, Nishizawa M, Kitagawa K, Kaibori M, Yamada M, Habara K, Kwon A, Kamiyama Y, Ito S, Okumura T: Up-regulation of IL-1 receptor through PI3K/Akt is essential for the induction of iNOS gene expression in hepatocytes, *J Hepatol* 2004, 40:616-623
  14. Skundric DS, Bealmear B, Lisak RP: Induced upregulation of IL-1, IL-1RA and IL-1R type I gene expression by Schwann cells, *J Neuroimmunol* 1997, 74:9-18
  15. Kowluru R, Zhong Q, Santos J: Matrix metalloproteinases in diabetic retinopathy: potential role of MMP-9, *Expert Opin Investig Drugs* 2012, 21:797-805
  16. Soh UJK, Dores MR, Chen B, Trejo J: Signal transduction by protease-activated receptors, *Br J Pharmacol* 2010, 160:191-203
  17. Uusitalo-Jarvinen H, Kurokawa T, Mueller BM, Andrade-Gordon P, Friedlander M, Ruf W: Role of Protease Activated Receptor 1 and 2 Signaling in Hypoxia-Induced Angiogenesis, *Arterioscler Thromb Vasc Biol* 2007, 27:1456-1462
  18. Belting M, Dorrell MI, Sandgren S, Aguilar E, Ahamed J, Dorfleutner A, Carmeliet P, Mueller BM, Friedlander M, Ruf W: Regulation of angiogenesis by tissue factor cytoplasmic domain signaling, *Nat Med* 2004, 10:502-509
  19. Tsai SH, Sheu MT, Liang YC, Cheng HT, Fang SS, Chen C: TGF- $\beta$  inhibits IL-1 $\beta$ -activated PAR-2 expression through multiple pathways in human primary synovial cells, *J Biomed Sci* 2009, 16:97-111
  20. Ritchie E, Saka M, MacKenzie C, Drummond R, Wheeler-Jones C, Kanke T, Plevin R: Cytokine upregulation of proteinase-activated-receptors 2 and 4 expression mediated by p38 MAP kinase and inhibitory kappa B kinase  $\beta$  in human endothelial cells, *Br J Pharmacol* 2007, 150:1044-1054
  21. Boileau C, Amiable N, Martel-Pelletier J, Fahmi H, Duval N, Pelletier J: Activation of proteinase-activated receptor 2 in human osteoarthritic cartilage upregulates catabolic and proinflammatory pathways capable of inducing cartilage degradation: a basic science study, *Arthritis Res Ther* 2007, 9:R121
  22. Noorbakhsh F, Vergnolle N, McArthur JC, Silva C, Andrade-Gordon P,

- Vodjgani M, Hollenberg M, Power C: Protease-activated Receptor-2 induction by neuroinflammation prevents neuronal death during HIV infection, *J Immunol* 2005, 174:7320-7329
23. Suharti C, van Gorp EC, Setiati TE, Dolmans WM, Djokomoeljanto RJ, Hack CE, Hugo ten C, van der Meer JW: The role of cytokines in activation of coagulation and fibrinolysis in dengue shock syndrome, *J Thromb Haemost* 2002, 87:42-46
  24. Smith LEH, Wesoloiuski E, McLellan A, SK Kostyk, DAMato XR, Sullivan R, DAMore PA: Oxygen-Induced Retinopathy in the Mouse, *Invest Ophthal Vis Sci* 1994, 35:101-111
  25. Stahl A, Connor KM, Sapiuha P, Chen J, Dennison RJ, Krah NM, Seaward MR, Willett KL, Aderman CM, Guerin KI, Hua J, Lofqvist C, Hellstrom A, Smith LEH: The Mouse Retina as an Angiogenesis Model, *Invest Ophthal Vis Sci* 2010, 51:2813-2826
  26. Stahl A, Connor KM, Sapiuha P, Willett KL, Krah NM, Dennison RJ, Chen J, Guerin KI, Smith LEH: Computer-aided quantification of retinal neovascularization, *Angiogenesis* 2009, 12:297-301
  27. Dull T, Zufferey R, Kelly M, Mandel RJ, Nguyen M, Trono D, Naldini L: A Third-Generation Lentivirus Vector with a Conditional Packaging System, *J Virol* 1998, 72:8463
  28. Sapiuha P, Sirinyan M, Hamel D, Zaniolo K, Joyal JS, Cho JH, Honoré JC, Kermorvant-Duchemin E, Varma DR, Tremblay S, Leduc M, Rihakova L, Hardy P, Klein WH, Mu X, Mamer O, Lachapelle P, Di Polo A, Beauséjour C, Andelfinger G, Mitchell G, Sennlaub F, Chemtob S: The succinate receptor GPR91 in neurons has a major role in retinal angiogenesis, *Nat Med* 2008, 14:1067-1076
  29. Barbaric I, Miller G, Dear T: Appearances can be deceiving: phenotypes of knockout mice, *Brief Funct Genomic Proteomic* 2007, 6:91-103
  30. Schmidlin F, Amadesi S, Dabbagh K, Lewis DE, Knott P, Bunnet NW, Gater PR, Geppetti P, Bertrand C, Stevens ME: Protease-Activated Receptor 2 Mediates Eosinophil Infiltration and Hyperreactivity in Allergic Inflammation of the Airway, *J Immunol* 2002, 169:5315-5321
  31. Binet F, Mawambo G, Sitaras N, Tetreault N, Lapalme E, Favret S, Cerani A, Leboeuf D, Tremblay S, Rezende F, Juan A, Stahl A, Joyal J, Milot É, Kaufman R, Guimond M, Kennedy T, Sapiuha P: Neuronal ER Stress Impedes Myeloid-Cell-Induced Vascular Regeneration through IRE1-alpha degradation of Netrin-1, *Cell Metab* 2013, 17: 353-371
  32. Cerani A, Tetreault N, Menard C, Lapalme E, Patel C, Sitaras N, Beaudoin F, Leboeuf D, De Guire V, Binet F, Dejda A, Rezende F, Miloudi K, Sapiuha P: Neuron-Derived Semaphorin 3A Is an Early Inducer of Vascular Permeability in Diabetic Retinopathy via Neuropilin-1, *Cell Metab* 2013, 18: 505-518
  33. Kaufmann R, Hollenberg M: Proteinase-Activated Receptors (PARs) and Calcium Signaling in Cancer, *Adv Exp Med Biol* 2012, 740:979-1000
  34. Kim Y, West XZ, Byzova TV: Inflammation and oxidative stress in angiogenesis and vascular disease, *J Mol Med* 2013, 91:323-328
  35. Gardiner TA, Gibson DS, de Gooyer TE, de la Cruz VF, McDonald DM, Stitt A:

Inhibition of Tumor Necrosis Factor- $\alpha$  Improves Physiological Angiogenesis and Reduces Pathological Neovascularization in Ischemic Retinopathy, *Am J Pathol* 2005, 166:637–644

36. Meyer N, Christoph J, Makrinioti H, Indermitte P, Rhyner C, Soyka M, Eiwegger T, Chalubinski T, KWanke, Fujita H, Wawrzyniak P, Burgler S, Zhang S, Akdis M, Menz G, Akdis C: Inhibition of angiogenesis by IL-32: Possible role in asthma, *J Allergy Clin Immunol* 2012, 129:964-973.e967

37. Massague J, Blain S, Lo R: TGF-beta Signaling in Growth Control, Cancer, and Heritable Disorders, *Cell* 2000, 103:295-309

38. Kermorvant-Duchemin E, Sennlaub F, Sirinyan M, Brault S, Andelfinger G, Kooli A, Germain S, Ong H, d'Orleans-Juste P, Gobeil F, Zhu T, Boisvert C, Hardy P, Jain K, Falck JR, Balazy M, Chemtob S: Trans-arachidonic acids generated during nitrate stress induce a thrombospondin-1–dependent microvascular degeneration, *Nat Med* 2005, 11:1339-1345

39. Minuzzo S, Moserle L, Indraccolo S, Amadori A: Angiogenesis meets immunology: Cytokine gene therapy of cancer, *Mol Aspects Med* 2007, 28:

40. Shen H, Yao P, Lee E, Greenhalgh D, Soulika A: Interferon-gamma inhibits healing post scald burn injury, *Wound Repair Regen* 2012, 20:580-591

41. Rothmeier A, Ruf W: Protease-activated receptor 2 signaling in inflammation, *Semin Immunopathol* 2012, 34:133-149

42. Ossovskaya VS, Nunnat N: Protease-Activated Receptors: Contribution to Physiology and Disease, *Physiol Rev* 2004, 84:579-621

43. Tremblay S, Miloudi K, Chaychi S, Favret S, Binet F, Polosa A, Lachapelle P, Chemtob S, Sapieha P: Systemic Inflammation Perturbs Developmental Retinal Angiogenesis and Neuroretinal Function, *Invest Ophthalmol Vis Sci* 2013, 54:8125-8139

44. Lange C, Ehlken C, Stahl A, Martin G, Hansen L, Agostini H: Kinetics of retinal vaso-obliteration and neovascularisation in the oxygen-induced retinopathy (OIR) mouse model, *Graefes Arch Clin Exp Ophthalmol* 2009, 247:1205-1211

45. Rasmussen J, Riis S, Frøbert O, Yang S, Kastrop J, Zachar V, Simonsen U, Fink T: Activation of Protease-Activated Receptor 2 Induces VEGF Independently of HIF-1, *PLoS ONE* 2012, 7:e46087

46. Bucci M, Roviezzo F, Cirino G: Protease-activated receptor-2 (PAR2) in cardiovascular system, *Vascul Pharmacol* 2005, 43:247-253

47. Ramachandran R, Hollenberg MD: Proteinases and signalling: pathophysiological and therapeutic implications via PARs and more, *Br J Pharmacol* 2008, 153:S263-S282

48. Luo W, Wang Y, Reiser G: Protease-activated receptors in the brain: Receptor expression, activation, and functions in neurodegeneration and neuroprotection, *Brain Res Rev* 2007, 56:331-345

49. Ramachandran R, Noorbakhsh F, DeFea K, Hollenberg MD: Targeting proteinase-activated receptors: therapeutic potential and challenges, *Nat Rev Drug Discov* 2012, 11:69-86

50. Afkhami-Goli A, Noorbakhsh F, Keller AJ, Vergnolle N, Westaway D, Jhamandas JH, Andrade-Gordon P, Hollenberg MD, Arab H, Dyck RH, Power C:

Proteinase-Activated Receptor-2 Exerts Protective and Pathogenic Cell Type-Specific Effects in Alzheimer's Disease, *J Immunol* 2007, 179:5493-5503

51. Noorbakhsh F, Tsutsui S, Vergnolle N, Boven LA, Shariat N, Vodjgani M, Warren KG, Andrade-Gordon P, Hollenberg MD, Power C: Proteinase-activated receptor 2 modulates neuroinflammation in experimental autoimmune encephalomyelitis and multiple sclerosis, *J Exp Med* 2006, 203:425-435

52. Jin G, Hayashi T, Kawagoe J, Takizawa T, Nagata T, Nagano I, Syoji M, Abe K: Deficiency of PAR-2 gene increases acute focal ischemic brain injury, *J Cereb Blood Flow Metab* 2005, 25:302-313

53. Wang H, Ubl J, Reiser G: Four subtypes of protease-activated receptors, co-expressed in rat astrocytes, evoke different physiological signaling, *Glia* 2002, 37:53-63

54. Hellström A, Smith LEH, Dammann O: Retinopathy of Prematurity, *Lancet* 2013, 382:1445-1457

55. Miller J, Couter JL, Strauss E, Ferrara N: Vascular Endothelial Growth Factor A in Intraocular Vascular Disease, *Ophthalmology* 2012, 120:106-114

56. Wang S, Park J, Duh E: Novel Targets Against Retinal Angiogenesis in Diabetic Retinopathy, *Curr Diab Rep* 2012, 12:355-363

57. Hernandez C, Simo R: Strategies for blocking angiogenesis in diabetic retinopathy: from basic science to clinical practice, *Expert Opin Investig Drugs* 2007, 16:1209-1226

58. Stewart MW: The Expanding Role of Vascular Endothelial Growth Factor Inhibitors in Ophthalmology, *Mayo Clinic Proc* 2012, 87:77-88

### *Specific contributions from the candidate*

In this study, we focused on a discrepancy that we observed in the previous Chapter, which is that of the autocrine, autostimulatory activation of microglia in the retina in IRs. IL-1 $\beta$  propagates this cycle and concomitantly induces Sema3A-mediated vascular decay. Bearing this in mind, I theorized the possibility of an intrinsic regulatory mechanism by which the retina (and more specifically, retinal ganglion cells) controls the exacerbated vascular degeneration precipitated by IL-1 $\beta$  and activated microglia. Since IL-1 $\beta$  also induces the expression of various proteases, which sequentially activates protease-activated receptors (PARs), we turned our

attention to PAR2 as a potential candidate—due to its previously described pro-angiogenic effects in the retina.

Precisely, I contributed enormously to the development of the project, which include planning, designing, optimizing and performing the majority of the experiments. I was chiefly involved in gathering and analyzing data. Dr. S Chemtob and myself prepared the figures with the aid of Dr. JC Rivera. Finally I scripted, proofed and finalized the entire manuscript. Dr. S Chemtob, Dr. JC Rivera and Dr. JS Joyal aided in editing and proofing the finalized version of the manuscript.

Dr. P Hardy and Dr. P Sapieha provided expert opinion in the study.

## Figures for Chapter 3

**Figure 1.**

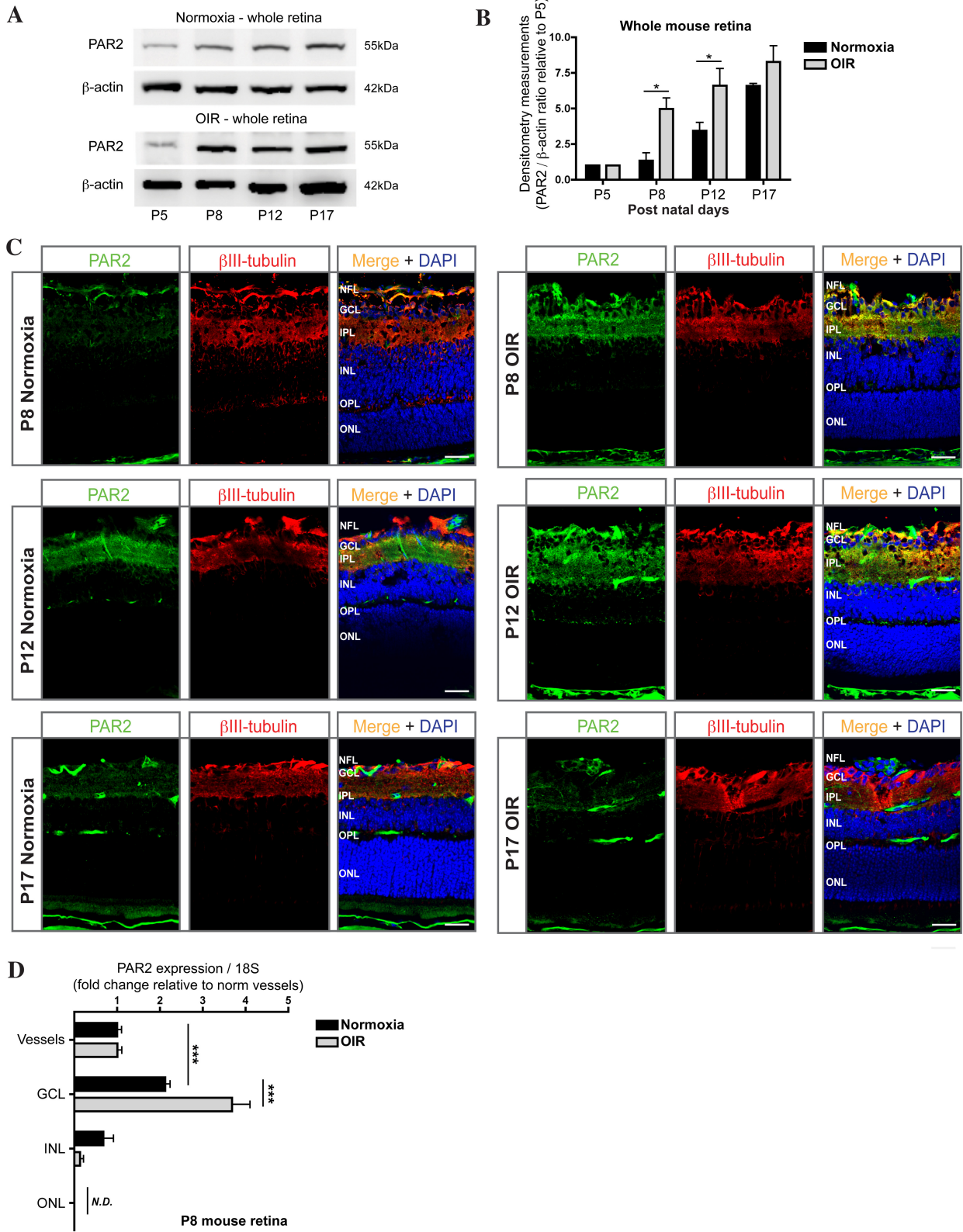


**Figure 1. Neuronal PAR2 increases in mice retina during Oxygen-induced retinopathy (OIR).** (A) Western Blot analysis of C57BL/6 mice whole retina at different time points of OIR<sup>24</sup> showing increases of PAR2 at P8 and P12 compared to room-air raised mice retinas (n=2 retinas per time point). (B) Densitometry quantification of A. Values are normalized to P5 retinas. (\*=p<0.05, n=3 independent experiments). (C) Immunohistochemical analysis on retinal coronal sections from P8, P12 and P17 C57BL/6 mice pups exposed for 24h in either 21 or 75 % O<sub>2</sub>. PAR2 (green) immunohistochemistry increases substantially in  $\beta$ III-tubulin-expressing retinal ganglion cells (red) during OIR at P8 and P12 similar to what is seen in A. At P17, PAR2 immunoreactivity in OIR mice retina was similar to normoxia-raised animals. Nuclei are counterstained with DAPI (blue) and vessels with CD31 (magenta). NFL, nerve fiber layer; GCL, ganglion cell layer; IPL, inner plexiform layer; INL; inner nuclear layer; OPL, outer plexiform layer; ONL, outer nuclear layer. Scale bar = 50  $\mu$ m. Original magnification 300x. (D) Laser-capture microdissected retinas from P8 pups exposed to 21 or 75 % O<sub>2</sub> (OIR). Real-time quantitative PCR (qPCR) on microdissected retinal layers demonstrate robust expression of PAR2 mRNA in GCL, which increases specifically in this layer following 24h exposure to high oxygen (\*\*\*=p<0.001, n=4 retinas).

**Relative contributions: Figure 1**

- A) Western Blot analysis performed by **N Sitaras** and M Bien-Aimé
- B) Immunohistochemistry, imaging and analysis performed by **N Sitaras** and JC Rivera
- C) Laser capture microdissection and qPCR analysis performed by **N Sitaras** and M Bien-Aimé

Animal handling and sample collection: **N Sitaras**

Figure preparation: **N Sitaras**, JC Rivera and S Chemtob

Approximate Figure contribution: 75%

**Figure 2.**

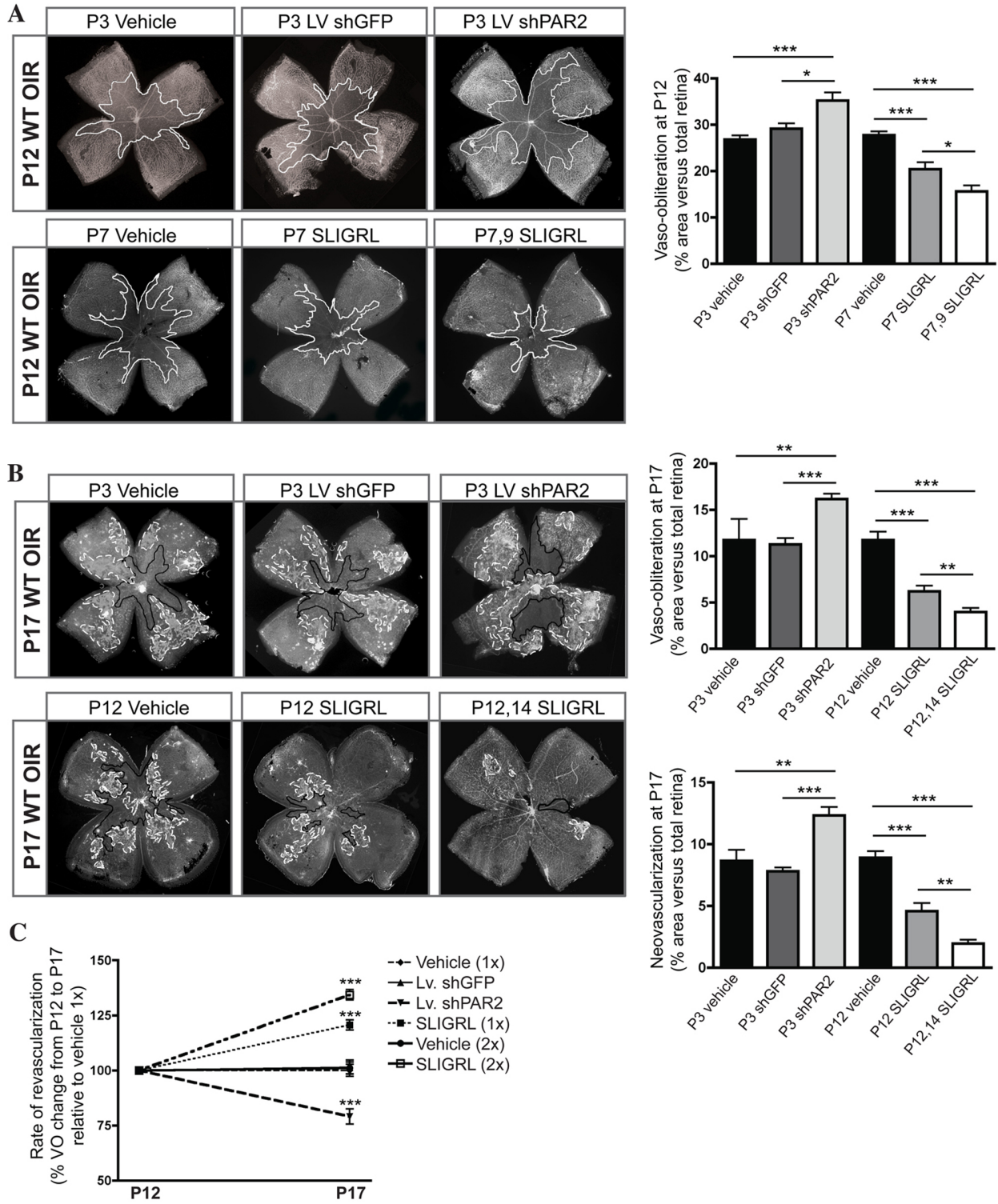


**Figure 2. Modulation of PAR2 activity during OIR affects vaso-obliteration and neovascularization.** (A) Representative photomicrographs from isolectin B4-stained retinal flatmounts from P12 C57BL/6 mice pups exposed to hyperoxia from P7 to P12<sup>24</sup>. Original magnification 100x. Vaso-obliterated (VO) areas are outlined with solid black line. Pups injected intravitreally with lentiviral (Lv.) particles containing shRNA versus PAR2 (~9.6 ng) show significant *increases* in VO compared to vehicle or control Lv. shGFP (~8.5 ng) injected animals. Mice pups injected intravitreally with PAR2 agonist peptide (PAR2-AP), SLIGRL-NH<sub>2</sub> (100μmol), however, display significant *decrease* in VO. Quantification of VO areas is shown in graph (\*=p<0.05, \*\*\*p<0.001, n=6-12 retinas). (B) Photomicrographs of P17 C57BL/6 mice pups exposed to OIR and injected intravitreally with Lv. shPAR2 demonstrate *increased* VO and neovascularization (NV) compared to control vehicle or Lv. shGFP treated animals, while, SLIGRL-treated mice pups demonstrate significant decreases in avascular area and NV. VO and NV areas are outlined with solid black lines and white-hashed lines, respectively. Quantification of avascular areas and NV areas by *SWIFT\_NV*<sup>26</sup> are shown in graphs (\*\*=p<0.01, \*\*\*p<0.001, n=6-12 retinas). (C) Calculated rate of revascularization from P12 to P17 of mice pup retinas following hyperoxic exposure previously injected with modulators of PAR2 activity. Change in VO was calculated for each group using VO at P12 as starting value (100%). Samples at P17 were compared relative to singly injected vehicle-treated animals. Lv. shPAR2 treatment translated to a retard in revascularization potential whereas administration of SLIGRL accelerated this process (\*=p<0.05, \*\*\*p<0.001, n=18-23 retinas).

**Relative contributions: Figure 2**

A) through C) Lentiviral preparations performed by **N Sitaras** and D Hamel  
Intravitreal injections performed by **N Sitaras**, JC Rivera, K Zaniolo and Z  
Shao  
Immunohistochemistry, imaging and analysis performed by **N Sitaras**, JC  
Rivera and K Zaniolo

Animal handling and sample collection: **N Sitaras**, K Zaniolo and Z Shao

Figure preparation: **N Sitaras** and S Chemtob

Approximate Figure contribution: 75%

**Figure 3.**

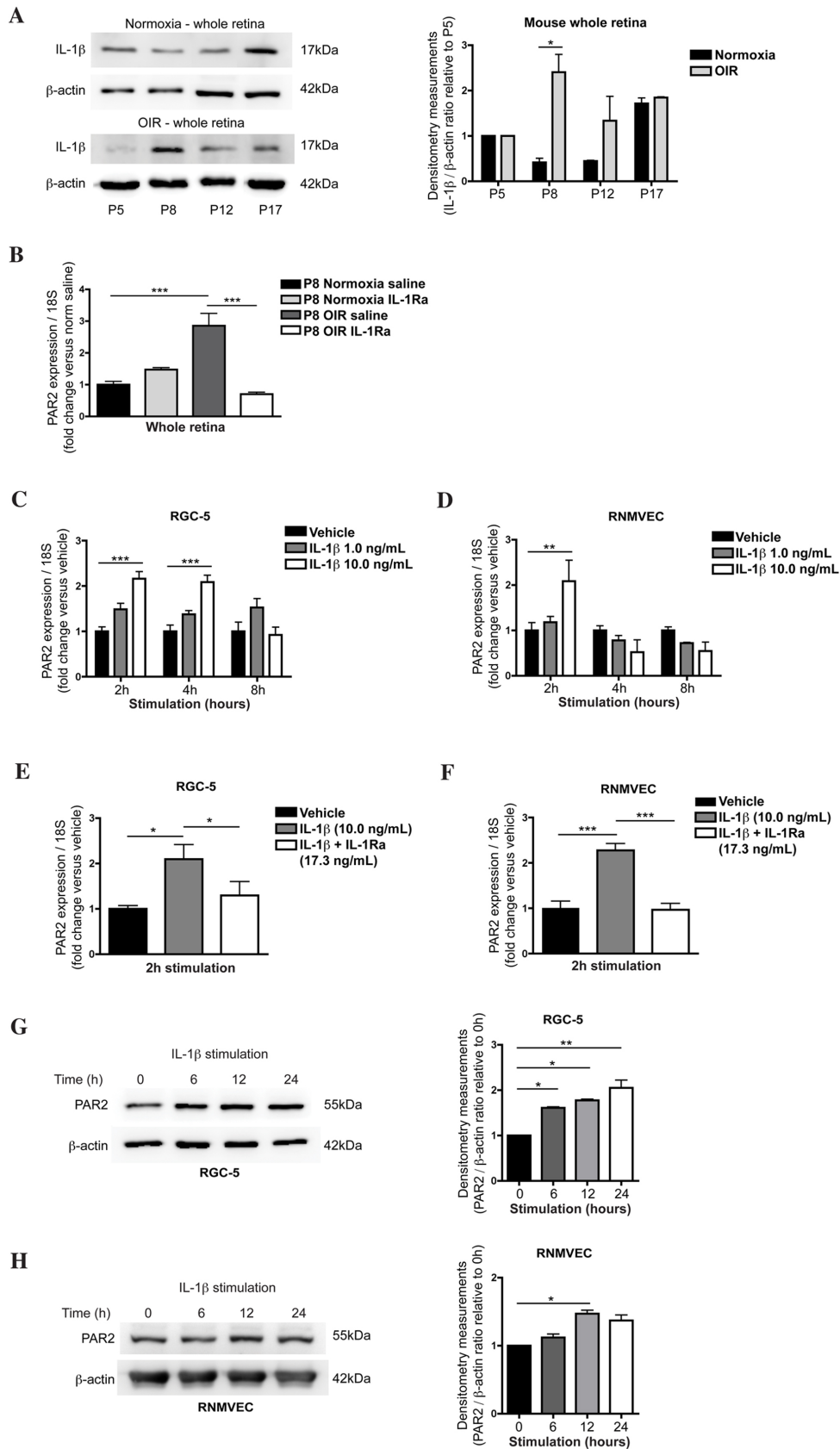


**Figure 3. Increased expression of IL-1 $\beta$  in the retina during OIR stimulates PAR2 expression.** (A) Western blot analysis of IL-1 $\beta$  in whole retina from mice pups at various time points of OIR showing increase in P8 compared to room-air raised C57BL/6 mice pups (n=2 retinas per time point). Densitometry quantification at right. Values are normalized to P5 retinas. (\*=p<0.05, n=3 independent experiments). (B) Real-time qPCR analysis of whole retina from P8 C57BL/6 mice pups showing an increase in PAR2 mRNA upon exposure to hyperoxia for 24h. Animals treated intraperitoneally with IL-1 receptor antagonist (IL-1Ra; Kineret®) display significantly less PAR2 mRNA (\*\*\*=p<0.001, n=3, pool of 2 retinas per n). IL-1 $\beta$  stimulated cultured (C) retinal neurons (RGC-5) and (D) rat brain microvascular endothelial cells (RBMVEC) display time- and dose-dependent increases in PAR2 mRNA as analyzed by qPCR analysis (\*\*=p<0.01, \*\*\*=p<0.001, n=4-8). Administration of IL-1Ra abrogated IL-1 $\beta$  dependent increases in PAR2 mRNA in both (E) RGC-5 and (F) RBMVEC as determined by qPCR analysis (\*=p<0.05, \*\*\*=p<0.001, n=6-8). (G) RGC-5 cells stimulated with IL-1 $\beta$  displayed time-dependent increase in PAR2 protein levels. Densitometry quantification at right (\*=p<0.05, \*\*=p<0.01, n=2 independent experiments). (H) RBMVEC cells stimulated with IL-1 $\beta$  displayed an increase in PAR2 protein levels at 12h only. Densitometry quantification at right (\*=p<0.05, n=2 independent experiments).

**Relative contributions: Figure 3**

- A) Western blot analysis performed by **N Sitaras** and M Bien-Aimé
- B) Kineret administration and qPCR analysis performed by N Sitaras
- C) though H) In vitro experiments and Western blot/qPCR analysis performed by **N Sitaras**, M Bien Aimé and B Noueihed

Animal handling and sample collection: **N Sitaras**, M Bien Aimé and B Noueihed

Figure preparation: **N Sitaras** and S Chemtob

Approximate Figure contribution: 60%

**Figure 4.**

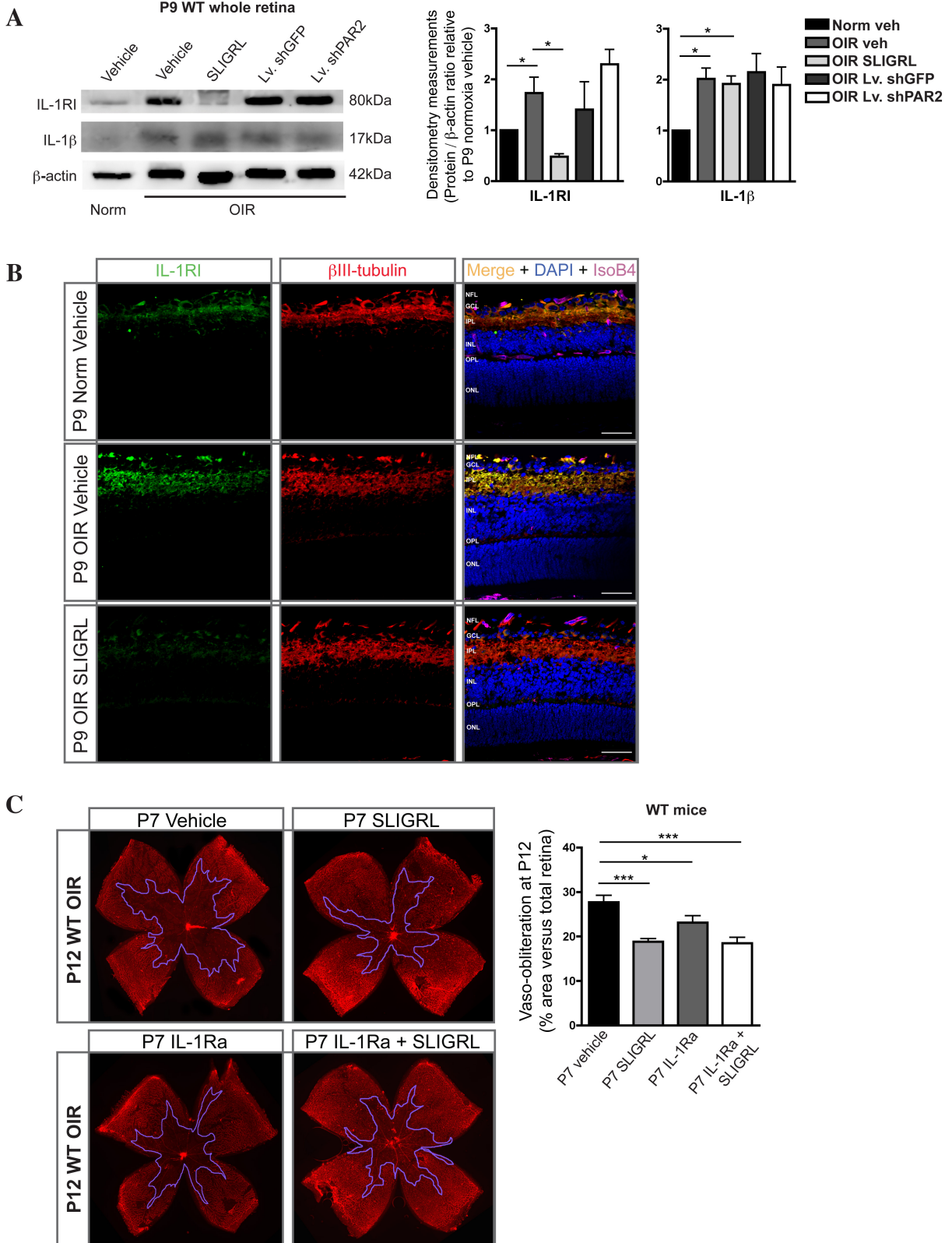


**Figure 4. PAR2 activation results in downregulation of IL-1RI in vivo.** (A) Western Blot analysis of IL-1 $\beta$  and IL-1RI in P9 C57BL/6 mice whole retina exposed to OIR and injected with vehicle, SLIGRL (100  $\mu$ M), Lv. shGFP or Lv. shPAR2 (n=2 retinas per group). Increases in IL-1 $\beta$  and IL-1RI were observed in OIR exposed retinas; however, treatment with SLIGRL significantly *reduced* IL-1RI expression but not IL-1 $\beta$ . Conversely, administration of Lv. shPAR2 *increased* IL-1RI levels while IL-1 $\beta$  levels remained the same. Densitometry quantification at right (\*=p<0.05, n=3 independent experiments). (B) Immunohistochemical analysis of P9 C57BL/6 mice retinas exposed to OIR (middle panels) displayed significant immuno-reactivity to IL-1RI (green) localized primarily in the ganglion cell layer ( $\beta$ III-tubulin; red) compared to normoxic-exposed retinas (upper panels). SLIGRL administration reversed this process (lower panels). Nuclei are counterstained with DAPI (blue) and vessels with isolectin B4 (magenta). NFL, nerve fiber layer; GCL, ganglion cell layer; IPL, inner plexiform layer; INL; inner nuclear layer; OPL, outer plexiform layer; ONL, outer nuclear layer. Scale bar = 50  $\mu$ m. Original magnification 300x. (C) Representative images from isolectin B4-stained retinal flatmounts from P12 C57BL/6 mice pups exposed to OIR and injected intravitreally with either SLIGRL (100  $\mu$ M) or IL-1Ra (10  $\mu$ M) or both. Original magnification 100x. VO areas are outlined with solid blue lines. Individually, administration of PAR-2 agonist and IL-1RI antagonist successfully inhibited hyperoxia-induced vaso-oblivation (\*=p<0.05, \*\*\*=p<0.001, n=6-8 retinas); however, there was no additive effect from co-administration of both SLIGRL and IL-1Ra.

**Relative contributions: Figure 4**

- A) Western blot analysis performed by **N Sitaras** and M Bien-Aimé
- B) and C) Intravitreal injections performed by **N Sitaras** and JC Rivera  
Immunohistochemistry, imaging and analysis performed by **N Sitaras** and JC Rivera

Animal handling and sample collection: **N Sitaras** and JC Rivera

Figure preparation: **N Sitaras**, JC Rivera and S Chemtob

Approximate Figure contribution: 75%

**Figure 5.**

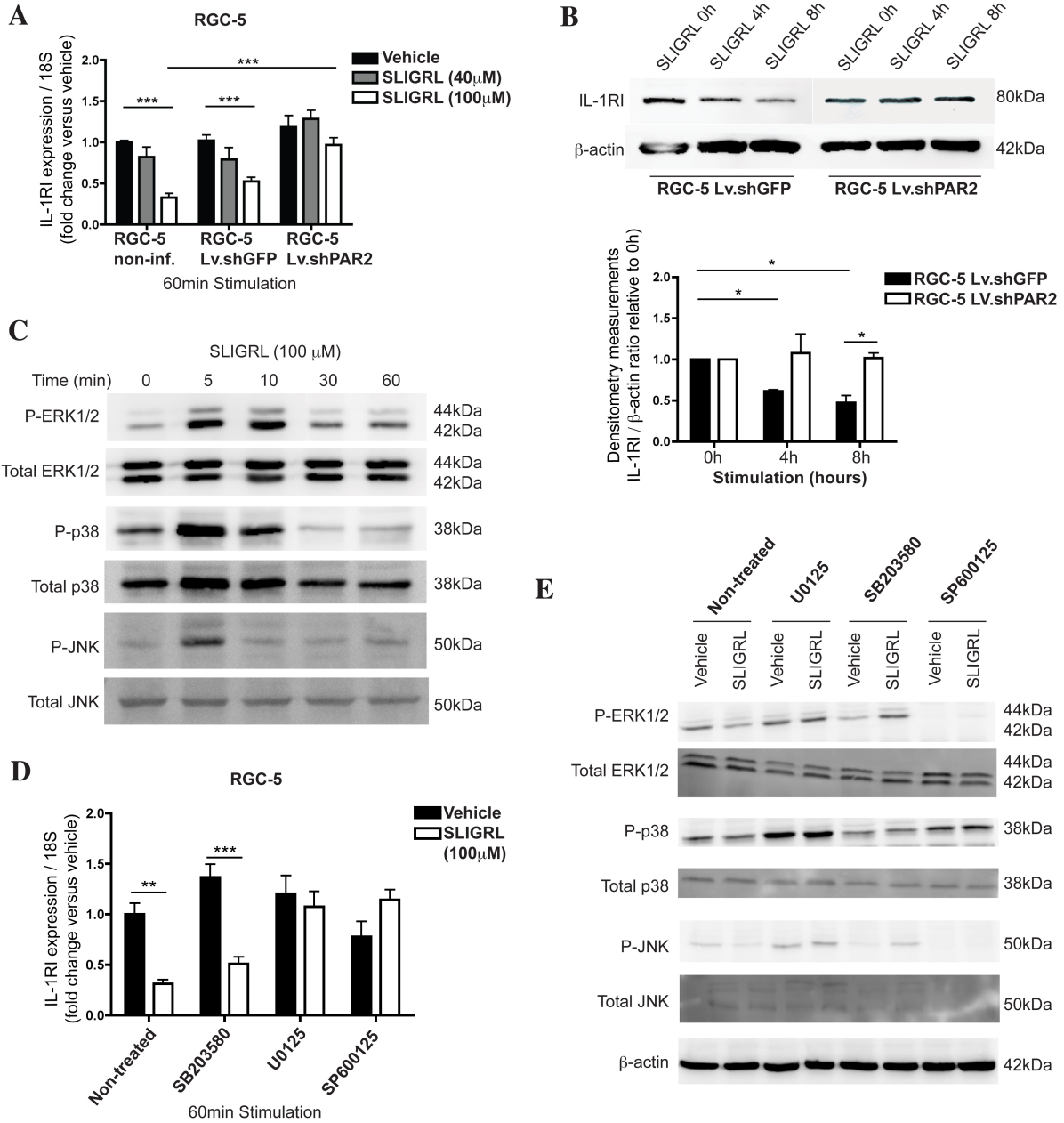


**Figure 5. JNK activates downstream ERK1/2, which is required for PAR2-dependent inhibition IL-1RI in retinal neurons.** (A) PAR2-expressing RGC-5 exhibit dose-dependent *decreases* in IL-1RI mRNA following 1h stimulation with SLIGRL (\*= $p < 0.05$ , \*\*\*= $p < 0.001$ ,  $n = 6-10$ ); RGC-5 infected with Lv. shPAR2 abrogated effect. Lv. shGFP-infected served as control RGC-5 (\*\*\*= $p < 0.001$ ,  $n = 10-14$ ). (B) RGC-5 cells show effective decrease in IL-1RI protein levels following SLIGRL treatment; Lv. shPAR2 did not respond to SLIGRL treatment. Densitometry quantification below (\*= $p < 0.05$ ,  $n = 2$  independent experiments). (C) Administration of SLIGRL activates various MAPK signaling pathways. (D) RGC-5 cells pre-treated with either MEK1/2 inhibitor (U0125) or JNK inhibitor (SP600125) *but not* p38 inhibitor (SB203580), abrogated the SLIGRL-dependent decreases in IL-1RI mRNA in RGC-5 (\*\*= $p < 0.01$ , \*\*\*= $p < 0.001$ ,  $n = 6$ ). (E) Activation of MAPK by SLIGRL in RGC-5 is abolished using specific inhibitors to MEK1/2 (U0125), p38 (SB203580) and JNK (SP600125); inhibition of JNK also translated to a downstream inhibition of ERK1/2 phosphorylation. JNK phosphorylation was not affected by MEK1/2 inhibitor.

**Relative contributions: Figure 5**

A) and D) In vitro preparation and qPCR analysis performed by **N Sitaras** and M Bien-Aimé

B) C) and E) In vitro preparation and Western blot analysis performed by B Noueihed, M Bien-Aimé, S Omri and **N Sitaras**

Figure preparation: **N Sitaras**, B Noueihed and S Chemtob

Approximate Figure contribution: 40%

**Figure 6.**

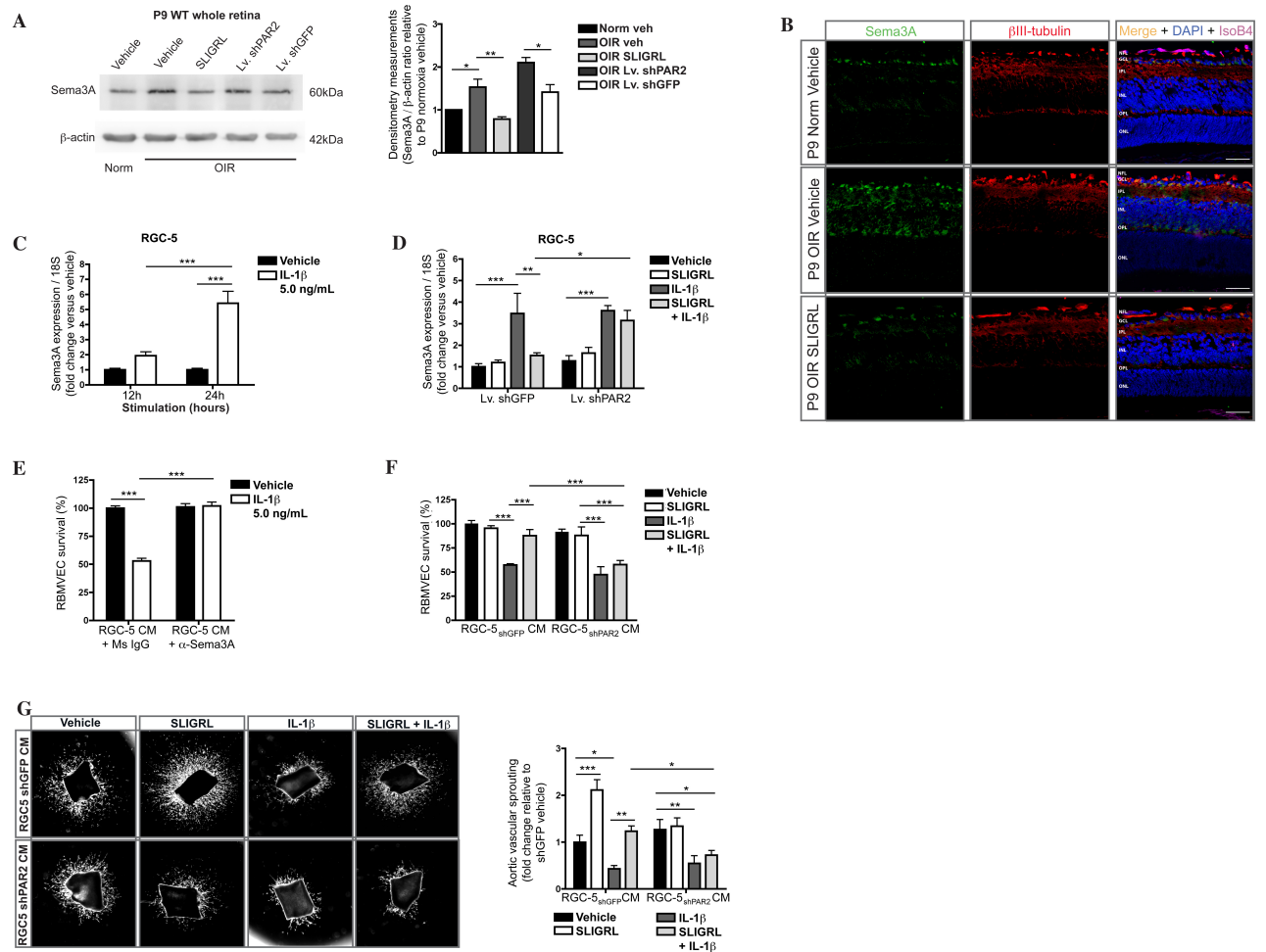


**Figure 6. Activation of PAR2 abolishes IL-1 $\beta$ -mediated Sema3A release, reducing endothelial cell death and promoting vascular sprouting.** (A) Western Blot analysis of Sema3A in P9 C57BL/6 mice whole retinas exposed to OIR and injected intravitreally. OIR exposure augmented Sema3A expression in P9 vehicle injected animals; however, OIR retinas treated with SLIGRL reduced Sema3A levels significantly compared to vehicle-injected eyes (n=2 retinas per group). Densitometry quantification at right (\*=p<0.05, n=3 independent experiments). Conversely, Lv. shPAR2 treatment augmented Sema3A levels compared to Lv. shGFP-injected retinas. (B) Immunohistochemical analysis on P9 C57BL/6 mice retina exposed to hyperoxia demonstrated significant immunoreactivity to Sema3A particularly in the ganglion cell layer. Treatment with SLIGRL, however, significantly reduced Sema3A levels in this layer. NFL, nerve fiber layer; GCL, ganglion cell layer; IPL, inner plexiform layer; INL; inner nuclear layer; OPL, outer plexiform layer; ONL, outer nuclear layer. Scale bar = 50  $\mu$ m. Original magnification 300x. (C) RGC-5 cells stimulated with IL-1 $\beta$  exhibit time-dependent increases in Sema3a mRNA (\*\*\*=p<0.001, n=6). (D) Control Lv. shGFP-infected RGC-5 stimulated with SLIGRL abrogated IL-1 $\beta$ -dependent increases in Sema3a mRNA after 24h; however, this effect was abolished in Lv. shPAR2-infected RGC-5 (\*=p<0.05, \*\*=p<0.01, \*\*\*=p<0.001, n=7-8). (E) MTT cell survival assay on RBMVEC exposed to CM from RGC-5 cells stimulated with IL-1 $\beta$  demonstrated significant reduction in EC survival. Treatment with an antibody to Sema3A abrogated this effect (\*\*\*=p<0.001, n=5-6). (F) Similar experiment as in E. but using CM from Lv. shGFP- or Lv. shPAR2-infected RGC-5 stimulated with either IL-1 $\beta$  or SLIGRL, or both. IL-1 $\beta$ -stimulated CM significantly reduced endothelial cell survival, while CM from Lv. shGFP RGC-5 co-stimulated with SLIGRL and IL-1 $\beta$  reversed this effect. Lv. shPAR2 RGC-5 co-stimulated with SLIGRL and IL-1 $\beta$  did not salvage the IL-1 $\beta$ -induced endothelial cell death (\*\*\*=p<0.001, n=6). (G) Aortic explants exposed to the same CM as in F. Explants treated with CM from SLIGRL-stimulated RGC-5 displayed increased sprouting whereas explants exposed to CM from IL-1 $\beta$ -stimulated RGC-5 exhibited diminished sprouting growth. CM from Lv. shGFP RGC-5 co-stimulated with SLIGRL and IL-1 $\beta$ , however, translated to normal aortic sprouting angiogenesis whereas CM from Lv. shPAR2 RGC-5 did not. Quantification of aortic vascular sprouting at right (\*=p<0.05, \*\*=p<0.01, \*\*\*=p<0.001, n=6-9).

**Relative contributions: Figure 6**

- A) Western blot analysis performed by **N Sitaras** and M Bien-Aimé
- B) Intravitreal injections performed by **N Sitaras**  
Immunohistochemistry, imaging and analysis performed by **N Sitaras** and JC Rivera
- C) In vitro preparations and qPCR performed by N Sitaras, JS Joyal, M Bien-Aimé and S Omri
- D) In vitro preparations and EC survival assay performed by **N Sitaras**
- E) Aortic explant preparations, imaging and analysis performed by **N Sitaras**

Animal handling and sample collection: **N Sitaras** and JC Rivera

Figure preparation: **N Sitaras**, JC Rivera and S Chemtob

Approximate Figure contribution: 75%

## Oxygen-Induced Retinopathy

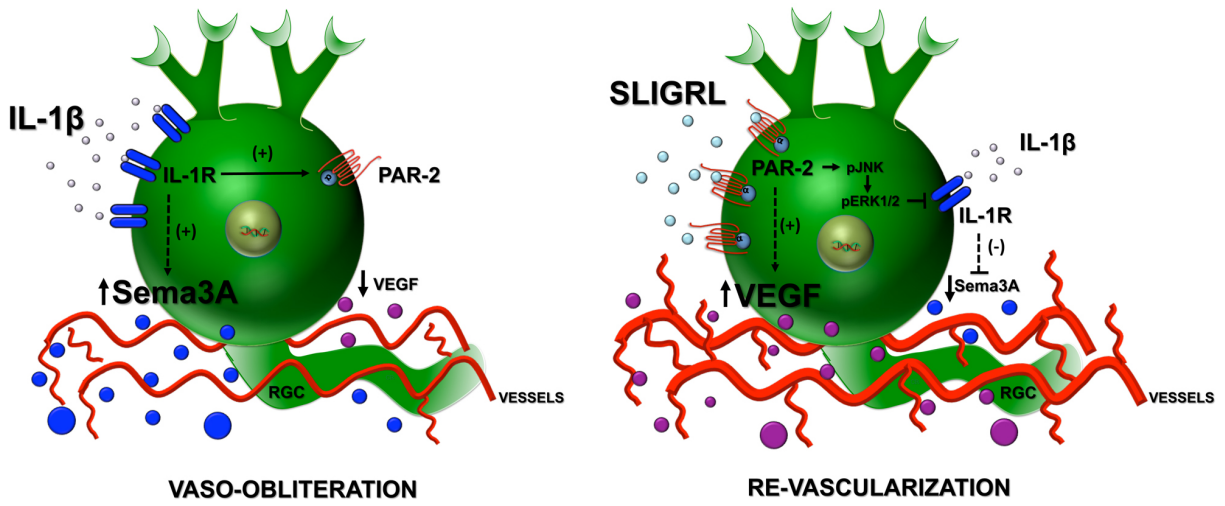


**Figure 7. PAR2 on retinal ganglion cells enhances revascularization by suppressing IL-1RI.** Augmented levels of secreted IL-1 $\beta$  stimulate rapid production of PAR2 to counteract the hyperoxic stress. However, exhaustive inflammation causes RGCs to suspend PAR2 production and instead induces Sema3A production, which leads to vaso-oblivation and contributes to pathological pre-retinal neovascularization (left panel). Conversely, timely activation of PAR2 – using peptide agonist, SLIGRL – abrogates this process by suppressing IL-1RI via JNK and ERK1/2-dependent processes in RGCs to blunt Sema3A production and concomitantly stimulate VEGF production to augment the revascularization process of the ischemic retina (right panel).

**Relative contributions: Figure 7**

Schematic provided by JC Rivera and **N Sitaras**

Figure preparation: **N Sitaras**, JC Rivera and S Chemtob

Approximate Figure contribution: 25%

## Final Discussion

The studies presented herein highlight several novel topics that are central to understanding the pathogenesis of Ischemic Retinopathies (IRs) with particular focus on developing new treatments for these sight-threatening diseases. The concept of vascular repulsion is highlighted as having a causal role in repelling nascent vessels away from the ischemic regions and instead towards the vitreous as seen in patients suffering from IRs. The source of these vaso-repulsive cues originates from the underlying RGCs, which interact with surrounding microglia to release vaso-modulatory factors. This tripartite cross-communication between neurons, vessels and immune cells is emphasized in these studies supporting the concept of neurovascular coupling and inflammation in ischemic diseases. The last concept covered herein is the varying functions of certain genes, which appear to be divergent depending on the cell type in which they are expressed. These concepts are discussed in detail below.

Current treatments for IRs focus on the latter stages of the disease, namely, pathological neovessel formation<sup>2,3</sup>; retinal ischemia, however—that provokes the formation of neovessels—imparts critical biochemical changes in retina that often result in observable reductions in vision health and function<sup>4,260</sup>. Herein, we demonstrate that timely revascularization of the retina can: 1) considerably diminish vessel loss early on in efforts to reduce retinal ischemia that affects retinal function, 2) reinstate the vascular network by maintaining neovessels on the surface of the retina and 3) significantly reducing misguidance of vessels toward the vitreous. As such, stimulating revascularization either by targeting specifically Netrin1, Sema3A or its upstream regulator, IL-1RI (via inhibition of IL-1 $\beta$  or activation of PAR2), may be potential therapeutic avenues in preventing pathological signatures of IRs.

## *The importance of balancing vascular guidance cues in IRs: lessons from Sema3A and Netrin1*

Vessels require both attractive and repulsive cues to properly guide them towards their non-perfused targets. An imbalance in these factors can cause vascular defects<sup>68</sup>, as seen in patients suffering from IRs. Herein, we show that during the initial phases of retinal ischemia, neurons secrete high amounts of VEGF, to stimulate angiogenesis in efforts to reinstate metabolic homeostasis. While this initially attracts vessels towards these avascular areas, severely ischemic neurons reverse their signaling machinery from VEGF production to that of vaso-repulsive Sema3A. Thus, while the levels of VEGF are high, the presence of Sema3A in severely ischemic zones repels nascent vessels away from these areas (via Nrp1). Similarly, another study showed that Sema3E released by the underlying RGCs is enriched in the avascular zone during retinal ischemia and, despite high levels of VEGF, also repel vessels from these zones (via PlexD1 signaling on ECs)<sup>261</sup>. Interestingly, this study demonstrated that Sema3E ensures that vessels do not dive prematurely into the retina towards the photoreceptors<sup>261</sup>, which likely accounts for why pathological neovessels are always found protruding into vitreous of DR and ROP patients and not into the retina.

Inhibiting Sema3A (either directly or indirectly) prevents abhorrent vessel growth and allows vessels to invade the ischemic regions enriched with VEGF. This can be seen at high magnification in the retina of animals treated with Sema3A inhibitor by the increased number of intact filopodia on tip cells projecting into the avascular zones. Consequently, the retinal vasculature of these mice looks 'normal' compared to untreated retina. A similar scenario is observed upon inhibition of Sema3E<sup>261</sup>. Essentially, tipping the balance between repulsive and attractive cues may reduce pathological vessel formation in efforts to ameliorate disease outcome. Similar strategies are exercised in various types of cancer, whereby treatment with class 3 semaphorins results in significant reduction of tumor growth and angiogenesis<sup>262,263</sup>. This is because various tumor cells increase production of VEGF

(or other growth factors)<sup>126</sup> while simultaneously suppressing class 3 semaphorins<sup>264,265</sup>, which are known for their anti-tumor capacities (Sema3A, 3B or 3F)<sup>185</sup>.

Netrin1 is a guidance molecules that can have varying effects in angiogenesis<sup>144,266</sup>. This is usually dependent on the netrin receptor present on the receptive cell, although Unc5b is the only reported endothelial Netrin1 receptor<sup>165</sup>. In a parallel study (Appendix 4), we unexpectedly found c-Myc-tagged Netrin1 on microglia/macrophages. Binding of Netrin1 to its receptor Adenosine A2B receptor on microglia/macrophages increased VEGF secretion, which translated to an increase in angiogenesis and accelerated revascularization of the ischemic retina. These important findings may account for the pro-angiogenic effects of Netrin1 observed in a mouse model of hindlimb ischemia<sup>107</sup> whereby macrophages are known to play a vital role in tissue repair<sup>267</sup>. Moreover, this study further demonstrates the importance of neuronal guidance cues in shaping vascular phenotypes whereby Netrin1 counteracts the ischemia-challenged retina following vascular injury. Interestingly, and in similar fashion as in VEGF mRNA suppression in ischemic RGCs, Netrin1 levels becomes suppressed upon exposure to long periods of hypoxia. Reduction in Netrin1 was mediated by the unfolded-protein response (UPR), a protective cellular pathway initiated by endoplasmic-reticulum (ER) stress, which was significantly increased in ischemic mice retina. We show that neuronal-derived Netrin1 mRNA is cleaved by inositol-requiring kinase 1 alpha (IRE-1 $\alpha$ ) following activation of the UPR pathway. This data shows that ER stress and UPR pathways may be an important in changing the balance between repulsive and attractive molecules in IRs. Whether or not VEGF is a substrate for IRE-1 $\alpha$ -mediated RNase in neurons has yet to be determined; however, one study discovered that VEGF degradation was *enhanced* upon inhibition of UPR pathways in retinal and choroidal ECs<sup>268</sup>, indicating that other cellular pathways may be involved in regulating VEGF in severely hypoxic RGCs. Elucidating these intracellular pathways may be important for understanding the

pathophysiological mechanisms by which ischemic neurons deviate from their pro-angiogenic phenotype.

### *Neurovascular interactions in IRs: RGCs, microglia and vessels*

In the retina, increased neuronal activity increases metabolic demand for nutrients and oxygen, which is satiated by the formation of an intricate vascular network. Glial cells which also make up the neurovascular unit were thought to precipitate the formation of the vascular network<sup>94</sup>; however, recent evidence demonstrates that RGCs impart a significant role in retinal vascular development. For instance, genetic ablation of retinal ganglion cells in mice (*brn3b*<sup>Z-dta/+</sup>; *six3-cre* mice) are completely devoid of an inner retinal capillary network<sup>129</sup>. Another study demonstrated that Math5 knockout mice, having 95% reduction in RGCs, also have an abhorrent and disorganized retinal vasculature<sup>269</sup>. Moreover, cell specific genetic deletion of VEGF, HIF-1 $\alpha$  or HIF-2 $\alpha$  in retinal astrocytes did not incur any perturbations in vascular development in mice<sup>270</sup> whereas genetic deletion of HIF-1 $\alpha$  in neurons caused abnormal vascular phenotypes<sup>271,272</sup>. Indeed, while astrocytes are necessary for providing the essential framework required for normal development of the retinal vasculature, it appears that RGCs play a more definitive role in providing necessary factors for stimulating vessel growth and development.

The relative contributions of neurovascular coupling in IRs, however, have only recently begun to come to light. In our studies, we demonstrate the neurons initially produce factors to counteract the ensuing oxidant/ischemic stress. PAR2 is rapidly upregulated on RGCs during the early phases of vascular dropout in mice retina to shut down exhaustive IL-1 $\beta$  signaling, which causes Sema3A-mediated vessel degeneration. Netrin1 is also secreted early on by RGCs, in response to ensuing stress, to counteract vessel loss. Other neuronally-derived molecules appear to precipitate the same effect. Neuronal-derived sirtuin1 is upregulated during OIR and was shown promote revascularization in attempts to counteract ischemic stress<sup>273</sup>.

Another study previously published by our lab demonstrated that ischemic neurons rapidly produce succinate, which induces expression of pro-angiogenic factors via GPR91 on RGCs to promote retinal angiogenesis<sup>129</sup>. On the other hand, persistent ischemia, if left unchecked, can induce Sema3A (and Sema3E<sup>261</sup>) which reproduce the cardinal features of IRs by repelling neovessels. Also, suppression of key vascular guidance molecules Netrin1 (by ER stress) and VEGF also results in delayed revascularization of avascular areas. A similar scenario is observed following stroke, whereby ischemic neurons secrete molecules to attract (or repel) growing neovessels<sup>274,275</sup>. Thus, harnessing the inherent angiogenic potential of neurons may provide novel therapeutic avenues in effort to reduce retinal ischemia and the subsequent pathological neovessel formation, which are central to the pathogenesis of IRs.

Glia are support cells in the retina (and CNS) that form part of the neurovascular unit<sup>226</sup>. While the relative contributions of astrocytes appear to be dispensable in formation of the retinal vascular network<sup>270</sup>, microglial cells appear to play a more central role in angiogenesis. During retinal development microglia are in close proximity to endothelial tip cells, which secrete factors that control neovessel formation<sup>118,137</sup>. Later microglia help maintain retinal homeostasis and form part of the innate immune response in the retina<sup>226</sup>. In retinal vasculopathies, however, microglia have a more disparaging role. In DR patients, microglia are associated with various vascular perturbations (microaneurysms, neovessel tufts)<sup>84</sup> and animal models of DR show that microglia increase cytokine production and inflammation<sup>89</sup>. In ROP, the role of microglia is less clear. Our study (Chapter 2) shows a direct causal role for microglia in ROP whereby they become activated during hyperoxia and release IL-1 $\beta$  in an autocrine and auto-stimulatory fashion. This induces paracrine release of Sema3A from proximal RGCs translating to microvascular decay and exacerbating pathological neovessel formation. Inhibition of IL-1 $\beta$  (via inhibition of IL-1RI) reversed these effects, which corroborates with the studies in diabetic mice showing a marked reduction in retinal inflammation following inhibition of microglia activation<sup>89</sup>.

However, upon binding Netrin1, microglia (and possibly macrophages) can induce revascularization (Annex 4), which challenges the initial studies in the literature and herein (Chapter 2) demonstrating the detrimental effects of microglia. This discrepancy can be described by the dynamics of microglial activity; resting microglia cells upon activation have the ability, depending on their environment, to adopt two functionally distinct phenotypes<sup>33,34</sup>: either pro-inflammatory, or 'M1', or anti-inflammatory, or 'M2'. While each microglia 'type' carries distinct molecular and phenotypical signatures, these polarized states are quite dynamic and likely interchangeable<sup>276,277</sup>. The same is true for macrophages<sup>232,278</sup>. Thus, Netrin1 may be polarizing what appear to be M1 microglia/macrophages in IRs towards a M2 phenotype, which promote anti-inflammation and repair. A similar observation has been shown in a cardiac ischemia reperfusion model whereby Netrin1 attenuates myocardial injury following activation of macrophages<sup>279</sup>. In this regard, Netrin1 may yet have a therapeutic benefit in ischemic diseases by specifically modulating the inherent phenotypes of invading macrophages / activated microglia.

While these two studies present the dual role of microglia in IRs, they also underline the importance of neurovascular cross-talk involving not only vessels and neurons, but glia too. The evidence herein shows that in retinal diseases, as well as other ischemic diseases in the CNS, this tripartite of cells continuously interact and do so in a highly dynamic and intimate fashion.

### *IL-1 $\beta$ and inflammation in IRs*

Inflammation plays an integral part of tissue's response to injury and foreign invasion. In pre-term infants, inflammation is known to exacerbate the severity of ROP<sup>207</sup> while in DR patients, increased levels of systemic pro-inflammatory cytokines (as a result of diabetes) precede the onset of retinal capillary dropout and contribute to the subsequent pathological neovascularization<sup>4,89</sup>. Elevated levels of inflammatory markers have been reported in the vitreous of IRs patients<sup>63,83,280</sup> and animals<sup>40,209</sup>;

among these, IL-1 $\beta$  has generally been proposed as having an impact in the pathogenesis of IRs<sup>63,281</sup>; however, despite its known prototypical pro-inflammatory properties<sup>211,282,283</sup>, the specific contributions of this important cytokine in modulating vascular phenotypes in IRs is not so well defined. In some cases, IL-1 $\beta$  has shown to stimulate angiogenesis directly<sup>213,284</sup>. In our studies, we demonstrate the inverse whereby elevated IL-1 $\beta$  expression contributes to both EC decay and vascular repulsion via induction of Sema3A from proximal RGCs. Importantly, we also demonstrate that IL-1 $\beta$  regulates its own activity in the retina by induction of PAR2 in RGCs; this intrinsic regulatory mechanism shuts down IL-1RI specifically in RGCs to prevent further exacerbation of vascular pathogenesis perpetuated by IL-1 $\beta$  adding to its already complex self-regulatory mechanisms<sup>211,283</sup>.

IL-1 $\beta$  is ubiquitously expressed in various organs and its expression reported in various cell types, particularly inflammatory cells<sup>211,283</sup>. Although, while IL-1 $\beta$  expression has been reported in IRs patients<sup>63</sup> and animals<sup>281</sup>, the major source of its expression remains ill defined. Herein, we demonstrate that resident microglia—upon activation by hyperoxia (and hypoxia [data not shown])—contribute largely to the augmented production of IL-1 $\beta$  in the retina in an autocrine and autostimulatory fashion. This unrelenting cytokine production thus perpetuates a continuous cycle of microglial auto-activation exacerbating retinal inflammation. Moreover, increased microglia number in the superficial plexus is likely associated with increased expression of ICAM-1, which is typically upregulated by IL-1 $\beta$  in retinal ECs<sup>220</sup>. Evidence of this can be seen in OIR animals treated with IL-1RI inhibitors whereby fewer microglia were detected in these layers compared to vehicle treated OIR animals. This indicates that microglial cells not only secrete IL-1 $\beta$  paracrinely in efforts to stimulate its own an auto-activation but it also contributes to their migration within the retina in IRs.

IL-1 $\beta$  mRNA is translated into a 33-kDa full length protein which includes a 16-kDa N-terminal pro-piece<sup>283</sup>. Activation of IL-1 $\beta$  requires proteolytic cleavage of its pro-piece generating a 17-kDa mature IL-1 $\beta$  protein<sup>283</sup>. This intracellular processing is

dependent on caspase-1, which itself is regulated by adaptor (Apoptosis-associated speck-like protein containing CARD, ASC) and regulatory proteins (NOD-like receptor proteins, NLRPs) together forming a signaling complex known as the inflammasome<sup>285</sup>. While this protein complex has important biological processes and contributes significantly to the innate and adaptive immune response<sup>285</sup>, the data surrounding its contribution to IRs are only beginning to be unraveled<sup>209,212</sup>. In chapter 3, we briefly underline the importance of the NLRP3 inflammasome (the most important isotype described in the retina<sup>286</sup>) in generating microglial-derived IL-1 $\beta$  in the retina, which offers insight into its contribution in modulating vascular phenotypes in IRs. However, NLRP3 is found in other cells including retinal-pigmented epithelium (RPE)<sup>287,288</sup> and infiltrating macrophages<sup>215</sup> indicating that it may have alternative functions in the retina and in IRs.

While these studies offer a more formal understanding of the role of the prototypic IL-1 $\beta$  in IRs, further studies on its activation (with particular focus on the NLRP3 inflammasome) will be necessary for highlighting its fine-tuned regulation in ischemic retinal vasculopathies.

### *Same protein, different roles: Lessons from PAR2 and Netrin1*

Genes that are ubiquitously expressed in different organs can have functionally distinct roles depending on the tissue that they are expressed. While some of the downstream signaling effectors can be similar, the final readout can vary significantly. Netrins was first identified to bind to DCC on commissural neurons and generating an attractive response for growing axon terminals<sup>160</sup>. It was later discovered that Netrins can bind to many other receptors, including Unc5 (a-d), Neogenin (part of the DCC family of Netrin receptors)<sup>144</sup>, Adenosine A2B receptor (AA2B)<sup>289</sup> and possibly other unidentified receptors. Heterodimerization between two Netrin receptors has also been described<sup>164</sup>.

Binding of Netrin1 to DCC typically generates attraction action whereas binding to Unc5b mediates repulsion on neurons<sup>144</sup>. In endothelial cells, Unc5b is the only receptor for Netrin1 expressed in tip cells<sup>144,266</sup>; however, this action results in repulsion, quite different than the response that we see in the retina. Rather than repelling vessels and contributing to vessel misguidance and pre-retinal neovascularization, Netrin1 generates the exact opposite. This is because it signals via a different receptor and yields a diverse vascular response in macrophages. Although not described in this study, Netrin1 has the ability to signal on macrophages in efforts to attract or retain them in atherosclerotic plaques<sup>290</sup> and in adipose tissue<sup>291</sup>. Thus, Netrin1 maybe be promoting migration from circulation into the retina to perform its pro-angiogenic functions. Intriguingly, Netrin1 signals macrophage retention in atherosclerotic plaques and adipose tissue via Unc5b receptor<sup>290,291</sup>, while in the retina this effect is mediated by AA2BR. Moreover, Netrin1/Unc5b signaling propagates inflammation and cytotoxicity in these models while in our study Netrin1/AA2BR incites protection, supporting the fact that Netrin1 has diverse functions depending on the receptor.

While the explanation for Netrin1 functional differences can be explained by the varying receptor expression on the target cell, the justification for PAR2 functional differences is not so clearly defined. Herein, we show that PAR2 in the retina is most prominently localized on RGCs and to a lesser extent on endothelium, where it exhibits functionally distinct cellular processes. Neuronal PAR2 appears to be mediating protective capacities by secreting pro-angiogenic cues (VEGF) to stimulate vessel growth, which also simultaneously function as neuroprotectants to counteract ischemic stress<sup>292</sup>. Furthermore, PAR2 dampens IL-1RI in efforts to curb neuronal inflammation, which have degenerative consequences on the retinal vasculature (via Sema3A) and on neurons themselves<sup>293</sup>. Thus, PAR2 on RGCs functions as an intrinsic regulatory mechanism for preventing exhaustive inflammation while simultaneously secreting pro-vascular modulators. Endothelial PAR2 appears to have prolific properties during development; activation of PAR2, via TF-FVII signaling or

agonist peptide induction, stimulates endothelial cell growth<sup>133,225,294</sup>, presumably via VEGF and TNF- $\alpha$ /Tie2<sup>133</sup>. During pathological processes, however, endothelial PAR2 function appears deleterious. We show that PAR2 activation increases IL-1RI expression, which may potentiate vascular injury by exacerbating IL-1 signaling. Notably, PAR2 stimulates IL-1 $\beta$  on ECs<sup>295</sup>, which can in turn increase ICAM-1 expression and thus inflammatory cell adhesion<sup>89</sup>, supporting this hypothesis.

In the brain, PAR2 can also have dichotomous roles during injury. In various animal of brain injury, PAR2 activity on neurons and astrocytes has neuroprotective functions<sup>296</sup>. Neuronal/astrocyte PAR2 protect against brain injury following transient middle carotid artery occlusion<sup>297</sup>, inhibits demyelination in a mouse model of experimental autoimmune encephalomyelitis<sup>298</sup> and protects against  $\beta$ -amyloid neurotoxicity in Alzheimer's Disease<sup>299</sup>. On the other hand, PAR2 on macrophages/microglia causes an upregulation of pro-inflammatory cytokines TNF- $\alpha$ , iNOS, IL-6, IL-12p40, IL-1 $\beta$ , IFN-inducible protein 10, MCP-1, and macrophage inflammatory protein 1 $\alpha$  (MIP-1 $\alpha$ )<sup>298</sup>, which translates to increased neuronal cell demyelination. Conversely, PAR2 deficiency in macrophages/microglia results in increased anti-inflammatory IL-10 expression<sup>298</sup> and protects neurons. Essentially, native PAR2 on neurons serves as a neuroprotective factor in the retina and brain, while EC and microglial/macrophage activity precipitates neurodegeneration. The reasoning why a paracellular dichotomy exists in the same tissue, however, remains a mystery.

Besides Netrin1 and PAR2, there are a plethora of genes that appear to have multiple functionalities. This work offers but one example of how evolutionary conserved molecules can diverge in their effector activation and read-out function in the cell that harbours their expression. This may be critical when developing therapeutic intervention for molecules that possess a variety of functions, such as VEGF, which imparts neuroprotective properties<sup>292</sup>.

## Conclusions

Vessel guidance is an important process required to ensure vessels reach their appropriate target to satisfy oxygen and nutrient demand while avoiding expenditure of metabolic stores on irrigating areas that do not require it. For this purpose attractive and repulsive signals exist, to function as intermediaries between the neurons and vessels. Having arisen later in evolution than nerves, vessels amalgamated the use of conserved neuronal guidance cues that help axons reach their target and do so in a highly concerted and regulated manner during vascular development. However, the interactions between neurons and vessels in ischemic retinal diseases are not fully understood. The studies presented herein demonstrate the important contribution of neuronal-derived vaso-modulatory cues (VEGF, Sema3A, Netrin1) in shaping vascular phenotypes in the neurovascular unit when under stress. Moreover, we identify important regulatory factors (IL-1 $\beta$ , PAR2, IRE1- $\alpha$ ) that modulate expression of these vaso-modulatory cues, which may be attractive candidates for therapeutic intervention for ischemic retinal diseases.

This work also supports the hypothesis that ischemic neurons shunt vessels away from perishing tissue by secreting vascular repulsive cues (and inhibiting vaso-chemotactic molecules) in efforts to redirect metabolic stores to more salvageable parts of the retina. Although, while some explanations can be offered (ER stress and the UPR), there are yet unidentified, inherent mechanisms by which ischemic neurons (specifically RGCs) proverbially 'switch' from a pro-vascular phenotype to one that is vaso-repulsive. Understanding the pathophysiological mechanisms by which neurons react to ischemic stress will aid in our understanding of how these cells interact during ischemic stress.

The current methods for treating IRs rely specifically on anti-angiogenic treatments, which aim at curbing retinal edema and vitreous hemorrhaging as well as pathological neovessel formation; however, these advents have variable success in IRs<sup>2,4,92</sup>. Moreover, these treatments do not address the underlying issue central to disease progression; namely, vessel loss and retinal ischemia. Exogenously

modifying the vascular response (possibly from neurons) in efforts to stimulate revascularization of ischemic tissue may present therapeutic avenues for treating IRs in the future.

## References: Introduction and Discussion

1. International, Diabetes, Federation. The Global Burden. *IDF World Atlas*. 2011;5th edition.
2. Hellström A, Smith LEH, Damman O. Retinopathy of Prematurity. *Lancet*. 2013;382(9902):1445-1457.
3. Heng L, Comyn O, Peto T, et al. Diabetic retinopathy: pathogenesis, clinical grading, management and future developments. *Diabet Med*. 2013;30(6):640-650.
4. Antonetti DA KR, Gardner TW. Diabetic Retinopathy. *N Engl J Med*. 2012;366:1227-1239.
5. Resnikoff S, Pascolini D, Etyaale D, et al. Global data on visual impairment in the year 2002. *Bullet World Health Organ*. 2005;80:844-851.
6. Goldenberg RL, Culhane JF, Iams JD, Romero R. Epidemiology and causes of preterm birth. *Lancet*. 2008;371:75-84.
7. Lawn JE, Gravett MG, Nunes TM, Rubens CE, Stanton C, GAPPS Review Group. Global report on preterm birth and stillbirth (1 of 7): definitions, description of the burden and opportunities to improve data. *BMC Pregnancy Childbirth*. 2010;10((suppl 1)):S1.
8. Hartnett ME, Penn S. Mechanisms and Management of Retinopathy of Prematurity. *N Engl J Med*. 2012;367(26):2515-2525.
9. Gilbert C. Retinopathy of prematurity: A global perspective of the epidemics, population of babies at risk and implications for control. *Early Hum Dev*. 2008;84:77-82.
10. Rivera JC, Sapieha P, Joyal J-S, et al. Understanding Retinopathy of Prematurity: Update on Pathogenesis. *Neonatology*. 2011;100(4):343-353.
11. Chen J, Stahl A, Hellstrom A, Smith LE. Current update on retinopathy of prematurity: screening and treatment. *Curr Opin Pediatr*. 2011;23(2):173-178.
12. Zepeda-Romero LC, Hård AL, Gomez-Ruiz LM, et al. Prediction of Retinopathy of Prematurity Using the Screening Algorithm WINROP in a Mexican Population of Preterm Infants. *Arch Ophthalmol*. 2012;130(2):720-723.
13. Sun H, Kang W, Cheng X, et al. The Use of the WINROP Screening Algorithm for the Prediction of Retinopathy of Prematurity in a Chinese Population. *Neonatology*. 2013;104(2):127-132.
14. Steinkuller PG, Du L, Gilbert C, Foster A, Collins ML, Coats DK. Childhood blindness. *J AAPOS*. 1999;3(1):26-32.
15. Fulton A, Hansen R, Moskowitz A, Akula J. The neurovascular retina in retinopathy of prematurity. *Prog Retin Eye Res*. 2009;28(6):452-482.
16. Sapieha P. Eyeing central neurons in vascular growth and reparative angiogenesis. *Blood*. 2012;120(11):2182-2194.
17. World, Health, Organization. Prevention of Blindness from Diabetes Mellitus. *World Health Organ Consult*. 2006:1-48.
18. Yau JWY, Rogers SL, Kawasaki R, et al. Global Prevalence and Major Risk Factors of Diabetic Retinopathy. *Diabetes Care*. 2012;35:556-564.

19. Diabetes, Control, and, Complications, Trial. Progression of retinopathy with intensive versus conventional treatment in the Diabetes Control and Complications Trial. *Ophthalmology*. 1995;102:647-661.
20. Zietz B, Buechler C, Kobuch K, Neumeier M, Schölmerich J, Schäffler A. Serum levels of adiponectin are associated with diabetic retinopathy and with adiponectin gene mutations in Caucasian patients with diabetes mellitus type 2. *Exp Clin Endocrinol Diabetes*. 2008;116(9):532-536.
21. Arnold E, Rivera J, Thebault S, et al. High Levels of Serum Prolactin Protect Against Diabetic Retinopathy by Increasing Ocular Vasoinhibins. *Diabetes*. 2010;59(12):3192-3197.
22. Nguyen T, Alibrahim E, Islam F, et al. Inflammatory, Hemostatic, and Other Novel Biomarkers for Diabetic Retinopathy: The Multi-Ethnic Study of Atherosclerosis. *Diabetes Care*. 2009;32(9):1704-1709.
23. Targher G, Bertolini L, Chonchol M, et al. Non-alcoholic fatty liver disease is independently associated with an increased prevalence of chronic kidney disease and retinopathy in type 1 diabetic patients. *Diabetologia*. 2010;53(7):1341-1348.
24. Hughes S YH, Chan-Ling T. Vascularization of the Human Fetal Retina: Roles of Vasculogenesis and Angiogenesis. *Invest Ophthal Vis Sci*. 2000;41(5):1217-1228.
25. Alon T, Hemo I, Itin A, Pe'er J, Stone J, Keshet E. Vascular endothelial growth factor acts as a survival factor for newly formed retinal vessels and has implications for retinopathy of prematurity. *Nat Med*. 1995;1(10):1024-1028.
26. Chen J, Connor KM, Aderman CM, Smith LEH. Erythropoietin deficiency decreases vascular stability in mice. *J Clin Invest*. 2008.
27. Smith LE, Shen W, Perruzzi C, et al. Regulation of vascular endothelial growth factor-dependent retinal neovascularization by insulin-like growth factor-1 receptor. *Nat Med*. 1999;5(12):1390-1396.
28. Smith LEH, Wesolowski E, McLellan A, et al. Oxygen-Induced Retinopathy in the Mouse. *Invest Ophthal Vis Sci*. 1994;35(1):101-111.
29. John S. Penn BLT, and Mark M. Henry. Oxygen-Induced Retinopathy in the Rat: Relationship of Retinal Nonperfusion to Subsequent Neovascularization. *Invest Ophthal Vis Sci*. 1994;35(9):3429-3436.
30. Shao Z, Dorfman A, Seshadri S, et al. Choroidal Involution Is a Key Component of Oxygen-Induced Retinopathy. *Invest Ophthal Vis Sci*. 2011;52(9):6238-6248.
31. Dorfman A, Dembinska O, Chemtob S, Lachapelle P. Early Manifestations of Postnatal Hyperoxia on the Retinal Structure and Function of the Neonatal Rat. *Invest Ophthal Vis Sci*. 2008;49(1):458-466.
32. Askie LM, Henderson-Smart DJ, Irwig L, JM S. Oxygen-Saturation Targets and Outcomes in Extremely Preterm Infants. *N Engl J Med*. 2003;349(10):959-968.
33. The, STOP-ROP, Multicenter, Study, Group. Supplemental Therapeutic Oxygen for Prethreshold Retinopathy of Prematurity (STOP-ROP), A Randomized, Controlled Trial. I: Primary Outcomes. *Pediatrics*. 2000;105(2):295-310.
34. Hardy P, Beauchamp M, Sennlaub F, et al. Inflammatory lipid mediators in ischemic retinopathy. *Pharmacol Rep*. 2005;57:169-190.

35. Sennlaub F, Courtois Y, Goureau O. Inducible Nitric Oxide Synthase Mediates Retinal Apoptosis in Ischemic Proliferative Retinopathy. *J Neurosci*. 2002;22(10):3987-3993.
36. GL Wang, B-H Jiang, EA Rue, GL Semenza. Hypoxia-inducible factor 1 is a basic-helix-loop-helix-PAS heterodimer regulated by cellular O<sub>2</sub> tension. *Proc Natl Acad Sci USA*. 1995;92(10):5510-5514.
37. Pierce EA, Avery RL, Foley ED, Aiello LP, Smith LE. Vascular endothelial growth factor/vascular permeability factor expression in a mouse model of retinal neovascularization. *Proc Natl Acad Sci USA*. 1995;92(1):905-909.
38. Christian Grimm AW, Matthias Groszer, Helmut Mayser, Mathias Seeliger, Marijana Samardzija, Christian Bauer, Max Gassmann & Charlotte E. Remé. HIF-1-induced erythropoietin in the hypoxic retina protects against light-induced retinal degeneration. *Nat Med*. 2002;8:718-724.
39. Kermorvant-Duchemin E, Sennlaub F, Sirinyan M, et al. Trans-arachidonic acids generated during oxidative stress induce a thrombospondin-1-dependent microvascular degeneration. *Nat Med*. 2005;11(12):1339-1345.
40. Gardiner TA, Gibson DS, de Gooyer TE, de la Cruz VF, McDonald DM, Stitt A. Inhibition of Tumor Necrosis Factor- $\alpha$  Improves Physiological Angiogenesis and Reduces Pathological Neovascularization in Ischemic Retinopathy. *Am J Pathol*. 2005;166(2):637-644.
41. Regev RH, Lusky A, Dolfin T, Litmanovitz I, Arnon S, Reichman B. Excess mortality and morbidity among small-for-gestational-age premature infants: a population-based study. *J Pediatr*. 2003;143:186-191.
42. Allegaert K, Vanhole C, Casteels I, et al. Perinatal growth characteristics and associated risk of developing threshold retinopathy of prematurity. *J AAPOS*. 2003;7:34-37.
43. Dhaliwal CA, Fleck BW, Wright E, Graham C, McIntosh N. Retinopathy of prematurity in small-for-gestational age infants compared with those of appropriate size for gestational age. *Arch Dis Child Fetal Neonatal Ed*. 2009;94(1):F193-195.
44. Fortes Filho JB, Valiatti FB, Eckert GU, Costa MC, Silveira RC, Procianny RS. Is being small for gestational age a risk factor for retinopathy of prematurity? A study with 345 very low birth weight preterm infants. *J Pediatr (Rio J)*. 2009;85(1):48-54.
45. Qiu X, Lodha A, Shah PS, et al. Neonatal outcomes of small for gestational age preterm infants in Canada. *Am J Perinatol*. 2012;29(2):87-94.
46. Hellstrom A, Engstrom E, Hard A, et al. Postnatal Serum Insulin-Like Growth Factor I Deficiency Is Associated With Retinopathy of Prematurity and Other Complications of Premature Birth. *Pediatrics*. 2003;112(5):1016-1020.
47. Stahl A, Chen J, Sapieha P, et al. Postnatal Weight Gain Modifies Severity and Functional Outcome of Oxygen-Induced Proliferative Retinopathy. *Am J Pathol*. 2010;177(6):2715-2723.
48. Lineham JD, Smith RM, Dahlenburg GW, et al. Circulating insulin-like growth factor I levels in newborn premature and full-term infants followed longitudinally. *Early Hum Dev*. 1986;13(1):37-46.

49. Lassarre C, Hardouin S, Daffos F, Forestier F, Frankenne F, Binoux M. Serum insulin-like growth factors and insulin-like growth factor binding proteins in the human fetus. Relationships with growth in normal subjects and in subjects with intrauterine growth retardation. *Pediatr Res*. 1991;29(3):219-225.
50. Sangiovanni J, Parra-Cabrera S, Colditz G, Berkey C, J D. Meta-analysis of Dietary Essential Fatty Acids and Long-Chain Polyunsaturated Fatty Acids as They Relate to Visual Resolution Acuity in Healthy Preterm Infants. *Pediatrics*. 2000;105(6):1292-1298.
51. Martin CR, Dasilva DA, Cluette-Brown JE, et al. Decreased postnatal docosahexaenoic and arachidonic acid blood levels in premature infants are associated with neonatal morbidities. *J Pediatr*. 2011;159(5):743-749.e741-742.
52. Crawford MA, Golfetto I, Ghebremeskel K, et al. The potential role for arachidonic and docosahexaenoic acids in protection against some central nervous system injuries in preterm infants. *Lipids*. 2003;38(4):303-315.
53. Liu JP, Baker J, Perkins AS, Robertson EJ, Efstratiadis A. Mice carrying null mutations of the genes encoding insulin-like growth factor I (Igf-1) and type 1 IGF receptor (Igf1r). *Cell*. 1993;75(1):59-72.
54. Lofqvist C, Chen J, Connor KM, et al. IGFBP3 suppresses retinopathy through suppression of oxygen-induced vessel loss and promotion of vascular regrowth. *Proc Natl Acad Sci USA*. 2007;104(25):10589-10594.
55. Vanhaesebrouck S, Daniëls H, Moons L, Vanhole C, Carmeliet P, F. DZ. Oxygen-Induced Retinopathy in Mice: Amplification by Neonatal IGF-I Deficit and Attenuation by IGF-I Administration. *Pediatr Res*. 2009;65(3):307-310.
56. Löfqvist C, Niklasson A, Engström E, et al. A pharmacokinetic and dosing study of intravenous insulin-like growth factor-I and IGF-binding protein-3 complex to preterm infants. *Pediatr Res*. 2009;65(5):574-579.
57. Hansen-Pupp I, Engstrom E, Niklasson A, et al. Fresh frozen plasma as a source of exogenous insulin-like growth factor I in the extremely preterm infant. *J Clin Endocrinol Metab*. 2009;94:477-482.
58. Stahl A, Sapiéha P, Connor K, et al. Short Communication: PPAR Mediates a Direct Antiangiogenic Effect of  $\omega$ -3-PUFAs in Proliferative Retinopathy. *Circ Res*. 2010;107(4):495-500.
59. Connor KM, SanGiovanni JP, Lofqvist C, et al. Increased dietary intake of omega-3-polyunsaturated fatty acids reduces pathological retinal angiogenesis. *Nat Med*. 2007;13(7):868-873.
60. Souied EH, Delcourt C, Querques G, et al. Oral Docosahexaenoic Acid in the Prevention of Exudative Age-Related Macular Degeneration: The Nutritional AMD Treatment 2 Study. *Ophthalmology*. 2013;120(8):1619-1631.
61. Sangiovanni J, Agron E, Meleth A, et al.  $\omega$ -3 Long-chain polyunsaturated fatty acid intake and 12-y incidence of neovascular age-related macular degeneration and central geographic atrophy: AREDS report 30, a prospective cohort study from the Age-Related Eye Disease Study. *Am J Clin Nutr*. 2009;90(6):1601-1607.
62. Hawkins BT, Davis TP. The Blood-Brain Barrier/Neurovascular Unit in Health and Disease. *Pharmacol Rev*. 2005;57(2):173-185.

63. Demircan N, Safran BG, Soylu M, Ozcan AA, Sizmaz S. Determination of vitreous interleukin-1 (il-1) and tumour necrosis factor (tnf) levels in proliferative diabetic retinopathy. *Eye (Lond)*. 2006;20:1366-1369.
64. McLeod DS, Lefer DJ, Merges C, Luty GA. Enhanced Expression of Intracellular Adhesion Molecule-1 and P-Selectin in the Diabetic Human Retina and Choroid. *Am J Pathol*. 1995;146(3):642-653.
65. Adamis A, Berman AJ. Immunological mechanisms in the pathogenesis of diabetic retinopathy. *Semin Immunopathol*. 2008;30(2):65-84.
66. H Dvorak, LF Brown, M Detmar, AM Dvorak. Vascular Permeability Factor/Nascular Endothelial Growth Factor, Microvascular Hyperpermeability, and Angiogenesis. *Am J Pathol*. 1995;146(5):1029-1040.
67. Mitamura Y, Harada C, Harada T. Role of Cytokines and Trophic Factors in the Pathogenesis of Diabetic Retinopathy. *Curr Diab Rev*. 2005;1(1):73-81.
68. Potente M GH, Carmeliet P. Basic and Therapeutic Aspects of Angiogenesis. *Cell*. 2011;146(6):873-887.
69. Gálvez MI. Protein kinase C inhibitors in the treatment of diabetic retinopathy. Review. *Current Pharm Biotechnol*. 2011;12(3):386-391.
70. Chen M, Curtis TM, Stitt AW. Advanced glycation end products and diabetic retinopathy. *Current Med Chem*. 2013;20(26):3234-3240.
71. Clermont A, Chilcote T, Kita T, et al. Plasma Kallikrein Mediates Retinal Vascular Dysfunction and Induces Retinal Thickening in Diabetic Rats. *Diabetes*. 2011;60(5):1590-1598.
72. Yuxiang Liu SRC, Toshisuke Morita, Stella Kourembanas. Hypoxia Regulates Vascular Endothelial Growth Factor Gene Expression in Endothelial Cells. *Circ Res*. 1995;77:638-643.
73. Adamis AP, Miller JW, Bernal MT, et al. Increased vascular endothelial growth factor levels in the vitreous of eyes with proliferative diabetic retinopathy. *Am J Ophthalmol*. 1994;118(4):445-450.
74. Watanabe D, Suzuma K, Matsui S, et al. Erythropoietin as a retinal angiogenic factor in proliferative diabetic retinopathy. *N Engl J Med*. 2005;353(8):782-792.
75. Giacco F, Brownlee M. Oxidative Stress and Diabetic Complications. *Circ Res*. 2010;107(9):1058-1070.
76. Goldin A, Beckman JA, Schmidt AM, Creager MA. Advanced glycation end products: sparking the development of diabetic vascular injury. *Circulation*. 2006;114(6):597-605.
77. Stitt AW. The role of advanced glycation in the pathogenesis of diabetic retinopathy. *Exp Mol Pathol*. 2003;75 (1):95-108.
78. Yao D, Taguchi T, Matsumura T, et al. High glucose increases angiopoietin-2 transcription in microvascular endothelial cells through methylglyoxal modification of mSin3A. *J Biol Chem*. 2007;282(42):31038-31045.
79. Yamagishi Si, Yonekura H, Yamamoto Y, et al. Advanced glycation end products-driven angiogenesis in vitro. Induction of the growth and tube formation of human microvascular endothelial cells through autocrine vascular endothelial growth factor. *J Biol Chem*. 1997; 272(13):8723-8730.

80. Gerald P, Hiraoka-Yamamoto J, Matsumoto M, et al. Activation of PKC- $\delta$  and SHP-1 by hyperglycemia causes vascular cell apoptosis and diabetic retinopathy. *Nat Med*. 2009;15(11):1298-1306.
81. Ali T, Al-Gayyar M, Matragoon S, et al. Diabetes-induced peroxynitrite impairs the balance of pro-nerve growth factor and nerve growth factor, and causes neurovascular injury. *Diabetologia*. 2011;54(3): 657-668.
82. Mysona B, Al-Gayyar M, Matragoon S, et al. Modulation of p75NTR prevents diabetes- and proNGF-induced retinal inflammation and blood–retina barrier breakdown in mice and rats. *Diabetologia*. 2013;56(10):2329-2339.
83. dell'Omo R, Semeraro F, Bamonte G, Cifariello F, Romano MR, Costagliola C. Vitreous Mediators in Retinal Hypoxic Diseases. *Mediators Inflamm*. 2013:1-16.
84. Zeng HY, Green WR, Tso MO. Microglial activation in human diabetic retinopathy. *Arch Ophthalmol*. 2008;126(2):227-232.
85. Butler J, Guthrie S, Koc M, et al. SDF-1 is both necessary and sufficient to promote proliferative retinopathy. *J Clin Invest*. 2005;115(1):86-93.
86. Nagineni C, Kommineni V, William A, Detrick B, Hooks J. Regulation of VEGF expression in human retinal cells by cytokines: Implications for the role of inflammation in age-related macular degeneration. *J Cell Physiol*. 2011;227(1):116-126.
87. Tikhonenko M, Lydic TA, Wang Y, et al. Remodeling of retinal Fatty acids in an animal model of diabetes: a decrease in long-chain polyunsaturated fatty acids is associated with a decrease in fatty acid elongases Elovl2 and Elovl4. *Diabetes*. 2010;59:219-227.
88. El-Asrar AM, Missotten L, Geboes K. Expression of cyclo-oxygenase-2 and downstream enzymes in diabetic fibrovascular epiretinal membranes. *Br J Ophthalmol*. 2008;92(11):1534-1539.
89. Tang J, Kern TS. Inflammation in diabetic retinopathy. *Prog Retin Eye Res*. 2011;30(5):343-358.
90. Ayalasomayajula SP, Kompella UB. Retinal delivery of celecoxib is several-fold higher following subconjunctival administration compared to systemic administration. *Pharm Res*. 2004;21(10):1797-1804.
91. Schwartzman ML, Iserovich P, Gotlinger K, et al. Profile of lipid and protein autacoids in diabetic vitreous correlates with the progression of diabetic retinopathy. *Diabetes*. 2010;59(7):1780-1788.
92. Miller J, Couter JL, Strauss E, Ferrara N. Vascular Endothelial Growth Factor A in Intraocular Vascular Disease. *Ophthalmology*. 2012;120(1):106-114.
93. Wang S, Park J, Duh E. Novel Targets Against Retinal Angiogenesis in Diabetic Retinopathy. *Curr Diab Rep*. 2012;12(4):355-363.
94. Fruttiger M. Development of the retinal vasculature. *Angiogenesis*. 2007;10(2):77-88.
95. Swift M, Weinstein B. Arterial-Venous Specification During Development. *Circ Res*. 2009;104(5):576-588.
96. Adams RH, Alitalo K. Molecular regulation of angiogenesis and lymphangiogenesis. *Nat Rev Mol Cell Biol*. 2007;8(6):464-478.

97. Roca C, Adams RH. Regulation of vascular morphogenesis by Notch signaling. *Genes Dev.* 2007;21(20):2511-2524.
98. Gering M, Patient R. Hedgehog Signaling Is Required for Adult Blood Stem Cell Formation in Zebrafish Embryos. *Dev Cell.* 2005;8(3):389-400.
99. Jones E, Le Noble F, Eichmann A. What Determines Blood Vessel Structure? Genetic Preshpecification vs. Hemodynamics. *Physiology.* 2006;21(6):388-395.
100. Djonov V, Makanya AN. New insights into intussusceptive angiogenesis. *EXS.* 2005;94:17-33.
101. Overall C, López-Otín C. Strategies for mmp inhibition in cancer: innovations for the post-trial era. *Nat Rev Cancer.* 2002;2(9):657-672.
102. Eble JA, Niland S. The extracellular matrix of blood vessels. *Curr Pharm Des.* 2009;15(12):1385-1400.
103. Phng L, Gerhardt H. Angiogenesis: A Team Effort Coordinated by Notch. *Dev Cell.* 2009;16(2):196-208.
104. Rui Benedito CR, Inga Sorensen, Susanne Adams, Achim Gossler, Marcus Fruttiger, and Ralf H. Adams. The Notch Ligands Dll4 and Jagged1 Have Opposing Effects on Angiogenesis. *Cell.* 2009;137:1124-1135.
105. De Smet F, Segura I, De Bock K, Hohensinner PJ, Carmeliet P. Mechanisms of vessel branching: filopodia on endothelial tip cells lead the way. *Arterioscler Thromb Vasc Biol.* 2009;29(5):639–649.
106. Carmeliet P, Tessier-Lavigne M. Common mechanisms of nerve and blood vessel wiring. *Nature.* 2005;436(7048):193-200.
107. Wilson BD, Li M, Park KW, et al. Netrins Promote Developmental and Therapeutic Angiogenesis. *Science.* 2006;313(5787):640-644.
108. Kim J, Oh WJ, Gaiano N, Yoshida Y, Gu C. Semaphorin 3E-Plexin-D1 signaling regulates VEGF function in developmental angiogenesis via a feedback mechanism. *Genes Dev.* 2011;25(13):1399-1411.
109. Shimizu A, Mammoto A, Italiano JE, et al. ABL2/ARG Tyrosine Kinase Mediates SEMA3F-induced RhoA Inactivation and Cytoskeleton Collapse in Human Glioma Cells. *J Biol Chem.* 2008;283(40):27230-27238.
110. Bielenberg DR, Hida Y, Shimizu A, et al. Semaphorin 3F, a chemorepellent for endothelial cells, induces a poorly vascularized, encapsulated, nonmetastatic tumor phenotype. *J Clin Invest.* 2004;114(9):1260-1271.
111. Kuijper S, Turner JT, Adams RH. Regulation of Angiogenesis by Eph–Ephrin Interactions. *Trends in Cardiovasc Med.* 2007;17(5):145-151.
112. Sawamiphak S, Seidel S, Essmann CL, et al. Ephrin-B2 regulates VEGFR2 function in developmental and tumour angiogenesis. *Nature.* 2010;465:487-491.
113. Wang Y, Nakayama M, Pitulescu ME, et al. Ephrin-B2 controls VEGF-induced angiogenesis and lymphangiogenesis. *Nature.* 2010;465:483–486.
114. Adams RH, Wilkinson GA, Weiss C, et al. Roles of ephrinB ligands and EphB receptors in cardiovascular development: demarcation of arterial/venous domains, vascular morphogenesis, and sprouting angiogenesis. *Genes & Development.* 1999;13:295-306.

115. Wang HU, Chen ZF, Anderson DJ. Molecular distinction and angiogenic interaction between embryonic arteries and veins revealed by ephrin-B2 and its receptor Eph-B4. *Cell*. 1998;93(5):741-753.
116. Marlow R, Binnewies M, Sorensen L, et al. Vascular Robo4 restricts proangiogenic VEGF signaling in breast. *Proc Natl Acad Sci USA*. 2010;107(23):10520-10525.
117. Jones C, London N, Chen H, et al. Robo4 stabilizes the vascular network by inhibiting pathologic angiogenesis and endothelial hyperpermeability. *Nat Med*. 2008;14(4):448-453.
118. Gerhardt H, M G, Fruttiger M, et al. VEGF guides angiogenic sprouting utilizing endothelial tip cell filopodia. *J Cell Biol*. 2003;161(6):1163-1177.
119. Iruela-Arispe ML, Davis GE. Cellular and molecular mechanisms of vascular lumen formation. *Dev Cell*. 2009;16:222-231.
120. Gaengel K, Genové G, Armulik A, Betsholtz C. Endothelial-Mural Cell Signaling in Vascular Development and Angiogenesis. *Arterioscler Thromb Vasc Biol*. 2009;29:630-638.
121. Pardali E, Goumans MJ, ten Dijke P. Signaling by members of the TGF- $\beta$  family in vascular morphogenesis and disease. *Trends Cell Biol*. 2010;20(9):556-567.
122. van Oostrom MC, van Oostrom O, Quax PH, Verhaar MC, Hofer IE. Insights into mechanisms behind arteriogenesis: what does the future hold? *J Leukoc Biol*. 2008;84(6):1379-1391.
123. Cai W, Schaper W. Mechanisms of arteriogenesis. *Acta Biochim Biophys Sin*. 2008;40(8):681-692.
124. MCLeod DS, Hasegawa T, Prow T, Merges C, Luty GA. The Initial Fetal Human Retinal Vasculature Develops by Vasculogenesis. *Dev Dyn*. 2006;235:3336 – 3347.
125. Stahl A, Connor KM, Sapienza P, et al. The Mouse Retina as an Angiogenesis Model. *Invest Ophthalmol Vis Sci*. 2010;51(6):2813-2826.
126. Carmeliet P, Jain RK. Molecular mechanisms and clinical applications of angiogenesis. *Nature*. 2011;473(7347):298-307.
127. Gariano RF. Cellular mechanisms in retinal vascular development. *Prog Retin Eye Res*. 2003;22:295-306.
128. Andrew Scott MBP, Pranita Gandhi, Claire Clarkin, David H. Gutmann, Randall S. Johnson, Napoleone Ferrara, Marcus Fruttiger Astrocyte-Derived Vascular Endothelial Growth Factor Stabilizes Vessels in the Developing Retinal Vasculature. *PLoS ONE*. 2010;5(7):e11863.
129. Sapienza P, Sirinyan M, Hamel D, et al. The succinate receptor GPR91 in neurons has a major role in retinal angiogenesis. *Nat Med*. 2008;14(10):1067-1076.
130. Shih S, Meihua Ju, Nan Liu, and Lois E.H. Smith. Selective stimulation of VEGFR-1 prevents oxygen-induced retinal vascular degeneration in retinopathy of prematurity. *J Clin Invest*. 2003;112(1):50-57.
131. Dorrell MI, Aguilar E, M F. Retinal Vascular Development Is Mediated by Endothelial Filopodia, a Preexisting Astrocytic Template and Specific R-Cadherin Adhesion. *Invest Ophthalmol Vis Sci*. 2002;43(11):3500-3510.

132. Arnold T, Ferrero G, Qiu H, et al. Defective Retinal Vascular Endothelial Cell Development As a Consequence of Impaired Integrin V $\beta$ 8-Mediated Activation of Transforming Growth Factor- $\beta$ . *J Neurosci*. 2012;32(4):1197-1206.
133. Zhu T, Sennlaub F, Beauchamp MH, et al. Proangiogenic Effects of Protease-Activated Receptor 2 Are Tumor Necrosis Factor- and Consecutively Tie2 Dependent. *Arterioscler Thromb Vasc Biol*. 2006;26(4):744-750.
134. Guttmann-Raviv N, Shraga-Heled N, Varshavsky A, Guimaraes-Sternberg C, Kessler O, Neufeld G. Semaphorin-3A and Semaphorin-3F Work Together to Repel Endothelial Cells and to Inhibit Their Survival by Induction of Apoptosis. *J Biol Chem*. 2007;282(36):26294-26305.
135. Dejana E, Tournier-Lasserre E, Weinstein BM. The Control of Vascular Integrity by Endothelial Cell Junctions: Molecular Basis and Pathological Implications. *Dev Cell*. 2009;16:209-222.
136. Ishida S, Yamashiro K, Usui T, et al. Leukocytes mediate retinal vascular remodeling during development and vaso-obliteration in disease. *Nat Med*. 2003;9(6):781-789.
137. Stefater III JA, Lewkowich I, Rao S, et al. Regulation of angiogenesis by a non-canonical Wnt–Flt1 pathway in myeloid cells. *Nature*. 2011;474(7352):511-515.
138. Xia C, Yablonka-Reuveni Z, Gong X. LRP5 Is Required for Vascular Development in Deeper Layers of the Retina. *PLoS ONE*. 2010;5(7):e11676.
139. Chen J, Stahl A, Krah N, et al. Retinopathy Wnt Signaling Mediates Pathological Vascular Growth in Proliferative. *Circulation*. 2011;124:1871-1881.
140. Ye X, Wang Y, Cahill H, et al. Norrin, Frizzled-4, and Lrp5 Signaling in Endothelial Cells Controls a Genetic Program for Retinal Vascularization. *Cell*. 2009;139(2):285-298.
141. Buehler A, Sitaras N, Favret S, et al. Semaphorin 3F forms an anti-angiogenic barrier in outer retina. *FEBS Letters*. 2013;587(11):1650-1655.
142. Vesalius A. *Humani Corporis Fabrica*. *Oporinus, Basel*. 1543.
143. Ramon y Cajal S. Sur l'origine et les ramifications des fibres nerveuses de la moelle embryonnaire. *Anat Anz*. 1890;5:609–613.
144. Larrivee B, Freitas C, Suchting S, Brunet I, A E. Guidance of Vascular Development: Lessons From the Nervous System. *Circ Res*. 2009:428-441.
145. Caporali A, Emanuelli C. Cardiovascular Actions of Neurotrophins. *Physiol Rev*. 2009;89:279-308.
146. Nishijima K, Ng Y-S, Zhong L, et al. Vascular Endothelial Growth Factor-A Is a Survival Factor for Retinal Neurons and a Critical Neuroprotectant during the Adaptive Response to Ischemic Injury. *Am J Pathol*. 2007;171(1):53-67.
147. Santos PM, Winterowd JG, Allen GG, Bothwell MA, Rubel EW. Nerve growth factor: increased angiogenesis without improved nerve regeneration. *Otolaryngol Head Neck Surg*. 1991;105(1):12-25.
148. Emanuelli C, Salis MB, Pinna A, Graiani G, L M, Madeddu P. Nerve Growth Factor Promotes Angiogenesis and Arteriogenesis in Ischemic Hindlimbs. *Circulation*. 2002;106(17):2257-2262.

149. Feng D, Kim T, Özkan E, et al. Molecular and Structural Insight into proNGF Engagement of P75NTR and Sortilin. *J Mol Biol.* 2010;396(4):967-984.
150. Caporali A, Pani E, Horrevoets A, et al. Neurotrophin p75 Receptor (p75NTR) Promotes Endothelial Cell Apoptosis and Inhibits Angiogenesis: Implications for Diabetes-Induced Impaired Neovascularization in Ischemic Limb Muscles. *Circ Res.* 2008;103(2):e15-e26.
151. Cantarella G, Lempereur L, Presta M, et al. Nerve growth factor-endothelial cell interaction leads to angiogenesis in vitro and in vivo. *FASEB J.* 2002;16(10):1307–1309.
152. Salis MB, Graiani G, Desortes E, Caldwell RB, Madeddu P, Emanuelli C. Nerve growth factor supplementation reverses the impairment, induced by Type 1 diabetes, of hindlimb post-ischaemic recovery in mice. *Diabetologia.* 2004;47(6):1055-1063.
153. Donovan MJ, Lin MI, Wiegand P, et al. Brain derived neurotrophic factor is an endothelial cell survival factor required for intramyocardial vessel stabilization. *Development.* 2000;127(21):4531–4540.
154. Wagner N, Wagner KD, Theres H, Englert C, Schedl A, Scholz H. Coronary vessel development requires activation of the TrkB neurotrophin receptor by the Wilms' tumor transcription factor Wt1. *Genes Dev.* 2005;19(21):2631–2642.
155. Shelton DL, Sutherland J, Gripp J, et al. Human trks: molecular cloning, tissue distribution, and expression of extracellular domain immunoadhesins. *J Neurosci.* 1995;15(1):477–491.
156. Donovan MJ, Hahn R, Tessarollo L, Hempstead BL. Identification of an essential nonneuronal function of neurotrophin 3 in mammalian cardiac development. *Nat Genet.* 1996;14(2):210-213.
157. Liu X, Wang D, Liu Y, et al. Neuronal-Driven Angiogenesis: Role of NGF in Retinal Neovascularization in an Oxygen-Induced Retinopathy Model. *Invest Ophthalmol Vis Sci.* 2010;51(7):3749-3757.
158. Liu X, Li Y, Liu Y, et al. Endothelial Progenitor Cells (EPCs) Mobilized and Activated by Neurotrophic Factors May Contribute to Pathologic Neovascularization in Diabetic Retinopathy. *Am J Pathol.* 2010;176(1):504-515.
159. Jadhao CS, Bhatwadekar AD, Jiang Y, Boulton ME, Steinle JJ, Grant MB. Nerve growth factor promotes endothelial progenitor cell-mediated angiogenic responses. *Invest Ophthalmol Vis Sci.* 2012;53(4):2030-2037.
160. Kennedy TE, Serafini T, de la Torre JR, Tessier-Lavigne M. Netrins are diffusible chemotropic factors for commissural axons in the embryonic spinal cord. *Cell.* 1994;78(3):425-435.
161. Fazeli A1, Dickinson SL, Hermiston ML, et al. Phenotype of mice lacking functional Deleted in colorectal cancer (Dcc) gene. *Nature.* 1997;386(6627):796–804.
162. Keino-Masu K, Masu M, Hinck L, et al. Deleted in Colorectal Cancer (DCC) encodes a netrin receptor. *Cell.* 1996;87(2):175-185.
163. Leonardo ED, Hinck L, Masu M, Keino-Masu K, Ackerman SL, Tessier-Lavigne M. Vertebrate homologues of *C. elegans* UNC-5 are candidate netrin receptors. *Nature.* 1997;386:833–838.

164. Hong K, Hinck L, Nishiyama M, Poo MM, Tessier-Lavigne M, Stein E. A ligand-gated association between cytoplasmic domains of UNC5 and DCC family receptors converts netrin-induced growth cone attraction to repulsion. *Cell*. 1999;97(7):927-941.
165. Lu X, Le Noble F, Yuan L, et al. The netrin receptor UNC5B mediates guidance events controlling morphogenesis of the vascular system. *Nature*. 2004;432(7014).
166. Lejmi E, Leconte L, Pédrón-Mazoyer S, et al. Netrin-4 inhibits angiogenesis via binding to neogenin and recruitment of Unc5B. *Proc Natl Acad Sci USA*. 2008;105(34):12491–12496.
167. Larrivé B, Freitas C, Trombe M, et al. Activation of the UNC5B receptor by Netrin-1 inhibits sprouting angiogenesis. *Genes Dev*. 2007;21(19):2433-2447.
168. Kolodkin AL, Matthes DJ, O'Connor TP, et al. Fasciclin IV: Sequence, Expression, and Function during Growth Cone Guidance in the Grasshopper Embryo. *Neuron*. 1992;9:831-845.
169. Luo Y, Raible D, Raper JA. Collapsin: a protein in brain that induces the collapse and paralysis of neuronal growth cones. *Cell*. 1993;75(2):217-227.
170. Goodman CS, Kolodkin AL, Luo Y, Püschel AW, Raper JA. Unified nomenclature for the semaphorins/collapsins. Semaphorin Nomenclature Committee. *Cell*. 1999;97(5):551-552.
171. Yazdani U, Terman JR. The Semaphorins. *Genome Biol*. 2006;7(3):211.
172. Pasterkamp RJ. R-Ras fills another GAP in semaphorin signalling. *Trends Cell Biol*. 2005;15(2):61-64.
173. Negishi M, Oinuma I, Katoh H. Plexins: axon guidance and signal transduction. *Cell Mol Life Sci*. 2005;62(12):1363-1371.
174. Toyofuku T, Yoshida J, Sugimoto T, et al. FARP2 triggers signals for Sema3A-mediated axonal repulsion. *Nat Neurosci*. 2005;8(12):1712-1719.
175. Oinuma I, Ishikawa Y, Katoh H, M N. The Semaphorin 4D Receptor Plexin-B1 Is a GTPase Activating Protein for R-Ras. *Science*. 2004;305(5685):862-865.
176. Tamagnone L, Comoglio PM. To move or not to move? Semaphorin signalling in cell migration. *EMBO J*. 2004;5(4):356-361.
177. Rice DS, Huang W, Jones HA, et al. Severe retinal degeneration associated with disruption of semaphorin 4A. *Invest Ophthal Vis Sci*. 2004;46(8):2767-2777.
178. Sahay A, Kim CH, Sepkuty JP, et al. Secreted semaphorins modulate synaptic transmission in the adult hippocampus. *J Neurosci*. 2005;25(14):3613-3620.
179. Acevedo LM, Barillas S, Weis SM, Gothert JR, Cheresh DA. Semaphorin 3A suppresses VEGF-mediated angiogenesis yet acts as a vascular permeability factor. *Blood*. 2008;111(5):2674-2680.
180. Appleton BA, Wu P, Maloney J, et al. Structural studies of neuropilin/antibody complexes provide insights into semaphorin and VEGF binding. *EMBO J*. 2007;26:4902-4912.
181. Miao H-Q, Soker S, Feiner L, Alonso JL, Raper JA, Klagsbrun M. Neuropilin-1 mediates collapsin-1/semaphorin III inhibition of endothelial cell motility: Functional competition of collapsin-1 and vascular endothelial growth factor-165. *J Cell Biol*. 1999;146:233-242.

182. Takahashi T, Fournier A, Nakamura F, et al. Plexin-Neuropilin-1 Complexes Form Functional Semaphorin-3A Receptors. *Cell*. 1999;99:59-69.
183. Maione F, Molla F, Meda C, et al. Semaphorin 3A is an endogenous angiogenesis inhibitor that blocks tumor growth and normalizes tumor vasculature in transgenic mouse models. *J Clin Invest*. 2009;119(11):113356-113372.
184. Varshavsky A, Kessler O, Abramovitch S, et al. Semaphorin-3B is an angiogenesis inhibitor that is inactivated by furin-like pro-protein convertases. *Cancer Res*. 2008;68(17):6922-6931.
185. Nasarre P, Constantin B, Drabkin HA, Roche J. Semaphorins and cancers : an up 'dating'. *Med Sci (Paris)*. 2005;21(6-7):641-647.
186. Nasarre P, Kusy S, Constantin B, et al. Semaphorin SEMA3F Has a Repulsing Activity on Breast Cancer Cells and Inhibits E-Cadherin–Mediated Cell Adhesion. *Neoplasia*. 2005;7(2):180-189.
187. Kusy S, Nasarre P, Chan D, et al. Selective Suppression of *In Vivo* Tumorigenicity by Semaphorin SEMA3F in Lung Cancer Cells. *Neoplasia*. 2005;7(5):457-465.
188. Konno R. Gene expression profiling of human ovarian epithelial tumors by digoxin nucleotide microarray. *Hum Cell*. 2001;14:261-256.
189. Kidd T, Brose K, Mitchell KJ, et al. Roundabout controls axon crossing of the CNS midline and defines a novel subfamily of evolutionarily conserved guidance receptors. *Cell*. 1998;92(2):205-215.
190. Zallen JA, Yi BA, Bargmann CI. The conserved immunoglobulin superfamily member SAX-3/Robo directs multiple aspects of axon guidance in *C. elegans*. *Cell*. 1998;92(2):217-227.
191. Huminiecki L, Gorn M, Suchting S, Poulosom R, Bicknell R. Magic roundabout is a new member of the roundabout receptor family that is endothelial specific and expressed at sites of active angiogenesis. *Genomics*. 2001;79(4):547-552.
192. Mambetisaeva ET, Andrews W, Camurri L, Annan A, Sundaresan V. Robo family of proteins exhibit differential expression in mouse spinal cord and Robo-Slit interaction is required for midline crossing in vertebrate spinal cord. *Dev Dyn*. 2005;233(1):41-51.
193. Grieshammer U, Le Ma, Plump AS, Wang F, Tessier-Lavigne M, Martin GR. SLIT2-mediated ROBO2 signaling restricts kidney induction to a single site. *Dev Cell*. 2004;6(5):709-717.
194. Wu JY, Feng L, Park HT, et al. The neuronal repellent Slit inhibits leukocyte chemotaxis induced by chemotactic factors. *Nature*. 2001;410:948–952.
195. Weitzman M, Bayley EB, Naik UP. Robo4: a guidance receptor that regulates angiogenesis. *Cell Adh Migr*. 2008;2(4):220-222.
196. Bedell VM, Yeo SY, Park KW, et al. roundabout4 is essential for angiogenesis in vivo. *Proc Natl Acad Sci USA*. 2005;102(18):6373–6378.
197. Drescher U, Kremoser C, Handwerker C, Löscher J, Noda M, Bonhoeffer F. In vitro guidance of retinal ganglion cell axons by RAGS, a 25 kDa tectal protein related to ligands for Eph receptor tyrosine kinases. *Cell*. 1995;82(3):359–370.

198. Cheng HJ, Nakamoto M, Bergemann AD, Flanagan JG. Complementary gradients in expression and binding of ELF-1 and Mek4 in development of the topographic retinotectal projection map. *Cell*. 1995;82(3):871-881.
199. Palmer A, Klein R. Multiple roles of ephrins in morphogenesis, neuronal networking, and brain function. *Genes Dev*. 2003;17(12):1429-1450.
200. Maekawa H, Oike Y, Kanda S, et al. Ephrin-B2 induces migration of endothelial cells through the phosphatidylinositol-3 kinase pathway and promotes angiogenesis in adult vasculature. *Arterioscler Thromb Vasc Biol*. 2003;23(11):2008-2014.
201. Steinle JJ, Meininger CJ, Forough R, Wu G, Wu MH, Granger HJ. Eph B4 receptor signaling mediates endothelial cell migration and proliferation via the phosphatidylinositol 3-kinase pathway. *J Biol Chem*. 2002;277(46):43830-43835.
202. Foo SS, Turner CJ, Adams S, et al. Ephrin-B2 controls cell motility and adhesion during blood-vessel-wall assembly. *Cell*. 2006;124(1):161-173.
203. Ogita H, Kunimoto S, Kamioka Y, Sawa H, Masuda M, Mochizuki N. EphA4-mediated Rho activation via Vsm-RhoGEF expressed specifically in vascular smooth muscle cells. *Circ Res*. 2003;93(1):23-31.
204. Deroanne C, Vouret-Craviari V, Wang B, Pouysségur J. EphrinA1 inactivates integrin-mediated vascular smooth muscle cell spreading via the Rac/PAK pathway. *J Cell Sci*. 2003;116:1367-1376.
205. Ogawa K, Pasqualini R, Lindberg RA, Kain R, Freeman AL, Pasquale EB. The ephrin-A1 ligand and its receptor, EphA2, are expressed during tumor neovascularization. *Oncogene*. 2000;19(52):6043-6052.
206. Kim Y, West XZ, Byzova TV. Inflammation and oxidative stress in angiogenesis and vascular disease. *J Mol Med*. 2013;91(3):323-328.
207. Dammann O. Inflammation and retinopathy of prematurity. *Acta Paediatrica*. 2010;99(7):975-977.
208. Ishida S, Usui T, Yamashiro K, et al. VEGF164 is proinflammatory in the diabetic retina. *Invest Ophthalmol Vis Sci*. 2003;44(5):2155-2162.
209. Krady JK, Basu A, Allen CM, et al. Minocycline reduces proinflammatory cytokine expression, microglial activation, and caspase-3 activation in a rodent model of diabetic retinopathy. *Diabetes*. 2005;54(5):1559-1565.
210. Ilg R, Davies M, Powers M. Altered Retinal Neovascularization in TNF Receptor-Deficient Mice. *Curr Eye Res*. 2005;30:1003-1013.
211. Dinarello CA. Immunological and Inflammatory Functions of the Interleukin-1 Family. *Annual Review of Immunology*. 2009;27(1):519-550.
212. Vincent JA, Mohr S. Inhibition of Caspase-1/Interleukin-1b signaling prevents degeneration of retinal capillaries in diabetes and galactosemia. *Diabetes*. 2007;56(1):224-230.
213. Lavalette S, Raoul W, Houssier M, et al. Interleukin-1 $\beta$  Inhibition Prevents Choroidal Neovascularization and Does Not Exacerbate Photoreceptor Degeneration. *Am J Pathol*. 2011;178(5):2416-2423.
214. Qiao H, Sonoda KH, Ikeda Y, et al. Interleukin-18 regulates pathological intraocular neovascularization. *J Leukoc Biol*. 2007;81(4):1012-1021.

215. Doyle SL, Campbell M, Ozaki E, et al. NLRP3 has a protective role in age-related macular degeneration through the induction of IL-18 by drusen components. *Nat Med*. 2012;18(5):791-798.
216. Ara T, Declerck YA. Interleukin-6 in bone metastasis and cancer progression. *Eur J Cancer*. 2010;46(7):1223-1231.
217. Kocak N, Alacacioglu I, Kaynak S, et al. Comparison of vitreous and plasma levels of vascular endothelial growth factor, interleukin-6 and hepatocyte growth factor in diabetic and non-diabetic retinal detachment cases. *Ann Ophthalmol (Skokie)*. 2010;42:10-14.
218. Hong KH, Ryu J, Han KH. Monocyte chemoattractant protein-1-induced angiogenesis is mediated by vascular endothelial growth factor-A. *Blood*. 2005;105(4):1405-1407.
219. Waugh DJ, Wilson C. The interleukin-8 pathway in cancer. *Clin Cancer Res*. 2008;14(21):6735-6741.
220. Jousseaume AM, Poulaki V, Le ML, et al. A central role for inflammation in the pathogenesis of diabetic retinopathy. *FASEB J*. 2004;18(12):1450-1452.
221. Ossovskaya VS, Nunez N. Protease-Activated Receptors: Contribution to Physiology and Disease. *Physiol Rev*. 2004;84:579-621.
222. Rothmeier A, Ruf W. Protease-activated receptor 2 signaling in inflammation. *Semin Immunopathol*. 2012;34(1):133-149.
223. Milia AF, Salis MB, Stacca T, et al. Protease-Activated Receptor-2 Stimulates Angiogenesis and Accelerates Hemodynamic Recovery in a Mouse Model of Hindlimb Ischemia. *Circulation Research*. 2002;91(4):346-352.
224. Uusitalo-Jarvinen H, Kurokawa T, Mueller BM, Andrade-Gordon P, Friedlander M, Ruf W. Role of Protease Activated Receptor 1 and 2 Signaling in Hypoxia-Induced Angiogenesis. *Arterioscler Thromb Vasc Biol*. 2007;27(6):1456-1462.
225. Belting M, Dorrell MI, Sandgren S, et al. Regulation of angiogenesis by tissue factor cytoplasmic domain signaling. *Nat Med*. 2004;10(5):502-509.
226. Coorey N, Shen W, Chung S, Zhu L, Gillies M. The role of glia in retinal vascular disease. *Clin Exp Optom*. 2012;95(3):266-281.
227. Barron KD. The Microglial cell: A historical review. *J Neurol Sci*. 1995;134(suppl):57-68.
228. Langmann T. Microglia activation in retinal degeneration. *J Leukoc Biol*. 2007;81(6):1345-1351.
229. Hotamisligil GS. Inflammation and metabolic disorders. *Nature*. 2006;444:860-867.
230. Kinnunen K, Puustjärvi T, Teräsvirta M, et al. Differences in retinal neovascular tissue and vitreous humour in patients with type 1 and type 2 diabetes. *Br J Ophthalmol*. 2009;93(8):1109-1115.
231. Kataoka K, Nishiguchi KM, Kaneko H, van Rooijen N, Kachi S, Terasaki H. The roles of vitreal macrophages and circulating leukocytes in retinal neovascularization. *Invest Ophthalmol Vis Sci*. 2011;52(3):1431-1438.
232. Jiang Z, Jiang JX, Zhang GX. Macrophages: a double-edged sword in experimental autoimmune encephalomyelitis. *Immunol Lett*. 2014;160(117-22).

233. Houston SK, Wykoff CC, Berrocal AM, Hess DJ, Murray TG. Laser treatment for retinopathy of prematurity. *Lasers Med Sci.* 2013;28:683–692.
234. Mintz-Hittner HA, Kennedy KA, Chuang AZ, Group. B-RC. Efficacy of Intravitreal Bevacizumab for Stage 3+ Retinopathy of Prematurity. *N Engl J Med.* 2011;364(7):603-615.
235. Harder B, Baltz S, Jonas J, Schlichtenbrede F. Intravitreal Bevacizumab for Retinopathy of Prematurity. *J Ocul Pharmacol Therap.* 2011;27(6):623-627.
236. Hu J, Blair MP, Shapiro MJ, Lichtenstein SJ, Galasso JM, R. K. Reactivation of retinopathy of prematurity after bevacizumab injection. *Arch Ophthalmol.* 2012;130(8):1000-1006.
237. Carmeliet P, Ferreira V, Breier G, et al. Abnormal blood vessel development and lethality in embryos lacking a single VEGF allele. *Nature.* 1996;380:435-439.
238. Sato T, Wada K, Arahori H, et al. Serum concentrations of bevacizumab (avastin) and vascular endothelial growth factor in infants with retinopathy of prematurity. *Am J Ophthalmol.* 2012;153(2):327-333.
239. Kurihara T, Westenskow P, Bravo S, Aguilar E, Friedlander M. Targeted deletion of Vegfa in adult mice induces vision loss. *J Clin Invest.* 2012;112(11):4213-4217.
240. Photocoagulation treatment of proliferative diabetic retinopathy: the second report of Diabetic Retinopathy Study findings. *Ophthalmology.* 1978;85:82-105.
241. Vujosevic S, Bottega E, Casciano M, Pilotto E, Convento E, Midena E. Microperimetry and fundus autofluorescence in diabetic macular edema: subthreshold micropulse diode laser versus modified early treatment diabetic retinopathy study laser photocoagulation. *Retina.* 2010;30:908–916.
242. Michaelides M, Fraser-Bell S, Hamilton R, et al. Macular perfusion determined by fundus fluorescein angiography at the 4-month time point in a prospective randomized trial of intravitreal bevacizumab or laser therapy in the management of diabetic macular edema (Bolt Study): Report 1. *Retina.* 2010;30(5):781-786.
243. Rajendram R, Fraser-Bell S, Kaines A, et al. A 2-year prospective randomized controlled trial of intravitreal bevacizumab or laser therapy (BOLT) in the management of diabetic macular edema: 24-month data: report 3. *Arch Ophthalmol.* 2012;130(8):972-979.
244. Michaelides M, Kaines A, Hamilton RD, et al. A prospective randomized trial of intravitreal bevacizumab or laser therapy in the management of diabetic macular edema (BOLT study) 12-month data: report 2. *Ophthalmology.* 2010;117(6):1078-1086.e1072.
245. Do DV, Schmidt-Erfurth U, Gonzalez VH, et al. The DA VINCI Study: phase 2 primary results of VEGF Trap-Eye in patients with diabetic macular edema. *Ophthalmology.* 2011;118(9):1819-1826.
246. Campochiaro PA, Brown DM, Pearson A, et al. Sustained delivery fluocinolone acetonide vitreous inserts provide benefit for at least 3 years in patients with diabetic macular edema. *Ophthalmology.* 2012;119(10):2125-2132.

247. Diabetic Retinopathy Clinical Research Network (DRCR.net), Beck RW, Edwards AR, et al. Three-year follow-up of a randomized trial comparing focal/grid photocoagulation and intravitreal triamcinolone for diabetic macular edema. *Arch Ophthalmol* 2009;127(3):245–251.
248. Coscas G, Augustin A, Bandello F, et al. Retreatment with Ozurdex for macular edema secondary to retinal vein occlusion. *Eur J Ophthalmol*. 2014;24(1):1-9.
249. Group TDCaCTR. The effect of intensive treatment of diabetes on the development and progression of long-term complications in insulin-dependent diabetes mellitus. *N Engl J Med*. 1993;329:977- 986.
250. Group TDCaCTR. Progression of retinopathy with intensive versus conventional treatment in the Diabetes Control and Complications Trial. *Ophthalmology*. 1995;102(2):647-661.
251. Stratton IM, Kohner EM, Aldington SJ, et al. UKPDS 50: risk factors for incidence and progression of retinopathy in Type II diabetes over 6 years from diagnosis. *Diabetologia*. 2001;44(2).
252. Chaturvedi N, Sjolie AK, Stephenson JM, et al. Effect of lisinopril on progression of retinopathy in normotensive people with type 1 diabetes. . *Lancet*. 1998;351(9095):28-31.
253. Matthews DR, Stratton IM, Aldington SJ, Holman RR, EM; K, UK Prospective Diabetes Study Group. Risks of progression of retinopathy and vision loss related to tight blood pressure control in type 2 diabetes mellitus: UKPDS 69. *Arch Ophthalmol*. 2004;122(11):1631-1640.
254. Mauer M, Zinman B, Gardiner R, et al. Renal and retinal effects of enalapril and losartan in type 1 diabetes. *N Engl J Med*. 2009;361(1):40-51.
255. Chaturvedi N, Porta M, Klein R, et al. Effect of candesartan on prevention (DIRECT-Prevent 1) and progression (DIRECT-Protect 1) of retinopathy in type 1 diabetes: randomised, placebo-controlled trials. *Lancet*. 2008;372(9647):1394-1402.
256. Group; AS, ACCORD Eye Study Group, Chew EY, et al. Effects of medical therapies on retinopathy progression in type 2 diabetes. *N Engl J Med*. 2010;363(3):233-244.
257. Keech AC, Mitchell P, Summanen PA, et al. Effect of fenofibrate on the need for laser treatment for diabetic retinopathy (FIELD study): a randomised controlled trial. *Lancet*. 2007;370(9600):1687-1697.
258. Dejda A, Mawambo G, Cerani A, et al. Neuropilin-1 mediates myeloid cell chemoattraction and influences retinal neuroimmune crosstalk. *J Clin Invest*. 2014;124(11):4807–4822.
259. Cerani A, Tetreault N, Menard C, et al. Neuron-Derived Semaphorin 3A Is an Early Inducer of Vascular Permeability in Diabetic Retinopathy via Neuropilin-1. *Cell Metab*. 2013;18(4): 505-518.
260. Fulton AB, Akula JD, Mocko JA, et al. Retinal degenerative and hypoxic ischemic disease. *Doc Ophthalmol*. 2008;118(1):55-61.
261. Fukushima Y, Okada M, Kataoka H, et al. Sema3E-PlexinD1 signaling selectively suppresses disoriented angiogenesis in ischemic retinopathy in mice *J Clin Invest*. 2011;121(5):1974-1986.

262. Gaur P, Bielenberg DR, Samuel S, et al. Role of Class 3 Semaphorins and Their Receptors in Tumor Growth and Angiogenesis. *Clinical Cancer Research*. 2009;15(22):6763-6770.
263. Bielenberg DR, Klagsbrun M. Targeting endothelial and tumor cells with semaphorins. *Cancer and Metastasis Reviews*. 2007;26(3-4):421-431.
264. Clarhaut J, Gemmill RM, Potiron VA, et al. ZEB-1, a Repressor of the Semaphorin 3F Tumor Suppressor Gene in Lung Cancer Cells. *Neoplasia*. 2009(11):157-166.
265. Beuten J, Garcia D, Brand TC, et al. Semaphorin 3B and 3F single nucleotide polymorphisms are associated with prostate cancer risk and poor prognosis. *J Urol*. 2009;182(4):1614-1620.
266. Adams RH, Eichmann A. Axon Guidance Molecules in Vascular Patterning. *Cold Spring Harb Perspect Biol*. 2010;2(5):1-19.
267. PK S. The chemokine system in arteriogenesis and hind limb ischemia. *J Vascul Surg*. 2007;45:A48-56.
268. Liu L, Qi X, Chen Z, et al. Targeting the IRE1 $\alpha$ /XBP1 and ATF6 arms of the unfolded protein response enhances VEGF blockade to prevent retinal and choroidal neovascularization. *Am J Pathol*. 2013;182(4):1412-1424.
269. Edwards M, Mcleod D, Li R, et al. The deletion of Math5 disrupts retinal blood vessel and glial development in mice. *Exp Eye Res*. 2012;96(1):147-156.
270. Weidemann A, Krohne TU, Aguilar E, et al. Astrocyte hypoxic response is essential for pathological but not developmental angiogenesis of the retina. *Glia*. 2010:NA-NA.
271. Caprara C, Thiersch M, Lange C, Joly S, Samardzija M, Grimm C. HIF1A is essential for the development of the intermediate plexus of the retinal vasculature. *Invest Ophthalmol Vis Sci*. 2011;52(5):2109-2117.
272. Nakamura-Ishizu A, Kurihara T, Okuno Y, et al. The formation of an angiogenic astrocyte template is regulated by the neuroretina in a HIF-1-dependent manner. *Dev Biol*. 2012;363(1):106-114.
273. Chen J MS, Juan AM, Hurst C, Hatton CJ, Pei D, Joyal J, Evans L, Cui Z, Stahl A, Sapienza P, Sinclair DA, Smith L. Neuronal sirtuin1 mediates retinal vascular regeneration in oxygen-induced ischemic retinopathy. *Angiogenesis*. 2013;16(4):985-992.
274. Arai K JG, Navaratna D, Lo E. Brain angiogenesis in developmental and pathological processes: neurovascular injury and angiogenic recovery after stroke. *FEBS Journal*. 2009;276(17):4644-4465.
275. Oliveira de Moraes O SD, Melo DA, Carvalho de Vasconcelos CA. Ischemic Cerebral Process: Risk Factors, Angiogenesis and Neuroprotection *Neurobiologica*. 2006;68(4):167-183.
276. Taylor RA, Sansing LH. Microglial responses after ischemic stroke and intracerebral hemorrhage. *Clin Dev Immunol*. 2013;Epub:746068.
277. Crain JM, Nikodemova M, Watters JJ. Microglia express distinct M1 and M2 phenotypic markers in the postnatal and adult central nervous system in male and female mice. *J Neurosci Res*. 2013;91(9):1143-1151.

278. Martinez FO, Gordon S. The M1 and M2 paradigm of macrophage activation: time for reassessment. *F1000Prime Rep*. 2014;6:13.
279. Mao X, Xing H, Mao A, et al. Netrin-1 attenuates cardiac ischemia reperfusion injury and generates alternatively activated macrophages. *Inflammation*. 2014;37(2):573-580.
280. Mocan MC, Kadayifcilar S, Eldem B. Elevated intravitreal interleukin-6 levels in patients with proliferative diabetic retinopathy. *Can J Ophthalmol*. 2006;41(6):747-752.
281. Liu Y BCM, Gerhardinger C. IL-1 $\beta$  Is Upregulated in the Diabetic Retina and Retinal Vessels: Cell-Specific Effect of High Glucose and IL-1 $\beta$  Autostimulation. *PLoS ONE*. 2012;7(5):e36949.
282. Gabay C, Lamacchia C, Palmer G. IL-1 pathways in inflammation and human diseases. *Nat Rev Rheumatol*. 2010;6(4):232-241.
283. Dinarello CA. Biologic Basis for Interleukin-1 in Disease. *Blood*. 1996;87(6):2095-2147.
284. Jung YJ. IL-1 mediated up-regulation of HIF-1 via an NF $\kappa$ B/COX-2 pathway identifies HIF-1 as a critical link between inflammation and oncogenesis. *The FASEB Journal*. 2003.
285. Lamkanfi M, Dixit V. Mechanisms and Functions of Inflammasomes. *Cell*. 2014;157(5):1013-1022.
286. Campbell M, Doyle SL, Ozaki E, et al. An overview of the involvement of interleukin-18 in degenerative retinopathies. *Adv Exp Med Biol*. 2014;801:409-415.
287. Kerur N, Hirano Y, Tarallo V, et al. TLR-independent and P2X7-dependent signaling mediate Alu RNA-induced NLRP3 inflammasome activation in Geographic Atrophy. *Invest Ophthalmol Vis Sci*. 2013;54(12):7395-7401.
288. Tarallo V, Hirano Y, Gelfand B, et al. DICER1 Loss and Alu RNA Induce Age-Related Macular Degeneration via the NLRP3 Inflammasome and MyD88. *Cell*. 2012;149(4):847-859.
289. Corset V, Nguyen-Ba-Charvet KT, Forcet C, Moyse E, Chedotal A, Mehlen P. Netrin-1-mediated axon outgrowth and cAMP production requires interaction with adenosine A2b receptor. *Nature*. 2000;407:747-750.
290. Ramkhelawon B, Yang Y, van Gils JM, et al. Hypoxia induces netrin-1 and Unc5b in atherosclerotic plaques: mechanism for macrophage retention and survival. *Arterioscler Thromb Vasc Biol*. 2013;33(6):1180-1188.
291. Ramkhelawon B, Hennessy EJ, Ménager M, et al. Netrin-1 promotes adipose tissue macrophage retention and insulin resistance in obesity. *Nat Med*. 2014;20(4):377-384.
292. Nishijima K, Ng Y, Zhong L, et al. Vascular Endothelial Growth Factor-A Is a Survival Factor for Retinal Neurons and a Critical Neuroprotectant during the Adaptive Response to Ischemic Injury. *Am J Pathol*. 2010;171(1):53-67.
293. Smith JA, Das A, Ray SK, Banik NL. Role of pro-inflammatory cytokines released from microglia in neurodegenerative diseases. *Brain Res Bull*. 2012;87(1):10-20.

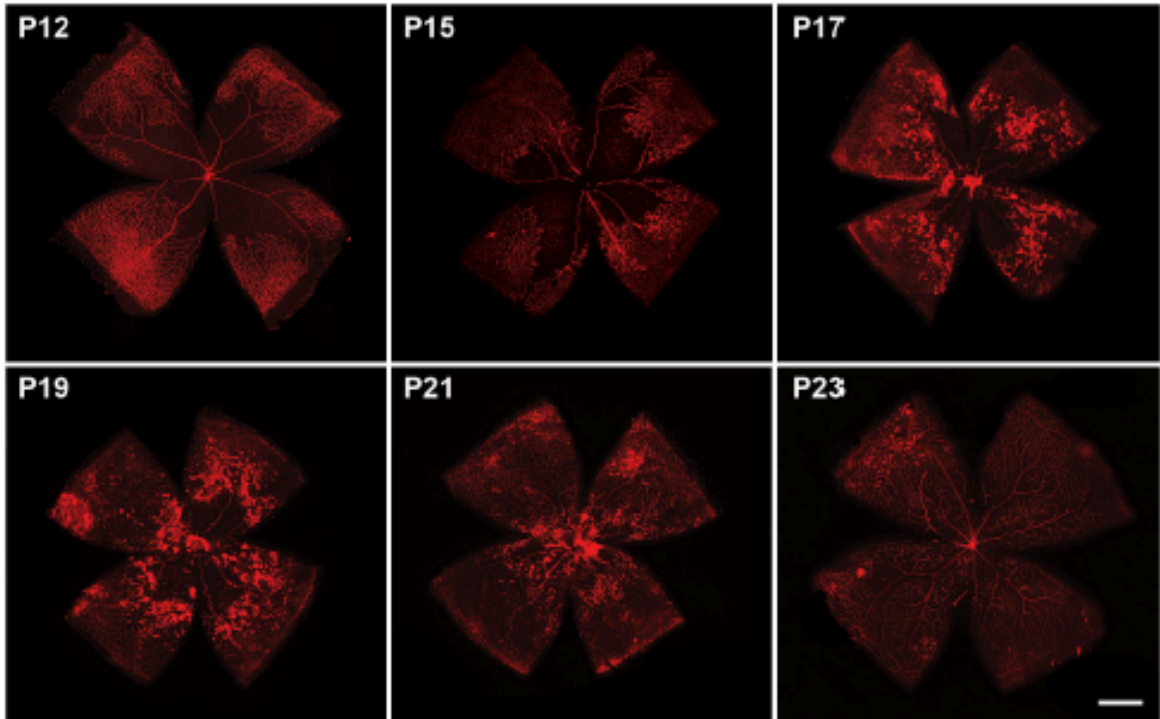
294. Fan L, Yotov WV, Zhu T, et al. Tissue factor enhances protease-activated receptor-2-mediated factor VIIa cell proliferative properties. *Journal of Thrombosis and Haemostasis*. 2005;3:1056–1063.
295. Ritchie E, Saka M, MacKenzie C, et al. Cytokine upregulation of proteinase-activated-receptors 2 and 4 expression mediated by p38 MAP kinase and inhibitory kappa B kinase  $\beta$  in human endothelial cells. *Br J Pharmacol*. 2007;150(8):1044-1054.
296. Luo W, Wang Y, Reiser G. Protease-activated receptors in the brain: Receptor expression, activation, and functions in neurodegeneration and neuroprotection. *Brain Res Rev*. 2007;56(2):331-345.
297. Jin G, Hayashi T, Kawagoe J, et al. Deficiency of PAR-2 gene increases acute focal ischemic brain injury. *J Cereb Blood Flow Metab*. 2005;25(3):302-313.
298. Noorbakhsh F, Tsutsui S, Vergnolle N, et al. Proteinase-activated receptor 2 modulates neuroinflammation in experimental autoimmune encephalomyelitis and multiple sclerosis. *J Exp Med*. 2006;203(2):425-435.
299. Afkhami-Goli A, Noorbakhsh F, Keller AJ, et al. Proteinase-Activated Receptor-2 Exerts Protective and Pathogenic Cell Type-Specific Effects in Alzheimer's Disease. *J Immunol*. 2007;179:5493-5503.

# Appendix 1

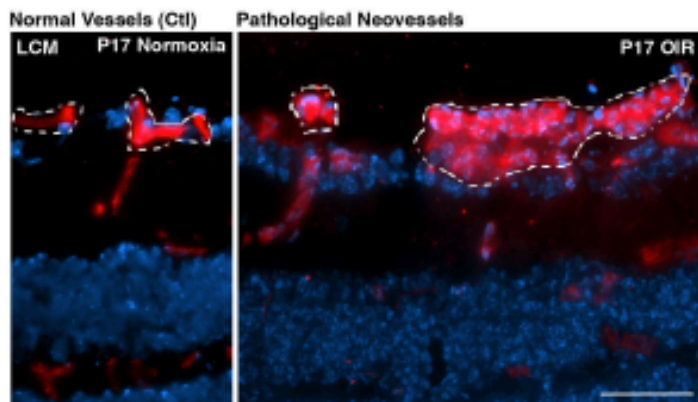
Supplementary Figures Joyal JS, Sitaras N, et al. Blood 2011

## Supplementary Figure 1

A



B



**Supplementary Figure 1. Timeline of revascularization in OIR and depiction of laser-capture microdissection.** (A) Representative photo-micrographs of *Griffonia simplicifolia* lectin-stained retinal flatmounts illustrate the progression of vascular growth following the initial vaso-obliteration in response to oxygen exposure from P7-12. At P12, immediately after exposure to hyperoxia, retinas present maximal vascular loss. As the retina attempts to revascularize, there is an initial delay in regrowth followed by misdirected preretinal vascular tuft formation that peaks at P17. Subsequently at P19-21, vessels enter the avascular retina, as the pre-retinal neovascularization regresses. By P23, the vaso-obiterated zone is fully revascularized. (B) Representative retinal cross-section of lectin-stained normal vessels before lasercapture, compared to (pre-retinal) vascular tufts. Dotted lines represent the laser dissection.

**Relative contributions: Suppl Figure 1**

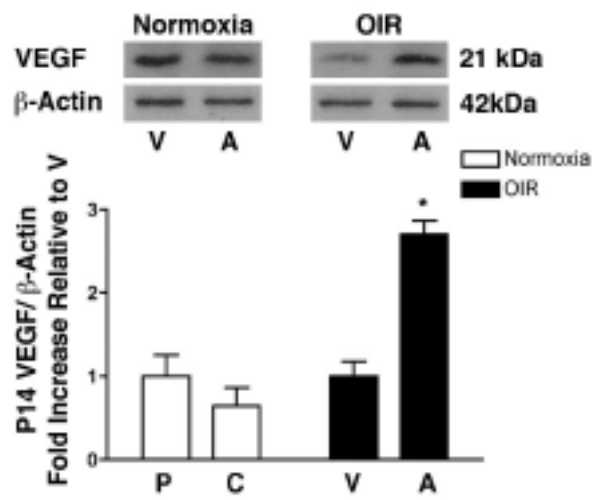
- A) Immunohistochemistry, imaging and analysis performed by **N Sitaras**, JS Joyal, K Zaniolo and Z Shao
- B) Immunohistochemistry, imaging and analysis performed by JS Joyal, A Stahl and P Sapieha

Animal handling and sample collection: **N Sitaras**, JS Joyal, K Zaniolo and Z Shao

Figure preparation: JS Joyal, **N Sitaras**, P Sapieha and S Chemtob

Approximate Figure contribution: 40%

Supplementary Figure 2



**Supplementary Figure 2. VEGF is upregulated in the central avascular region of the OIR retina.** Micro-dissection of avascular (A) and vascularized (V) areas of retinas from mice (P14) subjected to OIR, reveals a ~3-fold induction in VEGF protein (by Western blotting) specifically in the avascular center during pathological neovascularization (n=4). There is no significant difference in VEGF expression between peripheral (P) and central (C) normoxic retina at P14. Values are shown relative to peripheral and vascularized retinas  $\pm$  s.e.m. \*p=0.019 compared to corresponding vascularized area (V).

**Relative contributions: Suppl Figure 2**

Western blot analysis performed by **N Sitaras** and A Zabeida

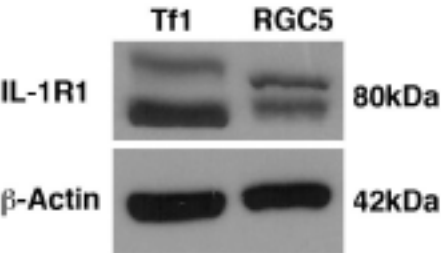
Animal handling and sample collection: **N Sitaras**, JS Joyal, K Zaniolo and Z Shao

Figure preparation: JS Joyal, **N Sitaras**, P Sapiuha and S Chemtob

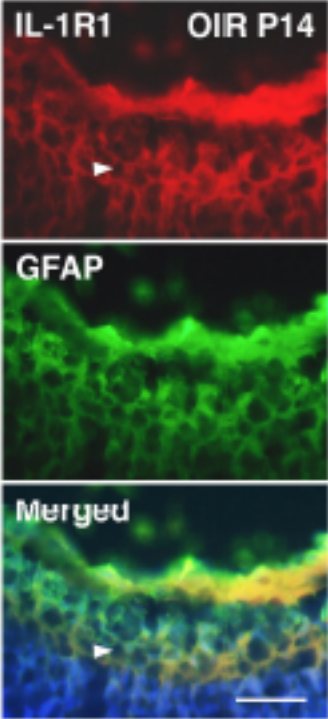
Approximate Figure contribution: 75%

Supplementary Figure 3

A



B



**Supplementary Figure 3. Expression of IL-1R1 in RGC-5 and astrocytes.** (A) Protein expression of IL-1R1 in unstimulated rat RGC-5 (by Western blot); human Tf-1 cells were used as positive control (n=3). (B) Confocal immunohistochemical imaging of retinal cross-sections from P14 mice subjected to OIR reveals expression of IL-1R in astrocytes (GFAP positive); note merged images. n=3. Scale bar: 25  $\mu$ m.

**Relative contributions: Suppl Figure 3**

- A) In vitro preparation and Western blot analysis performed by **N Sitaras**
- B) Immunohistochemistry, imaging and analysis performed by T Zhu

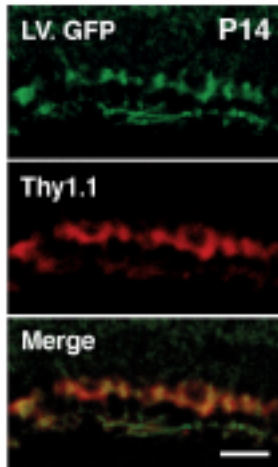
Animal handling and sample collection: **N Sitaras**, JS Joyal, K Zaniolo and Z Shao

Figure preparation: JS Joyal, **N Sitaras**, P Sapieha and S Chemtob

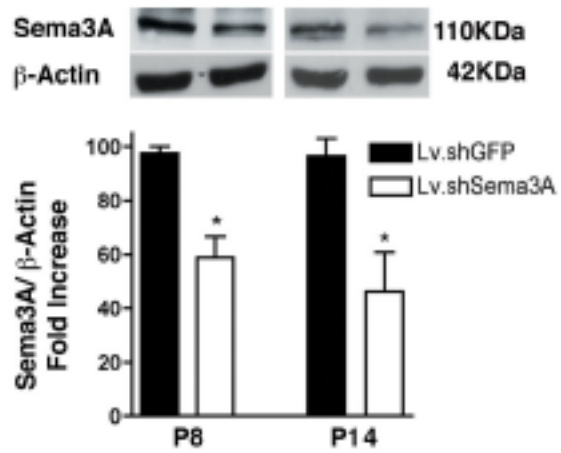
Approximate Figure contribution: 40%

## Supplementary Figure 4

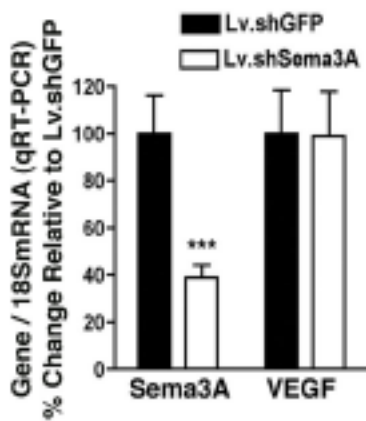
**A**



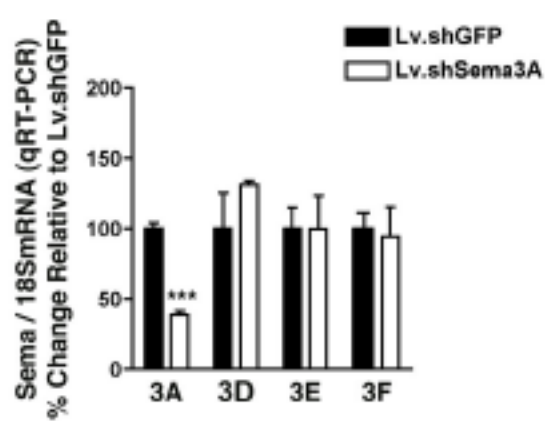
**B**



**C**



**D**



**Supplementary Figure 4. Intravitreal injection of Lentivirus efficiently infects RGCs.** (A) LV vectors containing a GFP transgene under a CMV promoter (Lv.GFP) were injected intravitreally into mouse pups at P2 and infected ~70% of RGCs as detected by co-localization with the RGC-specific marker Thy1.1. at P14 (n=3). (B) Intravitreal injections of Lv.shSema3A at P2 resulted in a ~38% reduction at P8 (n=3, \*p=0.043) and ~54% reduction at P14 (n=3, \*p=0.034) of Sema3A protein, relative to values for corresponding Lv.shGFP. (C, D) Specificity of shSema3A was confirmed as neither VEGF nor other related Semaphorins such as Sema3D, Sema3E or Sema3F were downregulated. n=3; \*\*\*p<0.005 compared to corresponding Lv.shGFP. Scale bar (A) 50  $\mu$ m.

#### **Relative contributions: Suppl Figure 4**

Lentiviral preparation performed by **N Sitaras**, JS Joyal, D Hamel and C Beauséjour

Intravitreal injections performed by **N Sitaras**, K Zaniolo and Z Shao

A) Immunohistochemistry, imaging and analysis performed by JS Joyal, K Zaniolo and P Sapieha

B) Sample preparation and Western blot analysis performed by **N Sitaras** and A Zabeida

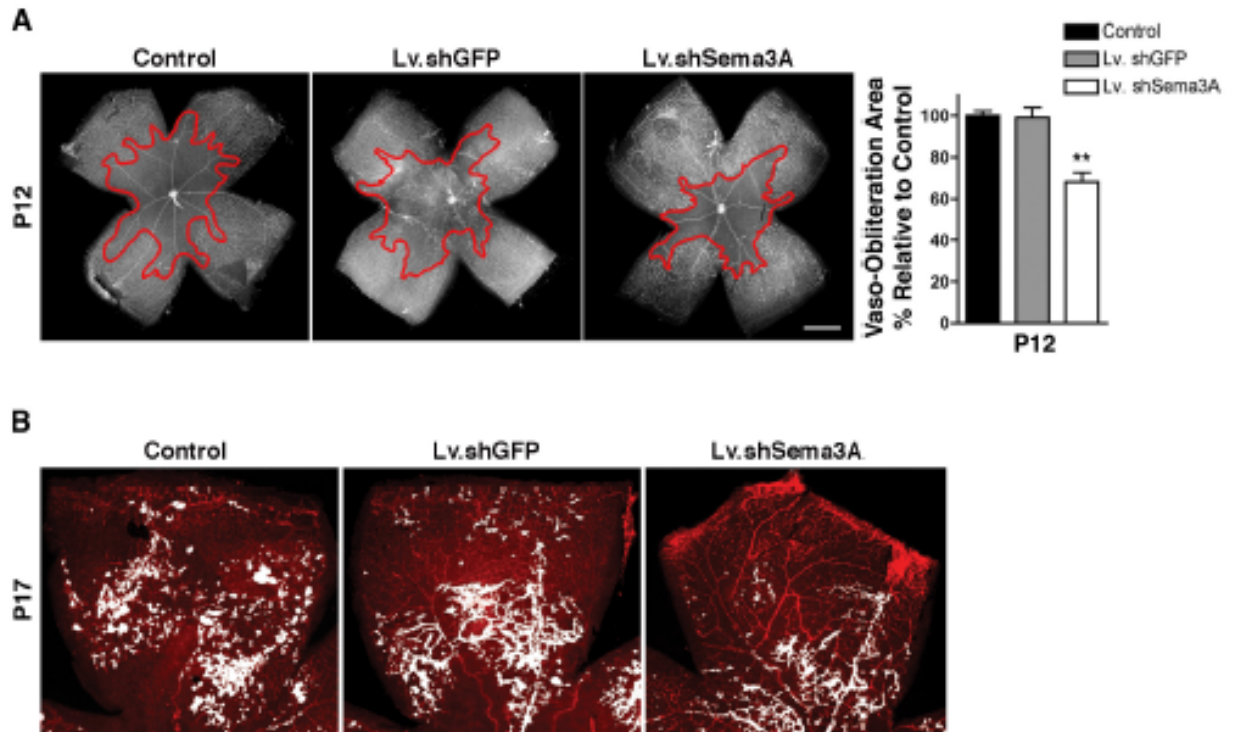
C) Sample preparation and qPCR analysis performed by **N Sitaras** and A Zabeida

Animal handling and sample collection: **N Sitaras**, JS Joyal, K Zaniolo and Z Shao

Figure preparation: JS Joyal, **N Sitaras**, P Sapieha and S Chemtob

Approximate Figure contribution: 40%

## Supplementary Figure 5



**Supplementary Figure 5. Lv.shSema3A protects against vaso-obliteration and neovascularization.** (A) Lectin-stained retinal flatmounts reveal that Lv.shSema3A treated retinas present significantly less vasoobliteration (67% relative to controls). n=13-15, \*\*p=0.01 compared to control. (B) Neovascular areas shown in Figure 3B were quantified using Swift NV1; representative quantification masks are presented.

**Relative contributions: Suppl Figure 5**

Lentiviral preparation performed by **N Sitaras**, JS Joyal, D Hamel and C Beauséjour

Intravitreal injections performed by **N Sitaras**, K Zaniolo and Z Shao

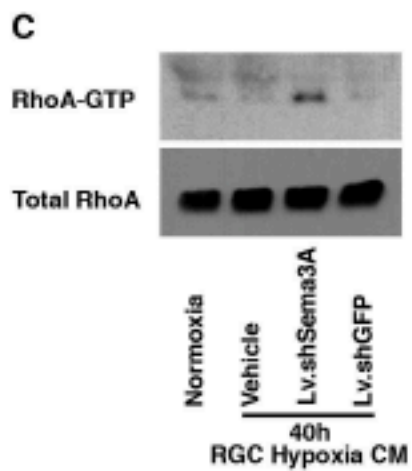
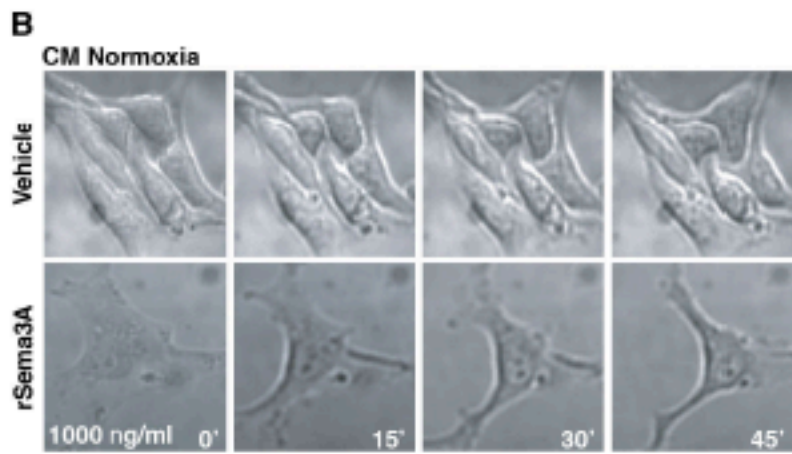
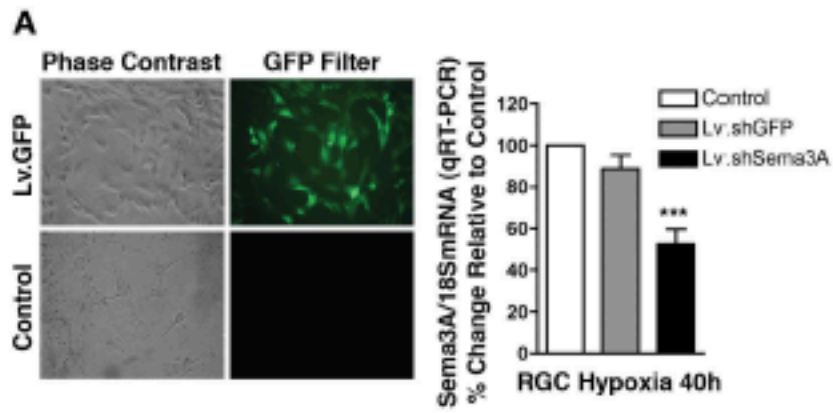
D) Immunohistochemistry, imaging and analysis performed by **N Sitaras**, JS Joyal, K Zaniolo and P Sapieha

Animal handling and sample collection: **N Sitaras**, JS Joyal, K Zaniolo and Z Shao

Figure preparation: JS Joyal, **N Sitaras**, P Sapieha and S Chemtob

Approximate Figure contribution: 40%

## Supplementary Figure 6



**Supplementary Figure 6. *In vitro* assessment of RGC-derived Sema3A.** (A) Lentivirus efficiently infects cultured RGCs and shSema3A reduces Sema3A expression by ~50%. n=3; \*\*\*p<0.01 compared to control. (B) Time lapse images (0 to 45 min) of EC contraction upon stimulation with rSema3A (1 µg/ml) or vehicle (control). (C) Pull-down of activated RhoA-GTP reveals that this permissive player in cytoskeletal growth and remodelling becomes activated when RGC-derived Sema3A is knocked down in CM.

**Relative contributions: Suppl Figure 6**

Lentiviral preparation performed by **N Sitaras**, JS Joyal, D Hamel and C Beauséjour

In vitro preparations performed by **N Sitaras**, F Binet and JS Joyal

A) Immunocytochemistry, imaging and analysis performed by **N Sitaras**, JS Joyal, and F Binet

qPCR analysis performed by **N Sitaras** and A Zabeida

B) Live imaging and analysis performed by F Binet, G Hickson and P Sapieha

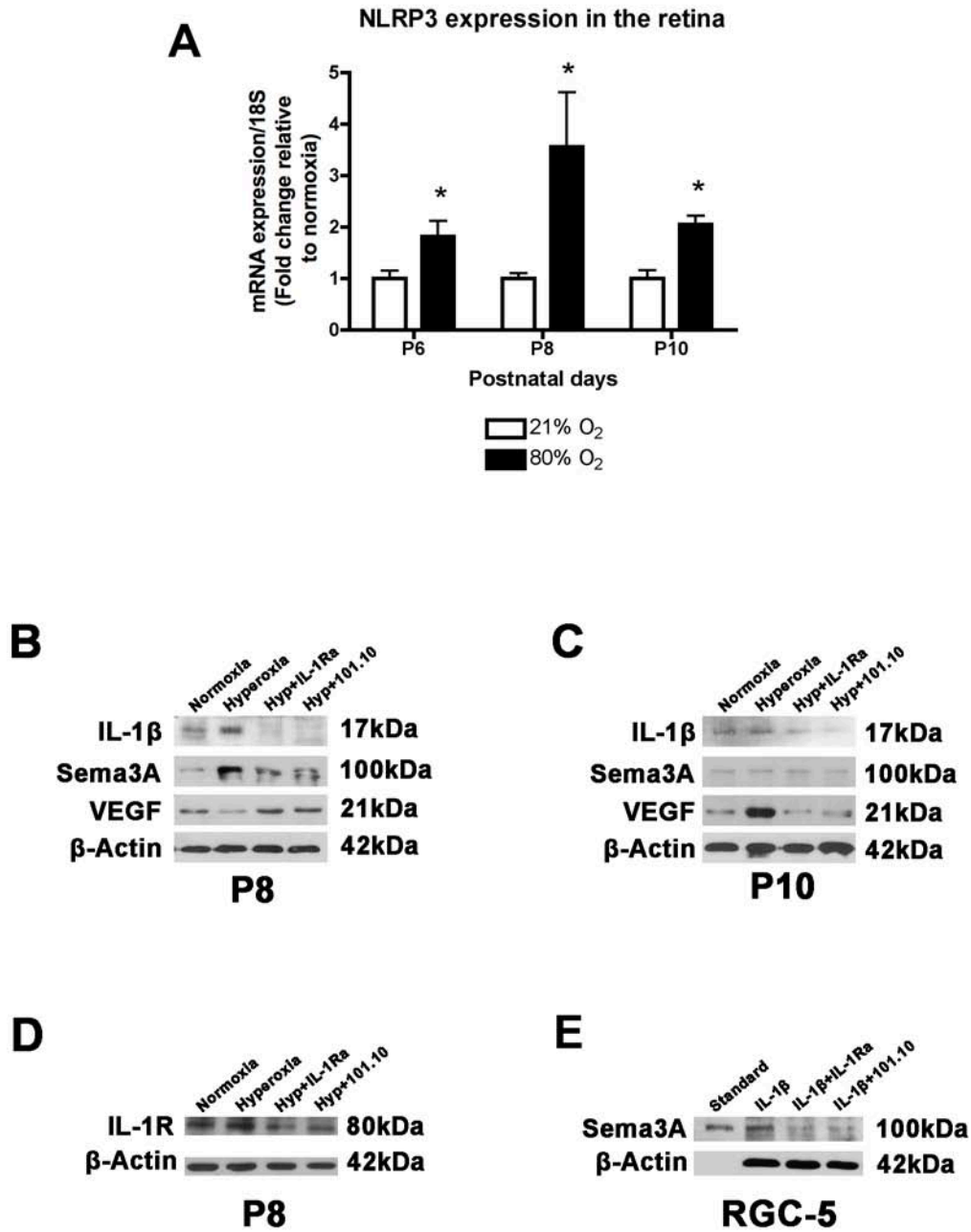
C) Pull down assay and Western blot analysis performed by F Binet

Figure preparation: F Binet, JS Joyal, **N Sitaras**, P Sapieha and S Chemtob

Approximate Figure contribution: 20%

## Appendix 2

Supplementary Figures for Rivera JC, Sitaras N et al. *Arterioscler Thromb Vasc Biol* 2013



**Supplemental Figure 1. NLRP3 inflammasome expression in the retina and protein detection of different mediators induced by hyperoxia.** Measurement by quantitative PCR of the mRNA expression of NLRP3 inflammasome in retinas (n=3) from rat pups exposed to normoxia (21% O<sub>2</sub>) or hyperoxia (80% O<sub>2</sub>) during 1, 3 and 5 days (**A**). \*p<0.01 vs 21% O<sub>2</sub>. Representative Western blots showing IL-1 $\beta$  (17 kD), Sema3A ( $\approx$ 95 kDa) and VEGF (21 kDa) immunoreactive bands in retinal homogenates at P8 (**B**) or P10 (**C**) after normoxic (21% O<sub>2</sub>; as control) or hyperoxic (80% O<sub>2</sub>) exposure treated with vehicle, IL-1Ra or 101.10. Expression of IL-1R (80 kDa) was increased by hyperoxia and suppressed by both IL-1R antagonists (**D**). RGC-5 cells treated with IL-1 $\beta$  (0.5 ng/ml) for 24 h and evaluated by Western blot in cell lysate showed increased Sema3A expression that was suppressed with IL-1Ra or 101.10 (**E**). In all the cases  $\beta$ -actin (42 kDa) was used as internal control.

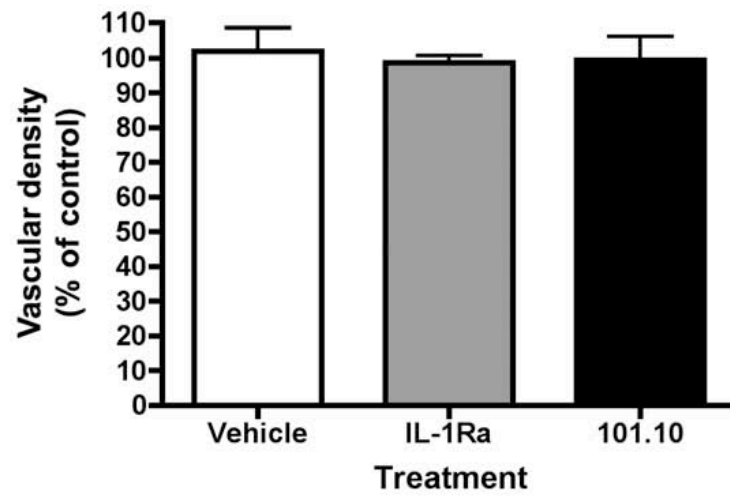
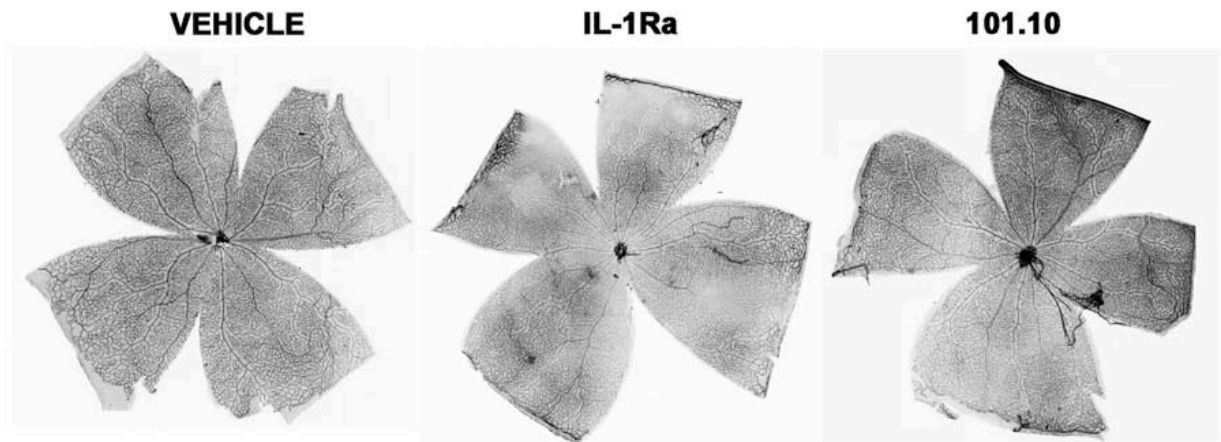
**Relative contributions: Suppl Figure 1**

- A) Sample preparation and qPCR analysis performed by **N Sitaras**, JC Rivera and B Noueihed
- B) through E) Sample preparation and Western blot analysis performed by JC Rivera, B Noueihed and A Madaan

Animal handling and sample collection: JC Rivera and **N Sitaras**

Figure preparation: JC Rivera, **N Sitaras**, B Noueihed and S Chemtob

Approximate Figure contribution: 20%



**Supplemental Figure 2. Administration of IL-1 antagonists does not affect normal retinal vascularization.** Representative lectin-stained retinal micrographs showing vascularisation, and vascular density histogram of animals treated with intraperitoneally with vehicle, IL-1Ra or 101.10 from P5 to P14 (sacrifice). Data are the mean  $\pm$  SEM for n=3 independent experiments.

**Relative contributions: Suppl Figure 2**

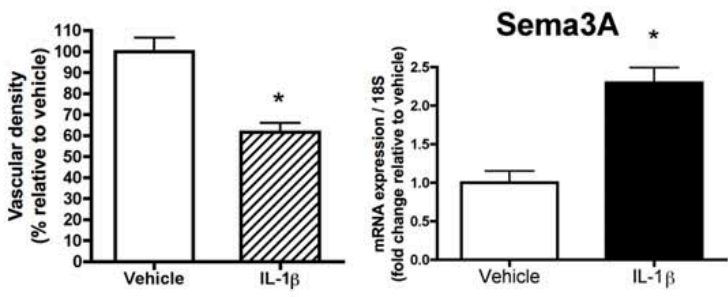
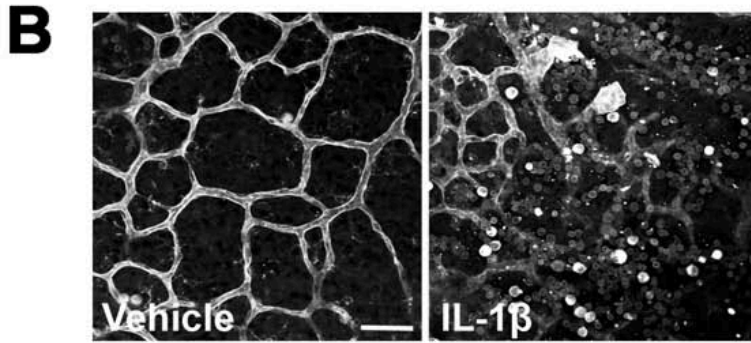
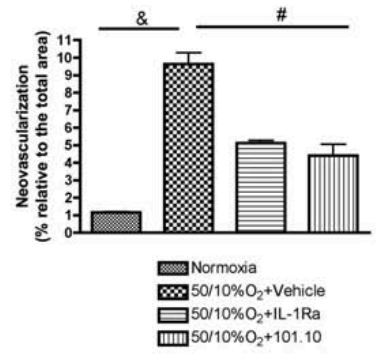
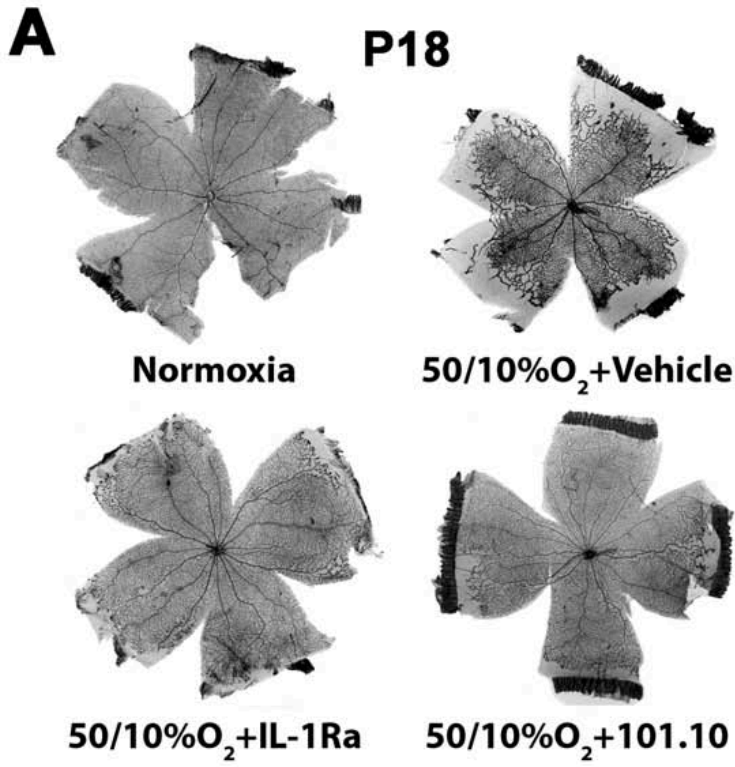
Drug administration performed by JC Rivera, **N Sitaras** and JC Honoré

Imaging and analysis performed by JC Rivera and **N Sitaras**

Animal handling and sample collection: JC Rivera

Figure preparation: JC Rivera and S Chemtob

Approximate Figure contribution: <10%



**Supplemental Figure 3. IL-1R inhibitors prevent pre-retinal neovascularization, and intravitreal IL-1 $\beta$  increases Sema3A expression and causes retinal microvascular injury.** Representative lectin-stained retinal flat mounts (showing vascularity) at P18 (A) and compiled histograms of percent neovascularization. Intraperitoneal administration of IL-1Ra or 101.10 from P0-P14 prevented pre-retinal neovascularization . Data are the mean  $\pm$  SEM for n=3 independent experiments.  $\&p<0.001$  vs normoxia,  $\#p<0.01$  vs OIR + vehicle. **(B)** Lectin-stained retinal photomicrographs in animals treated with intravitreal IL-1 $\beta$  (5ng/1 $\mu$ l) or vehicle (PBS). Below representative micrographs are the compiled histograms of vascular density and Sema3A mRNA expression. \*  $p<0.01$  vs vehicle. Scale bar = 50  $\mu$ m.

### **Relative contributions: Suppl Figure 3**

Drug administration performed by JC Rivera, **N Sitaras** and JC Honoré

A) Immunohistochemistry, imaging and analysis performed by JC Rivera

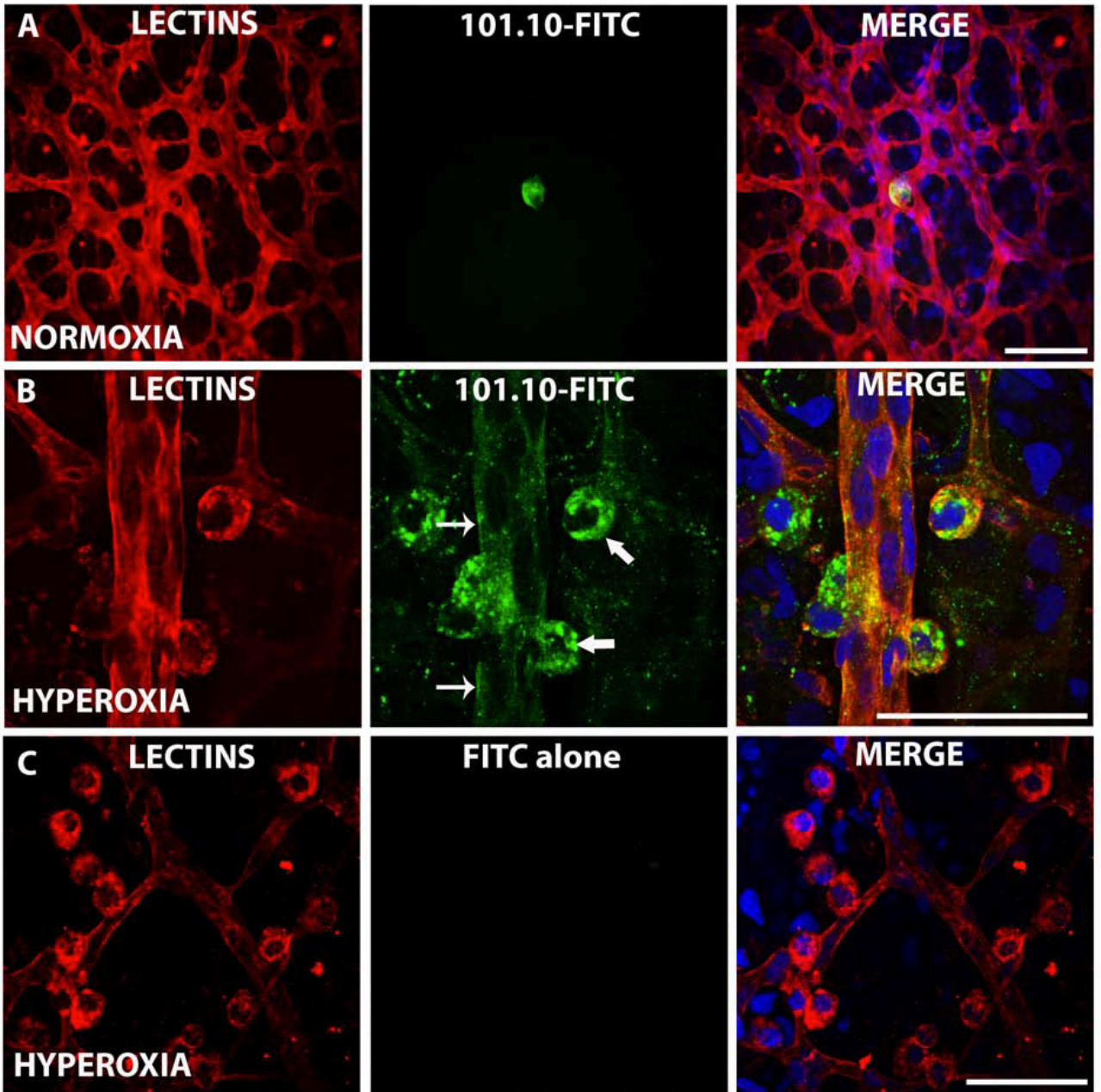
B) Immunohistochemistry, imaging and analysis performed by JC Rivera

qPCR analysis performed by **N Sitaras**

Animal handling and sample collection: JC Rivera

Figure preparation: JC Rivera and S Chemtob

Approximate Figure contribution: 10%



**Supplemental Figure 4. The peptide 101.10 (*rytvela*) is mostly distributed in the retina in microglia and endothelial cells during hyperoxia.** Peptide 101.10 was conjugated to FITC (green) and injected intraperitoneally in animals (at P5) exposed to normoxia (**A**) or hyperoxia (**B**); FITC alone was used as a negative control (**C**). Fluorescence was analyzed 3-6 hours after peptide administration by confocal microscopy in retinal flat-mounts stained with lectin (red). Primarily upon exposure to hyperoxia (80% O<sub>2</sub>), 101.10-FITC co-localized with lectin (yellow), corresponding to microglial (thick arrows) and endothelial (thin arrows) cells. Nuclei were counter-stained with DAPI (blue). Scale bars = 50µm.

**Relative contributions: Suppl Figure 4**

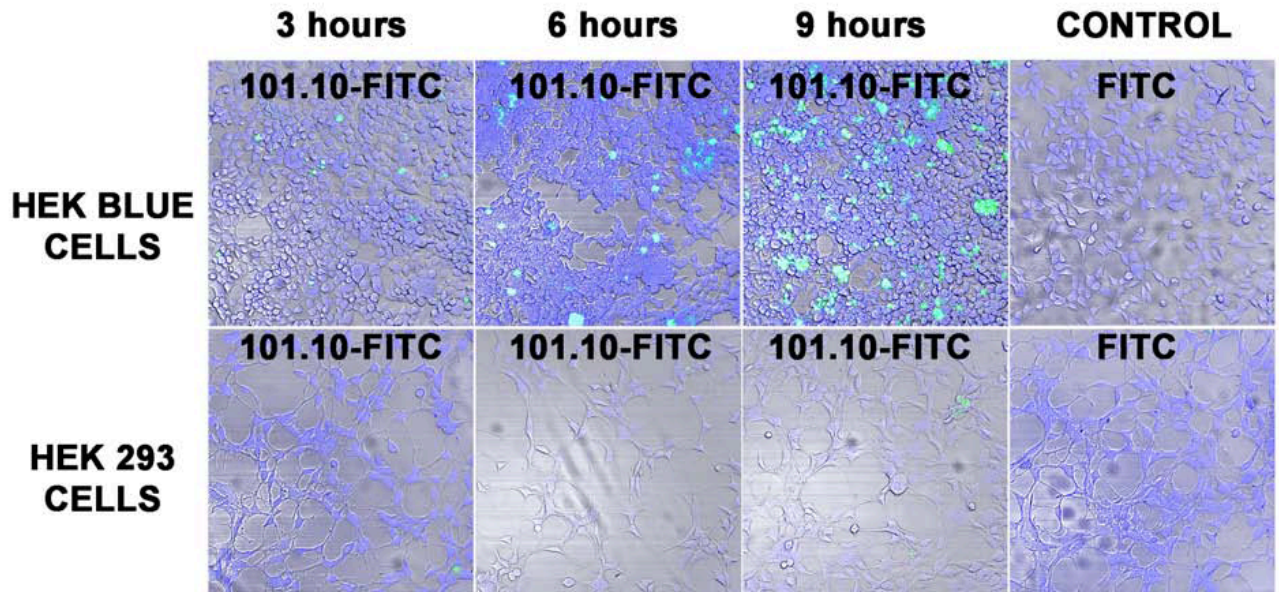
Drug administration performed by JC Rivera, **N Sitaras** and JC Honoré

Imaging and analysis performed by JC Rivera and **N Sitaras**

Animal handling and sample collection: JC Rivera

Figure preparation: JC Rivera and S Chemtob

Approximate Figure contribution: <10%



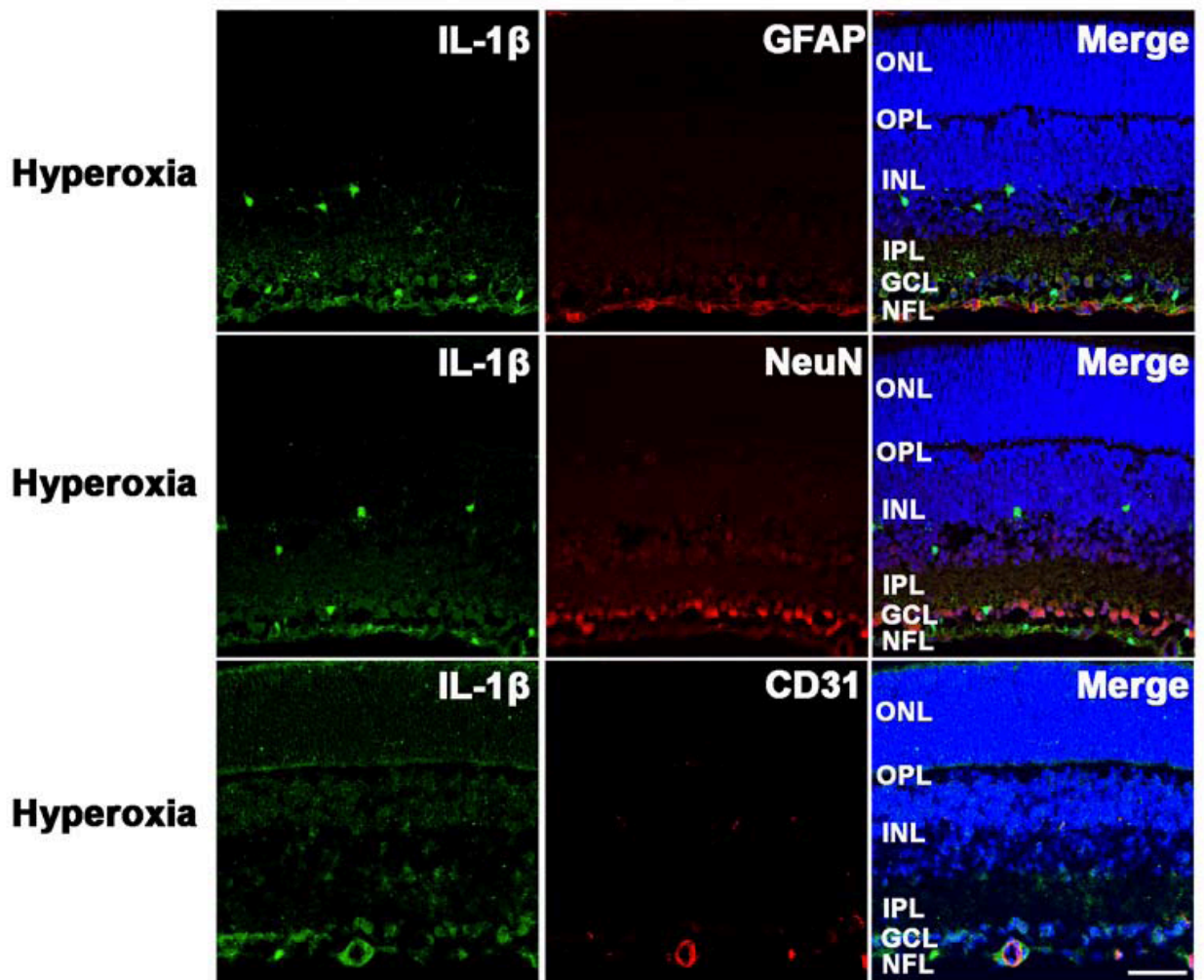
**Supplemental Figure 5. Cellular internalization of 101.10 is dependent on the presence of the IL-1R.** Internalization of 101.10-FITC in HEK blue cells (expressing IL-1R) was increased time-dependently at 3, 6 and 9 hours after stimulation with IL-1 $\beta$ ; HEK 293 cells (devoid of IL-1R) do not internalize IL-1R. FITC alone was used as control (n=3-4 per group).

**Relative contributions: Suppl Figure 5**

In vitro preparations, immunocytochemistry and analysis performed by JC Rivera and C Quiniou

Figure preparation: JC Rivera, C Quiniou and S Chemtob

Approximate Figure contribution: 0%



**Supplemental Figure 6. IL-1 $\beta$  is minimally produced by astrocytes, neurons and endothelium during hyperoxia.** Representative confocal images showing immunoreactivity to IL-1 $\beta$  (green), GFAP, NeuN, CD31 (red), merged with DAPI (blue and yellow) in retinal cryosections (n=3) from 8-day-old rats after 3 days of hyperoxia (80% O<sub>2</sub>). A slight colocalization of IL-1 $\beta$  with CD31 (endothelial marker) was detected. Scale bar = 50  $\mu$ m.

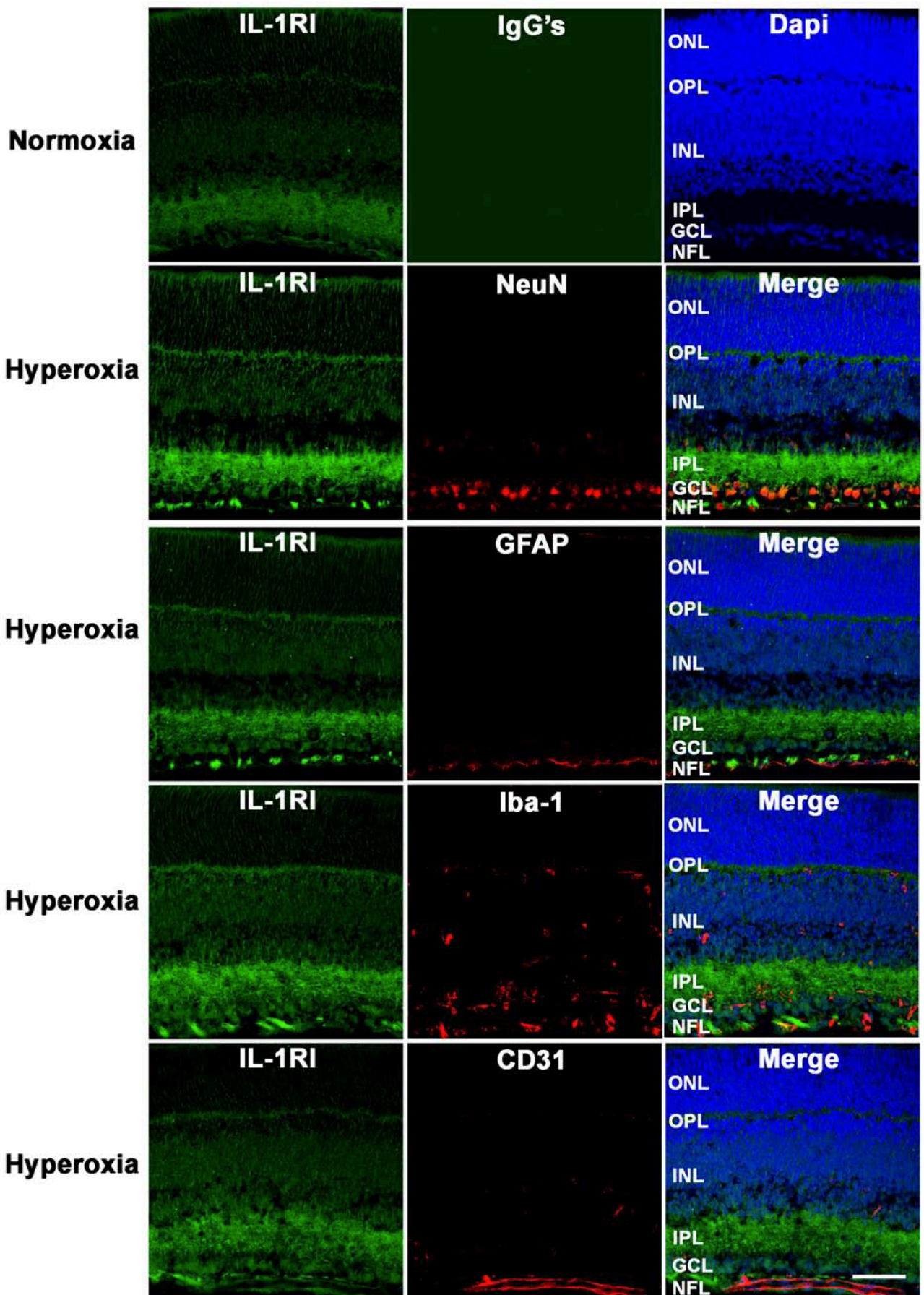
**Relative contributions: Suppl Figure 6**

Imaging and analysis performed by JC Rivera and **N Sitaras**

Animal handling and sample collection: JC Rivera and **N Sitaras**

Figure preparation: JC Rivera and S Chemtob

Approximate Figure contribution: 20%



**Supplemental Figure 7. Localization of IL-1R in the retina.** Representative confocal images from 3 experiments showing the immunoreactivity to IL-1RI (principally the inner plexiform layer [IPL], in green), IgG's (Control) and DAPI in retinal cryosections from 8-day-old rats exposed for 3 days to normoxia or hyperoxia (80% O<sub>2</sub>). IL-1RI immunoreactivity was increased by hyperoxia and mainly detected on neurons (NeuN) in the ganglion cell layer (GCL), and very slightly in microglia (Iba-1) and vessels (CD31), but not in astrocytes (GFAP). Scale bar = 50  $\mu$ m.

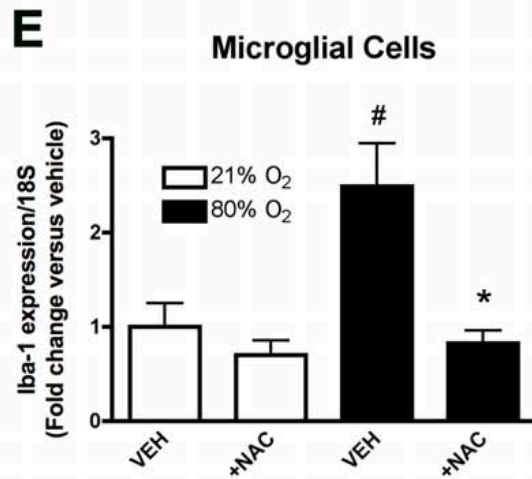
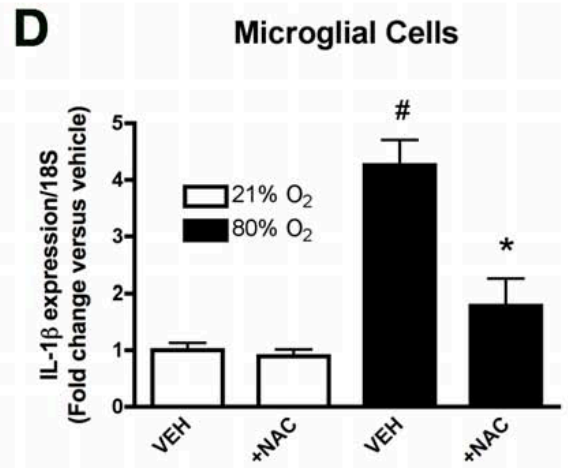
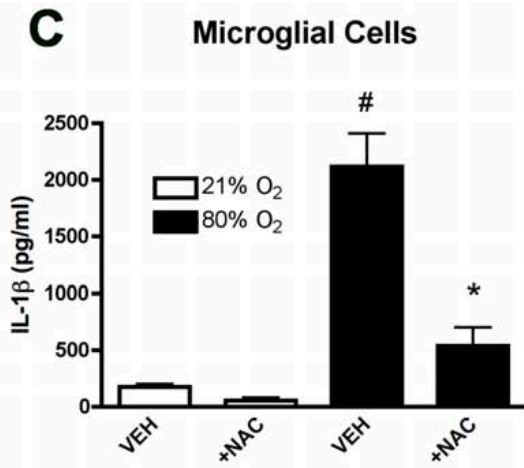
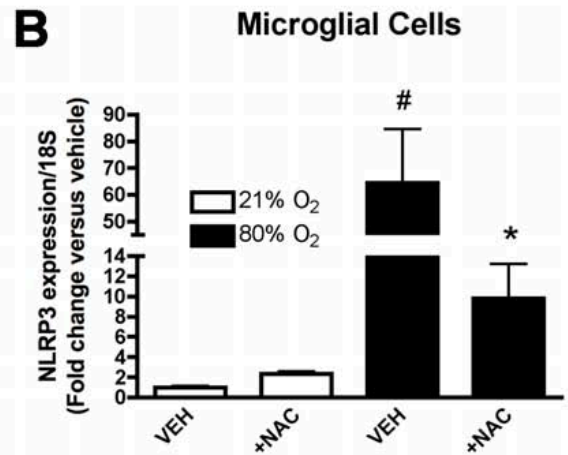
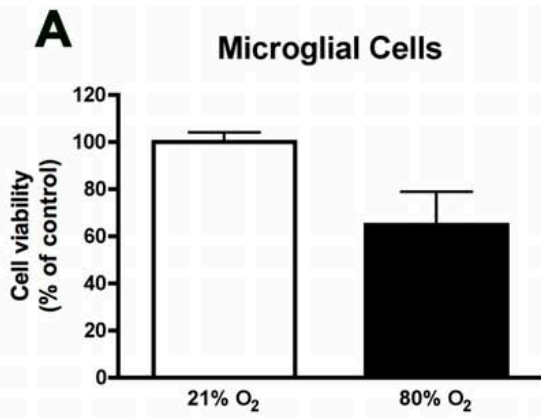
**Relative contributions: Suppl Figure 7**

Imaging and analysis performed by JC Rivera and **N Sitaras**

Animal handling and sample collection: JC Rivera and **N Sitaras**

Figure preparation: JC Rivera and S Chemtob

Approximate Figure contribution: 20%



**Supplemental Figure 8. NLRP3 inflammasome, IL-1 $\beta$  and Iba-1 expression in microglia cultures are increased during hyperoxia.** Measurement by quantitative PCR of the mRNA expression of NLRP3 (**B**), IL-1 $\beta$  (**C**), Iba-1 (**F**) and IL-1 $\beta$  secretion measured by ELISA (**D**) or cell viability evaluated by MTT assay (**E**) in primary microglial cultures exposed to hyperoxia (80% O<sub>2</sub>) or normoxia (21% O<sub>2</sub>) in presence or absence of *N*-acetylcysteine (NAC; 8mM). Data are the mean  $\pm$  SEM for n=4-5 independent experiments. #\*p<0.01 versus 21% O<sub>2</sub>.

**Relative contributions: Suppl Figure 8**

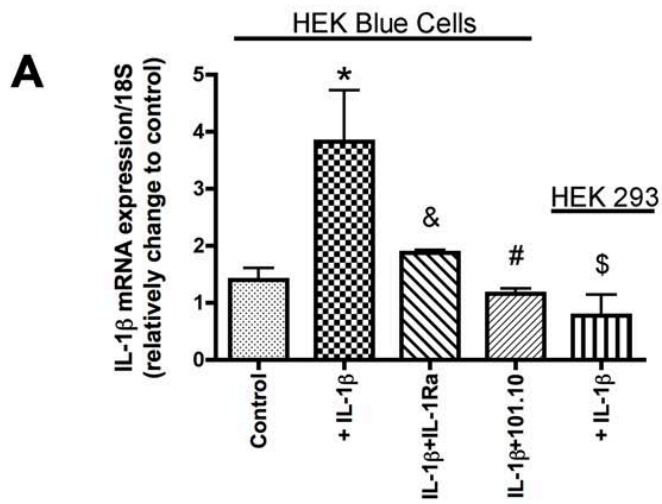
In vitro preparations performed by JC Rivera and N Sitaras

- A) Microglial cell viability assay performed by JC Rivera
- B) D) and E) qPCR performed by **N Sitaras** and B Noueihed
- C) ELISA performed by JC Rivera

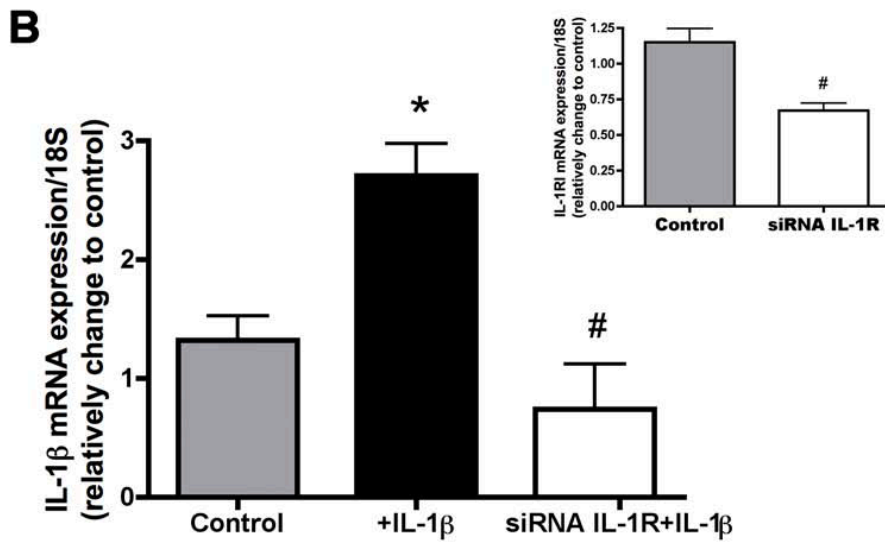
Animal handling and sample collection: JC Rivera and **N Sitaras**

Figure preparation: JC Rivera, **N Sitaras**, B Noueihed and S Chemtob

Approximate Figure contribution: 40%



**RAW BLUE MOUSE MACROPHAGES**



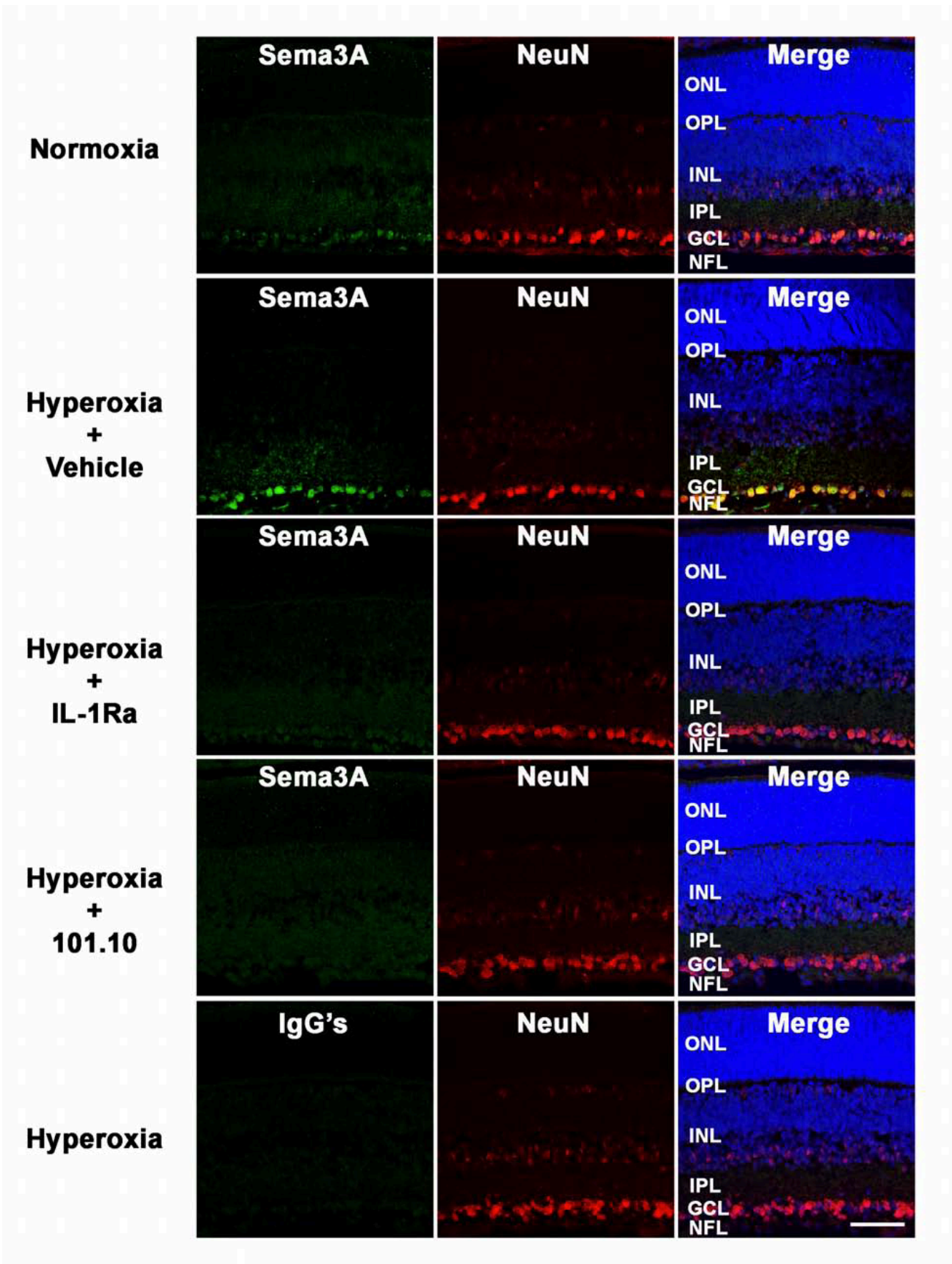
**Supplemental Figure 9. Autostimulation of IL-1 $\beta$  in HEK blue cells and macrophages.** (A) Exogenous IL-1 $\beta$  (50 ng/ml; 4 h) induced IL-1 $\beta$  mRNA expression (qPCR) in HEK blue cells (containing IL-1R) but not in HEK 293 cells devoid of IL-1R; induction was prevented by IL-1Ra and 101.10. Histogram values are mean  $\pm$  SD of three independent experiments. \* p<0.05 vs Control, &##\* p<0.05 vs IL-1 $\beta$  treatment. (B) Exogenous IL-1 $\beta$  (50 ng/ml; 4 h) induced IL-1 $\beta$  mRNA expression (qPCR) in RAW-Blue mouse macrophages; silencing of IL-1RI (siRNA-IL-1RI [see insert]) prevented this induction. Histogram values are mean  $\pm$  SD of three independent experiments. # p<0.05 vs Control.

**Relative contributions: Suppl Figure 9**

A) and B) In vitro preparations, immunocytochemistry and analysis performed by  
JC Rivera and C Quiniou

Figure preparation: JC Rivera, C Quiniou and S Chemtob

Approximate Figure contribution: 0%



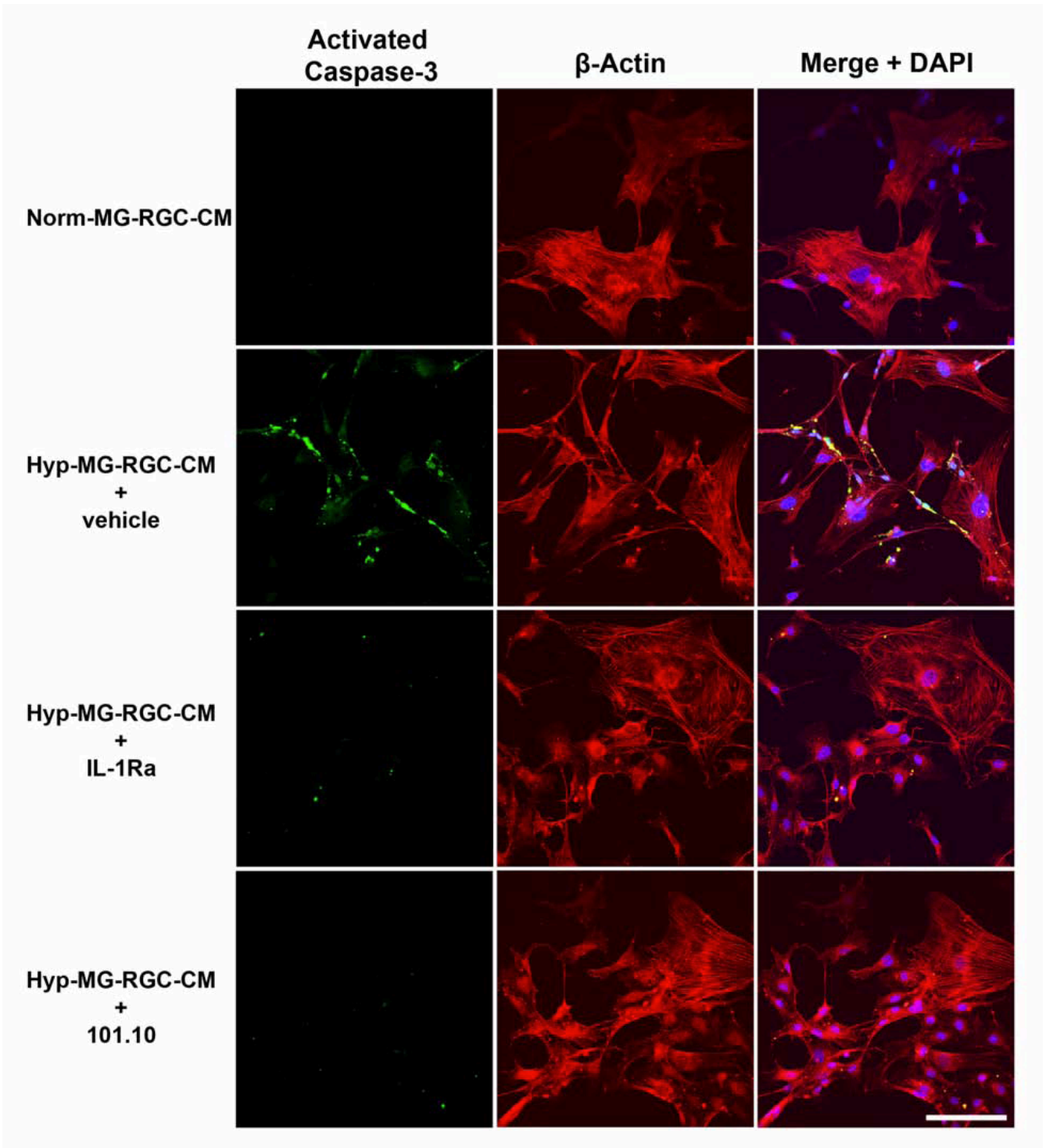
**Supplemental Figure 10. Semaphorin 3A (Sema3A) is largely produced by retinal ganglion cells (RGC) in the retina under hyperoxia.** Representative confocal images showing immunoreactivity of Sema3A (green) and NeuN (red) merged with DAPI (blue) in retinal cryosections (n=3) from 8-day-old rats after 3 days in normoxia (21% O<sub>2</sub>) or hyperoxia (80% O<sub>2</sub>). Co-staining of Sema3A with NeuN (yellow) was detected mainly on retinal ganglion cells (RGC) from hyperoxic pups treated with vehicle. Retinas from hyperoxic rat pups treated with IL-1Ra or 101.10 reveal a decrement in Sema3A staining similar to the normoxic animals in the ganglion cell layer (GCL). Scale bar = 50 μm.

**Relative contributions: Suppl Figure 9**

In vitro preparations, immunocytochemistry and analysis performed by JC Rivera and **N Sitaras**

Figure preparation: JC Rivera, **N Sitaras** and S Chemtob

Approximate Figure contribution: 20%



**Supplemental Figure 11. Conditioned media from retinal ganglion cells (RGC-5) stimulated with hyperoxic-microglia conditioned media (Hyp-MG-RGC-CM) induces activation of caspase-3 on endothelial cells (RBMVEC).** Representative photomicrographs of endothelial cells (n=3) positively labeled with activated caspase-3 polyclonal antibody (green) or  $\beta$ -actin monoclonal antibody (red) on RBMVEC treated for 48 hours with conditioned medium from RGC-5 cells previously stimulated with normoxia-(21% O<sub>2</sub>; Norm-MG-RGC-CM) or hyperoxia-exposed (80% O<sub>2</sub>) microglia media in absence (vehicle; Hyp-MG-RGC-CM) or presence of IL-1Ra or 101.10. Co-localization of activated caspase-3 and  $\beta$ -actin staining was merged with RBMVECs nucleus stained with DAPI (blue). Scale bar = 50 $\mu$ m.

**Relative contributions: Suppl Figure 11**

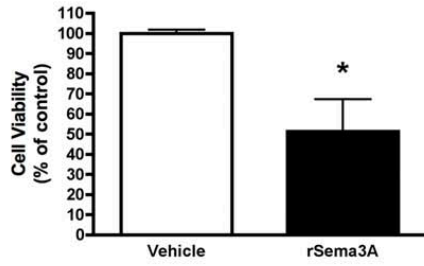
In vitro preparations, immunocytochemistry and analysis performed by JC Rivera

Figure preparation: JC Rivera and S Chemtob

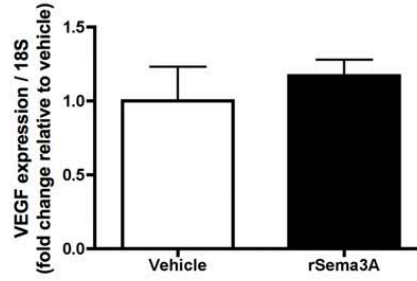
Approximate Figure contribution: 0%

# RBMVEC

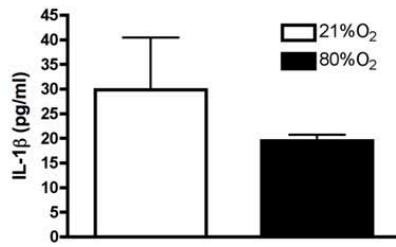
**A**



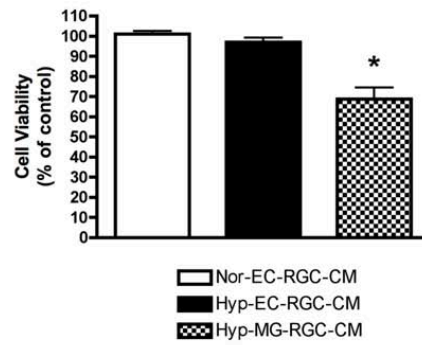
**B**



**C**



**D**



**Supplemental Figure 12. IL-1 $\beta$  released from neuro-microvascular endothelial cells (RBMVEC) exposed to hyperoxia does not induced Sema3A release on RGC-5 cells.** The treatment with recombinant Sema3A (4.5 nM) for 24 hours decreased significantly (48%) the cell viability (evaluated by MTT assay) on RBMVEC cells compared to the control (**A**). \* $p < 0.05$  vs Vehicle. But, the mRNA VEGF levels determined by qPCR did not change with the Sema3A treatment (**B**). IL-1 $\beta$  protein was evaluated by ELISA (**C**) in the media of RBMVEC exposed to 21% or 80% of oxygen levels for 24 hours. IL-1 $\beta$  levels from RBMVEC exposed to hyperoxia does not significantly change compared to control. No changes were observed in cell viability (**D**) evaluated by MTT assay on RBMVEC cells (n=3) treated with conditioned media from RGC-5 previously treated with hyperoxic endothelial cell conditioned media (Hyp-EC-RGC-CM, containing IL-1 $\beta$ ). By contrast, the conditioned media from RGC-5 cells treated with hyperoxic microglial cell conditioned media (Hyp-MG-RGC-CM, containing high levels of IL-1 $\beta$ , used as positive control), increased the expression of the pro-apoptotic Sema3A from cultured RGC and induced a significant decrement (35%;  $p < 0.05$ ) in the endothelial cell viability compared to the control (**D**). \* $p < 0.05$  vs Nor-EC-RGC-CM.

### **Relative contributions: Suppl Figure 11**

In vitro preparations performed by JC Rivera and **N Sitaras**

A) and D) Cell survival assay and analysis performed by JC Rivera and **N Sitaras**

B) qPCR analysis performed by **N Sitaras** and B Noueihed

C) ELISA performed and analyzed by JC Rivera

Figure preparation: JC Rivera, **N Sitaras** and S Chemtob

Approximate Figure contribution: 20%

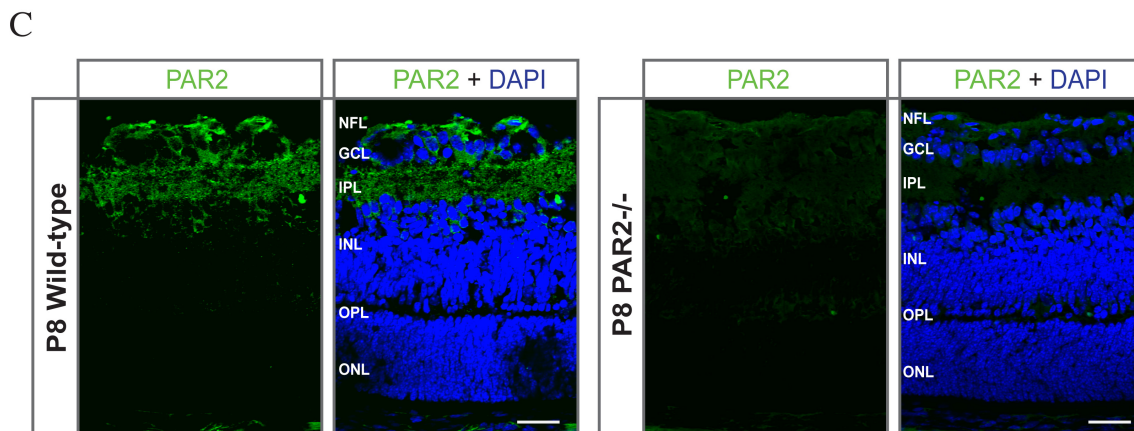
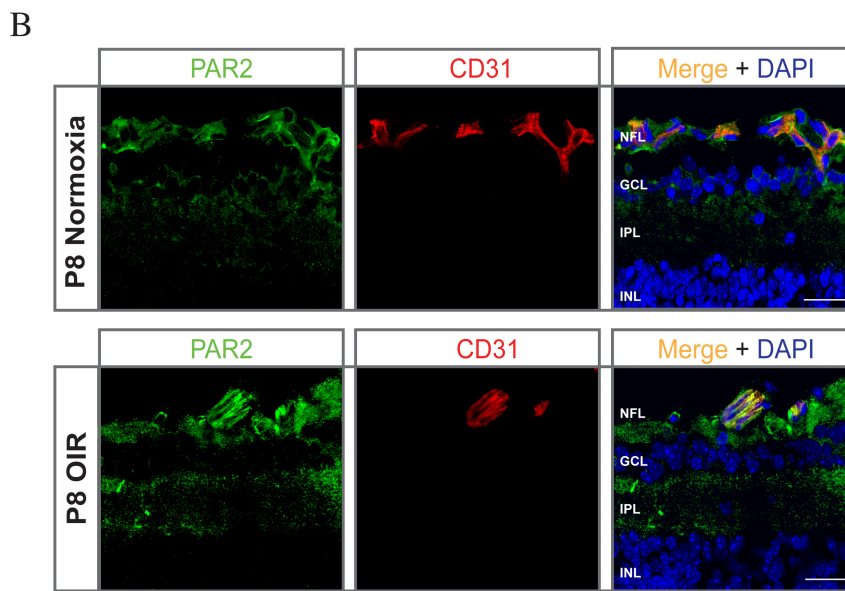
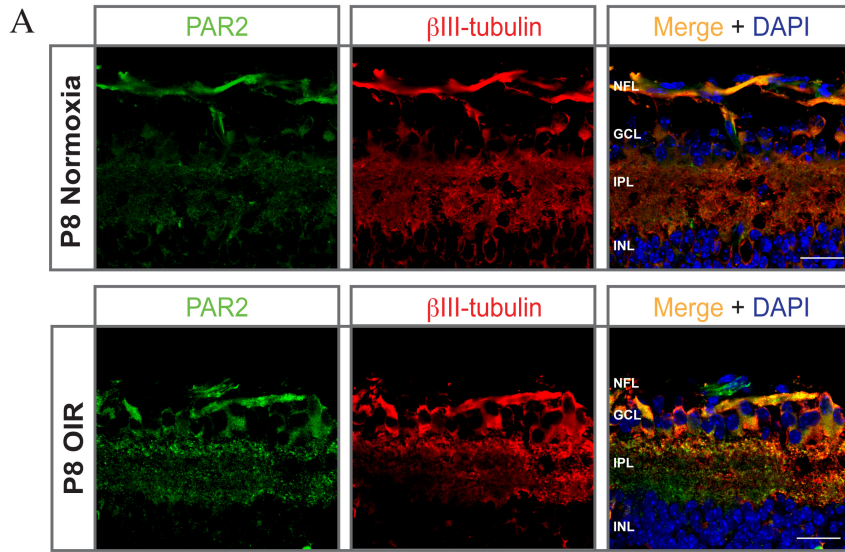
### Appendix 3

Supplementary Figures Sitaras N, et al. Am J Pathol 2014.

**Supplementary Table 1.** Primers used for detecting mRNA expression

Primer	Species	Sequence 5' to 3'	Annealing Temp. (°C)	Primer Conc. (nM)	Amplicon Size (bp)
<b>PAR2 Fwd</b> <b>PAR2 Rev</b>	Mouse	TGACCACGGTCTTTCTTCCG TCAGGGGGAACCAGATGACA	58.0	<b>500</b>	175
<b>PAR2 Fwd</b> <b>PAR2 Rev</b>	Rat	TGGGAGGTATCACCCCTTCTG GGGGAACCAGATGACAGAGA	58.0	<b>500</b>	350
<b>IL-1<math>\beta</math> Fwd</b> <b>IL-1<math>\beta</math> Rev</b>	Mouse	CTGGTACATCAGCACCTCACA GAGCTCCTTAACATGCCCTG	58.0	<b>500</b>	155
<b>IL-1RI Fwd</b> <b>IL-1RI Rev</b>	Mouse & Rat	TGAATGTGGCTGAAGAGCAC CGTGACGTTGCAGACAGTT	58.0	<b>500</b>	235
<b>Sema3A Fwd</b> <b>Sema3A Rev</b>	Mouse	GCTCCTGCTCCGTAGCCTGC TCGGCGTTGCTTTCGGTCCC	58.0	<b>500</b>	304
<b>VEGF-A Fwd</b> <b>VEGF-A Rev</b>	Mouse	GCCCTGAGTCAAGAGGACAG CTCCTAGGCCCTCAGAAGT	58.0	<b>500</b>	215
<b>Cyclophilin A Fwd</b> <b>Cyclophilin A Rev</b>	Mouse	CAGACGCCACTGTCGCTTT	58.0	<b>500</b>	133
<b><math>\beta</math>III-tubulin Fwd</b> <b><math>\beta</math>III-tubulin Rev</b>	Mouse	TAGACCCAGCGGCAACTAT GTTCCAGGTTCCAAGTCCACC	58.0	<b>500</b>	127
<b>CD-31 Fwd</b> <b>CD-31 Rev</b>	Mouse	ACCGGGTGCTGTTCTATAAGG TCACCTCGTACTCAATCGTGG	58.0	<b>500</b>	165
<b>Thy1.1 Fwd</b> <b>Thy1.1 Rev</b>	Mouse	TGCTCTCAGTCTTGCAGGTG TGGATGGAGTTATCCTTGGTGT	58.0	<b>500</b>	121
<b>Rhodopsin Fwd</b> <b>Rhodopsin Rev</b>	Mouse	TCATGGTCTTCGGAGGATTCAC TCACCTCCAAGTGTGGCAAAG	58.0	<b>500</b>	112

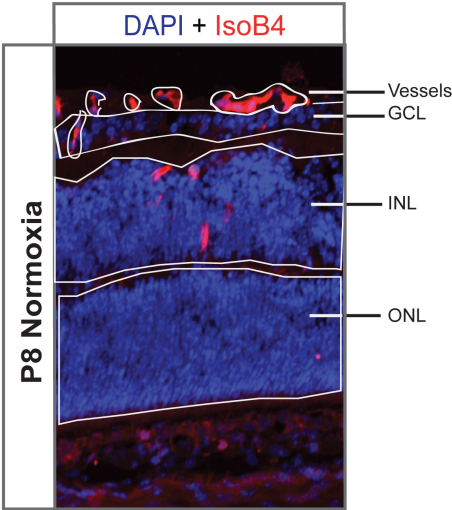
**Supplementary Figure 1.**



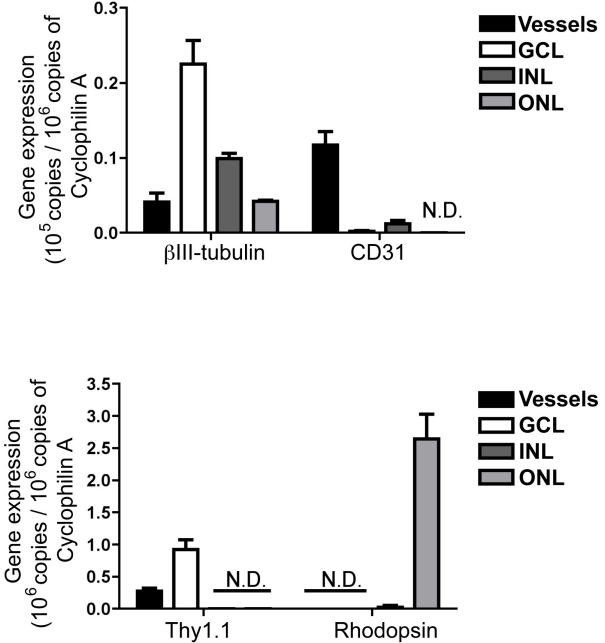
**Supplementary Figure 1. PAR2 expression in neural retina.** (A) High magnification immunohistochemical images of sagittal sections from P8 C57BL/6 mice showing colocalization of PAR2 (green) in  $\beta$ III-tubulin-positive RGCs (red). (B) PAR2 (green) also colocalizes with endothelial cells (CD31; red) albeit to a lesser extent. Nuclei are counterstained with DAPI (blue). NFL, nerve fiber layer; GCL, ganglion cell layer; IPL, inner plexiform layer; INL; inner nuclear layer. Scale bar = 30  $\mu$ m; original magnification 600x. (C) Comparison of wild-type and PAR2 null P8 mice retina stained with SAM11 antibody. PAR2<sup>-/-</sup> mice are devoid of immunofluorescent signal using SAM11 antibody.

Supplementary Figure 2.

A



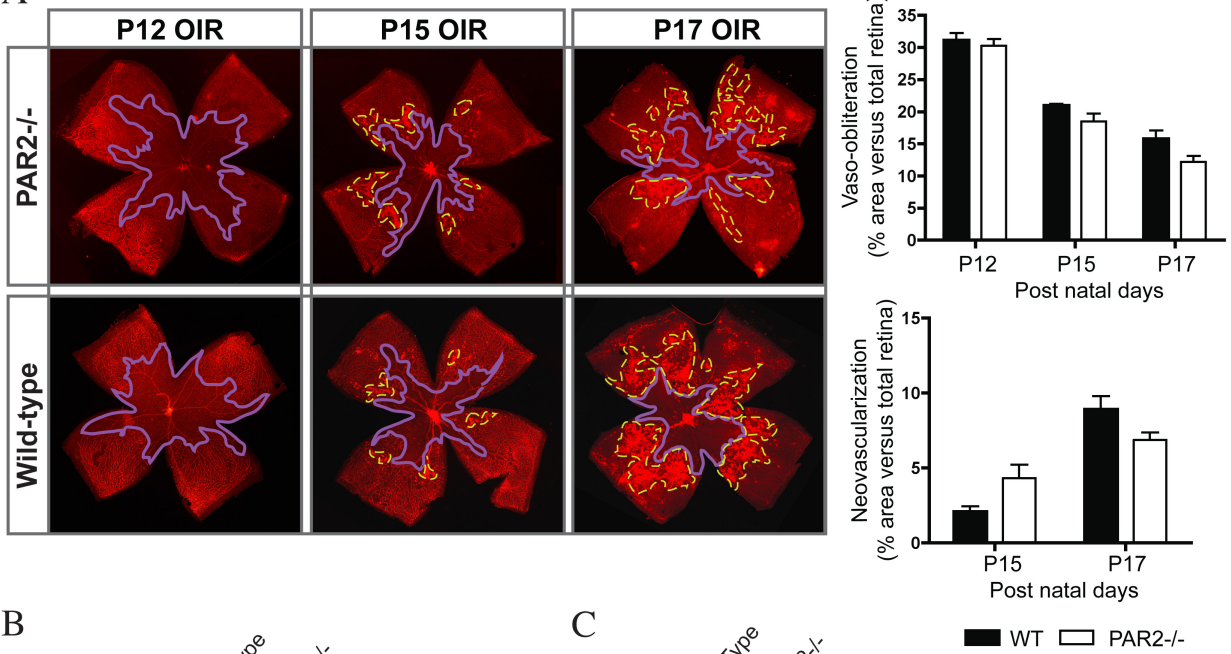
B



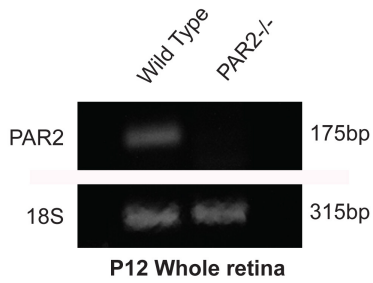
**Supplementary Figure 2. Laser capture microdissection on sagittal P8 mouse retina.** (A) Cross sectional image of a P8 mouse retina depicting the delineated areas captured using laser-capture microdissection. Vessels are stained with lectin (red) while nuclei are counterstained with DAPI (blue). NFL, nerve fiber layer; GCL, ganglion cell layer; INL; inner nuclear layer; ONL, outer nuclear layer. Scale bar = 50  $\mu\text{m}$ ; original magnification 300x (B) Expression profile of laser dissected retinal layers probed for cell markers CD31 (vessels), Thy1.1 (GCL),  $\beta$ III-tubulin (GCL & INL) and Rhodopsin (ONL).

### Supplementary Figure 3.

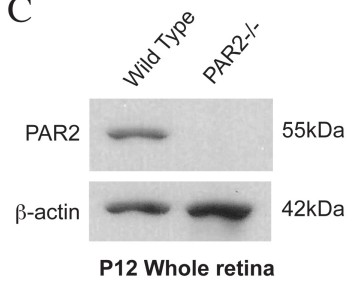
A



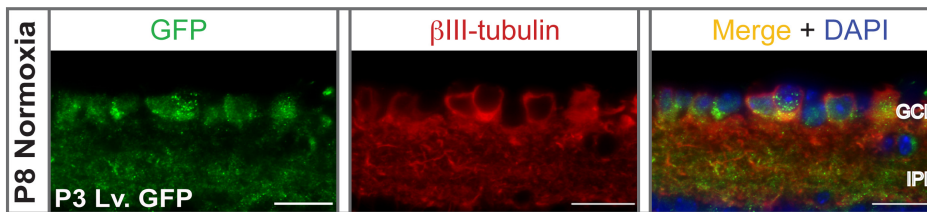
B



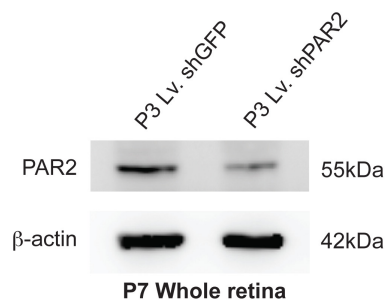
C



D



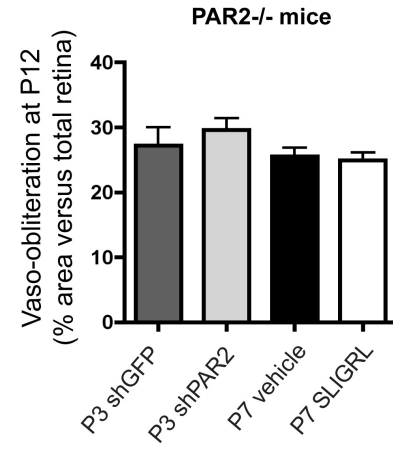
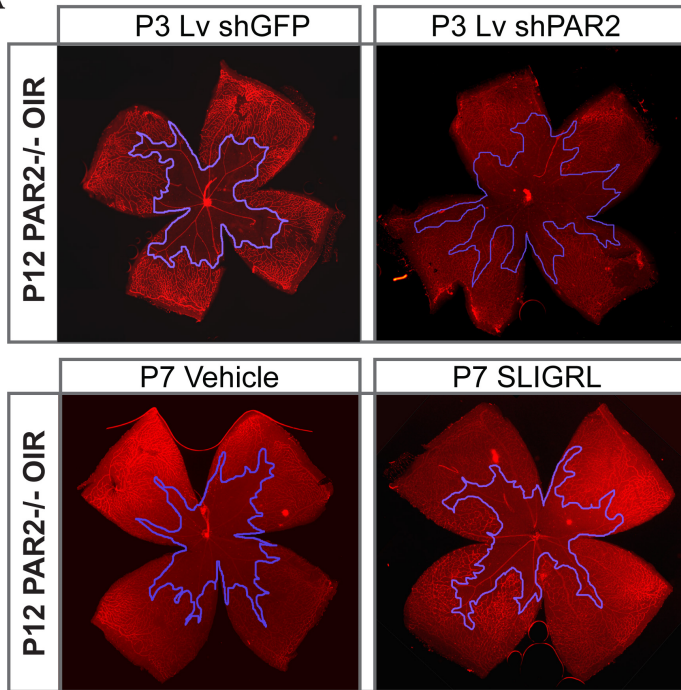
E



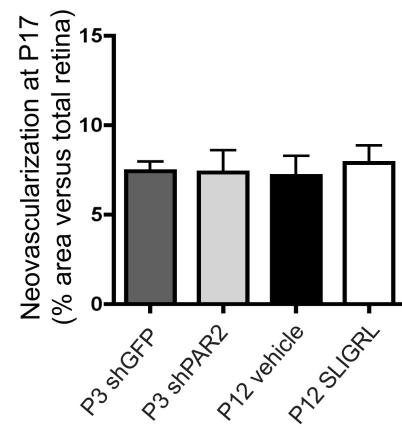
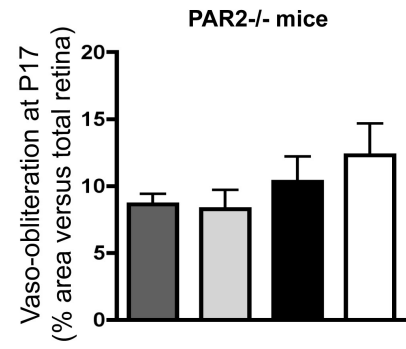
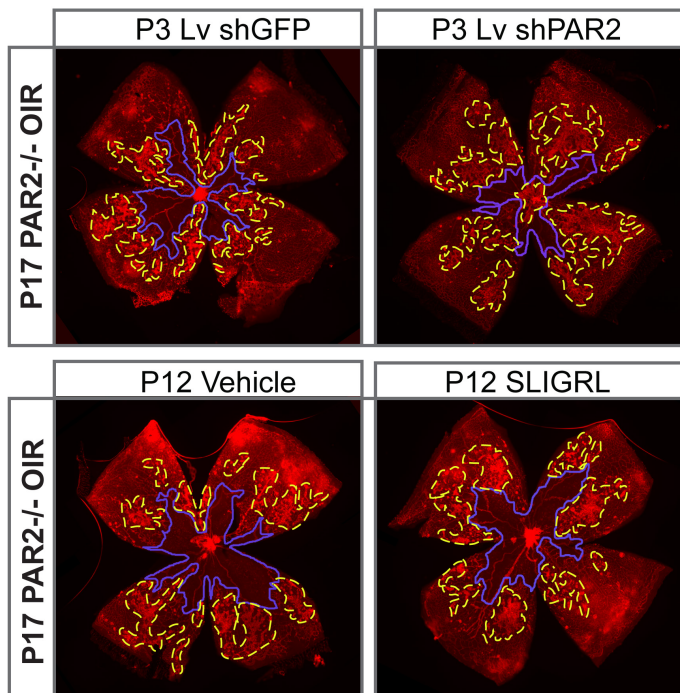
**Supplementary Figure 3. PAR2 intact and transgenic mice share similar vascular phenotypes in OIR; shRNA-bearing Lentiviral constructs target PAR2 in retinal ganglion cells.** (A) Representative flatmounts of isolectin B4-stained retinas from PAR2 intact (Wild-Type C57BL/6) and transgenic (PAR2<sup>-/-</sup>) mice at P12, 15 and P17 previously exposed to hyperoxia from P7 to P12. Original magnification 100x. VO and NV areas are outlined with solid blue lines and yellow-hashed lines, respectively. Avascular areas and neovascularization is shown in right panels; no significant differences were observed between mice populations (n=5-12 retinas). RT-PCR data (B) and Western blot data (C) from P12 PAR2 intact (C57BL/6) and transgenic (PAR2<sup>-/-</sup>) mice retina showing the presence or absence of PAR2 gene and protein, respectively. (D) Immunohistochemical staining showing colocalization of GFP (green) with retinal ganglion cells ( $\beta$ III-tubulin; red) in P8 C57BL/6 mice retina following intravitreal injection (P3) with GFP reporter Lentiviral particles (~15.0 ng). Nuclei are counterstained with DAPI (blue). GCL, ganglion cell layer; IPL, inner plexiform layer. Scale bar = 30  $\mu$ m. Original magnification 600x. (E) Western blot analysis of whole retina from P7 mice demonstrating effective knockdown of PAR2 following intravitreal injection with Lv. shPAR2; contralateral eyes injected with Lv. shGFP served as control (n=2 retinas per group).

# Supplementary Figure 4.

**A**



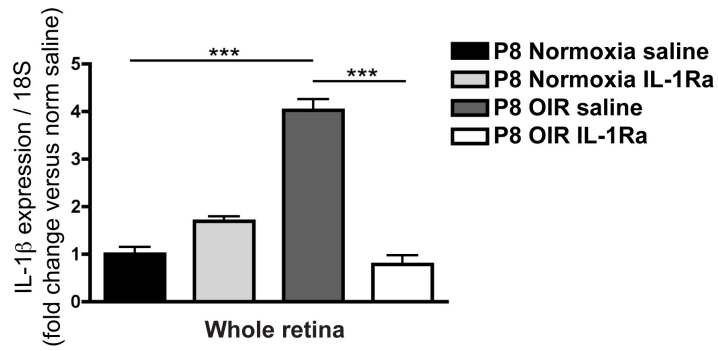
**B**



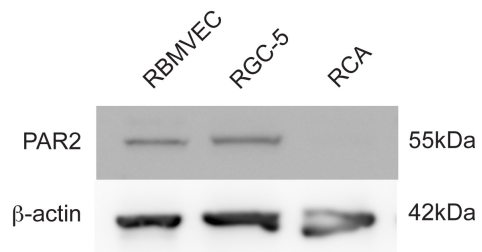
**Supplementary Figure 4. PAR2 transgenic mice do not respond to SLIGRL or Lv. shPAR2 treatment.** (A) Representative flatmounts from isolectin B4-stained P12 PAR2<sup>-/-</sup> exposed to OIR and injected intravitreally at P7 with either vehicle (PBS), SLIGRL (100 μM), Lv. shGFP (~8.5 ng) or Lv. shPAR2 (~9.6 ng) show no change in VO (n=7-9 retinas). (B) Similar effects were observed in P17 PAR2<sup>-/-</sup> OIR mice injected intravitreally at P12 showing no change in VO or NV (n= 7-8 retinas). VO and NV areas are outlined with solid blue lines and yellow-hashed lines, respectively.

## Supplementary Figure 5.

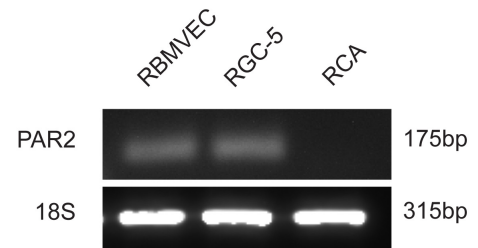
**A**



**B**

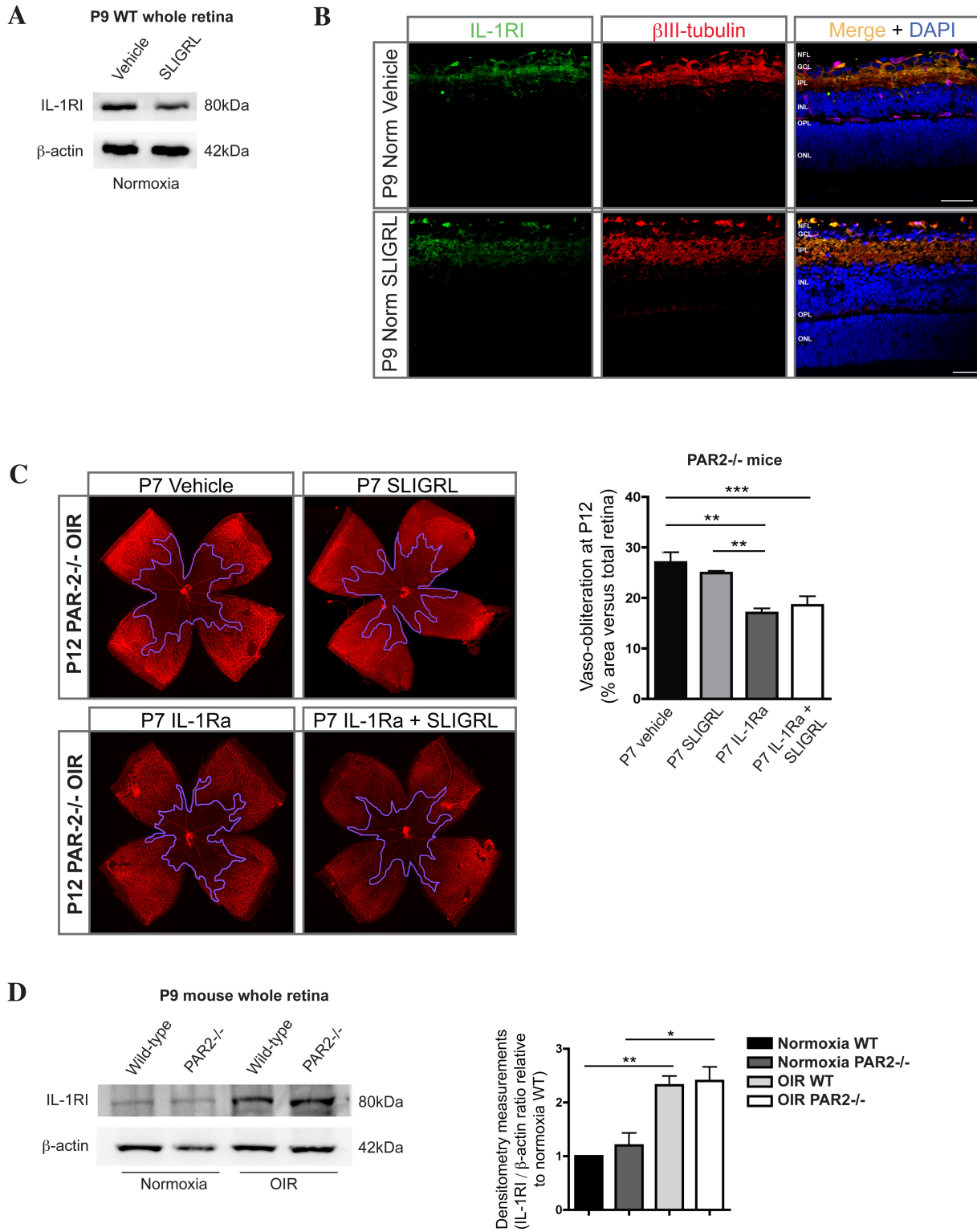


**C**



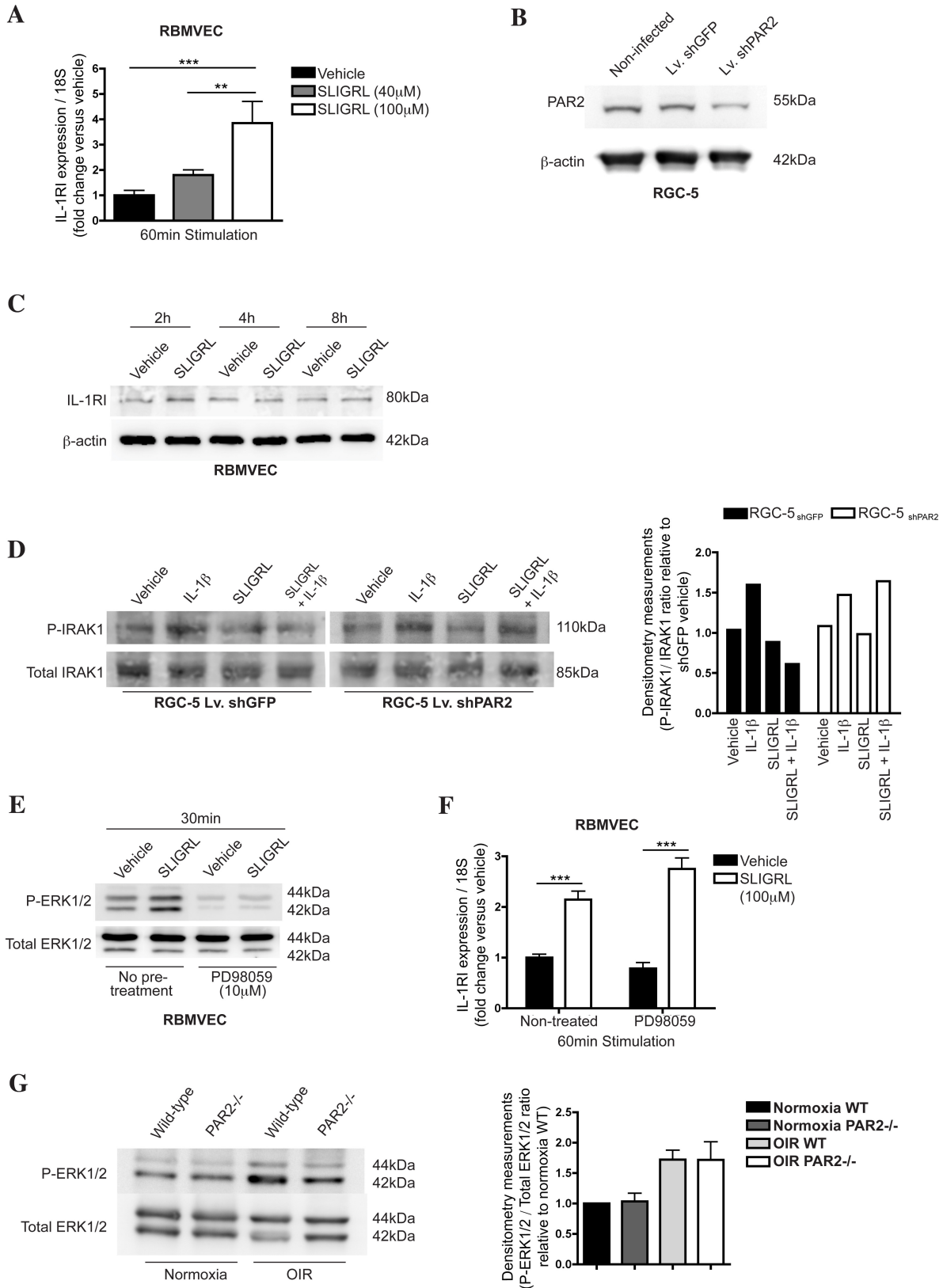
**Supplementary Figure 5. Kineret treatment in vivo successfully dampens IL-1 $\beta$  in whole retina and PAR2 expression in various cell lines.** (A) Intraperitoneal administration of Kineret® translated to decreased IL-1 $\beta$  mRNA in P8 mice whole retina exposed to OIR compared to saline treated animals (\*\*= $p < 0.001$ ; n=2 retinas per group). (B) Cell lysates from RBMVEC, RGC-5 and rat cerebral astrocytes (RCA) immunoblotted with PAR2 SAM11 antibody. RCA devoid of PAR2 show no band at 55kDa. (C) PCR analysis of RBMVEC, RGC-5 and RCA showing PAR2 mRNA expression in these cell lines; PAR2 was not detected in RCA.

### Supplementary Figure 6.



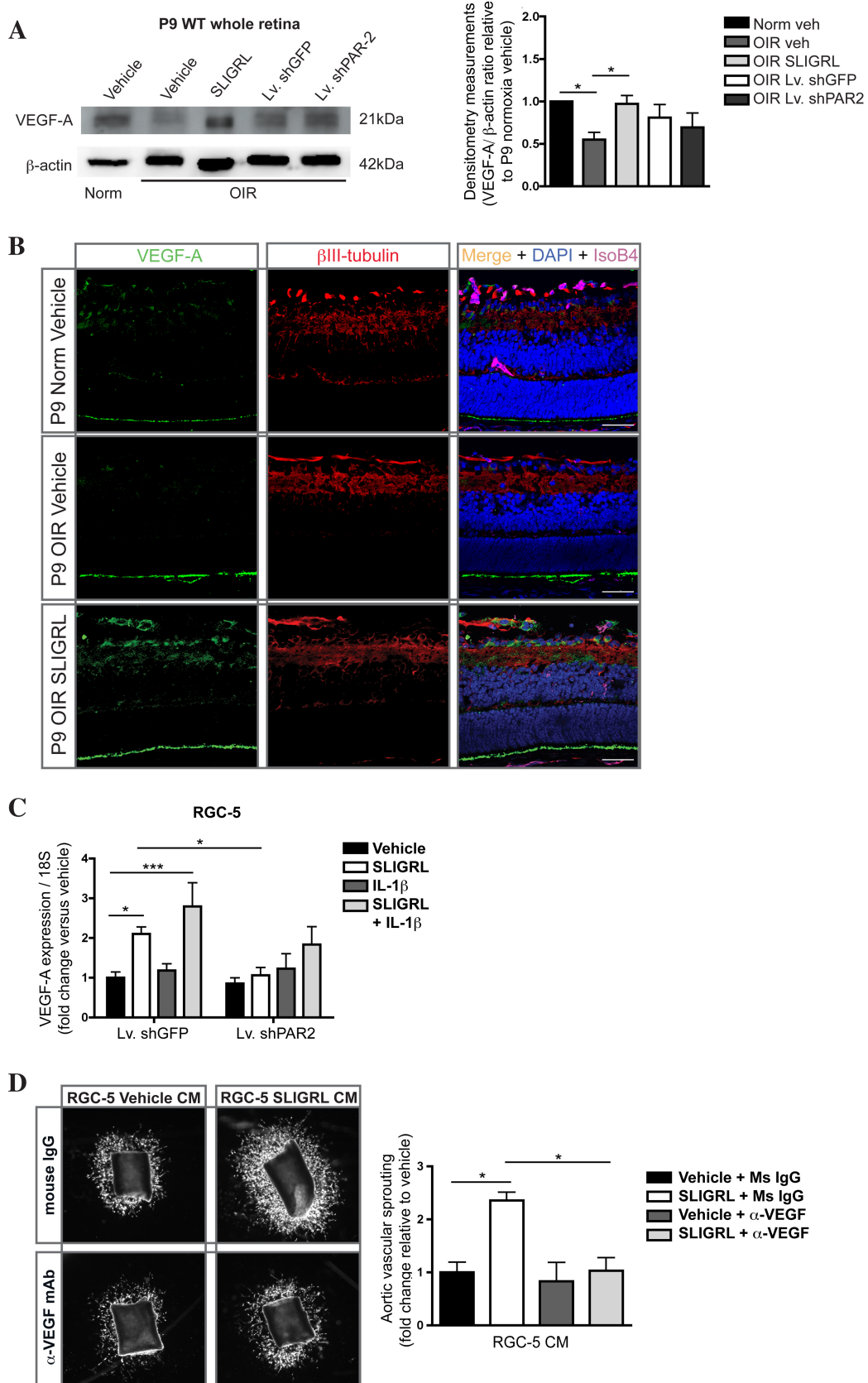
**Supplementary Figure 6. SLIGRL treatment in normoxia raised mice pups; PAR2 transgenic mice respond to IL-1Ra but not to SLIGRL treatment.** (A) Western blot analysis and (B) immunohistochemical analysis of retinas from normoxia raised P9 C57Bl6 injected with vehicle or SLIGRL (contralateral eye) demonstrate slight decreases in IL-1RI levels. IL-1RI stained in green, retinal ganglion cells in red (bIII-tubulin) and nuclei are counterstained in blue. NFL, nerve fiber layer; GCL, ganglion cell layer; IPL, inner plexiform layer; INL; inner nuclear layer; OPL, outer plexiform layer; ONL, outer nuclear layer. Scale bar = 50  $\mu$ m; original magnification 300x. (C) Representative flatmounts from isolectin B4-stained P12 PAR2<sup>-/-</sup> exposed to OIR and injected intravitreally at P7 with either vehicle, SLIGRL (100  $\mu$ M), IL-1Ra (10  $\mu$ M) or both (\*=p<0.05, \*\*\*=p<0.001, n=6-8 retinas). VO areas are outlined with solid blue lines. Original magnification 100x. (D) Western blot analysis of P9 mice retina from WT (C57Bl6) and PAR2<sup>-/-</sup> mice showing an effective increase in IL-1RI upon exposure to OIR; however, there was no variation in IL-1RI levels in PAR2<sup>-/-</sup> compared to WT mice retina. Densitometry quantification at right (\*=p<0.05, \*\*=p<0.01, n=3 independent experiments).

## Supplementary Figure 7.



**Supplementary Figure 7. PAR2-mediated regulation of IL-1RI in RBMVEC; PAR2-induced reduction of IRAK1 phosphorylation in RGC-5.** (A) PAR2-expressing RBMVEC display dose-dependent *increases* in IL-1RI mRNA following 1h stimulation with SLIGRL as analyzed by qPCR (\*= $p < 0.05$ , \*\*= $p < 0.01$ , \*\*\*= $p < 0.001$ ,  $n=8$ ). (B) RGC-5 infected with Lv. shPAR2 demonstrated effective decrease in PAR2 levels; Lv. shGFP-infected RGC-5 served as controls. (C) RBMVEC cells show increased IL-1RI protein levels following SLIGRL stimulation. (D) Control RGC-5 cells pre-treated with SLIGRL successfully abolish IL-1 $\beta$ -dependent IRAK-1 phosphorylation whereas PAR2-deficient RGC-5 do not. (E) RBMVEC cells pre-treated with ERK1/2 inhibitor, PD98059, displayed no increase in SLIGRL-dependent ERK1/2 phosphorylation. (F) ERK1/2 inhibition using PD98059 did not affect SLIGRL-dependent increases in IL-1RI mRNA in RBMVEC (\*\*\*= $p < 0.001$ ,  $n=6$ ). (G) Western blot analysis of P9 mice retina from WT (C57Bl6) and PAR2<sup>-/-</sup> mice showing an effective increase in ERK1/2 phosphorylation upon exposure to OIR; however, there was no variation in phospho-ERK1/2 levels in PAR2<sup>-/-</sup> compared to WT mice retina. Densitometry quantification at right (\*= $p < 0.05$ ,  $n=3$  independent experiments).

### Supplementary Figure 8.



**Supplementary Figure 8. PAR2 stimulates production of VEGF in retinal ganglion cells and promotes VEGF-dependent vascular sprouting.** (A) Western blot analysis demonstrating effective *downregulation* of VEGF in P9 C57BL/6 mice whole retina exposed to OIR. Intravitreal injection of SLIGRL, however, *increased* VEGF levels compared to vehicle treated animals. Densitometry quantification at right (n=3 independent experiments). (B) Immunohistochemical analysis of coronal sections from P9 C57BL/6 mice retina exposed to OIR and injected intravitreally with vehicle or SLIGRL. While hyperoxia treatment *decreased* VEGF immunoreactivity in the retina proper, intravitreal administration of SLIGRL *augmented* VEGF specifically in the GCL. Scale bar = 50  $\mu$ m; original magnification 300x. (C) Control Lv.shGFP-infected RGC-5 treated with SLIGRL but not IL-1 $\beta$  exhibited *increased* VEGF mRNA compared to vehicle controls after 24 h; Lv. shPAR2-infected RGC-5, however, showed no increases in VEGF mRNA following treatment with SLIGRL (\*=p<0.05, \*\*\*=p<0.001, n=8). (D) Aortic explants stimulated with SLIGRL reveal *increased* vascular sprouting; however, treatment with neutralizing antibody to VEGF abrogated SLIGRL-induced aortic sprouting (\*=p<0.05, n=4-5).

## Appendix 4

### Neuronal ER Stress Impedes Myeloid-Cell-Induced Vascular Regeneration through IRE1a Degradation of Netrin-1

Francois Binet,<sup>1</sup> Gaelle Mawambo,<sup>2</sup> Nicholas Sitaras,<sup>1</sup> Nicolas Tetreault,<sup>4</sup> Eric Lapalme,<sup>1</sup> Sandra Favret,<sup>1</sup> Agustin Cerani,<sup>2</sup> Dominique Leboeuf,<sup>3</sup> Sophie Tremblay,<sup>1</sup> Flavio Rezende,<sup>1</sup> Aimee M. Juan,<sup>1</sup> Andreas Stahl,<sup>5</sup> Jean-Sebastien Joyal,<sup>1</sup> Eric Milot,<sup>2</sup> Randal J. Kaufman,<sup>6</sup> Martin Guimond,<sup>3</sup> Timothy E. Kennedy,<sup>4</sup> and Przemyslaw Sapieha<sup>1,2,4,\*</sup>

<sup>1</sup>Department of Ophthalmology

<sup>2</sup>Department of Biochemistry

<sup>3</sup>Department of Immunology Maisonneuve-Rosemont Hospital Research Centre, University of Montreal, Montreal, QC H1T 2M4, Canada

<sup>4</sup>Department of Neurology and Neurosurgery, McGill University, Montreal, QC H3A 2B4, Canada <sup>5</sup>University Eye Hospital Freiburg, Killianstrasse

<sup>5</sup> University Eye Hospital Freiburg, Killianstrasse 5, 79106 Freiburg, Germany

<sup>6</sup> Sanford-Burnham Medical Research Institute, La Jolla, CA 92037, USA

#### *Summary*

In stroke and proliferative retinopathy, despite hypoxia driven angiogenesis, delayed revascularization of ischemic tissue aggravates the loss of neuronal function. What hinders vascular regrowth in the ischemic central nervous system remains largely unknown. Using the ischemic retina as a model of neurovascular interaction in the CNS, we provide evidence that the failure of reparative angiogenesis is temporally and spatially associated with endoplasmic reticulum (ER) stress. The canonical ER stress pathways of protein kinase RNA-like ER kinase (PERK) and inositol-requiring

enzyme-1a (IRE1a) are activated within hypoxic/ischemic retinal ganglion neurons, initiating a cascade that results in angiostatic signals. Our findings demonstrate that the endoribonuclease IRE1a degrades the classical guidance cue netrin-1. This neuron-derived cue triggers a critical reparative-angiogenic switch in neural macrophage/microglial cells. Degradation of netrin-1, by persistent neuronal ER stress, thereby hinders vascular regeneration. These data identify a neuronal-immune mechanism that directly regulates reparative angiogenesis.

### *Introduction*

Central neurons require a secure metabolic supply to ensure adequate function and transmission of sensory information. The breakdown of vascular beds in ischemic conditions such as stroke and proliferative retinopathies prevents nutrient and oxygen delivery and leads to hypoxic/ischemic events and a constellation of biochemical changes that compromises cellular function (Eichmann and Thomas, 2012; Lo, 2008; Moskowitz et al., 2010; Sapieha, 2012, Sapieha et al., 2010a). While the ensuing hypoxia is a potent stimulator of vascular growth itself (Lange et al., 2011; Ritter et al., 2006; Sapieha et al., 2010a, 2010b), initial attempts to revascularize the ischemic nervous tissue are typically inadequate (Fukushima et al., 2011; Joyal et al., 2011). Promoting faster revascularization is of great therapeutic interest, as this will decrease the damage secondary to ischemia and could prevent the destructive hypoxia-driven pathological neovascular phase associated with diseases such as diabetic retinopathy and retinopathy of prematurity (ROP).

In the central nervous system (CNS), one cellular manifestation of hypoxia/ischemia is endoplasmic reticulum (ER) stress (Chen et al., 2008; Hayashi et al., 2005; Paschen and Doutheil, 1999; Tajiri et al., 2004), which activates a collection of signaling pathways that initially promote cellular survival in a compromised metabolic situation. When ER homeostasis is perturbed, the unfolded protein response (UPR) is initiated and activates phosphorylation of protein kinase RNA-like

ER kinase (PERK) and inositol-requiring enzyme-1a (IRE1a) (Bernales et al., 2006; Marciniak and Ron, 2006; Ron and Walter, 2007; Schröder and Kaufman, 2005). Together, these pathways signal to reduce the workload of folding machinery inside the ER (Figure 1A). ER stress is a short-term adaptive response, yet if it persists and is not resolved, it will contribute to tissue dysfunction (Tabas and Ron, 2011; Xu et al., 2005). To date, the physiological repercussions of ER stress have largely been investigated in the context of insulin resistance (Lee et al., 2011), atherosclerosis (Tabas, 2010), or liver disease (Malhi and Kaufman, 2011) while its influence in neurovascular homeostasis remains undefined.

The retina is a relevant model in which to study CNS neurovascular crosstalk due to its highly stereotyped apposition of central neurons, capillaries, venules, arteries, and veins (Dorrell and Friedlander, 2006; Joyal et al., 2011; Sapiéha, 2012) (Figure S1A). Moreover, of immediate clinical relevance, compromised neurovascular networks result in proliferative retinopathies (PRs) such as diabetic retinopathy (Aiello, 2005) and retinopathy of prematurity (Sapiéha et al., 2010b), which are the principal blinding diseases affecting pediatric and working-age populations in industrialized countries (Gilbert et al., 1997; Kempner et al., 2004). PRs are generally characterized by initial microvascular degeneration followed by an excessive and pathological neovascularization provoked by the hypoxic retina attempting to reinstate oxygen and energy supply (Chen and Smith, 2007; Cheung and Wong, 2008; Smith, 2008). This attempted compensatory vascular regrowth is initially concentrated at the avascular border of the injured retina and hence fails to adequately perfuse the hypoxic tissue (Figure 1B). Instead, the new vessels are misdirected into the vitreous chamber, resulting in tangential shearing of the retina and consequent vision loss.

There has been a recent surge in our knowledge of the molecular mechanisms governing blood vessel growth (Carmeliet and Jain, 2011). During vascular development, several conserved regulatory cues are shared between neurons and vessels (Adams and Eichmann, 2010; Carmeliet and Tessier-Lavigne, 2005; Erskine

et al., 2011; Larivée et al. 2009; Miao et al., 1999; Soker et al., 1998). Vascular tip cells (Gerhardt et al., 2003) (analogous to axonal growth cones) probe and sense chemotropic attractant and repellent environmental cues and respond to the vascular endothelial growth factor (VEGF) by forming motile filopodia enriched in VEGFR2 and rich in guidance receptors for semaphorins (Neuropilins), netrins (UNC5B and DCC), ephrins (Ephs), and slits (roundabout) (Adams et al., 1999; Klagsbrun and Eichmann, 2005; Larivée et al. 2009, 2007; Wilson et al., 2006). In addition, there is mounting evidence for the role of myeloid cells in vascular development (Stefater et al., 2011a, 2011b), repair (Checchin et al., 2006; Ritter et al., 2006), remodeling (Lang and Bishop, 1993), and anastomosis (Fantin et al., 2010) where these cells associate directly with vessels at the vascular front to exert their modulatory effects. To date, the influence of guidance cues on myeloid-induced vascular growth and remodeling has not been addressed.

Using the neural retina and its vascular system as a model of central neurovascular interaction, we set out to determine the outcome of hypoxia-induced neuronal ER stress on the vascular beds that perfuse this highly metabolic tissue. Employing the oxygen-induced retinopathy (OIR) model of vascular degeneration and regeneration (Smith et al., 1994), which serves as a proxy for human proliferative retinopathies such as diabetic retinopathy and retinopathy of prematurity, we uncovered a paradigm where ER stress in ischemic neurons provokes the suppression of vascular regeneration into hypoxic regions of CNS tissue. This results from an IRE1a-dependent downregulation of netrin-1, a protein we demonstrated to be required for myeloid-dependent revascularization. Either inhibition of IRE1a or treatment with netrin-1 accelerates retinal vascular regeneration and consequently alleviates the hypoxic stimulus for destructive neovascularization. Our data reveal an inherent capacity of CNS neurons to repair neighboring tissue by summoning a reparative innate immune response and provide evidence for neuronal-immune communication in ischemic retinopathies. Approaches to foster revascularization may be desirable to counter ischemic stress in the CNS.

## *Experimental Procedures*

### Animals

All studies were performed according to the Association for Research in Vision and Ophthalmology (ARVO) Statement for the Use of Animals in Ophthalmic and Vision Research and were approved by the Animal Care Committee of the University of Montreal in agreement with the guidelines established by the Canadian Council on Animal Care. C57Bl/6 wild-type were purchased from The Jackson Laboratory and CD1 nursing mothers from Charles River Laboratories.

### Depletion of Macrophages by Clodronate Liposomes

We prepared clodronate liposomes (0.7 M) or control empty-liposomes (PBS-filled) as described (van Rooijen and van Kesteren-Hendrikx, 2003) and delivered them by intravitreal injection (0.5 mL) at P11. To visualize and ascertain uptake of liposomes in macrophages in vitro and in vivo, we incubated liposomes with the fluorescent lipophilic marker Dil according to the manufacturer's protocol (Invitrogen).

### O<sub>2</sub>-Induced Retinopathy

Mouse pups (C57Bl6; The Jackson Laboratory) and their fostering mothers (CD1; Charles River Laboratories) were exposed to 75% O<sub>2</sub> from P7–P12 and returned to room air. This model serves as a proxy to human ocular neovascular diseases such as ROP and diabetic retinopathy characterized by a late phase of destructive pathological angiogenesis (Sapieha, 2012; Stahl et al., 2010). Upon return to room air, hypoxia-driven neovascularization (NV) develops from P14 onward (Smith et al., 1994). We enucleated eyes at different time points and dissected the retinas for mRNA or protein assays as described. Dissected retinas were flatmounted and incubated overnight with fluoresceinated isolectin B4 (1:100) in 1 mM CaCl<sub>2</sub> to determine the extent of avascular area or neovascularization area at P17 using ImageJ and the SWIFT-NV method (Stahl et al., 2009).

### Semiquantitative and Real-Time PCR Analysis

We isolated RNA using the GenElute Mammalian Total RNA Miniprep Kit (Sigma-Aldrich) and performed a digestion with deoxyribonuclease I (DNase I) to prevent amplification of genomic DNA. We reverse transcribed the RNA using M-MLV reverse transcriptase and analyzed gene expression using Sybr Green in an ABI real-time PCR machine (Applied Biosystems). b-actin was used as a reference gene. Primers sequences are displayed in Figure S7. We investigated the splicing of XBP1 by incubating the XBP1 semiquantitative PCR product with 0.4 U/mL of PstI enzyme for 5 hr at 37\_C followed by separation on 2.5% agarose gel.

#### Laser-Capture Microdissection

Eyes were enucleated from P14 pups in OIR or normoxic littermates and flash frozen in OCT. We then cut 12 mm sections using a Leica cryostat at -20\_C and air dried for 10 min. We dissected retinal layers using a Zeiss Observer microscope equipped with a PALM MicroBeam device for laser capture microdissection. We isolated mRNA from these sections and performed qPCRs as described above.

#### Western Blotting

For assessment of retinal protein levels, we enucleated eyes at varying time points and rapidly dissected and homogenized retinas. Protein concentrations were assessed by BCA assay (Sigma), and then 30 ug of protein was analyzed for each condition by standard SDS-PAGE technique. Antibodies used for western blotting are listed in Figure S7.

#### Immunohistochemistry

To localize protein expression, eyes were enucleated from mice and fixed in 4% paraformaldehyde at room temperature for 4 hr, incubated in 30% sucrose overnight, and then frozen in OCT compound. We then embedded the whole eye in optimal cutting temperature compound at -20.C and performed 12 mm serial sections. We carried out immunohistochemistry experiments and visualized the sections with an epifluorescent microscope (Zeiss Axio Imager). Antibodies used for immunohistochemistry are listed in Figure S7. For visualization of panretinal vasculature, flatmount retinas were stained with fluoresceinated Isolectin B4 (Alexa

Fluor 594 [I21413]; Molecular Probes) in 1 mM CaCl<sub>2</sub> in PBS for retinal vasculature. For assessment of vascular permeability, we injected the mice intracardially with 10 mg/mL of 70 kDa FITC-dextran. After 5 min, the eyes were harvested and retinas were dissected for flatmounting and visualization under a fluorescent microscope.

#### Preparation of Lentivirus

We produced infectious lentiviral vectors by transfecting lentivector and packaging vectors into HEK293T cells (Invitrogen) as previously described (Dull et al., 1998). Viral supernatants were concentrated by ultracentrifugation (>500-fold) and titers determined by ELISA for viral p24 antigen using a commercial kit (Clontech). The titers of the lentiviruses used were (in ng p24) LV.GFP (15.0 ng/mL), LV.sh.RNA IRE1a (8.52 ng/mL), and LV.sh.RNA.GFP (8.47 ng/mL).

#### Generation of Stable PERK- and IRE1a-Deficient RGC-5 Cell Lines and Transfections

We stably transfected RGC-5 cells with 500 ng of shRNA plasmids targeting PERK or IRE1a (Open Biosystems) or an unrelated shRNA (shGFP) for 16 hr at 37°C using Lipofectamine 2000 following the manufacturer's directions. We generated stable cell lines by selecting with 2 mg of puromycin over 2 weeks. For analysis of cleavage of netrin-1, we transfected 1 mg of an expression plasmid for chicken netrin-1 with or without the expression plasmids for shGFP, IRE1a or a dominant-negative mutant of IRE1a K599A, or the RNase dead mutant K907A in HEK293T cells using Lipofectamine 2000. Plasmids for IRE1a and IRE1a K599A were a gift from Fumihiko Urano (Addgene plasmid #20744 and #20745), and plasmid K907A was kindly provided by Randal J. Kaufman (Sanford-Burnham Medical Research Institute).

#### Detection of Intravitreally Delivered Netrin-1

We injected a recombinant Myc-tagged netrin-1 protein in P14 OIR animals. We collected eyes 3 hr later then fixed and dissected the retinas. We stained the retinas using a Myc antibody, Iba1, and fluoresceinated isolectin B4. Flatmounted retinas were visualized using a confocal microscope equipped with an argon laser

(LMS5; Zeiss). We generated a 3D reconstruction of >20 z stack layers using the Velocity software.

#### Microvascular Sprouting of Aortic Rings

Aortae from adult C57Bl6 mice were dissected and sectioned into 1 mm rings, which were immediately transferred to reduced growth factor Matrigel. After 3 days in EBM basal medium (Lonza), we incubated the rings with 500  $\mu$ L of macrophage-conditioned media. Rings were photographed with an inverted microscope (Zeiss Axio Imager) before and 48 hr post-treatment. Variation in the vascular area surrounding the aortic ring was calculated using ImageJ software.

#### CyQUANT Proliferation Assay

Primary human retinal microvascular endothelial cells (HRMEC passages six to ten from Cell Systems) were starved for 12 hr in EBM-2 medium (Lonza) plus 0.5% fetal bovine serum prior to treatment with macrophage-conditioned media or controls. We assessed the proliferation rates of 5,000 HRMEC cells/well using the CyQUANT NF Cell Proliferation Assay Kit (Invitrogen) (according to instructions given by the manufacturer) after 48 hr of incubation.

#### Isolation of Primary Microglia

Brains from P14 pups were homogenized in ice-cold L15 medium (GIBCO) and incubated for 15 min in 0.05% trypsin-EDTA (GIBCO) at 37°C. The reaction was stopped by addition of equal volumes of fetal bovine serum. We added 75 U/mL of DNase I (Sigma) before filtering through a 70  $\mu$ m cell strainer. After 9 days of incubation in DMEM media (Invitrogen) supplemented with 10% fetal bovine serum and penicillin/streptomycin, microglia were detached from the plates by gentle shaking (150 rpm for 2 hr at 37°C). Purity of preparations was confirmed by FACS analysis.

#### Matrigel Plug Assay

Macrophage-conditioned media (80  $\mu$ l) was mixed with 500  $\mu$ L of reduced growth factor Matrigel (BD Biosciences) at 4°C. The mixture was injected subcutaneously in the abdominal region of C57Bl6 mice (6 weeks old). After 10 days,

we injected 200 ml of FITC-dextran (2,000,000 MW; 25 mg/mL) intravenously 15 min prior to dissection of the overlying skin and harvesting of the Matrigel plug. We photographed the plugs using an epifluorescent microscope (Zeiss Axiolmager) then weighted and homogenized the plugs in 1 mg/mL of collagenase/dispase (Roche) overnight at 37\_C in the dark. The next day, we centrifuged homogenates and measured fluorescence intensity of supernatants at 480/520 nm.

#### FACS of Digested Retinas

Retinas from clodronate or empty liposome-injected eyes were homogenized with a solution of 750 U/mL DNaseI (Sigma) and 0.5 mg/mL of collagenase D (Roche) for 15 min at 37\_C with gentle shaking. Homogenates were filtered with a 70 mm cell strainer and washed in RPMI + 2% fetal bovine serum. We used PE-F4/80, FITC-CD11b, 7-AAD antibodies for detection of macrophages and performed analysis using a BD FACSCanto device (BD Biosciences) and the FlowJo 7.6 software. Antibodies are listed in Figure S7.

#### Preparation of Macrophage-Conditioned Media

Supernatants were collected from J774 cells that had been incubated for 24 hr in the presence of various concentrations of netrin-1 and/or inhibitors. Supernatants were centrifuged, filtered, and then frozen for subsequent use. Secondary Structure Reconstruction of Netrin-1 mRNA

For prediction of the secondary structure of mRNA, we analyzed the murine sequence of netrin-1 mRNA using CentroidFold program (<http://www.ncrna.org/centroidfold>).

#### IRE1a In Vitro Cleavage Assay

Thirty micrograms of total RNA extracted from HEK transfected or not with an expression plasmid for netrin-1 was subjected to digestion by the IRE1a recombinant enzyme (5 mg) for 2 hr at 37\_C in a 53 digestion buffer (250 mM Tris [pH 7.5], 600 mM NaCl, 5 mM MgCl<sub>2</sub>, 5 mM MnCl<sub>2</sub>, 25 mM b-mercaptoethanol, 10 mM ATP). The digested RNA was analyzed by semi-quantitative PCR using sets of primers spanning different regions in the netrin-1 mRNA.

## Northern Blotting

Fifty micrograms of total RNA was separated on a formaldehyde agarose gel and transferred to a nitrocellulose membrane. The membrane was then incubated with a radiolabelled netrin-1-specific probe (<500 pb fragment of a SacII-PvuII digestion product of the netrin-1 expression plasmid) overnight at 42°C.

## Statistical Analyses

Data are presented as mean  $\pm$  SEM. We used Student's t test to compare the different groups;  $p < 0.05$  was considered statistically different.

## Supplemental Information

Supplemental Information includes seven figures and one movie and can be found with this article online at <http://dx.doi.org/10.1016/j.cmet.2013.02.003>.

## *Results*

### Neuronal ER stress Is Induced in Ischemic Conditions

The activation of canonical ER stress pathways is a conserved mechanism that enhances cellular survival under low metabolic conditions by reducing protein synthesis. This is achieved via phosphorylation of ER membrane-resident proteins such as PERK and IRE1a (Figure 1A). PERK restricts the translational machinery to a selected subset of messenger RNAs (mRNAs) such as ATF4, whereas phosphorylated, active IRE1a promotes splicing of XBP1 into an active transcription factor (XBP1s) that promotes expression of genes involved in UPR while the unspliced form (XBP1u) blocks transcription of genes involved in UPR. ATF4 and XBP1s induce transcription of specific homeostasis genes, such as the chaperone GRP78, to increase the protein-folding capacity of the ER (Figure 1A) (Ron and Walter, 2007). To determine if ischemia in central nervous tissue can provoke ER stress, we used the mouse model of OIR (75% oxygen from P7–P12 [postnatal day 7–12] and room air until P17), which yields a central avascular retina (Smith et al., 1994). This vascular degeneration is followed by a second phase of deregulated

(albeit compensatory) vascular regeneration (Figure 1B). The secondary regrowth occurs upon return to room air (P12) for a period of approximately 7 days (Stahl et al., 2010).

We initially performed a time course for the expression of classical markers of ER stress throughout OIR. We focused on time points corresponding to the hyperoxic vasoobliterative phase (P10), upon return to normal air (P12), and in the initial phase of progressive vascular regrowth (P14). Phosphorylated PERK and IRE1a were found primarily in the ganglion cell layer (GCL) and colocalized with the RGC marker  $\beta$ -tubulin (Figures 1C and 1D). The phosphorylation was evident in P14 OIR retinas during the early phase of vascular regeneration when reparative angiogenesis proceeds at a slow pace and the central retina remains hypoxic (Figures 1C and 1D). No phosphorylation of IRE1a and PERK was observed in the vascular layers (Figure 1E), highlighting the neuronal nature of the ER stress. This expression pattern was associated robustly with the central avascular area of the retina as confirmed with endothelial isolectin B4 staining (Figure 1F). Moreover, using laser capture microdissection (LCM), we specifically isolated the RGC layer from the retina (Figure 1G) and analyzed the expression of downstream effectors of ER stress pathways. Significantly enhanced expression of ATF4 and GRP78 transcripts was found in OIR mice compared to normoxic littermates at P14 (Figures 1H and 1I).

These findings were confirmed using an *in vitro* model of retinal neuron precursors cells (RGC-5) (Joyal et al., 2011; Sapieha et al., 2008) exposed to hypoxic conditions (1% O<sub>2</sub>) in order to mimic the retinal ischemia present at P14 of OIR. First, we noted a pronounced phosphorylation of PERK and IRE1a (Figure 1J) representing the activation of ER stress pathways upon exposing RGC-5s to hypoxic conditions (starting at 4 hr). The activation of these pathways coincided with a marked upregulation of their effectors. ATF4 induction was detected at 8 hr and reached a greater than 8-fold increase in expression after 48 hr (Figure 1K). Concordantly, an increased splicing of XBP1 was observed, confirming the activation of IRE1a (ratio of 0.6327 at 0 hr and 1.826 at 4 hr of spliced versus unspliced XBP1 mRNA) (Figure 1L). GRP78

expression was similarly elevated at 12 hr and increased by 8-fold at 24 hr (Figure 1M). The same pattern was noted for C/EBP homologous protein (CHOP), a transcription factor whose expression is controlled primarily by ATF4 and to a lesser extent by XBP1s (Oyadomari and Mori, 2004) (Figure S1B). Together, these findings indicate that the microvascular degeneration and ensuing ischemia characteristic of proliferative retinopathies triggers ER stress in retinal ganglion neurons.

### Neuronal ER Stress Provokes Failure of Vascular Regeneration

Recent studies demonstrate that RGCs are important effector cells for retinal angiogenesis (Edwards et al., 2012; Fukushima et al., 2011; Joyal et al., 2011; Kim et al., 2011; Sapieha et al., 2008). We therefore sought to determine if ER stress in these neurons could influence retinal revascularization in OIR. To specifically hinder ER stress in RGCs in vivo, we generated lentiviral (Lv) vectors carrying small hairpin RNAs (shRNAs). These Lv vectors exhibit high tropism for RGCs when delivered intravitreally (Joyal et al., 2011; Sapieha et al., 2008) (Figure S2A). A single intravitreal injection of lentivirus shIRE1a (Lv.shIRE1a) or Lv.shPERK at P7 led to a significant reduction in IRE1a and PERK expression in whole retinas (Figures S2B and S2C, respectively). Lv.shIRE1a injections robustly enhanced retinal vascular regeneration by 3.7-fold compared to vehicle-treated controls (as determined by the extent of remaining avascular areas at P17; Figure 1N). Importantly, the enhanced rate of reparative angiogenesis profoundly reduced destructive pre-retinal neovascularization associated with ischemic retinopathies by over 65% (Figure 1O). This is likely attributed to the alleviation of hypoxic stress. Conversely, injections of Lv.shPERK did not result in any significant changes in retinal vascularization (Figure 1N) or neovascular tuft formation (Figure 1O), highlighting the central role of IRE1a in the control of reparative retinal angiogenesis. Importantly, we did not observe any differences in the extent of vasoobliteration at P12 upon treatment with either Lv.shIRE1a or Lv.shPERK (Figure 1P), thus confirming that the observed ER stress is primarily affecting the second phase regeneration and not the initial phase of vascular

degeneration. These findings illustrate that ER stress (more specifically IRE1a activity) in hypoxic retinal ganglion neurons contributes to stalling vascular regrowth. Inhibiting this neuron-associated stress directly impacts reparative vascularization and thus highlights the importance of neurovascular crosstalk in this model of ischemic retinopathies.

### Netrin-1 Is Degraded in Hypoxic Conditions by ER Stress

ER stress has been classically described as evoking a non-specific response to restore cellular function. However, growing evidence points to a degree of selectivity with specific substrates being preferentially targeted by the effectors of the ER stress response. This is the case specifically with the endoribonuclease activity of IRE1a (Han et al., 2009; Hollien and Weissman, 2006). Given the elucidation of key roles for neuronal guidance cues in retinal vascularization (Eichmann and Thomas, 2012; Fukushima et al., 2011; Jones et al., 2008; Joyal et al., 2011; Kim et al., 2011; Larivée et al 2007), we turned our attention to these molecules.

Upon subjecting mice to the OIR model, we observed that the neuronal guidance protein netrin-1 (Kennedy et al., 1994) was profoundly downregulated at P14 (Figure 2A), a time that corresponds to elevated ER stress and initial attempts at vascular restoration (Figure 1B). In the retina, netrin-1 is mainly produced in the ganglion cell layer and colocalizes with the RGC marker  $\beta$ -tubulin (Figure 2B). In addition, cells of the inner nuclear layer showed a modest level of netrin-1 expression. This was confirmed by performing LCM on retinal layers where netrin-1 expression was 16-fold higher in the ganglion cell layer when compared to the RPE layer. Cells of the outer and inner nuclear layers showed only modest expression of netrin-1 (Figure 2C). We also confirmed that the expression of netrin-1 mRNA drops in the GCL layer as determined in LCM-isolated samples from P14 OIR and compared to normoxic littermates (Figure 2D). Interestingly, this drop in netrin-1 correlates with an increase in IRE1a-mediated XBP1 splicing activity at P14 OIR and thus temporally links IRE1a activity with a drop in netrin-1 mRNA (Figure 2D). Importantly, the decrease in

netrin-1 mRNA seen at P14 (Figure 2E) is largely prevented by lentivirus small hairpin (Lv.sh)- mediated knockdown of IRE1a following intravitreal injection (Figure 2F), an effect not seen with Lv.shPERK. These data identify a specific link between the IRE1a arm of the ER stress pathway and netrin-1. Moreover, as observed in whole retinal mRNA at P14 OIR, the degradation of netrin-1 by IRE1a is selective for netrin-1 since levels of VEGF are not affected by intravitreal administration of Lv.shPERK or Lv.shIRE1a (Figure 2F). While the levels of VEGF are not elevated in whole retinas, analysis at the microenvironmental level will be required to tease out the contribution of individual cell populations to VEGF production. Concordantly, netrin-1 decreases in cultured RGC-5s under hypoxic conditions (1% O<sub>2</sub>) that mimic the ischemic phase of retinopathy while other transcripts such as VEGF increased as expected (Figure 2G). In this experimental paradigm, cultured RGC-5s were not serum starved in order to prevent premature induction of ER stress and UPR by amino acid deficiency.

To ascertain if ER stress pathways are responsible for the downregulation of netrin-1 in RGCs under hypoxic conditions, we generated PERK- and IRE1a-deficient RGCs by stable transfection with shRNA. Using these cell lines, we determined that IRE1a is the primary negative regulator of netrin-1 mRNA, as IRE1a-deficient cells showed significantly increased levels of netrin-1 under hypoxic conditions. Importantly, PERK-deficient cells or cells deficient for both PERK and IRE1a did not show any additional preservation of netrin-1 mRNA when compared to IRE1a alone, thus confirming the prominent role for IRE1a in the downregulation of netrin-1 (Figure 2H).

**Netrin-1 Is Cleaved by the RNase Activity of IRE1a** Recent evidence suggests that the ribonuclease (RNase) activity of IRE1a, also termed IRE1-dependent decay (RIDD), specifically targets mRNAs encoding proteins that traverse the ER-Golgi secretory pathway (Hollien and Weissman, 2006). Therefore, to determine if netrin-1 could be a substrate for IRE1a, we cotransfected human embryonic kidney (HEK) cells that express endogenously low levels of netrin-1 (Shekarabi and Kennedy, 2002) with a plasmid encoding netrin-1 with or without an expression plasmid for IRE1a, a

kinase-inactive/RNase-dead IREa (K599A), or an exclusively RNase-dead IRE1a (K907A) (Figure 3A) (Lipson et al., 2008). The overexpression of IRE1a drastically decreased the level of netrin-1 mRNA (Figure 3B), an effect also seen at the protein level (Figure 3C). In contrast, the degradation of netrin-1 was not observed with the kinase/endoribonuclease inactive dominant-negative mutant K599A (Lipson et al., 2008) or the endoribonuclease-dead mutant K907A (Figures 3B and 3C). In this experimental paradigm employing HEK cells, no effect was noted on the level of VEGF in the time frame (48 hr) investigated, demonstrating the selectivity of the reaction (Figures 3B and 3C). These results were confirmed by northern blot using a netrin-1-specific probe (Figure 3D).

IRE1a has been shown to target specific scission sites; these include 5'-CAGCAG-3' in adjacent mRNA stem loops. This was demonstrated for the transcripts of mouse insulin II (Han et al., 2009) or makorin RING finger protein 2 (Oikawa et al., 2010). Using a bioinformatics approach, we generated the 2D structure of netrin-1 transcript (Figure 3E) and noted two putative cleavage sites for IRE1a in positions 1605–1610 and 1670–1675 located in stem loops (Figure 3E, red arrows). Exposure of cultured RGC-5s to hypoxia for 24 hr led to a substantial drop in netrin-1 mRNA as determined by semiquantitative PCR and was largely reversed when blocking IRE1a expression with shRNAs (Figure 3F). Netrin-1 fragments were very unstable using a cell transfection system, and no cleavage fragments were found by northern blot (Figure 3D), which could be due to the rapid activity of 5'-to-3' and 3'-to-5' exonucleases. We therefore employed a cell-free system to analyze the presence of these fragments using recombinant GST-fused IRE1a. We designed distinct sets of primers spanning the predicted sequences of IRE1a cleavage sites in netrin-1 mRNA. Loss of netrin-1 transcript was only observed when amplifying across the prospective IRE1a scission sites (959–1683 but not 511–891) (Figure 3G), thus confirming that IRE1a targets netrin-1. Together these data demonstrate that netrin-1 mRNA is a substrate for IRE1a.

## Restoring Netrin-1 Accelerates Revascularization of the Ischemic Retina

Given the pronounced reduction of netrin-1 (noted above; Figure 2) during a period in which retinal revascularization is compromised (Joyal et al., 2011; Stahl et al., 2010), we sought to determine if restoring netrin-1 levels by ectopic intravitreal administration would enhance reparative angiogenesis following OIR. A single intravitreal injection of netrin-1 at P14 accelerated vascular regeneration and consequently decreased the avascular area of retina in a dose-dependent manner: 25% reduction with 50 ng/mL, 57% with 100 ng/mL, and 67% reduction with 200 ng/mL (Figure 4A). This rapid restoration of retinal vascularization led to reduced pathological preretinal neovascularization with the 100 ng/ml dose abrogating close to 70% of this destructive angiogenesis (Figure 4B). To ascertain whether the regenerated vessels were healthy, we determined their barrier function by angiography with fluorescein isothiocyanate (FITC)-dextran. Regenerated vessels in netrin-1-injected retinas assumed a healthy disposition and did not present any signs of vascular leakage in contrast to vehicle-injected controls, which showed blebbing and poor retention of FITC-dextran (Figure 4C). These data attest to the stability of the neovessels in netrin-1-treated retinas.

To further confirm the role of netrin in retinal angiogenesis, we designed a lentiviral vector carrying an shRNA targeting netrin-1 and administered it to the developing retina. Intravitreal injection of Lv.shNtn1 at P2 significantly reduced the expression of netrin-1 at P7 (Figure S3A) and resulted in an abnormal vascular front with several retracted tip cells (Figure S3B, solid white arrows). Isolectin-B4-positive microglial cells were found in the general vicinity of the growing vascular front, yet were less in direct contact with vascular tip cells in Lv.shNtn-1-treated retinas (Figure S3B, gray dotted arrows). Taken with the previous, these data demonstrate that a specific substrate of neuronal ER stress, namely netrin-1, has potent vasoregenerative properties.

## Netrin-1 Modulates the Expression of VEGF in Macrophage/Microglial Cells

To gain insight into the mechanisms by which netrin-1 accelerates retinal revascularization, we explored its influence on the prominent retinal proangiogenic factor VEGF (Pierce et al., 1995; Pierce et al., 1996). The same intravitreal injection of netrin-1 that significantly enhanced revascularization (Figure 4) induced a significant yet very modest increase in gene expression of VEGF in the total retina 24 hr postinjection (Figure 5A). Elevated panretinal levels of VEGF are associated with pathological ocular neovascularization (Aiello et al., 1995). However, we observed only a modest rise in retinal VEGF in our experimental paradigm. Yet this increase in VEGF precipitated reparative angiogenesis. We therefore sought to explore the source of the VEGF production at a microenvironmental level and elucidate which cell population was responsible for this netrin-1-induced production of VEGF.

Following administration of Myc-tagged recombinant netrin-1 protein to the vitreous as described above (Figure 4), we detected Myc-netrin-1 specifically localized to lectin and Iba1-positive microglia/macrophages at the vascular front (Figure 5B) in close proximity with tip cells (Figure 5B, white arrows). Confocal images were taken 3 hr post-injection. A 3D reconstruction shows the binding of exogenously applied netrin-1 to the cell surface of microglia/macrophages (Movie S1).

To determine whether netrin-1 can have biological effects on these cells, we evaluated the expression of netrin-1 receptors in a murine macrophage cell line (J774) (Figure 5C) and in primary microglia (Figure S4A). Our results demonstrate that UNC5B, neogenin, and the putative receptor for netrin, adenosine A2B receptor (AA2BR), are expressed in macrophages (Figure 5C), with a similar pattern in primary microglial cells (Figure S4A). Conversely, UNC5A and DCC are undetectable or negligibly expressed in macrophages or microglia. Macrophages may thus be required for netrin-1 to exert proangiogenic effects, as netrin-1 alone has been elegantly shown to inhibit sprouting angiogenesis (Larrivée et al. 2007).

We next analyzed the ability of netrin-1 to induce expression of VEGF and angiopoietins directly in macrophages. Netrin-1 (100 or 200 ng/ml) induced a 3-fold

increase of VEGF expression in macrophages (Figure 5D). Moreover, a significant increase in other proangiogenic factors such as Angiopoietin 2 was noted while the vasostabilizing Angiopoietin 1 was affected minimally, suggesting a general proangiogenic modulation by Netrin-1 (Figure S4B). Increased expression of VEGF was induced similarly in primary microglia by application of netrin-1 (Figure S4C). Given that Angiopoietin 2 requires VEGF to induce angiogenic growth, we focused our study on VEGF. We therefore analyzed the expression of VEGF in the presence of various blockers of netrin-1 receptors. In this context, only the AA2BR antagonist PSB1115 or an AA2BR siRNA were able to decrease the induction of VEGF while neutralizing antibodies or siRNAs against UNC5B (Ly et al., 2005; Tadagavadi et al., 2010), and Neogenin (Lejmi et al., 2008) did not prevent this induction (Figure 5D). We verified that these siRNAs were transfected effectively in macrophages using siGLO and fluorescence-activated cell sorting (FACS) analysis (Figure 5D, inset) and certified their specificity and potency (Figure S4D).

To confirm that netrin-1 can exert a biological effect on macrophages, we analyzed the activation of the mitogen activated protein kinase (MAPK) ERK1/ERK2 as a generic readout of intracellular activity. Relevantly, ERK1 and ERK2 are known to be activated by the AA2BR (Yang et al., 2011) and stimulated following netrin-1 exposure to epithelial cells (Wang et al., 2009). Treatment of macrophages with a 100 ng/mL dose of netrin-1 induced a rapid increase of ERK1/ERK2 phosphorylation starting at 5 min and peaking at 30 min (Figure 5E). Pre-incubation with PSB1115 reversed ERK1/ERK2 phosphorylation (Figure 5F), confirming the involvement of this receptor in netrin-1-mediated signaling in macrophages. These data reveal that netrin-1 can prompt myeloid cell production of proangiogenic factors such as VEGF. This provides a paradigm in which netrin-1 induces an angiogenic switch in microglial cells and drives reparative angiogenesis at a microenvironmental level, thus promoting localized vascular regeneration without increasing overall pathological angiogenesis.

## The Proangiogenic Properties of Netrin-1 Are Driven by Macrophages

To investigate the contribution of macrophages to the proangiogenic effects of netrin-1, we conducted a series of *ex vivo* and *in vitro* angiogenesis assays. Cultured macrophages were exposed to 100 ng/mL netrin-1 for a period of 24 hr and used to condition fresh culture media (Figure 6A). The conditioned media (CM) containing factors secreted by macrophages secondary to netrin-1 stimulation was collected, filtered, and used to culture human retinal microvascular endothelial cells (HRMECs). Using a CyQUANT Cell Proliferation Assay, we found that supernatants from netrin-1-stimulated macrophages induced a robust 30-fold induction in HRMEC proliferation compared to nonstimulated controls (Figure 6B). In line with the results above, the AA2BR inhibitor, PSB1115, abolished the proliferative effects of netrin-1 (Figure 6B). Direct addition of netrin-1 lead to less pronounced endothelial proliferation, suggesting that the proangiogenic effects of CM are mediated by factors produced by netrin-1-stimulated macrophages and not by exogenously added netrin-1. In order to confirm the angiogenic potential of netrin-1-stimulated macrophages *in vivo*, we used a Matrigel plug assay in which CM was solubilized with Matrigel and injected subcutaneously in mice. Ten days following introduction of plugs, mice were perfused with FITC-dextran, and the extent of invading vascularization was quantified by spectrofluorometry. Netrin-1 CM induced a 4-fold increase in plug angiogenesis (Figure 6C), an effect visualized by fluorescent microscopy (Figure 6C). Consistent with the data above, inhibition of AA2BR efficiently abolished the capacity of netrin-1 to induce macrophage-dependent vascularization, as revealed by a decrease in vascular networks observed in PSB1115-CM-treated Matrigel plugs (Figure 6C).

Next, we verified if netrin-1 CM from macrophages could induce sprouting angiogenesis in aortic explants. The results presented in Figure 6D demonstrate that CM from macrophages incubated with netrin-1 significantly increased aortic ring sprouting area compared to controls. As above, the CM harvested from macrophages pretreated with PSB1115 provoked considerably less vascular growth, thus confirming the role of this receptor in netrin-1-induced angiogenesis (Figure 6D).

Importantly, consistent with previous studies (Larrivée et al. 2007), direct incubation of aortic explants with netrin-1 alone lead to a dose-dependent reduction in vascular sprouting (Figure S5). These results underscore the importance of macrophages in mediating the proangiogenic effects of netrin-1. Given the central role of VEGF in angiogenesis, including as a positive modulator of the effects of angiopoietins, we sought to determine if neutralization of VEGF would abrogate the proangiogenic effects of the CM from netrin-1-treated macrophages. Indeed, our data confirm that VEGF was the major proangiogenic effector in the CM, given that addition of a VEGF-neutralizing antibody reversed the observed sprouting angiogenesis (Figure 6E), an effect not seen with addition of a control goat immunoglobulin G (IgG) antibody. Combined, the findings presented in Figure 6 provide evidence that the direct effect of netrin-1 on proliferation and migration of endothelial cells was either not significant or negligible compared to the pronounced effect of netrin-1 CM that was obtained from macrophages. Moreover, we showed that VEGF is a central proangiogenic effector secreted by netrin-1-stimulated macrophages.

#### Neurovascular Regeneration by Netrin-1 In Vivo Is Macrophage/Microglial Cell Dependent

Retinal myeloid cells (macrophages/microglia) participate in vascularization both during development (Stefater et al., 2011a, 2011b) and in pathological neovascularization (Stahl et al., 2010). To confirm that retinal macrophages/microglia mediate the observed netrin-1-induced vascular regeneration of the ischemic retina (Figure 4) and to further rule out a direct effect of netrin-1 on endothelium, we proceeded to deplete the retina of myeloid cells by intravitreal injection of clodronate liposomes prior to treatment with netrin-1. Clodronate liposomes have been used successfully to remove macrophages from distal organs (van Rooijen and van Kesteren-Hendriks, 2002) as well as the retina (Ishida et al., 2003; Ritter et al., 2006).

We first confirmed the ability of our clodronate liposome preparation to induce apoptosis of macrophages in vitro (Figure S6).

We next verified the efficacy with which clodronate liposomes deplete retinal macrophages/microglia by FACS analysis. Treatment with clodronate liposomes lead to a significant 2-fold reduction in retinal macrophages/microglia compared to control empty liposomes as confirmed by 7-AAD negative- F4-80/CD11b positive cells (4,500 microglia for empty liposomes and ~2,300 microglia for clodronate liposomes/retina). 7-AAD negative cells are viable (Figure 7A).

As expected, intravitreal injection of netrin-1 enhanced vascular regeneration by ~50% as observed at P17 in empty-liposome-injected animals. Conversely, delivery of netrin-1 to macrophage/microglia-depleted retinas did not induce any significant difference in vascular regeneration, thus underscoring the importance of these immune cells in netrin-1-induced angiogenesis (Figure 7B). We next verified the contribution of the macrophage/microglial-derived VEGF produced in response to netrin-1 (described in Figures 5 and 6). To this end, we simultaneously injected netrin-1 and anti-VEGF neutralizing antibodies and analyzed the outcome on vascular regeneration at P17. Blocking antibodies for VEGF effectively abolished the pro-regenerative effect of netrin-1, confirming the key role of this factor in the regeneration of the vasculature observed in our paradigm (Figure 7C). Our data indicate that netrin-1 activates an angiogenic switch in macrophages/microglia, and thus drives microenvironmental revascularization, but does not contribute to pathological pre-retinal neovascularization. Taken together, we demonstrate that sustained ER stress specifically targets netrin-1, which we identify as a potent retinal revascularization factor that mediates its effects through retinal myeloid cells.

## *Discussion*

The neurovascular unit has been increasingly investigated in health and disease over the course of the last decade. In this study, we put forward two concepts

pertaining to the role of ER stress in hindering reparative angiogenesis within the CNS. First, we demonstrate that sustained neuronal ER stress, through the endoribonuclease IRE1a, provokes the degradation of netrin-1 and results in revascularization failure of the ischemic retina. Second, we present neuronal-derived netrin-1 as a potent mediator of myeloid-cell-induced CNS vascular regeneration (Figure 7C). Although mechanisms governing vascular degeneration and the ensuing pre-retinal neovascularization in proliferative retinopathies have been extensively studied (Ashton et al., 1954; Campbell, 1951; D'Amore and Sweet, 1987; Lundbaek et al., 1970; Michaelson, 1948; Simons and Flynn, 1999; Smith, 2004; Smith et al., 1994; Tesfamariam, 1994), there are no strategies to date to accelerate revascularization of the vaso-obliterated retina and consequently alleviate the ischemic stress that is central to disease progression. Gaining insight into why vascular regeneration stalls or proceeds at compromised rates will be key to understanding the pathomechanisms of ischemic neuropathies.

Hypoxia is an activator of the unfolded protein response in conditions such as ischemic heart disease or cerebral ischemia (Tajiri et al., 2004). We demonstrate that both arms of the ER stress response, IRE1a (cleavage of XBP1) and PERK (induction of ATF4), are profoundly induced in response to neuronal hypoxia. Although it is well established that mild hypoxia (via hypoxia-inducible factor [HIF]) drives a cluster of over 70 genes that encode proteins that promote the adjustment to an oxygen deficient state (Bruick, 2003; Lange and Bainbridge, 2012; Paul et al., 2004), it is conceivable that when the ischemic shock persists, the nervous tissue segregates irreversibly damaged regions in an attempt to deviate metabolic stores to less-affected and more-salvageable areas (Joyal et al., 2011). Globally, this concept may in part explain the production of vasorepulsive guidance cues in ischemic cores secondary to severe vascular injury in stroke (Fujita et al., 2001) or in vasodeficient areas of the retina in retinopathy (Fukushima et al., 2011; Joyal et al., 2011). The sustained activation of ER stress pathways, and specifically IRE1a, may provide the neuron with the appropriate enzymatic machinery to shift from a

prosurvival program to one that repels vessels and thus redistributes oxygen and nutrients to sectors of tissue that would preferentially benefit. In agreement, degradation of netrin-1 transcripts by IRE1a during a state of sustained hypoxia perturbs revascularization and thus permits vasorepellant factors such as semaphorins 3A and 3E to deviate nascent angiogenic sprouts from severely ischemic areas of nervous tissue (Fukushima et al., 2011; Joyal et al., 2011).

The paradigm we present suggests that the cellular consequences of ER stress are finely tuned and selective. In an attempt to elucidate the mechanism by which ER stress in retinal ganglion neurons stalls neurovascular regeneration, we identified netrin-1 as a selective substrate for IRE1a via a mechanism previously described as IRE1a-dependent decay (RIDD) of messenger RNA (Hollien and Weissman, 2006). Specifically targeting effectors such as netrin-1, while permitting VEGF levels to increase, will hinder netrin-1-induced revascularization while maintaining adequate VEGF levels to provide neurotrophic support of neighboring retinal neural tissue (Robinson et al., 2001). Similarly, it is now believed that several substrates for IRE1a exist including the mRNAs encoding insulin (Lipson et al., 2008), CD59 (Oikawa et al., 2007), HMG-CoA reductase, b2-microglobulin, and the microRNA for TXNIP (miR-17) (Lerner et al., 2012). IRE1a-mediated mRNA degradation provides a rapid mechanism to deplete cells of ER-localized mRNAs and alleviate the metabolic burden of protein folding inside the ER. Interestingly, in our experimental paradigms, we did not observe any direct effects of IRE1a on the induction of VEGF, as has been suggested (Drogat et al., 2007; Ghosh et al., 2010). This could be attributed to IRE1a's ability to adjust its RNase versus transcriptional activity (via activation of XBP1) under conditions of prolonged ER stress (Hollien et al., 2009). In conditions in which homeostasis could not be restored, such as that observed in our experimental paradigms, the RNase activity of IRE1a would be favored over the prosurvival transcriptional induction of angiogenic genes such as VEGF (Han et al., 2009) by IRE1a. Interestingly, as demonstrated in this study, VEGF

was found by other reports to be insensitive to the RIDD activity of IRE1a (Ghosh et al., 2010).

Although the nervous system has long been considered immunologically privileged, evidence for direct interplay between the nervous and immune systems is mounting (Farina et al., 2007; London et al., 2011; Nguyen et al., 2002; Rosas-Ballina et al., 2011; Wong et al., 2011). Specifically, the innate immune system has been intimately tied to CNS health and disease. Neuroimmune crosstalk can orchestrate an innate response that participates in beneficial events such as nerve remyelination and microglia-derived neuroprotective trophic support of injured neurons (Nguyen et al., 2002). In the retina, monocyte-derived macrophages participate in promoting RGC survival and nerve regeneration following traumatic optic nerve injury (Leon et al., 2000) as well as neuroprotection against glutamate cytotoxicity and elevated intraocular pressure (London et al., 2011). Of direct pertinence, resident retinal microglia participate actively in promoting developmental vascularization of the ganglion cell layer (Checchin et al., 2006), and resident myeloid cells have the propensity to suppress angiogenic branching (Stefater et al., 2011). Bone marrow-derived myeloid progenitors migrate to avascular areas, differentiate into microglia, and promote revascularization (Ritter et al., 2006). We demonstrate that netrin-1 provokes an angiogenic switch in retinal macrophages and participates in guiding vascular regrowth into avascular areas of the retina. We show that microglial depletion by clodronate liposomes abolishes the enhanced rate of revascularization induced by netrin-1. In addition, ex vivo and in vitro assays indicate that the proangiogenic effects of netrin-1 are mediated via macrophages in a manner that is dependent on AA2BR function and activation of the ERK1/ERK2 kinase. Hence, the upregulation of VEGF occurs at a microenvironmental level at the vascular front and thus does not precipitate destructive preretinal growth as would be expected by an overall rise in VEGF during the vasoproliferative phase of retinopathy. Interestingly, selective antagonists of the AA2BR were shown to reduce preretinal neovascularization (Mino et al., 2001), suggesting a correlation between this G

protein-coupled receptor (GPCR) and retinal angiogenesis. Our data indicate that AA2BR is required for netrin-1 to activate microglia to provide the tissue with an adequate level of VEGF to revascularize the retina without contributing to extraretinal growth. This approach may be considered counterintuitive given the uncontestable involvement of VEGF in the pathogenesis of ocular neovascular disease (Aiello et al., 1995; Caldwell et al., 2003; Ferrara and Kerbel, 2005) and the currently employed anti-angiogenic strategies for proliferative ocular disease (Stewart, 2012). However, providing minute doses of VEGF has been shown to reduce OIR-associated pathology (Dorrell et al., 2010). Consistent with our findings, the ability of physiological doses of netrin-1 (50–200 ng/mL) to promote vascularization and survival of endothelial cells has previously been demonstrated (Park et al., 2004; Wilson et al., 2006). At the same time, however, well-designed and sophisticated studies have

described antiangiogenic properties for netrin-1 (Larrivée et al., 2007) acting through the UNC5B receptor (Lu et al., 2004). Our findings indicate that beyond a direct effect on endothelium, netrin-1 influences cell populations associated with the vasculature and suggest that this may account for some of the noted discrepancies (Castets and Mehlen, 2010). It is important to note that although it has been suggested that AA2BR functions as a receptor for netrin-1 (Corset et al., 2000; Mirakaj et al., 2011; Rosenberger et al., 2009), these results have been controversial (Stein et al., 2001). Alternatively, manipulating AA2BR function directly regulates the intracellular concentration of cyclic AMP (cAMP), which in neurons regulates the switch between chemoattractant and chemorepellent responses to a netrin-1 gradient (Nishiyama et al., 2003; Shewan et al., 2002). We speculate that a similar paradigm may thus apply to macrophages, with intracellular levels of cAMP potentiating the angiogenic switch.

Collectively, these findings provide mechanistic insight into vascular regeneration in neuroischemic conditions. Our data present the ER of CNS neurons as a key sensor of hypoxic stress that has the propensity to modulate the reparative

innate immune response under ischemic conditions. In doing so, we provide evidence for neuroimmune communication in neuroischemic conditions such as proliferative retinopathies. When driven beyond a hypoxic threshold however, central neurons via IRE1a have the ability to halt vascularization, possibly in order to deviate metabolic stores to more salvageable areas. To date, there are no therapeutic strategies that aim to enhance vascular regeneration in ischemic CNS tissue. In this regard, netrin-1-stimulated macrophages may be able to override the vaso-inhibitory cues present within the ischemic neuronal retina (Fukushima et al., 2011; Joyal et al., 2011) and achieve functional vascular regeneration. The work presented in this study provides proof of concept for the modulation of ER stress and netrin-1 for an ischemic disorder of the CNS. Future investigation and streamlining will be required to translate these findings and design therapeutic strategies to counter neuroischemic conditions such as retinopathies.

### *Acknowledgments*

This work was supported by operating grants to P.S. from the Canadian Institutes of Health Research (221478), the Canadian Diabetes Association (OG-3-11-3329-PS), and the Natural Sciences and Engineering Research Council of Canada (418637). P.S. holds a Canada Research Chair in Retinal Cell Biology and The Alcon Research Institute Young Investigator Award. F.B. holds a Fonds de la recherche en sante du Quebec (FRSQ) postdoctoral fellowship. G.M. and A.C. are supported by scholarships from the Reseau de Recherche en Sante de la Vision du Quebec. N.S. holds an FRSQ doctoral scholarship. T.E.K. holds an FRSQ Chercheurs Nationaux award and is a Killam Foundation Scholar. NIH grants R37DK042394, R01DK088227, P01HL057346R01, and R01HL052173 were awarded to R.J.K. We would like to thank Isabelle Louarn for the artwork in Figure 1. We thank Dr. Jing Chen for critical comments on the manuscript. We also wish to acknowledge Vincent Bourgoin, Stefania Bottardi, and Vincent Lemay for technical advices. F.B., N.T., M.G., T.E.K.,

and P.S. conceived and designed the experiments; F.B., G.M., N.S., N.T., S.F., E.L., A.C., D.L., S.T., F.R., A.M.J., and J.-S.J. performed the experiments; F.B. and P.S. analyzed the data; A.S., E.M., R.K., and M.G. provided expert advice; and P.S., F.B., and T.E.K. wrote the paper.

## *References*

- Adams, R.H., and Eichmann, A. (2010). Axon guidance molecules in vascular patterning. *Cold Spring Harb. Perspect. Biol.* 2, a001875.
- Adams, R.H., Wilkinson, G.A., Weiss, C., Diella, F., Gale, N.W., Deutsch, U., Risau, W., and Klein, R. (1999). Roles of ephrinB ligands and EphB receptors in cardiovascular development: demarcation of arterial/venous domains, vascular morphogenesis, and sprouting angiogenesis. *Genes Dev.* 13, 295–306.
- Aiello, L.P. (2005). Angiogenic pathways in diabetic retinopathy. *N. Engl. J. Med.* 353, 839–841.
- Aiello, L.P., Pierce, E.A., Foley, E.D., Takagi, H., Chen, H., Riddle, L., Ferrara, N., King, G.L., and Smith, L.E. (1995). Suppression of retinal neovascularization in vivo by inhibition of vascular endothelial growth factor (VEGF) using soluble VEGF-receptor chimeric proteins. *Proc. Natl. Acad. Sci. USA* 92, 10457–10461.
- Ashton, N., Ward, B., and Serpell, G. (1954). Effect of oxygen on developing retinal vessels with particular reference to the problem of retrolental fibroplasia. *Br. J. Ophthalmol.* 38, 397–432.
- Bernales, S., Papa, F.R., and Walter, P. (2006). Intracellular signaling by the unfolded protein response. *Annu. Rev. Cell Dev. Biol.* 22, 487–508.
- Bruick, R.K. (2003). Oxygen sensing in the hypoxic response pathway: regulation of the hypoxia-inducible transcription factor. *Genes Dev.* 17, 2614–2623.
- Caldwell, R.B., Bartoli, M., Behzadian, M.A., El-Remessy, A.E., Al-Shabrawey, M., Platt, D.H., and Caldwell, R.W. (2003). Vascular endothelial growth factor and diabetic retinopathy: pathophysiological mechanisms and treatment perspectives. *Diabetes Metab. Res. Rev.* 19, 442–455.
- Campbell, K. (1951). Intensive oxygen therapy as a possible cause of retrolental fibroplasia; a clinical approach. *Med. J. Aust.* 2, 48–50.
- Carmeliet, P., and Jain, R.K. (2011). Molecular mechanisms and clinical applications of angiogenesis. *Nature* 473, 298–307.
- Carmeliet, P., and Tessier-Lavigne, M. (2005). Common mechanisms of nerve and blood vessel wiring. *Nature* 436, 193–200.
- Castets, M., and Mehlen, P. (2010). Netrin-1 role in angiogenesis: to be or not to be a pro-angiogenic factor? *Cell Cycle* 9, 1466–1471.
- Checchin, D., Sennlaub, F., Levavasseur, E., Leduc, M., and Chemtob, S. (2006). Potential role of microglia in retinal blood vessel formation. *Invest. Ophthalmol. Vis.*

Sci. 47, 3595–3602.

Chen, J., and Smith, L.E. (2007). Retinopathy of prematurity. *Angiogenesis* 10, 133–140.

Chen, X., Kintner, D.B., Luo, J., Baba, A., Matsuda, T., and Sun, D. (2008). Endoplasmic reticulum Ca<sup>2+</sup> dysregulation and endoplasmic reticulum stress following in vitro neuronal ischemia: role of Na<sup>+</sup>-K<sup>+</sup>-Cl<sup>-</sup> cotransporter. *J. Neurochem.* 106, 1563–1576.

Cheung, N., and Wong, T.Y. (2008). Diabetic retinopathy and systemic vascular complications. *Prog. Retin. Eye Res.* 27, 161–176.

Corset, V., Nguyen-Ba-Charvet, K.T., Forcet, C., Moyses, E., Chedotal, A., and Mehlen, P. (2000). Netrin-1-mediated axon outgrowth and cAMP production requires interaction with adenosine A2b receptor. *Nature* 407, 747–750.

D'Amore, P.A., and Sweet, E. (1987). Effects of hyperoxia on microvascular cells in vitro. *In Vitro Cell. Dev. Biol.* 23, 123–128.

Dorrell, M.I., and Friedlander, M. (2006). Mechanisms of endothelial cell guidance and vascular patterning in the developing mouse retina. *Prog. Retin. Eye Res.* 25, 277–295.

Dorrell, M.I., Aguilar, E., Jacobson, R., Trauger, S.A., Friedlander, J., Siuzdak, G., and Friedlander, M. (2010). Maintaining retinal astrocytes normalizes revascularization and prevents vascular pathology associated with oxygen-induced retinopathy. *Glia* 58, 43–54.

Drogat, B., Auguste, P., Nguyen, D.T., Bouhecareilh, M., Pineau, R., Nalbantoglu, J., Kaufman, R.J., Chevet, E., Bikfalvi, A., and Moenner, M. (2007). IRE1 signaling is essential for ischemia-induced vascular endothelial growth factor-A expression and contributes to angiogenesis and tumor growth in vivo. *Cancer Res.* 67, 6700–6707.

Dull, T., Zufferey, R., Kelly, M., Mandel, R.J., Nguyen, M., Trono, D., and Naldini, L. (1998). A third-generation lentivirus vector with a conditional packaging system. *J. Virol.* 72, 8463–8471.

Edwards, M.M., McLeod, D.S., Li, R., Grebe, R., Bhutto, I., Mu, X., and Lutty, G.A. (2012). The deletion of Math5 disrupts retinal blood vessel and glial development in mice. *Exp. Eye Res.* 96, 147–156.

Eichmann, A., and Thomas, J.L. (2012). *Molecular Parallels between Neural and Vascular Development* (New York: Cold Spring Harbor Perspect Med).

Erskine, L., Reijntjes, S., Pratt, T., Denti, L., Schwarz, Q., Vieira, J.M., Alakakone, B., Shewan, D., and Ruhrberg, C. (2011). VEGF signaling through neuropilin 1 guides commissural axon crossing at the optic chiasm. *Neuron* 70, 951–965.

Fantin, A., Vieira, J.M., Gestri, G., Denti, L., Schwarz, Q., Prykhodzhiy, S., Peri, F., Wilson, S.W., and Ruhrberg, C. (2010). Tissue macrophages act as cellular chaperones for vascular anastomosis downstream of VEGF-mediated endothelial tip cell induction. *Blood* 116, 829–840.

Farina, C., Aloisi, F., and Meinl, E. (2007). Astrocytes are active players in cerebral innate immunity. *Trends Immunol.* 28, 138–145.

Ferrara, N., and Kerbel, R.S. (2005). Angiogenesis as a therapeutic target. *Nature* 438, 967–974.

Fujita, H., Zhang, B., Sato, K., Tanaka, J., and Sakanaka, M. (2001). Expressions of neuropilin-1, neuropilin-2 and semaphorin 3A mRNA in the rat brain after middle cerebral artery occlusion. *Brain Res.* 914, 1–14.

Fukushima, Y., Okada, M., Kataoka, H., Hirashima, M., Yoshida, Y., Mann, F., Gomi, F., Nishida, K., Nishikawa, S., and Uemura, A. (2011). Sema3E-PlexinD1 signaling selectively suppresses disoriented angiogenesis in ischemic retinopathy in mice. *J. Clin. Invest.* 121, 1974–1985.

Gerhardt, H., Golding, M., Fruttiger, M., Ruhrberg, C., Lundkvist, A., Abramsson, A., Jeltsch, M., Mitchell, C., Alitalo, K., Shima, D., and Betsholtz, C. (2003). VEGF guides angiogenic sprouting utilizing endothelial tip cell filopodia. *J. Cell Biol.* 161, 1163–1177.

Ghosh, R., Lipson, K.L., Sargent, K.E., Mercurio, A.M., Hunt, J.S., Ron, D., and Urano, F. (2010). Transcriptional regulation of VEGF-A by the unfolded protein response pathway. *PLoS ONE* 5, e9575.

Gilbert, C., Rahi, J., Eckstein, M., O’Sullivan, J., and Foster, A. (1997). Retinopathy of prematurity in middle-income countries. *Lancet* 350, 12–14.

Han, D., Lerner, A.G., Vande Walle, L., Upton, J.-P., Xu, W., Hagen, A., Backes, B.J., Oakes, S.A., and Papa, F.R. (2009). IRE1 $\alpha$  kinase activation modes control alternate endoribonuclease outputs to determine divergent cell fates. *Cell* 138, 562–575.

Hayashi, T., Saito, A., Okuno, S., Ferrand-Drake, M., Dodd, R.L., and Chan, P.H. (2005). Damage to the endoplasmic reticulum and activation of apoptotic machinery by oxidative stress in ischemic neurons. *J. Cereb. Blood Flow Metab.* 25, 41–53.

Hollien, J., and Weissman, J.S. (2006). Decay of endoplasmic reticulum-localized mRNAs during the unfolded protein response. *Science* 313, 104–107.

Hollien, J., Lin, J.H., Li, H., Stevens, N., Walter, P., and Weissman, J.S. (2009). Regulated Ire1-dependent decay of messenger RNAs in mammalian cells. *J. Cell Biol.* 186, 323–331.

Ishida, S., Usui, T., Yamashiro, K., Kaji, Y., Amano, S., Ogura, Y., Hida, T., Oguchi, Y., Ambati, J., Miller, J.W., et al. (2003). VEGF<sub>164</sub>-mediated inflammation is required for pathological, but not physiological, ischemia-induced retinal neovascularization. *J. Exp. Med.* 198, 483–489.

Jones, C.A., London, N.R., Chen, H., Park, K.W., Sauvaget, D., Stockton, R.A., Wythe, J.D., Suh, W., Larrieu-Lahargue, F., Mukoyama, Y.S., et al. (2008). Robo4 stabilizes the vascular network by inhibiting pathologic angiogenesis and endothelial hyperpermeability. *Nat. Med.* 14, 448–453.

Joyal, J.-S., Sitaras, N., Binet, F., Rivera, J.C., Stahl, A., Zaniolo, K., Shao, Z., Polosa, A., Zhu, T., Hamel, D., et al. (2011). Ischemic neurons prevent vascular regeneration of neural tissue by secreting semaphorin 3A. *Blood* 117, 6024–6035.

Kempner, J.H., O’Colmain, B.J., Leske, M.C., Haffner, S.M., Klein, R., Moss, S.E., Taylor, H.R., and Hamman, R.F.; Eye Diseases Prevalence Research Group. (2004). The prevalence of diabetic retinopathy among adults in the United States. *Arch. Ophthalmol.* 122, 552–563.

Kennedy, T.E., Serafini, T., de la Torre, J.R., and Tessier-Lavigne, M. (1994). Netrins

are diffusible chemotropic factors for commissural axons in the embryonic spinal cord. *Cell* 78, 425–435.

Kim, J., Oh, W.J., Gaiano, N., Yoshida, Y., and Gu, C. (2011). Semaphorin 3E-Plexin-D1 signaling regulates VEGF function in developmental angiogenesis via a feedback mechanism. *Genes Dev.* 25, 1399–1411.

Klagsbrun, M., and Eichmann, A. (2005). A role for axon guidance receptors and ligands in blood vessel development and tumor angiogenesis. *Cytokine Growth Factor Rev.* 16, 535–548.

Lang, R.A., and Bishop, J.M. (1993). Macrophages are required for cell death and tissue remodeling in the developing mouse eye. *Cell* 74, 453–462.

Lange, C.A., and Bainbridge, J.W. (2012). Oxygen sensing in retinal health and disease. *Ophthalmologica* 227, 115–131.

Lange, C.A., Stavrakas, P., Luhmann, U.F., de Silva, D.J., Ali, R.R., Gregor, Z.J., and Bainbridge, J.W. (2011). Intraocular oxygen distribution in advanced proliferative diabetic retinopathy. *Am. J. Ophthalmol.* 152, 406–412, e3.

Larrivee, B., Freitas, C., Trombe, M., Lv, X., Delafarge, B., Yuan, L., Bouvree, K., Breant, C., Del Toro, R., Brechot, N., et al. (2007). Activation of the UNC5B receptor by Netrin-1 inhibits sprouting angiogenesis. *Genes Dev.* 21, 2433–2447.

Larrivee, B., Freitas, C., Suchting, S., Brunet, I., and Eichmann, A. (2009). Guidance of vascular development: lessons from the nervous system. *Circ. Res.* 104, 428–441.

Lee, J., Sun, C., Zhou, Y., Lee, J., Gokalp, D., Herrema, H., Park, S.W., Davis, R.J., and Ozcan, U. (2011). p38 MAPK-mediated regulation of Xbp1s is crucial for glucose homeostasis. *Nat. Med.* 17, 1251–1260.

Lejmi, E., Leconte, L., Pedron-Mazoyer, S., Ropert, S., Raoul, W., Lavalette, S., Bouras, I., Feron, J.G., Maitre-Boube, M., Assayag, F., et al. (2008). Netrin-4 inhibits angiogenesis via binding to neogenin and recruitment of Unc5B. *Proc. Natl. Acad. Sci. USA* 105, 12491–12496.

Leon, S., Yin, Y., Nguyen, J., Irwin, N., and Benowitz, L.I. (2000). Lens injury stimulates axon regeneration in the mature rat optic nerve. *J. Neurosci.* 20, 4615–4626.

Lerner, A.G., Upton, J.P., Praveen, P.V., Ghosh, R., Nakagawa, Y., Igbaria, A., Shen, S., Nguyen, V., Backes, B.J., Heiman, M., et al. (2012). IRE1a induces thioredoxin-interacting protein to activate the NLRP3 inflammasome and promote programmed cell death under irremediable ER stress. *Cell Metab.* 16, 250–264.

Lipson, K.L., Ghosh, R., and Urano, F. (2008). The role of IRE1alpha in the degradation of insulin mRNA in pancreatic beta-cells. *PLoS ONE* 3, e1648.

Lo, E.H. (2008). A new penumbra: transitioning from injury into repair after stroke. *Nat. Med.* 14, 497–500.

London, A., Itskovich, E., Benhar, I., Kalchenko, V., Mack, M., Jung, S., and Schwartz, M. (2011). Neuroprotection and progenitor cell renewal in the injured adult murine retina requires healing monocyte-derived macrophages. *J. Exp. Med.* 208, 23–39.

Lu, X., Le Noble, F., Yuan, L., Jiang, Q., De Lafarge, B., Sugiyama, D., Breant, C., Claes, F., De Smet, F., Thomas, J.L., et al. (2004). The netrin receptor UNC5B mediates

guidance events controlling morphogenesis of the vascular system. *Nature* 432, 179–186.

Lundbaek, K., Christensen, N.J., Jensen, V.A., Johansen, K., Olsen, T.S., Hansen, A.P., Orskov, H., and Osterby, R. (1970). Diabetes, diabetic angiopathy, and growth hormone. *Lancet* 2, 131–133.

Ly, N.P., Komatsuzaki, K., Fraser, I.P., Tseng, A.A., Prodhon, P., Moore, K.J., and Kinane, T.B. (2005). Netrin-1 inhibits leukocyte migration in vitro and in vivo. *Proc. Natl. Acad. Sci. USA* 102, 14729–14734.

Malhi, H., and Kaufman, R.J. (2011). Endoplasmic reticulum stress in liver disease. *J. Hepatol.* 54, 795–809.

Marciniak, S.J., and Ron, D. (2006). Endoplasmic reticulum stress signaling in disease. *Physiol. Rev.* 86, 1133–1149.

Miao, H.Q., Soker, S., Feiner, L., Alonso, J.L., Raper, J.A., and Klagsbrun, M. (1999). Neuropilin-1 mediates collapsin-1/semaphorin III inhibition of endothelial cell motility: functional competition of collapsin-1 and vascular endothelial growth factor-165. *J. Cell Biol.* 146, 233–242.

Michaelson, I.C. (1948). The mode of development of the vascular system of the retina with some observations on its significance for certain retinal disorders. *Trans. Ophthalmol. Soc. UK.* 68, 137–180.

Mino, R.P., Spoerri, P.E., Caballero, S., Player, D., Belardinelli, L., Biaggioni, I., and Grant, M.B. (2001). Adenosine receptor antagonists and retinal neovascularization in vivo. *Invest. Ophthalmol. Vis. Sci.* 42, 3320–3324.

Mirakaj, V., Gatidou, D., Potzsch, C., König, K., and Rosenberger, P. (2011). Netrin-1 signaling dampens inflammatory peritonitis. *J. Immunol.* 186, 549–555.

Moskowitz, M.A., Lo, E.H., and Iadecola, C. (2010). The science of stroke: mechanisms in search of treatments. *Neuron* 67, 181–198.

Nguyen, M.D., Julien, J.P., and Rivest, S. (2002). Innate immunity: the missing link in neuroprotection and neurodegeneration? *Nat. Rev. Neurosci.* 3, 216–227.

Nishiyama, M., Hoshino, A., Tsai, L., Henley, J.R., Goshima, Y., Tessier-Lavigne, M., Poo, M.M., and Hong, K. (2003). Cyclic AMP/GMP-dependent modulation of Ca<sup>2+</sup> channels sets the polarity of nerve growth-cone turning. *Nature* 423, 990–995.

Oikawa, D., Tokuda, M., and Iwawaki, T. (2007). Site-specific cleavage of CD59 mRNA by endoplasmic reticulum-localized ribonuclease, IRE1. *Biochem. Biophys. Res. Commun.* 360, 122–127.

Oikawa, D., Tokuda, M., Hosoda, A., and Iwawaki, T. (2010). Identification of a consensus element recognized and cleaved by IRE1 alpha. *Nucleic Acids Res.* 38, 6265–6273.

Oyadomari, S., and Mori, M. (2004). Roles of CHOP/GADD153 in endoplasmic reticulum stress. *Cell Death Differ.* 11, 381–389.

Park, K.W., Crouse, D., Lee, M., Karnik, S.K., Sorensen, L.K., Murphy, K.J., Kuo, C.J., and Li, D.Y. (2004). The axonal attractant Netrin-1 is an angiogenic factor. *Proc. Natl. Acad. Sci. USA* 101, 16210–16215.

Paschen, W., and Doutheil, J. (1999). Disturbances of the functioning of endoplasmic reticulum: a key mechanism underlying neuronal cell injury? *J. Cereb. Blood Flow Metab.* 19, 1–18.

Paul, S.A., Simons, J.W., and Mabeesh, N.J. (2004). HIF at the crossroads between ischemia and carcinogenesis. *J. Cell. Physiol.* 200, 20–30.

Pierce, E.A., Avery, R.L., Foley, E.D., Aiello, L.P., and Smith, L.E. (1995). Vascular endothelial growth factor/vascular permeability factor expression in a mouse model of retinal neovascularization. *Proc. Natl. Acad. Sci. USA* 92, 905–909.

Pierce, E.A., Foley, E.D., and Smith, L.E. (1996). Regulation of vascular endothelial growth factor by oxygen in a model of retinopathy of prematurity. *Arch. Ophthalmol.* 114, 1219–1228.

Ritter, M.R., Banin, E., Moreno, S.K., Aguilar, E., Dorrell, M.I., and Friedlander, M. (2006). Myeloid progenitors differentiate into microglia and promote vascular repair in a model of ischemic retinopathy. *J. Clin. Invest.* 116, 3266–3276.

Robinson, G.S., Ju, M., Shih, S.C., Xu, X., McMahon, G., Caldwell, R.B., and Smith, L.E. (2001). Nonvascular role for VEGF: VEGFR-1, 2 activity is critical for neural retinal development. *FASEB J.* 15, 1215–1217.

Ron, D., and Walter, P. (2007). Signal integration in the endoplasmic reticulum unfolded protein response. *Nat. Rev. Mol. Cell Biol.* 8, 519–529.

Rosas-Ballina, M., Olofsson, P.S., Ochani, M., Valde s-Ferrer, S.I., Levine, Y.A., Reardon, C., Tusche, M.W., Pavlov, V.A., Andersson, U., Chavan, S., et al. (2011). Acetylcholine-synthesizing T cells relay neural signals in a vagus nerve circuit. *Science* 334, 98–101.

Rosenberger, P., Schwab, J.M., Mirakaj, V., Masekowsky, E., Mager, A., Morote-Garcia, J.C., Unertl, K., and Eltzschig, H.K. (2009). Hypoxia-inducible factor-dependent induction of netrin-1 dampens inflammation caused by hypoxia. *Nat. Immunol.* 10, 195–202.

Sapieha, P. (2012). Eyeing central neurons in vascular growth and reparative angiogenesis. *Blood* 120, 2182–2194.

Sapieha, P., Sirinyan, M., Hamel, D., Zaniolo, K., Joyal, J.-S., Cho, J.-H., Honore, J.-C., Kermorvant-Duchemin, E., Varma, D.R., Tremblay, S., et al. (2008). The succinate receptor GPR91 in neurons has a major role in retinal angiogenesis. *Nat. Med.* 14, 1067–1076.

Sapieha, P., Hamel, D., Shao, Z., Rivera, J.C., Zaniolo, K., Joyal, J.S., and Chemtob, S. (2010a). Proliferative retinopathies: angiogenesis that blinds. *Int. J. Biochem. Cell Biol.* 42, 5–12.

Sapieha, P., Joyal, J.S., Rivera, J.C., Kermorvant-Duchemin, E., Sennlaub, F., Hardy, P., Lachapelle, P., and Chemtob, S. (2010b). Retinopathy of prematurity: understanding ischemic retinal vasculopathies at an extreme of life. *J. Clin. Invest.* 120, 3022–3032.

Schroder, M., and Kaufman, R.J. (2005). ER stress and the unfolded protein response. *Mutat. Res.* 569, 29–63.

Shekarabi, M., and Kennedy, T.E. (2002). The netrin-1 receptor DCC promotes filopodia formation and cell spreading by activating Cdc42 and Rac1. *Mol. Cell. Neurosci.* 19, 1–17.

Shewan, D., Dwivedy, A., Anderson, R., and Holt, C.E. (2002). Age-related changes underlie switch in netrin-1 responsiveness as growth cones advance along visual

pathway. *Nat. Neurosci.* 5, 955–962.

Simons, B.D., and Flynn, J.T. (1999). Retinopathy of prematurity and associated factors. *Int. Ophthalmol. Clin.* 39, 29–48.

Smith, L.E. (2004). Pathogenesis of retinopathy of prematurity. *Growth Horm. IGF Res.* 14(Suppl A ), S140–S144.

Smith, L.E. (2008). Through the eyes of a child: understanding retinopathy through ROP the Friedenwald lecture. *Invest. Ophthalmol. Vis. Sci.* 49, 5177–5182.

Smith, L.E., Wesolowski, E., McLellan, A., Kostyk, S.K., D’Amato, R., Sullivan, R., and D’Amore, P.A. (1994). Oxygen-induced retinopathy in the mouse. *Invest. Ophthalmol. Vis. Sci.* 35, 101–111.

Soker, S., Takashima, S., Miao, H.Q., Neufeld, G., and Klagsbrun, M. (1998). Neuropilin-1 is expressed by endothelial and tumor cells as an isoform-specific receptor for vascular endothelial growth factor. *Cell* 92, 735–745.

Stahl, A., Connor, K.M., Sapieha, P., Willett, K.L., Krah, N.M., Dennison, R.J., Chen, J., Guerin, K.I., and Smith, L.E. (2009). Computer-aided quantification of retinal neovascularization. *Angiogenesis* 12, 297–301.

Stahl, A., Connor, K.M., Sapieha, P., Chen, J., Dennison, R.J., Krah, N.M., Seaward, M.R., Willett, K.L., Aderman, C.M., Guerin, K.I., et al. (2010). The mouse retina as an angiogenesis model. *Invest. Ophthalmol. Vis. Sci.* 51, 2813–2826.

Stefater, J.A., 3rd, Lewkowich, I., Rao, S., Mariggi, G., Carpenter, A.C., Burr, A.R., Fan, J., Ajima, R., Molkentin, J.D., Williams, B.O., et al. (2011). Regulation of angiogenesis by a non-canonical Wnt-Flt1 pathway in myeloid cells. *Nature* 474, 511–515.

Stefater, J.A., 3rd, Lewkowich, I., Rao, S., Mariggi, G., Carpenter, A.C., Burr, A.R., Fan, J., Ajima, R., Molkentin, J.D., Williams, B.O., et al. (2011a). Regulation of angiogenesis by a non-canonical Wnt-Flt1 pathway in myeloid cells. *Nature* 474, 511–515.

Stefater, J.A., 3rd, Ren, S., Lang, R.A., and Duffield, J.S. (2011b). Metchnikoff’s policemen: macrophages in development, homeostasis and regeneration. *Trends Mol. Med.* 17, 743–752.

Stein, E., Zou, Y., Poo, M., and Tessier-Lavigne, M. (2001). Binding of DCC by netrin-1 to mediate axon guidance independent of adenosine A2B receptor activation. *Science* 291, 1976–1982.

Stewart, M.W. (2012). The expanding role of vascular endothelial growth factor inhibitors in ophthalmology. *Mayo Clin. Proc.* 87, 77–88.

Tabas, I. (2010). The role of endoplasmic reticulum stress in the progression of atherosclerosis. *Circ. Res.* 107, 839–850.

Tabas, I., and Ron, D. (2011). Integrating the mechanisms of apoptosis induced by endoplasmic reticulum stress. *Nat. Cell Biol.* 13, 184–190.

Tadavadi, R.K., Wang, W., and Ramesh, G. (2010). Netrin-1 regulates Th1/Th2/Th17 cytokine production and inflammation through UNC5B receptor and protects kidney against ischemia-reperfusion injury. *J. Immunol.* 185, 3750–3758.

Tajiri, S., Oyadomari, S., Yano, S., Morioka, M., Gotoh, T., Hamada, J.I., Ushio, Y., and Mori, M. (2004). Ischemia-induced neuronal cell death is mediated by the

endoplasmic reticulum stress pathway involving CHOP. *Cell Death Differ.* 11, 403–415.

Tesfamariam, B. (1994). Free radicals in diabetic endothelial cell dysfunction. *Free Radic. Biol. Med.* 16, 383–391.

van Rooijen, N., and van Kesteren-Hendrikx, E. (2002). Clodronate liposomes: perspectives in research and therapeutics. *J. Liposome Res.* 12, 81–94.

van Rooijen, N., and van Kesteren-Hendrikx, E. (2003). “In vivo” depletion of macrophages by liposome-mediated “suicide”. *Methods Enzymol.* 373, 3–16.

Wang, W., Reeves, W.B., and Ramesh, G. (2009). Netrin-1 increases proliferation and migration of renal proximal tubular epithelial cells via the UNC5B receptor. *Am. J. Physiol. Renal Physiol.* 296, F723–F729.

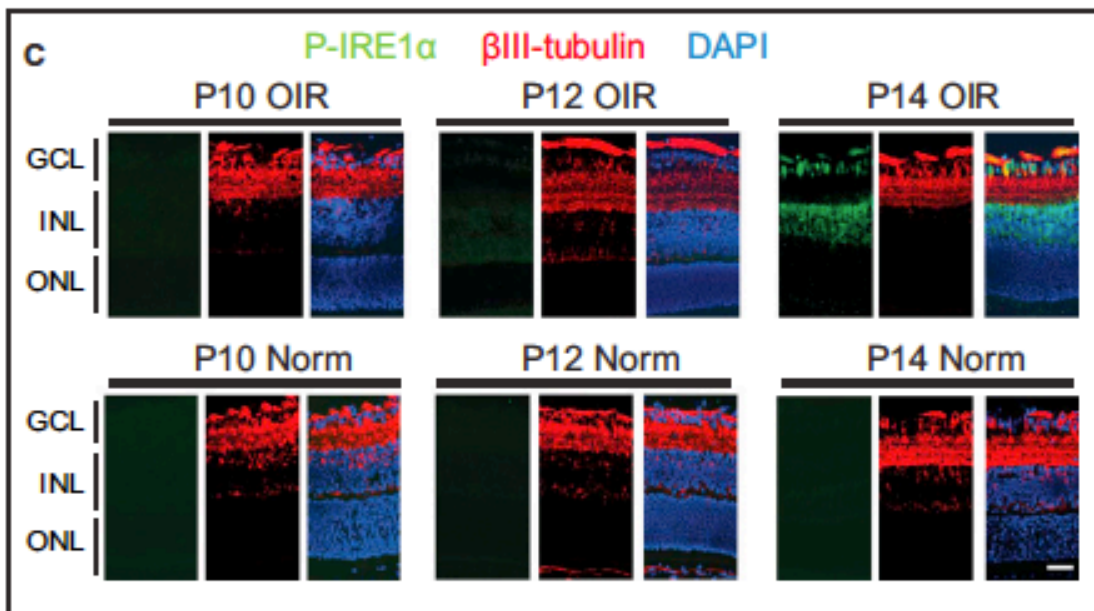
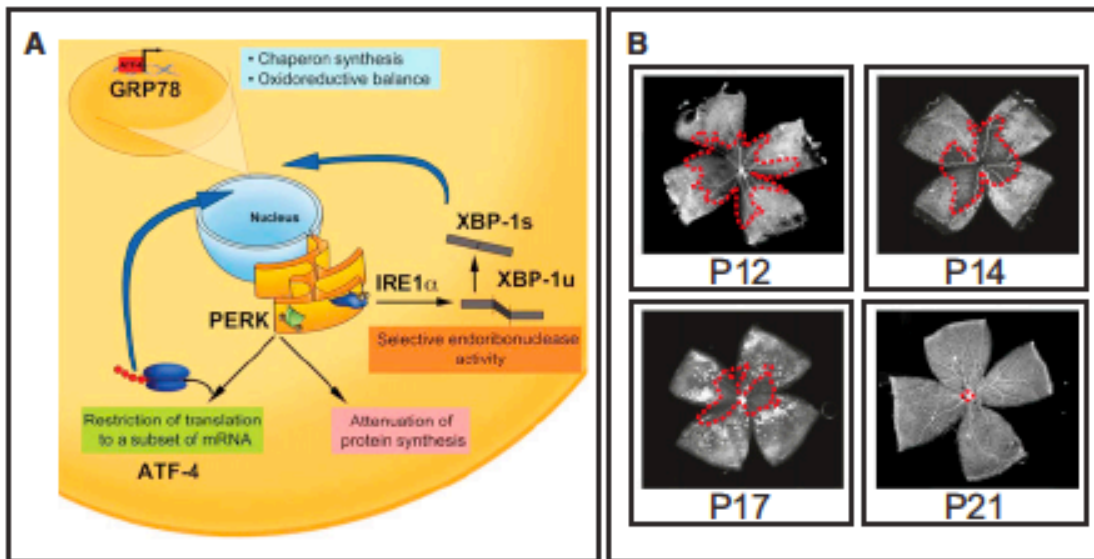
Wilson, B.D., Li, M., Park, K.W., Suli, A., Sorensen, L.K., Larrieu-Lahargue, F., Urness, L.D., Suh, W., Asai, J., Kock, G.A., et al. (2006). Netrins promote developmental and therapeutic angiogenesis. *Science* 313, 640–644.

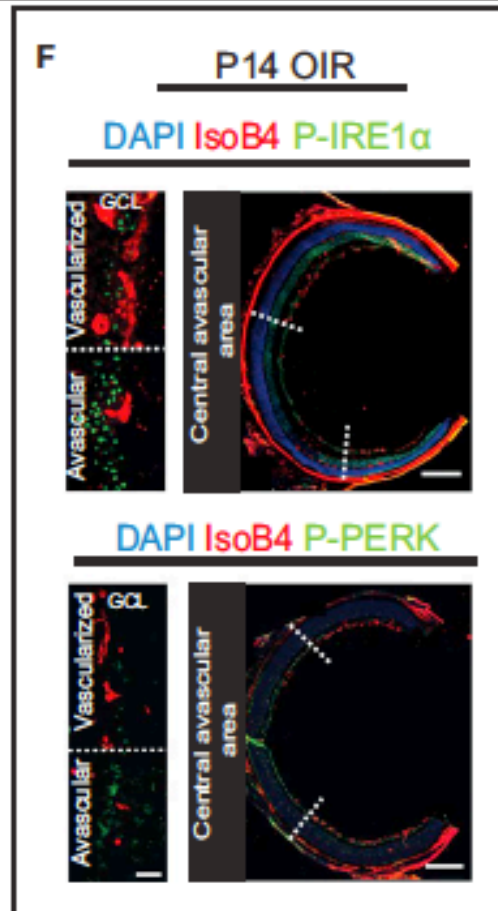
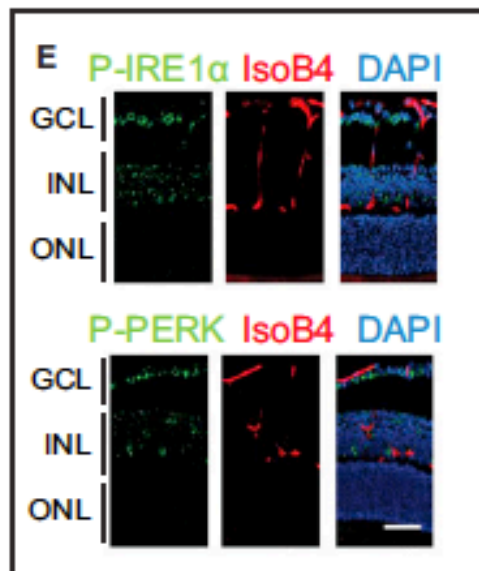
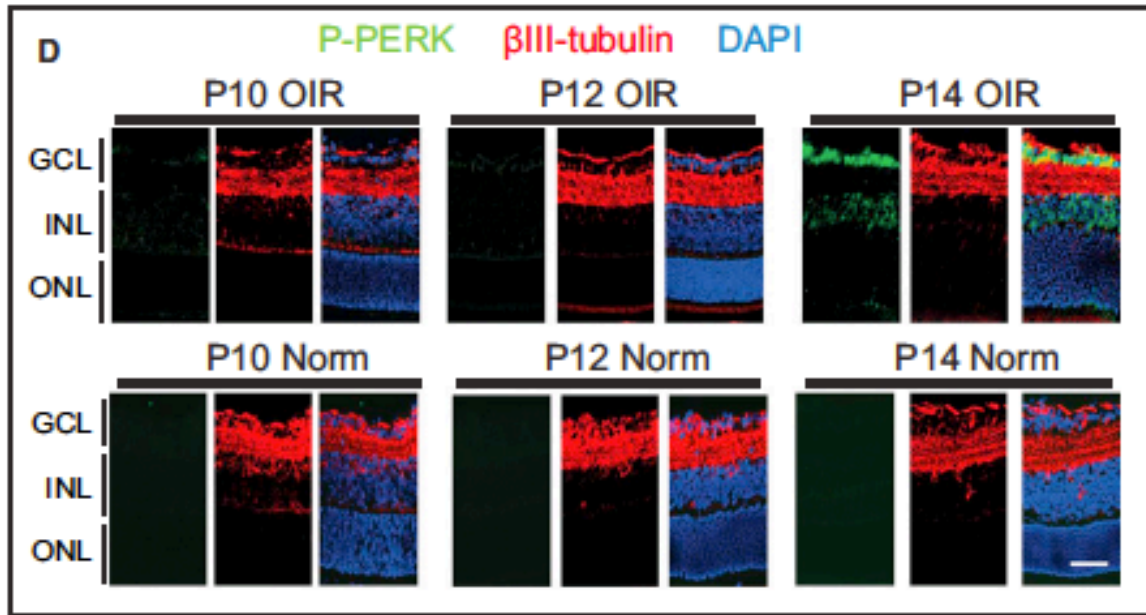
Xu, C., Bailly-Maitre, B., and Reed, J.C. (2005). Endoplasmic reticulum stress: cell life and death decisions. *J. Clin. Invest.* 115, 2656–2664.

Wong, C.H., Jenne, C.N., Lee, W.Y., Leger, C., and Kubes, P. (2011). Functional innervation of hepatic iNKT cells is immunosuppressive following stroke *Science* 334, 101–105.

J.M. (2011). A2B adenosine receptors inhibit superoxide production from mitochondrial complex I in rabbit cardiomyocytes via a mechanism sensitive to Pertussis toxin. *Br. J. Pharmacol.* 163, 995–1006.

## Figures for Appendix 4





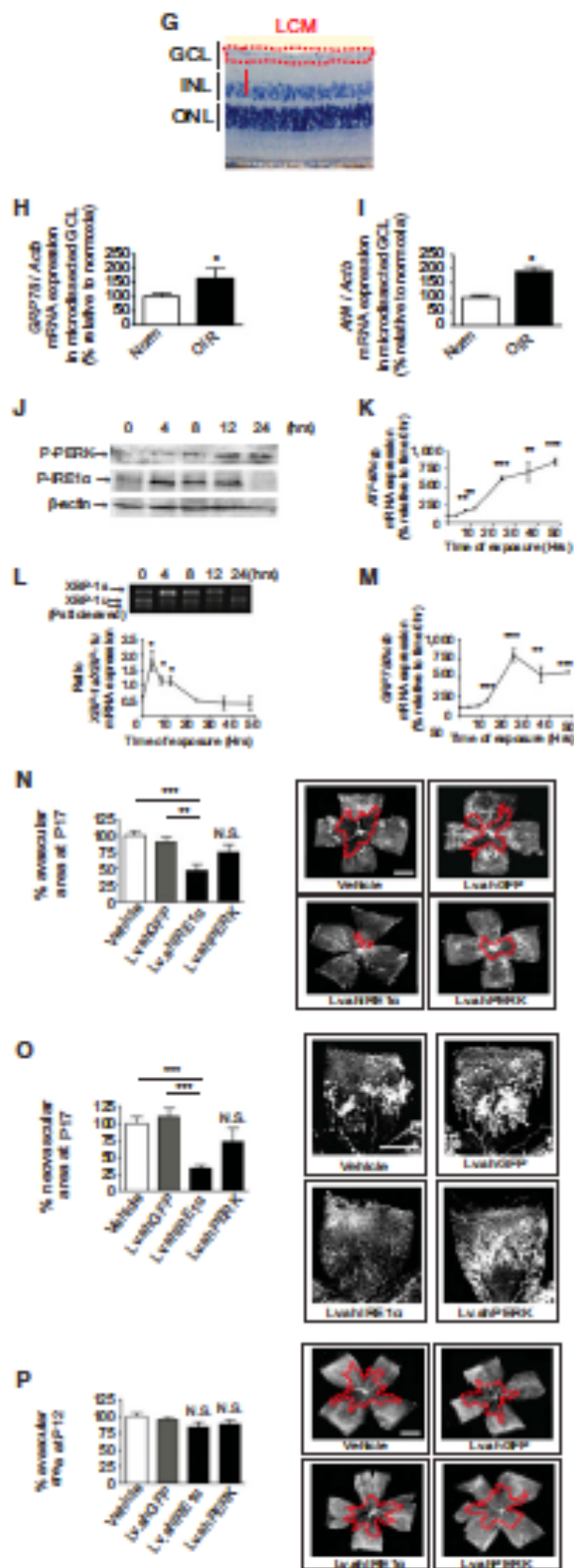


**Figure 1. Neuronal ER Stress Is Induced in Hypoxic Retinas and Associated with Failure of Revascularization** (A) Graphic depiction of canonical ER stress pathways. The PERK arm controls ATF4 expression while IRE1a mediates XBP1 splicing. Both lead to GRP78 expression. (B) Representative photomicrographs of isolectin B4-stained flatmount retinas from the OIR model illustrate the progression of vascular growth following initial vasoobliteration. Upon exit from O2 at P12, the retina attempts to revascularize, yet there is an initial stall in regrowth followed by pathological preretinal neovascularization (white sprouts) that peaks at P17. Successively, vessels enter the avascular retina toward P19–P21, and the preretinal neovascularization regresses. (C) Sagittal retinal sections show that phosphorylated IRE1a is robustly induced at P14 OIR and expressed in the retinal ganglion cell layer (GCL) as demonstrated by colocalization with  $\beta$ III-tubulin-positive RGCs. P-IRE1a also stains cells of the inner nuclear layer (INL). Scale bar: 20  $\mu$ m. (D) Sagittal retinal sections show that phosphorylated PERK is induced at P14 OIR and expressed in the retinal GCL as demonstrated by colocalization with  $\beta$ III-tubulin-positive RGCs. (E) The expression of both markers is more robust in the avascular zones of the retina and does not colocalize with isolectin B4 staining. ONL, outer nuclear layer; INL, inner nuclear layer; GCL, ganglion cell layer. Scale bar: 50  $\mu$ m. (F) Whole retinal cross-sections from P14 OIR confirm that p-IRE1a and p-PERK are expressed robustly in the central avascular area of the retina. Scale bar left panel: 20  $\mu$ m, right panel: 500  $\mu$ m. Images and analysis are representatives of three independent experiments. (G) Sagittal sections of the retina showing the area harvested by LCM. (H and I) ATF4 (H) and GRP78 (I) gene expressions are increased in OIR compared to normoxic littermates as determined by LCM of the ganglion cell layer of the retina. (J) PERK and IRE1a are phosphorylated in response to hypoxia in cultured RGCs. (K–M) ATF4 gene expression (K), XBP1 mRNA splicing (L), and GRP78 gene expression (M) are increased following prolonged hypoxic exposure ( $n = 4$  independent experiments for each gene studied).  $**p < 0.01$  and  $***p < 0.001$ . Values represent a fold increase relative to time 0 hr  $\pm$  SEM. (N–P) During the phase of vascular dropout (P8), an injection of a lentivirus coding for an sh.IRE1a at P3 dramatically enhanced vascular regeneration (N) and decreased the preretinal neovascular area (O) in the regrowth phase of OIR at P17. Injection with a shPERK lentivirus did not result in any significant amelioration of vascular regeneration or reduction of preretinal neovascularization. Treatment with either sh.IRE1a or shPERK at P3 did not lead to noticeable variations in vasoobliteration (P). Representative images of retinas from each condition are presented. Scale bar: 1 mm.  $n = 8$  animals/group;  $*p < 0.05$ ,  $**p < 0.01$ ,  $***p < 0.001$  relative to vehicle-treated retinas  $\pm$  SEM.

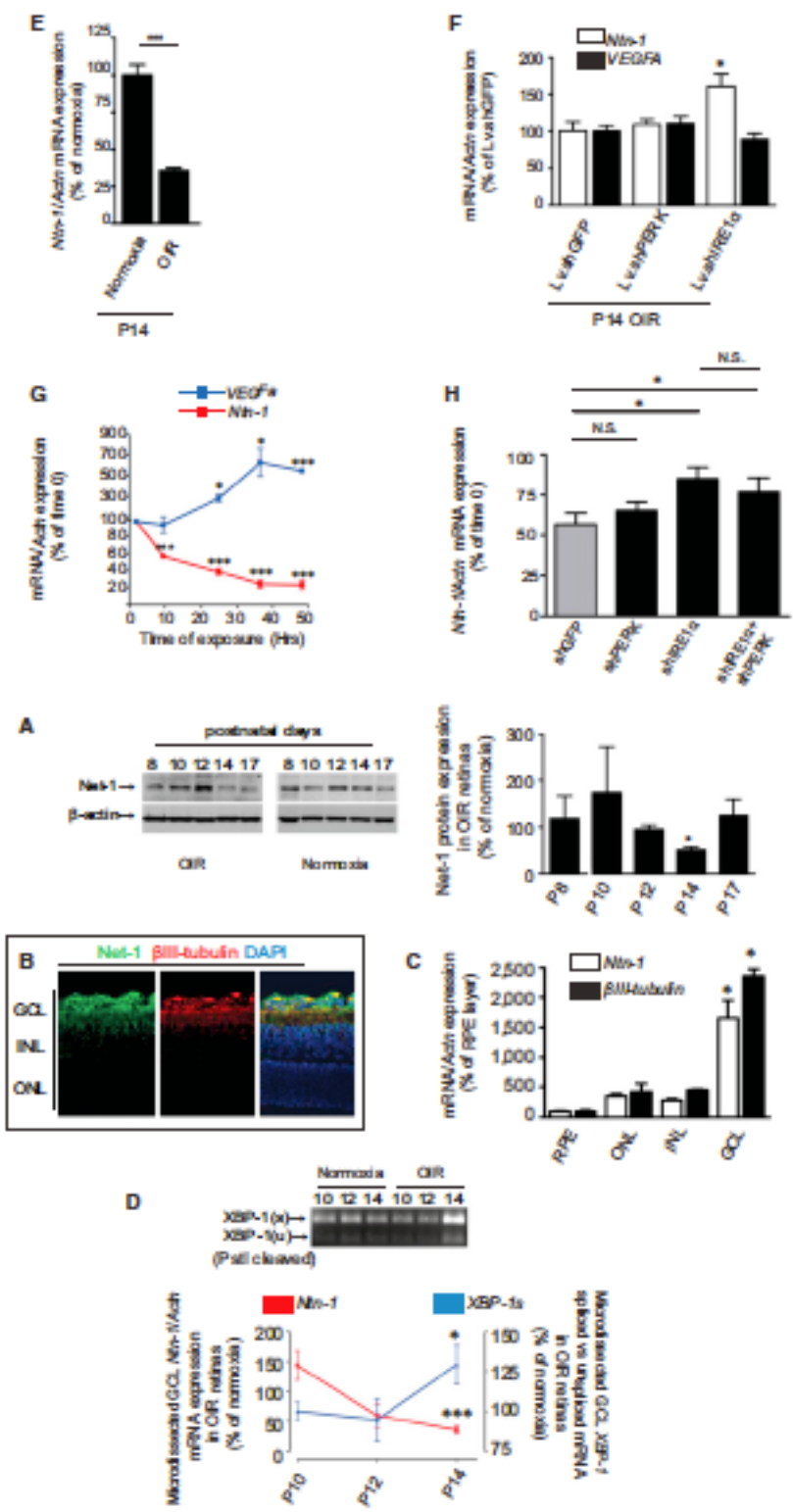
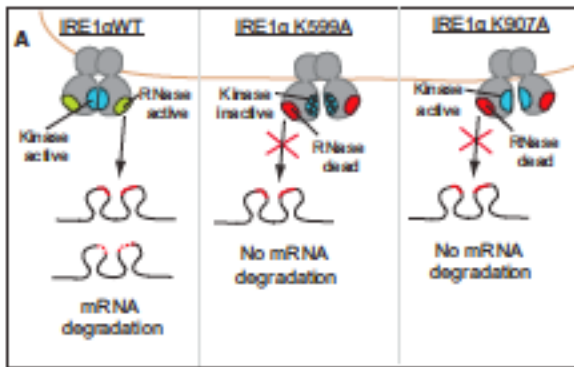


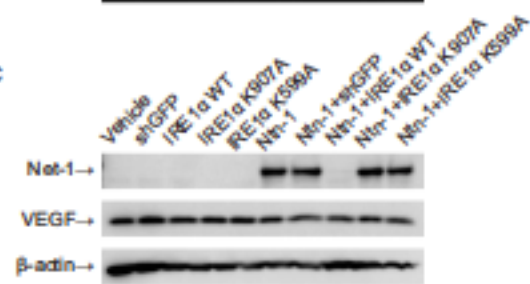
**Figure 2. Netrin-1 Is Downregulated by Hypoxia-Triggered ER Stress (A–C)** Retinal Netrin-1 protein levels (western blot) drop during periods associated with elevated ER stress and vascular regeneration failure in OIR.  $n = 4$  retinas/group,  $*p < 0.05$  relative to normoxia. Netrin-1 is predominantly expressed in the retinal ganglion cell layer and colocalizes with bIII-positive RGCs, as assessed by IHC (B) and LCM (C). RPE = retinal pigment epithelium (representative of three independent experiments; P10 normoxic mouse eye). Scale bar, 50  $\mu$ m;  $*p < 0.05$ . (D) The drop in netrin-1 expression correlates with increased splicing of IRE1a in the ganglion cell layer isolated by LCM.  $*p < 0.05$ ,  $***p < 0.001$  relative to normoxic controls and normalized to P10  $\pm$  SEM.  $n = 3$  independent experiments. (E and F) Netrin-1 gene expression is significantly reduced at P14 OIR (E) but preserved in Lv.sh.IRE1a-injected retinas (F). VEGF expression is not altered by Lv.shPERK and Lv.shIRE1a injections at P14 of OIR.  $n = 4$  retinas. Injection of Lv.sh.PERK does not induce any significant change in netrin-1 gene expression. N.S., not significant;  $*p < 0.05$ ,  $**p < 0.01$  relative to normoxic vehicle or Lv.shGFP-injected retinas  $\pm$  SEM. (G) Temporal gene expression of netrin-1 and VEGF in hypoxic cultured RGC-5 demonstrate the gradual increase of VEGF and the sharp drop in netrin-1.  $n = 4$  independent experiments;  $*p < 0.05$ ,  $***p < 0.001$  relative to time 0 hr  $\pm$  SEM. (H) Lv.shIRE1a preserves netrin-1 mRNA against hypoxic exposure. Graph depicts netrin-1 gene expression after 8 hr of hypoxia in cultured RGCs stably expressing shRNAs for either PERK, IRE1, PERK and IRE1a, or controls.  $n = 5$  independent experiments;  $*p < 0.05$  relative to shGFP-transfected cells  $\pm$  SEM.

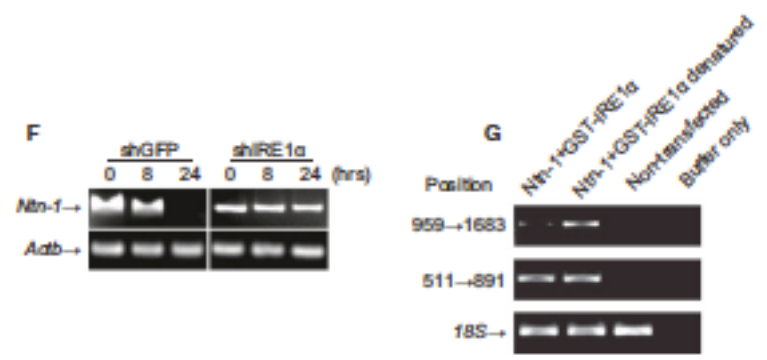
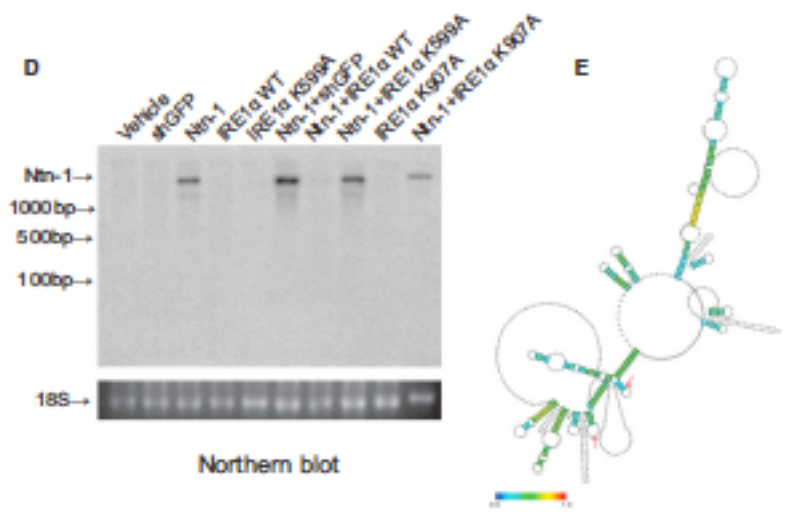


**B**

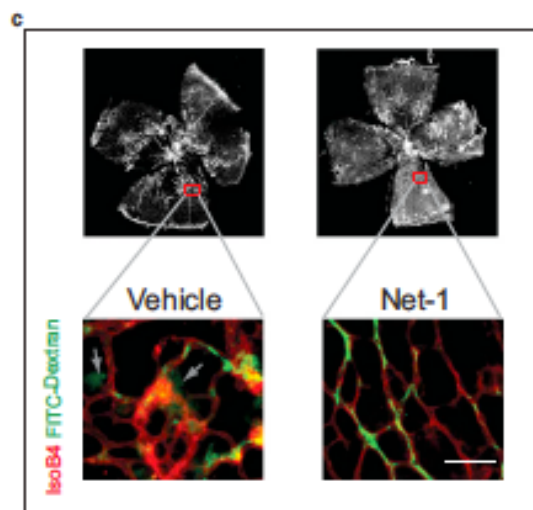
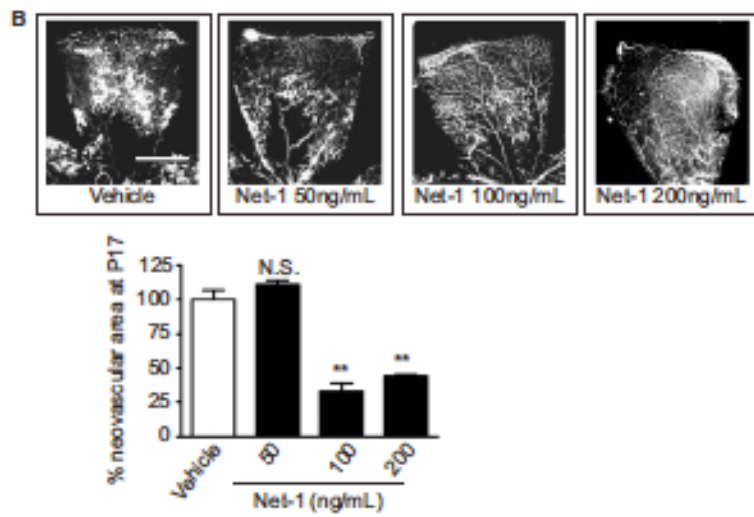
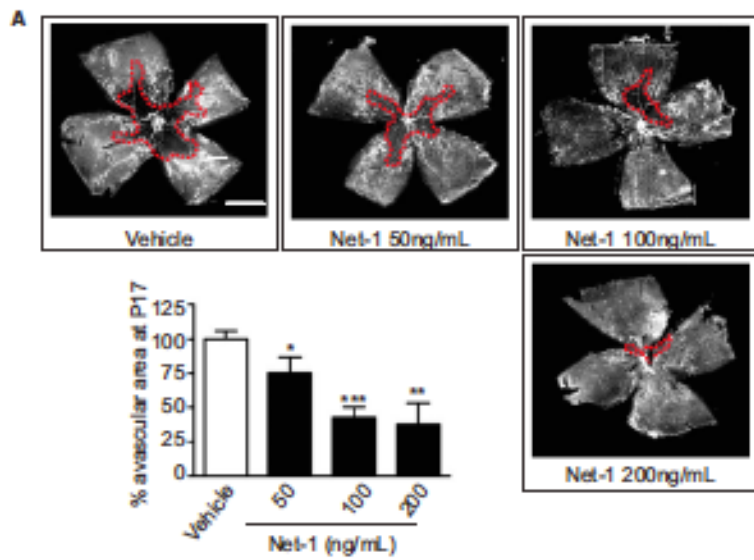


**C**

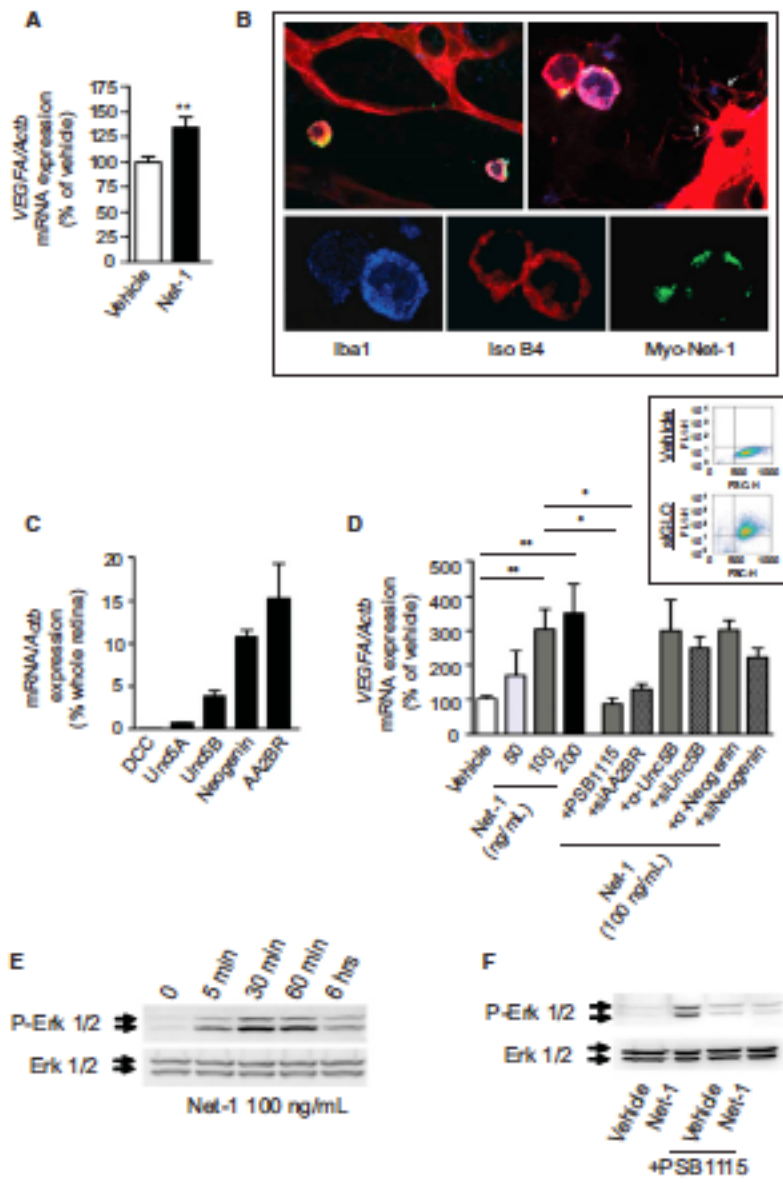




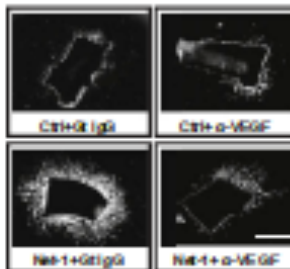
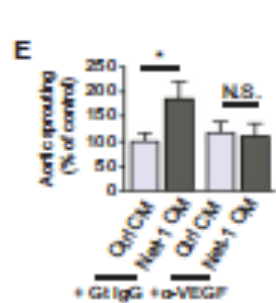
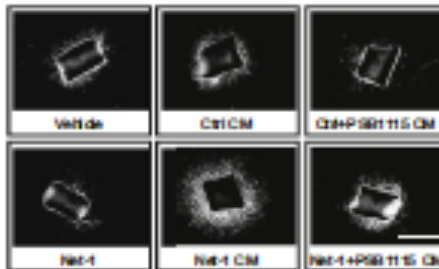
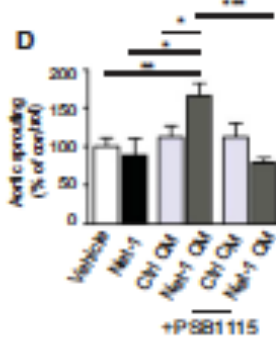
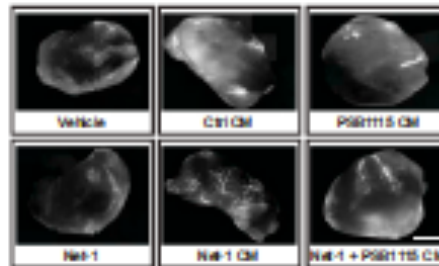
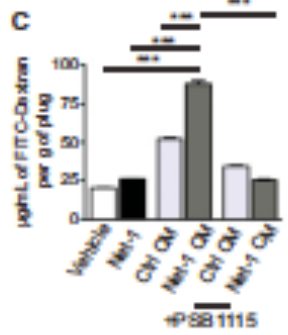
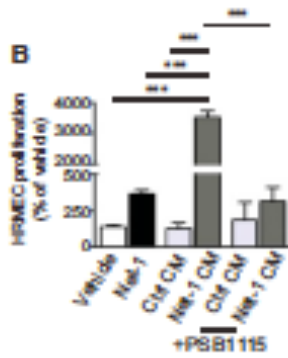
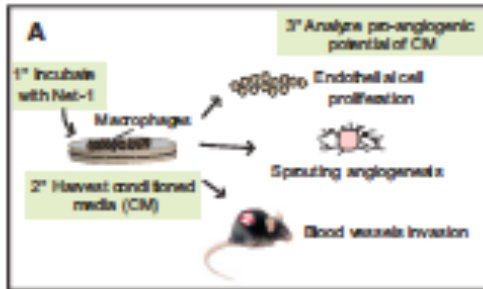
**Figure 3. Netrin-1 Is Cleaved by the RNase Activity of IRE1a** (A) Schematic representation of IRE1a RNase activity following kinase activation, which can be abolished using a K599A or K907A mutant. (B and C) Netrin-1 and IRE1a WT expression plasmid cotransfection results in the degradation of netrin-1 mRNA (B) and protein (C). Cotransfection with an IRE1a endoribonuclease/kinase-dead mutant (K599A), an endoribonuclease inactivated mutant (K907A), or an irrelevant expression plasmid (shGFP) does not induce degradation of netrin-1 mRNA (B) or protein (C). VEGF mRNA (B) and protein (C) are not degraded by IRE1a activity. IRE1a is highly expressed following transfection with IRE1a WT, K599A, or K907A plasmids (third panel) (B). (D) Northern blot showing degradation of the netrin-1 mRNA using the same conditions as in (B) and (C). (E) 2D reconstitution of secondary structure of netrin-1 murine mRNA (position 1191–1960). Red arrows depict putative 50-CAGCAG-30 recognition sites for IRE1a RNase activity in stem loops (position 1605–1610 and 1670–1675). Each predicted base pair is colored with the heat color gradation from blue to red, indicating the base-pairing probability from 0 to 1. (F) Netrin-1 mRNA degradation in hypoxic RGCs (1% O<sub>2</sub>) can be reversed with an shRNA directed against IRE1a. (G) Amplification products with primers spanning the putative cleavage sites (959–1683) show degradation of netrin-1 mRNA with recombinant IREa, an effect not seen with primers outside the cleavage sites (511–891). Panels (B), (C), (D), (F), and (G) are representative of at least three separate experiments.



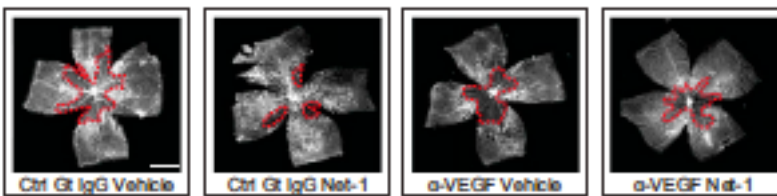
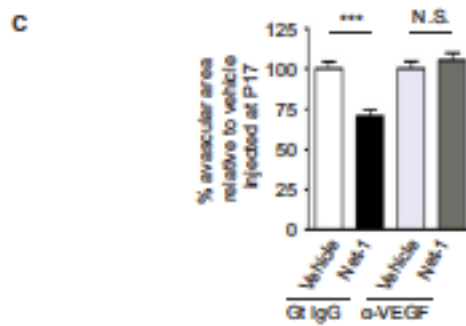
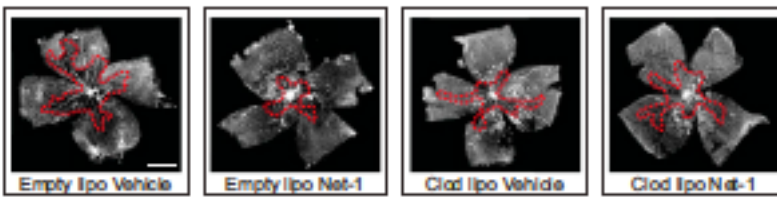
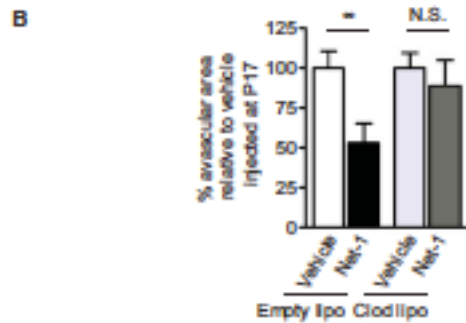
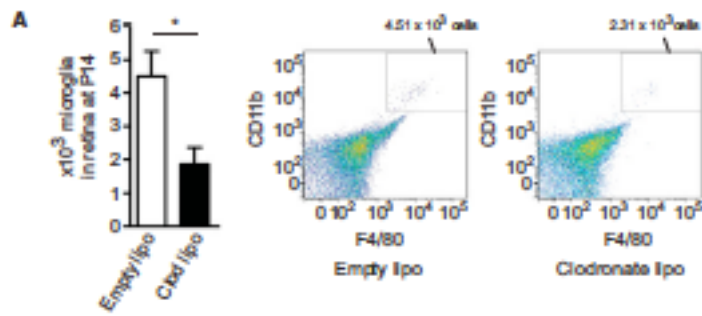
**Figure 4. Administration of Netrin-1 to Ischemic Retinas Enhances Vascular Regeneration and Suppresses Pathologic Neovascularization** (A and B) Isolectin B4 stained retinas from P17 mice injected intravitreally at P14 with 50, 100, or 200 ng/mL of recombinant netrin-1 or vehicle (PBS). Netrin-1 effectively enhanced reparative angiogenesis (A) and diminished neovascular areas (B) as determined at P17. Representative images of retinas for each condition are presented.  $n = 10\text{--}13$  animals/group for each calculation;  $*p < 0.05$ ,  $**p < 0.01$ ,  $***p < 0.001$  relative to vehicle-injected retinas  $\pm$  SEM. Scale bar: 1 mm. (C) Neovessels induced by netrin-1 treatment do not show any signs of leakage of FITC-dextran, as opposed to vehicle-injected retinas. Representative images of three independent experiments. Scale bar: 100  $\mu$ m.



**Figure 5. Netrin-1 Activates AA2BR on Macrophages and Provokes the Release of VEGF in an ERK1/ERK2-Dependent Manner** (A) Intravitreal injection of netrin-1 (100 ng/mL at P14) induces retinal VEGF gene expression at P15 OIR. n = 6 animals/group; \*\*p < 0.01 relative to vehicle injected retinas  $\pm$  SEM. (B) Confocal images of c-Myc-tagged netrin-1 reveals binding to Iba1-positive macrophages/microglia 3 hr postinjection (P14 OIR). Representative images of three independent experiments. (C) Macrophages express classic netrin-1 receptors UNC5B, Neogenin, and AA2BR. Expression was normalized relative to retinas of normoxic mice at P10. n = 3 independent experiments. (D) Netrin-1 induced VEGF gene expression in macrophages after 24 hr of incubation with varying doses of netrin-1. Pretreatment with PSB1115 (5 mM) lead to a significant reduction in VEGF expression while anti-UNC5B or anti-neogenin neutralizing antibody (both used at 5 mg/mL) did not affect netrin-1-induced VEGF expression. n = 6 independent experiments. These results were confirmed using siRNA against AA2BR, UNC5B, and neogenin (checkered columns). \*p < 0.05, \*\*p < 0.01 relative to vehicle or 100 ng/mL netrin-1  $\pm$  SEM. Inset: FACS analysis shows that transfection was effective in macrophages using siGLO reagents (>90% FL-1+ in transfected cells as opposed to <5% FL-1+ in vehicle-transfected controls). Representative of three independent experiments. (E and F) Netrin-1 (100 ng/mL) induced ERK1/ERK2 phosphorylation in macrophages while pretreatment with PSB1115 (5 mM) blocked the activation of ERK1/ERK2 (depicted at 30 min following stimulation) (F). Representative image of three independent experiments.



**Figure 6. Netrin-1 Triggers a VEGF-Dependent Proangiogenic Response in Macrophages** (A) Schematic description of the experimental design used for assessing the angiogenic potential of macrophage supernatants after netrin-1 challenge. (B) HRMEC proliferation was assessed by CyQUANT assay after a 48 hr incubation with conditioned media (CM) from macrophages stimulated with vehicle (Ctrl), netrin-1 (100 ng/mL), or netrin-1 stimulation following pretreatment with PSB1115 (5 mM) for 30 min. Cells were incubated in the presence of vehicle (PBS), netrin-1 (100 ng/mL), or macrophage CM. CM from Netrin-1-stimulated macrophages yielded a pronounced increase in cell proliferation in an AA2BR-dependent manner while netrin-1 alone provoked a more modest proliferation (n = 3 separate experiments). (C) Matrigel plug assay was employed to investigate the ability of macrophage CM to induce vascularization in vivo. CM from same conditions as in (B) were solubilized in Matrigel and implanted in adult mice. Vascular growth inside the subcutaneously injected Matrigel was evaluated by intravenous FITCdextran injections and spectrophotometric quantification. CM from netrin-1-stimulated macrophages yielded a robust increase in vascular growth in an AA2BR-dependent manner while netrin-1 alone did not influence vascularization. Representative images from Matrigel plugs collected 10 days postintroduction. Scale bar: 2 mm. n = 3 separate experiments. (D) Area of vascular sprouting from aortic explants incubated with same conditions as in (B). Assessment was made after 48 hr of incubation. Representative images from each condition assessed are shown. n = 12–16 aortic rings from four separate experiments. Scale bar: 1mm. (E) CM were preincubated with either goat IgG (Gt IgG) or an anti-VEGF neutralizing antibody (5 mg/mL) before addition to aortic explants. Representative images are shown. Scale bar: 1 mm; n = 9–11 aortic rings from three different experiments. \*p < 0.05, \*\*p < 0.01, \*\*\*p < 0.001 relative to vehicle, netrin-1 100ng/mL, Ctrl CM, or netrin-1 CM ± SEM.



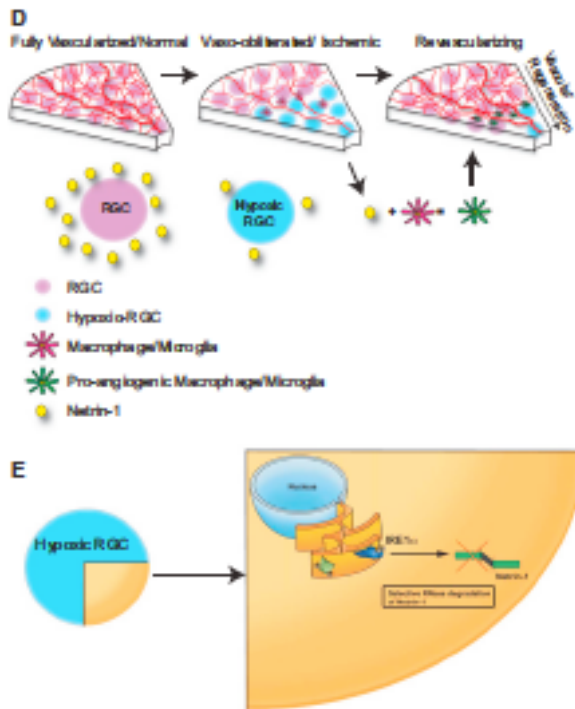


**Figure 7. Netrin-1-Dependent Vascular Regeneration Is Macrophage/Microglial Cell and VEGF Dependent** (A) Intravitreal injection of clodronate liposomes efficiently eliminated retinal macrophages/microglia. Retinas were injected at P11 with 1 mL of empty (PBS) or clodronate liposomes and collected at P14 for FACS analysis. The proportion of CD11b+/F4-80+ (microglia) was calculated by first gating the 7-AAD negative (viable) population. Histograms showing the numbers of macrophages/microglia according to the proportion measured by FACS analysis. Representative dot plots are shown; n = 6 retinas/group. (B) Depletion of retinal macrophages abrogated netrin-1-induced revascularization of OIR retinas. Avascular areas were determined in retinas pretreated with 0.5 mL of empty or clodronate-containing liposomes at P11 then injected with 100 ng/mL netrin-1 at P14. Retinas were analyzed at P17. Representative images of flatmount retinas are shown; n = 8–10 animals/group. \*p < 0.05, \*\*p < 0.01 relative to vehicle-injected retinas ± SEM. Scale bar: 1 mm. (C) Simultaneous injections of anti-VEGF neutralizing antibodies at P14 abolished the ability of netrin-1 to induce vascular regeneration. Representative images of n = 8–10 retinal flatmounts per group are shown below. \*\*\*p < 0.001 relative to vehicle-injected retinas ± SEM. (D and E) Graphical depiction of principal findings of the study. Mildly ischemic retinal ganglion neurons produce netrin-1, which activates a critical reparative angiogenic switch in macrophages/microglia and precipitates vascular regeneration of ischemic retinas (D). Sustained hypoxic stress on RGCs provokes the degradation of netrin-1 mRNA by an IRE1a-dependent mechanism and consequently impedes vascular regeneration (E).